



Binks, Alexander William David (2018) The role of immunogenic cell death in oncolytic herpes simplex virus-1 infection of cancer cells. PhD thesis.

<https://theses.gla.ac.uk/30718/>

Copyright and moral rights for this work are retained by the author

A copy can be downloaded for personal non-commercial research or study, without prior permission or charge

This work cannot be reproduced or quoted extensively from without first obtaining permission in writing from the author

The content must not be changed in any way or sold commercially in any format or medium without the formal permission of the author

When referring to this work, full bibliographic details including the author, title, awarding institution and date of the thesis must be given

Enlighten: Theses

<https://theses.gla.ac.uk/>  
[research-enlighten@glasgow.ac.uk](mailto:research-enlighten@glasgow.ac.uk)



University  
of Glasgow

**The role of immunogenic cell death in oncolytic  
herpes simplex virus-1 infection of cancer cells**

Alexander William David Binks

B.Sc.

Submitted in fulfilment of the requirements for the Degree of Doctor  
of Philosophy

Institute of Cancer Sciences

College of Medical, Veterinary and Life Sciences  
University of Glasgow

May 2018



## Abstract

Patients living with many cancers, including ovarian cancer (OC), often suffer from a lack of adequate treatment options. In the case of OC, primary debulking surgery followed by platinum and paclitaxel chemotherapy has led to a vast improvement in patient survival over the past few decades, however, rates of drug-resistant recurrence remain high. Research into new, experimental treatment options is therefore warranted for OC and other cancers.

Oncolytic viruses (OVs) are replication-competent viruses that can selectively infect and destroy cancerous cell types, while leaving healthy cells unharmed. OVs do this by exploiting differences between cancer and normal cell phenotypes. Herpes simplex virus (HSV)-1, strain 1716 is one example of this type of virus that has shown selectivity for cancer cells in previous preclinical studies, as well as high levels of safety in humans. One prominent area of current OV study seeks to investigate the ability of OVs to induce immunogenic cell death (ICD) - this term describes multiple modes of programmed death pathways that culminate in release of proimmunogenic factors, which facilitate a modification of the host immune system. Two of the most prominent of these pathways are necroptosis and immunogenic apoptosis (IA).

Here, I show that while many OV cell lines express the necessary components for necroptosis, they are unable to undergo classical necroptotic death (induced by TSZ). Despite this, HSV-1716 can infect and kill a range of OC lines successfully. I showed that HSV-1716-induced cell death displays two markers of IA yet does not seem to rely solely on apoptosis to kill cells. In addition, it appears not to rely on any components of the necrosome in order to kill cells, even in cells that are competent to typical necroptosis. However, when RIPK3 is overexpressed in HeLa cells, virus-induced cell death increases, as do markers of both necroptosis and IA.

To investigate the role of ICP6 in HSV-1716-induced ICD, viral and cell mutants were made possessing various forms of the protein. Full-length ICP6 protein expressed in cell lines had the effect of blocking cellular response to TSZ, but constructs lacking a region known as the RHIM did not. A functionally similar

mutation was produced within the RHIM of live HSV-1716 using CRISPR/Cas9 technology, which was shown to have the effect of disrupting ICP6/RIPK3 binding - thought to be the determinant of necroptotic cell death. Despite this, no changes in cell death signalling could be determined between the viruses at all.

Interestingly, when cells were infected in combination with TNF- $\alpha$ , or TNF- $\alpha$  in addition to SMAC mimetic, the RHIM-modified virus produced significantly more death than HSV-1716. This suggests that while loss of RIPK3 inhibition is not sufficient to lead to increased necrosis alone, cells infected with this virus are more sensitive to further necrosis induction. This finding may prove to have great utility for producing the next generation of oncolytic viral therapeutics which can induce greater levels of proimmunogenic cell death.

From this we can conclude that HSV-1716 is capable of inducing IA in OC cells. Death is not dependent on necroptosis, however additional RIPK3 seems to sensitise cells to death by other means. Cellular binding of viral ICP6 and RIPK3 can be disrupted by modification of the RHIM, although this change has no bearing on ICD signalling alone but can sensitise cells to TNF- $\alpha$ -induced death.

# Table of Contents

<b>Abstract</b> .....	<b>1</b>
<b>List of Tables</b> .....	<b>7</b>
<b>List of Figures</b> .....	<b>8</b>
<b>Acknowledgements</b> .....	<b>10</b>
<b>Author's Declaration</b> .....	<b>12</b>
<b>Table of Abbreviations</b> .....	<b>13</b>
<b>1 Introduction</b> .....	<b>17</b>
<b>1.1 Ovarian Cancer</b> .....	<b>20</b>
1.1.1 Epidemiology.....	20
1.1.2 Molecular Pathology.....	21
1.1.3 Staging.....	25
1.1.4 Presentation and Diagnosis.....	26
1.1.5 Ovarian Cancer Tumour Immunology.....	27
1.1.6 Current Treatment Standards.....	29
1.1.7 New Therapies.....	31
<b>1.2 Oncolytic Virotherapy</b> .....	<b>34</b>
1.2.1 Introduction.....	34
1.2.2 Oncolytic Viruses in Clinical Development.....	36
1.2.3 Oncolytic Viruses and Tumour Immunology.....	38
1.2.4 Oncolytic Viruses and Clinical Ovarian Cancer Studies.....	42
<b>1.3 Herpes Simplex Virus 1</b> .....	<b>43</b>
1.3.1 Introduction and History.....	43
1.3.2 Viral Structure.....	44
1.3.3 Viral Genome Organisation.....	45
1.3.4 Viral Life Cycle.....	47
<b>1.4 Herpes Simplex Virus 1 as an Oncolytic Agent</b> .....	<b>53</b>
1.4.1 Introduction.....	53
1.4.2 HSV-1716.....	56
1.4.3 Other Notable HSV-based Oncolytic Viruses.....	59
<b>1.5 Cell Death</b> .....	<b>61</b>
1.5.1 Introduction to Death Modalities.....	61
1.5.2 Apoptosis.....	63
1.5.3 Necrosis.....	70
1.5.4 Autophagy.....	74
1.5.5 Non-Classical Cell Death Modalities.....	75
<b>1.6 Immunogenic Cell Death and Oncolytic Virus Therapy</b> .....	<b>77</b>
1.6.1 Oncolytic Viruses that Induce Immunogenic Cell Death.....	77
1.6.2 Herpesviruses and Immunogenic Cell Death.....	79
<b>1.7 Aims of the Project</b> .....	<b>83</b>
1.7.1 Evaluate HSV-1716 as a treatment for ovarian cancer.....	83
1.7.2 Produce novel models for assessing ICP6 function.....	83
1.7.3 Determine the role of immunogenic cell death during HSV-1716 infection.....	83
1.7.4 Determine the roles of ICP6 and RIPK3 in HSV-1716-induced immunogenic cell death.....	83
<b>2 Materials and methods</b> .....	<b>85</b>
<b>2.1 Cell and virus culture</b> .....	<b>86</b>

2.1.1	Cell lines .....	86
2.1.2	Viruses .....	87
<b>2.2</b>	<b>Cell infection and drug treatment .....</b>	<b>87</b>
2.2.1	Infection .....	87
2.2.2	Drug treatment.....	87
2.2.3	Transfection of siRNA .....	88
<b>2.3</b>	<b>Cell Viability Assays.....</b>	<b>89</b>
2.3.1	MTT cytotoxicity assay.....	89
2.3.2	Sytox nuclear staining for NK cell co-culture .....	89
<b>2.4</b>	<b>HSV production, purification and titration .....</b>	<b>90</b>
2.4.1	Virus production .....	90
2.4.2	Virus Purification .....	90
2.4.3	Titration of viral stocks .....	91
<b>2.5</b>	<b>Cloning techniques.....</b>	<b>91</b>
2.5.1	DNA extraction from cells and viruses .....	91
2.5.2	Polymerase chain reaction for amplification of DNA fragments .....	92
2.5.3	Restriction enzyme digestion of DNA .....	92
2.5.4	Ligation .....	93
2.5.5	TA ligation of PCR products into pCR TOPO 2.1 vector .....	93
2.5.6	Separation and visualisation of DNA fragments on agarose gel .....	94
2.5.7	Gel extraction and purification of DNA.....	94
2.5.8	Determination of nucleic acid concentration .....	94
2.5.9	Transformation of competent <i>E.coli</i> .....	95
2.5.10	Mini and Maxi preparation of DNA from <i>E.coli</i> .....	95
<b>2.6</b>	<b>Creation of ICP6 expressing cell lines by lentiviral transduction .....</b>	<b>96</b>
2.6.1	Creation of lentiviruses from plasmid constructs .....	96
2.6.2	Transduction of cell lines with lentiviruses .....	97
2.6.3	Dilution cloning of ICP6 cells .....	98
<b>2.7</b>	<b>CRISPR/Cas9 gene editing of HSV-1716. ....</b>	<b>98</b>
2.7.1	Guide design.....	98
2.7.2	Transfection .....	98
2.7.3	Isolation of viral clones.....	99
2.7.4	Screening for gene edited viral clones.....	99
<b>Sequencing .....</b>		<b>99</b>
<b>2.8</b>	<b>Quantitative PCR.....</b>	<b>100</b>
2.8.1	Viral replication .....	100
2.8.2	RNA extraction for RT-PCR from cells .....	101
2.8.3	Complementary DNA (cDNA) generation .....	101
2.8.4	qPCR following reverse transcription.....	102
2.8.5	RT <sup>2</sup> Profiler array .....	102
<b>2.9</b>	<b>Protein expression levels .....</b>	<b>103</b>
2.9.1	Preparation of whole cell lysates .....	103
2.9.2	Determination of protein concentration.....	103
2.9.3	Preparation of polyacrylamide gels.....	104
2.9.4	Preparation of samples.....	104
2.9.5	SDS-PAGE and Western blotting .....	104
2.9.6	Antibody staining.....	105
2.9.7	Co-immunoprecipitation (CoIP) .....	105
2.9.8	Fluorescent antibody detection array.....	107

2.10	<b>Flow cytometry</b> .....	<b>108</b>
2.10.1	Cell surface expression of Calreticulin .....	108
2.10.2	Annexin V/Zombie Violet staining for determination of cell death.....	109
2.10.3	Analysis by flow cytometry .....	109
2.11	<b>Transmission Electron Microscopy</b> .....	<b>110</b>
2.12	<b>Luminescence detection of ATP release</b> .....	<b>111</b>
2.13	<b>Statistical analyses</b> .....	<b>111</b>
3	<b>Basic observations of HSV-1716 in cancer cells</b> .....	<b>113</b>
3.1	<b>Introduction</b> .....	<b>114</b>
3.2	<b>HSV-1716 replicates within human ovarian cancer cells</b> .....	<b>115</b>
3.3	<b>HSV-1716 kills both continuous and primary human ovarian cancer cells</b> .....	<b>116</b>
3.4	<b>Susceptibility of ovarian cancer cell lines to necroptosis</b> .....	<b>119</b>
3.5	<b>Assessing the characteristics of a RIPK3 over-expression model in HeLa cells</b> ..	<b>121</b>
3.6	<b>Discussion</b> .....	<b>124</b>
4	<b>Creation of ICP6 modified Virus and Cell Lines</b> .....	<b>128</b>
4.1	<b>Introduction</b> .....	<b>129</b>
4.2	<b>Creation of ICP6 modified viruses using a CRISPR/Cas9- based system</b> .....	<b>129</b>
4.2.1	Developing a CRISPR/Cas9 gene-editing technique for viruses .....	129
4.2.2	Design of Guide Sequences .....	133
4.2.3	Isolating and identifying CRISPR viral clones .....	134
4.3	<b>Creation of a range of ICP6-modified cell lines</b> .....	<b>137</b>
4.4	<b>Effect of ICP6 RHIM on sensitivity to TSZ</b> .....	<b>139</b>
4.5	<b>Effect of CRISPR-mediated ICP6 mutations on viral activity</b> .....	<b>141</b>
4.5.1	Effect on viral replication .....	141
4.5.2	Effect on viral killing.....	143
4.5.3	Effect on RIPK3 binding .....	146
4.6	<b>Complementation of <math>\Delta</math>ICP6 HSV-1716 with ICP6 expressing ovarian cancer cells</b> <b>148</b>	
4.7	<b>Discussion</b> .....	<b>149</b>
5	<b>Understanding the Role of Immunogenic Cell Death in HSV-1716 infection</b> .....	<b>156</b>
5.1	<b>Introduction</b> .....	<b>157</b>
5.2	<b>Markers of immunogenic apoptosis following HSV-1716 or HSV-3D7 infection</b> ....	<b>158</b>
5.2.1	Extracellular calreticulin exposure.....	158
5.2.2	HMGB1 release.....	159
5.2.3	ATP release.....	161
5.2.4	Response to inhibition of caspase-8 .....	163
5.3	<b>Markers of general necrosis following viral infection</b> .....	<b>165</b>
5.3.1	Annexin V/ Zombie Violet staining .....	165
5.3.2	Visual evidence of necrosis by TEM .....	167
5.4	<b>Markers of necroptosis following viral infection</b> .....	<b>173</b>
5.4.1	Phosphorylation of MLKL .....	173
5.4.2	Response to necrosome inhibitors.....	174
5.4.3	Response to short interfering RNA knockdown of RIPK3 and MLKL .....	176
5.4.4	Effect of RIPK3 overexpression on HSV-1716 and HSV-3D7-induced cell death..	178
5.4.5	Effect of Genomic MLKL Knock-Down on Viral Killing.....	179
5.5	<b>Effect of ICP6-RIPK3 binding on response to TNF-<math>\alpha</math></b> .....	<b>181</b>
5.6	<b>Discussion</b> .....	<b>183</b>
6	<b>Immune system responses to HSV-1716 and HSV-3D7 infection</b> .....	<b>193</b>
6.1	<b>Introduction</b> .....	<b>194</b>
6.2	<b>Cytokine and chemokine regulation following viral infection</b> .....	<b>194</b>

6.2.1	mRNA regulation.....	194
6.2.2	Protein regulation.....	196
<b>6.3</b>	<b>NK cell killing induced by viral infection.....</b>	<b>200</b>
<b>6.4</b>	<b>Discussion.....</b>	<b>202</b>
<b>7</b>	<b>Final Discussion.....</b>	<b>209</b>
7.1	Results summary.....	210
7.2	Future directions.....	212
7.3	Translational significance.....	213
7.4	Final remarks.....	214
<b>8</b>	<b>Appendices.....</b>	<b>216</b>
8.1	Fold-change values for RT <sup>2</sup> chemokine/cytokine array.....	217
8.2	Fold change values for Raybiotech chemokine array.....	218
<b>9</b>	<b>List of References.....</b>	<b>222</b>

# List of Tables

Table 1.1: Nationally approved and orphan drug designated oncolytic viruses.....	38
Table 1.2: Human herpes virus species.....	44
Table 2.1: List of drugs used with working concentrations and suppliers.....	88
Table 2.2: List of restriction enzymes used with buffer and supplier .....	93
Table 2.3: ICP6-expressing plasmid information and naming. ....	97
Table 2.4: Lentivirus reagent quantities for cell line transduction. ....	97
Table 2.5: Standard qPCR cycling conditions. ....	101
Table 2.6: cDNA generation thermocycler conditions. ....	102
Table 2.7: RT <sup>2</sup> cytokine and chemokine profiler array cycle conditions.....	103
Table 2.8: List of antibodies and suppliers used.....	107
Table 2.9: List of flow cytometry antibodies used with suppliers .....	110
Table 8.1: Log2 fold-change values for HSV-1716 compared to uninfected cells in TOV21G. .....	217
Table 8.2: Log2 fold-change values for HSV-1716 infection compared to HSV-3D7 in TOV21G cells. ....	218
Table 8.3: Relative fold changes in chemokine expression for TOV21G cells infected with HSV-1716 or HSV-3D7.....	219
Table 8.4: Relative fold changes in chemokine expression for HeLa cells infected with HSV- 1716. ....	220
Table 8.5: Relative fold changes in chemokine expression for HeLa-RIPK3 cells infected with HSV-1716 or HSV-3D7.....	221

# List of Figures

Figure 1.1 The ten hallmarks of cancer. ....	19
Figure 1.2 Histological subtypes of ovarian cancer and common mutations.....	21
Figure 1.3 Oncolytic virotherapy concept.....	35
Figure 1.4 Immune modulation of the tumour microenvironment by oncolytic viruses.....	40
Figure 1.5 Simplified structure of Herpesvirus virion.....	45
Figure 1.6 Map of the HSV-1 genome. ....	46
Figure 1.7 Life cycle of HSV-1. ....	52
Figure 1.8 Comparison of BAC and CRISPR methods for modification of large viruses. ....	55
Figure 1.9 Gene modifications of several oHSV strains.....	57
Figure 1.10 Visual map of cell death modalities.....	63
Figure 1.11 Mechanisms of classical apoptosis.....	66
Figure 1.12 Mechanisms of DAMP release from immunogenic apoptotic cells.....	68
Figure 1.13 Interconnected pathways of necroptosis and apoptosis. ....	72
Figure 1.14 RIP-homotypic interaction motif sequences of cellular and viral proteins. ....	80
Figure 1.15 Various cell death roles of HSV-1 ICP6. ....	81
Figure 3.1 Replication of HSV-1716 within ovarian cancer cells. ....	115
Figure 3.2 HSV-1716 killing of primary and established ovarian cancer cell lines.....	118
Figure 3.3 Assessing the necroptosis-competency of ovarian cancer cell lines. ....	120
Figure 3.4 Assessing the characteristics of a HeLa-RIPK3 over-expression model.....	122
Figure 4.1 CRISPR-based method for HSV genome editing. ....	130
Figure 4.2 Assessing the suitability of puromycin and Vero cells for CRISPR gene editing of HSV-1716. ....	132
Figure 4.3 CRISPR guide sequences used for ICP6 gene editing. ....	134
Figure 4.4 Isolation of CRISPR-edited viral clones. ....	135
Figure 4.5 Illustration of nucleotide changes in ICP6 virus mutants. ....	137
Figure 4.6 Schematic representation of ICP6 mutant constructs overexpressed in TOV21G and OVCAR4 cells. ....	138
Figure 4.7 Visualisation of ICP6-expressing cell lines by immunoblot. ....	139
Figure 4.8 Susceptibility of ICP6-expressing cell lines to TSZ treatment. ....	140
Figure 4.9 Replication of ICP6-modified viruses in TOV21G cells. ....	142
Figure 4.10 Effect of CRISPR-mediated ICP6 alterations on viral killing in cell lines. ....	144
Figure 4.11 Effect of CRISPR-mediated ICP6 alterations on viral killing in primary OC cells. ....	145
Figure 4.12 Co-immunoprecipitation of ICP6 and RIPK3 in HSV-infected cells.....	147
Figure 4.13 Complementation of ICP6-null viruses with ICP6-expressing cells.....	149
Figure 5.1 Calreticulin release from HSV-1716-infected cells.....	159
Figure 5.2 HMGB1 release following HSV-1716 and HSV-3D7 infection of TOV21G and HeLa cells. ....	160
Figure 5.3 Release of ATP from HSV-1716 and HSV-3D7 infected cells.....	162
Figure 5.4 Effect of caspase inhibition on HSV killing in TOV21G cells.....	164
Figure 5.5 Effect of HSV-1716 and HSV-3D7 infection on Annexin V exposure and pore formation. ....	166
Figure 5.6 Electron micrograph images of uninfected TOV21G cells. ....	168
Figure 5.7 Electron micrograph images of TOV21G cells treated with TSZ. ....	169
Figure 5.8 Electron micrograph images of TOV21G cells infected with HSV-1716. ....	171
Figure 5.9 Electron micrograph images of TOV21G cells infected with HSV-3D7.....	172
Figure 5.10 Phosphorylation of MLKL following HSV-1716 or HSV-3D7 infection of cancer cells. ....	173

Figure 5.11 Effect of pharmacological necrosome inhibition on HSV-1716 and HSV-3D7-induced cell death.....	175
Figure 5.12 Effect of siRNA knockdown of RIPK3 and MLKL on HSV-1716-mediated killing. ....	177
Figure 5.13 Effect of RIPK3 overexpression on HSV-1716 and HSV-3D7-induced cell death. ....	178
Figure 5.14 Effect of Genomic Knockdown of MLKL on HSV-1716 and HSV-3D7-mediated killing. ....	180
Figure 5.15 Effect of co-treatment of HeLa-RIPK3 cells with virus and TNF- $\alpha$ on cell death. ....	182
Figure 6.1 Effect of HSV-1716 or HSV-3D7 infection on cytokine and chemokine regulation. ....	195
Figure 6.2 Cytokine and Chemokine protein release following infection of cell lines with HSV-1716 or HSV-3D7.....	197
Figure 6.3 Correlation between whole protein and mRNA expression of selected chemokines in TOV21G cells infected with HSV-1716. ....	199
Figure 6.4 Effect of co-treatment of TOV21G cells with NK92 cells and HSV-1716. ....	201

## Acknowledgements

First and foremost, I'd like to thank my supervisor, Iain. I think you definitely hit the supervisor sweet-spot by providing the right amount of nurturing and guidance, while at the same time leaving enough space to grow. In addition, your near-encyclopaedic knowledge of cancer and ability to channel the biology spirits through your predictive scribbles provided not only immense help, but also plenty of material for bullshit bingo. I particularly want to thank you for your flexibility and help with allowing me to come and pester you for an extra few months at Imperial.

I want to thank all the members of the McNeish lab for your help with getting me settled and quickly making me feel at home. I'd like to especially thank Suzanne for showing me the ropes with tissue culture, being a reliable liquid nitrogen buddy, and always going the extra mile to help me figure out a problem. I'm grateful for my friendships with everyone in the carefully titled "MO4 PhDs + JW + Eirini" group, for always providing a source of laughter when unpacking the daily lab madness - particularly Josephine, my cake and bingo partner in crime; Elaine, my Ka Ka Lok guide and total lab guru; Pavlina and Amber, my equally awesome desk buddies, and of course; Melanie, my necrosis twin. I'd like to give a shout out to Otto, the cutest little idiot puppy I've ever met. Those cuddles turned out to be extremely therapeutic, so thanks. I should probably also give a mention to his daddies, Darren and Luciano, who, in addition to being the ones that introduced me to Otto, are also pretty solid guys. Additional thanks to Sophie, Sarah and Jaya, who helped me transition into the new London lab.

I'd like to thank everyone else who helped me get through my time in Glasgow, starting with Mara - you singlehandedly turned what would have been a good year into one of the best years of my life. I'm truly grateful for you bringing so many excellent people together in one place with your epic parties - people like Gwen, Dorine, Stephan, Pepper, Marissa, Jacquie, Eleanor, Kevan and Maria and many more! It was heart-breaking to see you all leave at once, but I'm thankful that more great friends were just around the corner. I'd of course like to give shout outs to Steph, Kayla and Michelle for keeping the party going throughout my second and third years. Steph, you have been a terrific friend to me and I'm

extremely grateful - you're even consoling me about my upcoming viva as I write this. Thanks to all the MRC "guys and gals" for those surprisingly frequent afternoons spent polishing off free wine and letting me know that you guys are just as freaked out as I am about this whole PhD thing.

Extra thanks to all the friends that came to visit me in Glasgow and keep me sane - Josh, Slava, Ellie, Simon, Chris and Nina, and to all my family. I of course need to give final, special thanks to my wonderful girlfriend, Sara. I'm wholly grateful for having someone so wonderful with whom to laugh and joke around. Those cuddles in the kitchen always got me off the ground. Here's to the next few years of London life!

## **Author's Declaration**

The material presented in this thesis is the result of original work carried out by the author, Alexander Binks, at the Wolfson Wohl Cancer Research Centre, Institute of Cancer Sciences, University of Glasgow. All external sources have been properly acknowledged, referenced and required licences obtained.

## Table of Abbreviations

Abbreviation	Description
3-O HS	3-O sulphated heparan sulphate
AA	amino acid
ACD	autophagic cell death
ADIPOQ	adiponectin
AIF	apoptosis-inducing factor
APAF-1	apoptotic protease-activating factor-1
APC	antigen-presenting cell
APS	ammonium per sulphate
ATP	adenosine triphosphate
AUC	area under curve
AV	annexin V
BAC	bacterial artificial chromosome
BCL-2	B-cell lymphoma-2
BiTEs	bispecific T cell engagers
bp	base-pair(s)
BRCA1	breast cancer 1
BRCA2	breast cancer 2
CA	cancer antigen
CAD	caspase-activated DNase
CAL	calreticulin
Cas	CRISPR-associated protein
CCC	clear cell carcinoma
CD	cluster of differentiation
CEA	carcinoembryonic antigen
ciAP	cellular inhibitor of apoptosis
CK	cytokeratin
CLYD	cylindromatosis
CMV	cytomegalovirus
CNS	central nervous system
CO <sub>2</sub>	carbon dioxide
CRISPR	clustered regularly-interspaced short palindromic repeats
CRUK	Cancer Research UK
CSF-1	colony-stimulating factor 1
CT	computed tomography
CTLA	cytotoxic T-lymphocyte associated protein
CVB3	Coxsackie virus B3
CXCL	interferon gamma-induced protein
Da	Dalton
DAI	DNA-dependent activator of interferon regulatory factors
DAMP	damage-associated molecular pattern
DED	death effector domain
DISC	death-inducing signalling complex

DMEM	Dulbecco's modified eagle medium
DMSO	dimethyl sulphoxide
DNA	deoxyribonucleic acid
DSB	double-strand break
EBV	Epstein-Barr virus
EC	endometrial carcinoma
EGF(R)	epidermal growth factor (receptor)
eIF-2 $\alpha$	eukaryotic initiation factor 2 $\alpha$
EMA	European Medicines Agency
ER	endoplasmic reticulum
FADD	Fas-associated protein with death domain
FBS	foetal bovine serum
FDA	Food and Drug Administration
FDG-PET	[18F]-fluorodeoxyglucose positron emission tomography
FIGO	The International Federation of Gynaecology and Obstetrics
FITC	fluorescein isothiocyanate
FOXP3	forkhead box P3
GI	gastrointestinal
GM-CSF	granulocyte macrophage colony-stimulating factor
GPX4	glutathione-dependent enzyme glutathione peroxidase 4
gRNA	guide RNA
GSDMD	gasdermin D
h	Hour(s)
H-1PV	parvovirus H-1
HGSOC	high-grade serous ovarian cancer
HHV	human herpesvirus
HIV	human immunodeficiency virus
HMGB1	high-mobility group box-1
HNF1- $\beta$	hepatocyte nuclear factor 1- $\beta$
HR	homologous recombination
HSP	heat-shock protein
HSPG	heparan sulphate proteoglycan
HSV	herpes simplex virus
HVEM	herpesvirus entry mediator
IA	immunogenic apoptosis
IBS	irritable bowel syndrome
IC <sub>50</sub>	half-maximal inhibitory concentration
ICD	immunogenic cell death
ICP	infected cell protein
(i)DC	(immature) dendritic cell
IFI16	interferon-inducible protein 16
IFNG	Interferon- $\gamma$
IGFR	insulin-like growth factor receptor
IL	interleukin
ITS	insulin, transferrin and sodium selenite
k	kilo

KSHV	Kaposi's sarcoma-associated virus
LAT	latency-associated transcript
LB	Lennox broth
LC3	microtubule-associated protein 1A/1B light chain 3
LGSOC	low-grade serous ovarian cancer
MC	mucinous carcinoma
MDSC	myeloid-derived suppressor cell
MHC	major histocompatibility complex
(M/H)CMV	(murine/human) cytomegalovirus
MIF	migration inhibitory factor
min	minute(s)
miRNA	micro RNA
MLKL	mixed-lineage kinase domain-like pseudokinase
MOI	multiplicity of infection
mRNA	messenger RNA
MT	microtubule
MTT	(3- (4,5- Dimethylthiazol-2-yl)-2,5-diphenyltetrazolium bromide)
MV	Measles virus
MW	molecular weight
NCCD	The Nomenclature Committee on Cell Death
NDV	Newcastle disease virus
NET	neutrophil extracellular trap
NK	natural killer
NLR	nod-like receptor
NLRP3	NACHT, LRR and PYD domains-containing protein 3
NPC	nuclear pore complex
OC	ovarian cancer
oHSV	oncolytic HSV
OV	oncolytic virus
p.i	post-infection
P/S	penicillin and streptomycin
PAM	protospacer adjacent motif
PAMP	pathogen-associated molecular pattern
PAR(P)	poly(ADP-ribose) (polymerase)
PBS	phosphate-buffered saline
PCD	programmed cell death
PCR	polymerase chain reaction
PD(L)-1	programmed cell death protein (ligand) 1
PDGF	platelet-derived growth factor
PE	phycoerythrin
PFA	paraformaldehyde
PFS	progression-free survival
PFU	plaque-forming units
PI	propidium iodide
PI	phosphatidylinositol
PKR	protein kinase R
pMLKL	phosphorylated MLKL

PP1 $\alpha$	protein phosphatase 1 $\alpha$
PS	phosphatidyl serine
PSA	prostate-specific antigen
RAGE	receptor for advanced glycation end products
RCD	regulated cell death
RHIM	RIP-homotypic interaction motif
RHOA	ras homolog family member A
RIPK1/3	receptor-interacting serine/threonine-protein kinase 1/3
RMI	risk of malignancy index
RNA	ribonucleic acid
ROS	reactive oxygen species
RPMI	Roswell Park Memorial Institute (medium)
RR	ribonucleotide reductase
RT	reverse transcriptase
s	second(s)
SD	standard deviation
SDS	sodium dodecyl sulphate
siRNA	small interfering RNA
SMAC	second mitochondria-derived activator of caspase
SSB	single-strand break
TAA	tumour-associated antigen
TAM	tumour-associated macrophage
TBS(T)	tris buffered saline (tween)
TEM	transmission electron microscopy
TIC	tubal intraepithelial carcinoma
TIL	tumour-infiltrating lymphocyte
TK	thymidine kinase
TLR	toll-like receptor
TNF	tumour necrosis factor
TP53	tumour protein 53
TRADD	TNF receptor type 1-associated death domain protein
TRAF	TNF receptor-associated factor
T reg	suppressor T cell
TRP	transient potential receptor
T-VEC	Talimogene Laherparepvec
UV	ultraviolet
VEGF(R)	vascular endothelial growth factor (receptor)
vIRA	viral inhibitor of RIP activation
VSV	varicella zoster virus
VV	Vaccinia virus
WT	wild-type
ZV	zombie Violet
zVAD-fmk	carbobenzoxy-valyl-alanyl-aspartyl-[O-methyl]- fluoromethylketone
$\beta$ -ME	$\beta$ -mercaptoethanol

# 1 Introduction

Cancer is the second leading cause of death in the world, representing one in every six deaths. In 2015, there were 8.8 million deaths globally and there are roughly 14 million new cases of cancer each year. The number of cancer cases is expected to rise by as much as 70% over the next two decades, making it one of the greatest health crises of this century (WHO, 2017).

Cancer is the term given to any disease caused by the uncontrolled regulation of cell growth and proliferation, leading to eventual spread of these cells throughout the body. Cancer is in fact not one disease, but a collection of diseases which differ greatly in their origins, behaviour, lethality and severity. In 2000, Hanahan and Weinberg published their 'hallmarks of cancer', outlining the characteristics and steps involved in the development of malignancy from normal cells (Hanahan and Weinberg, 2000). In 2011, this overview was updated to include more recent developments in the biology of cancer (Hanahan and Weinberg, 2011). These papers identify 10 hallmarks that cells acquire during the multi-step path to malignancy (Figure 1.1). These consist of the following: sustaining proliferative signalling; evading growth suppressors; avoiding immune destruction; enabling replicative immortality; tumour-promoting inflammation; activating invasion and metastasis; inducing angiogenesis; genome instability and mutation; resisting cell death; and deregulating cellular energetics.

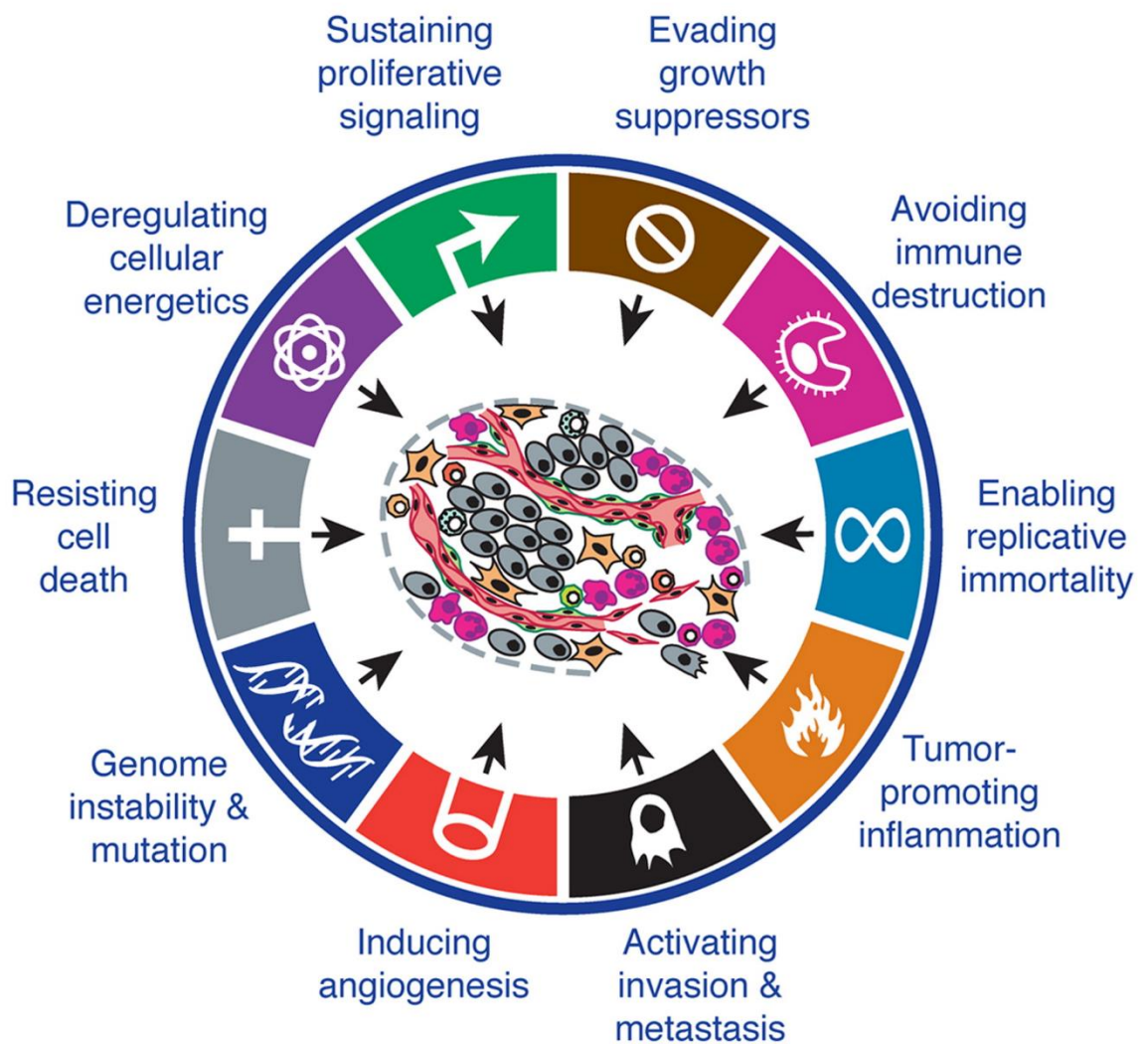


**Figure 1.1** The ten hallmarks of cancer. Figure adapted from *Cell* 2011 **144**, 646-674

This introduction will touch on a number of these hallmarks by exploring first how ovarian cancer forms, how it is treated, and what the remaining obstacles are for future therapies. I will then introduce the concept of oncolytic virotherapy and discuss how viruses can be used to directly destroy cancer cells via a number of regulated cell death mechanisms. Finally, I will discuss how different modes of cell death can have important consequences for how cancer is identified and targeted by the immune system.

# 1.1 Ovarian Cancer

## 1.1.1 Epidemiology

Ovarian cancer (OC) is the fifth most common form of cancer in women in the developed world (sixth in the UK, in particular), and is the leading cause of gynaecological cancer associated death. In the UK, this amounts to 7400 cases every year, with 4100 deaths. The lifetime risk of developing the disease in the UK for women is 1 in 52. The highest incidence occurs in women aged 75-79, with over half of cases in those over the age of 65. OC is the 15<sup>th</sup> most common form of cancer in the UK, but the 14<sup>th</sup> most common cause of cancer death; this amounts to 3% of all female cancer deaths.

Survival rates are poor, with one, five and ten-year survival rates being 73%, 46% and 35% respectively. Younger age at diagnosis and earlier stage at presentation are both associated with greater survival rates. This effect is dramatic for those that present at an early age, with 90% surviving five years or more when diagnosed before age 40.

It is estimated that 21% of OC can be attributed to lifestyle factors, including smoking (3%), hormonal replacement therapy (1%) or occupational exposures such as radiation (1%). There are also some links to use of talcum powder, height and obesity. Oral contraceptive use and breast feeding have been shown to have a protective effect against OC - as many as 18% of OC cases may be a result of breastfeeding for less than 6 months.

The most recent data provided above for OC are from 2014 for incidence and mortality, and 2010-2011 for survival (CRUK, 2017).

Genetic predispositions for OC exist, with germline *BRCA1* and *BRCA2* mutations being the best known. Carrying a *BRCA1* mutation puts the individual at a roughly 39% chance of developing OC by age 70; for *BRCA2* mutations, the probability is 11%, although the range of risk is very high and poorly understood (Antoniou *et al.*, 2003). These mutations are common in Ashkenazi Jewish populations, putting these groups at higher risk of developing OC (Simchoni *et al.*, 2006).

## 1.1.2 Molecular Pathology

Once thought of as a single disease with histological subtypes, OC is now recognised as several distinct diseases with differing origins, behaviour, severity and molecular characteristics (Prat, 2012). The five OC types and their relative incidences are: high-grade serous (70%), endometrioid (10%), clear cell (10%), mucinous (3%) and low-grade serous (<5%) (Figure 1.2).

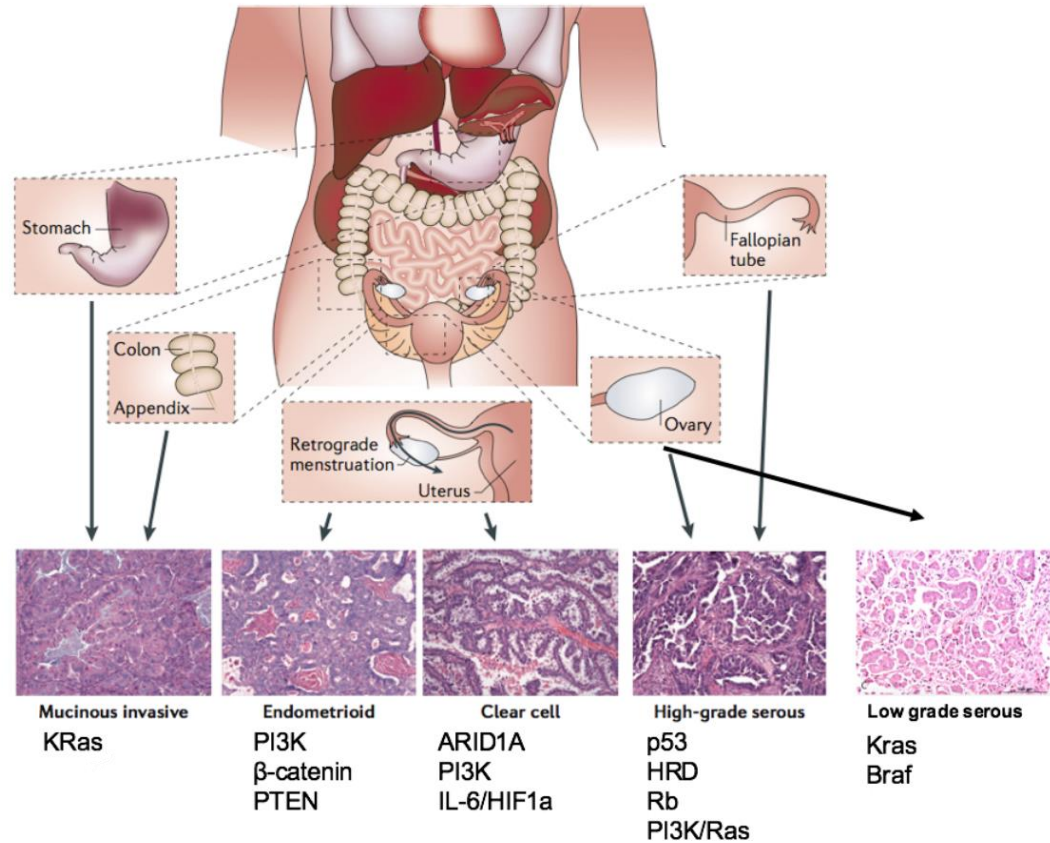


**Figure 1.2 Histological subtypes of ovarian cancer and common mutations.** The five main histological subtypes of epithelial ovarian cancer are shown. High grade serous is the most common subtype and has recently been proposed to originate from the fallopian tubes as well as the ovarian surface epithelium. Homologous recombination deficiency (HRD) is common in HGSOE, in addition to universal p53 loss, and Rb and PI3K/Ras mutation. Sites of origin other than the ovary are known for mucinous, endometrioid and clear cell subtypes. Mutational profiles also differ significantly between subtypes. Image adapted from Nature Reviews Cancer 2011 11, 719-725 by Iain McNeish.

### 1.1.2.1 High-Grade Serous

High grade serous OC (HGSOC) makes up approximately 70% of epithelial OCs. Histologically, tumour cells appear intermediate in size, with the occasional giant cell containing a prominent nucleus (Figure 1.2). Nuclei of the cells vary in size by as much as three times, with this being a major differentiating characteristic from low-grade serous types. Mitotic activity is also much higher in HGSOC. Immunostaining is commonly positive for WT1, PAX8 and CK7 and negative for CK20 and CDX2. Staining for p16 should be strong and diffuse to be positive. Staining for p53 can vary based on the type of mutation seen in the specific tumour (e.g. missense/gain of function or null).

Current evidence suggests that HGSOC is likely derived from fallopian tube precursor lesions (tubal intraepithelial carcinoma (TIC)) (Piek *et al.*, 2001; Medeiros *et al.*, 2006; Folkins *et al.*, 2008), which can migrate to sites on the ovary itself. As most OCs present in such a late stage, it is difficult in many cases to tell what proportion of HGSOC is ovarian or tubal in origin.

HGSOCs have universal *TP53* mutations (Ahmed *et al.*, 2010). Carcinomas arising in those with germline *BRCA1* or *BRCA2* mutations are almost always of high-grade serous type. *TP53* mutation is thought to be the earliest event in oncogenesis, occurring in p53 signature foci, leading to TIC in the distal fallopian tube. In non-germline carriers, *BRCA1 and 2* mutations are thought to occur early, but after *TP53* mutation (Bowtell, 2010), although *BRCA1/2* mutation may help promote development of TIC. In addition to these, *NF1*, *FAT3*, *CDK12*, *CSMD3* and *GABRA6* are the next most common mutations, most of which occurring in fewer than 1% of cases (Bell, Berchuck and Birrer, 2011). Typically, mutations are caused by copy-number alterations and structural rearrangements, although *TP53* mutations are frequently due to mis-sense point mutations (Patch *et al.*, 2015).

### 1.1.2.2 Low-Grade Serous

Low-grade serous OC (LGSOC) accounts for fewer than 5% of all OC cases (Gershenson *et al.*, 2006). Microscopically, LGSOC contain small papillae of tumour cells with uniform nuclei contained within hyalinized stroma, which

often contains psammoma bodies (Figure 1.2). LGSOC only very rarely progresses to HGSOC.

LGSOC possesses similar histological markers to HGSOC, with the main difference being a lower level of Ki-67 staining (2.5% vs 22.4%) (Köbel *et al.*, 2008) reflecting lower rates of cell division and growth and wild-type p53 staining reflecting the absence of *TP53* mutations. Genetically, mutations in *KRAS* and *BRAF* are the most common, with prevalence of 19% and 38% respectively (Jones *et al.*, 2012; Ardighieri *et al.*, 2014). More recent evidence has identified *NRAS* as recurrently mutated in LGSOC, although the prevalence is low at 3.6%, suggesting it plays a minor role in disease progression (Xing *et al.*, 2017). Deletions of 1p36 and 9p21 are associated with LGSOC progression, although LGSOC does not show chromosomal instability and do not possess the complex genetic abnormalities seen in HGSOC (Kuo *et al.*, 2009).

### 1.1.2.3 Mucinous

Mucinous tumours account for 10-15% of ovarian tumours. However, 80% of these are benign, and many of the remaining 20% are borderline or metastases from the GI tract (Prat, 2012). The cells resemble those of GI origin, particularly gastric pylorus and intestine, or those from the endocervix (Figure 1.2). Malignant tumours are often heterogeneous, with invasive components present within borderline, benign-appearing surroundings (Rodríguez and Prat, 2002).

Mucinous carcinomas (MCs) are often found to harbour mutations in genes involved in intestinal differentiation, such as *CDX2* and *KRAS* (Cuatrecasas *et al.*, 1997), with *KRAS* mutations appearing early. Staining for cytokeratin (CK)7 and CK20 is present in 80% and 65% of MCs, respectively. CK20 and CDX-2 staining is fairly weak in true ovarian MC, which can help differentiate from strongly stained colorectal adenocarcinoma. CK7 is also absent in colorectal adenocarcinoma, allowing its use as an identifier (Park *et al.*, 2002; Vang *et al.*, 2006). MCs also lack both WT1 and oestrogen receptor (ER) staining, which allow differentiation from both endometrioid (ER+, WT1-) and serous (ER+, WT1+) types.

#### 1.1.2.4 Endometrioid

Endometrioid carcinomas (ECs) account for 10% of OCs, primarily affecting women of perimenopausal age (~30-50 years old). ECs have a strong association with the endometrium, with 15-20% of cases occurring concurrently with endometrial carcinoma and others with endometriotic cysts (Irving *et al.*, 2005). There is still some debate on whether these carcinomas represent separate diseases, or whether the ovarian disease is a metastasis from the endometrium (Anglesio *et al.*, 2015). Many cases occur in tandem with ipsilateral pelvic or ovarian endometriosis. EC can be graded as high or low, with high grade appearing very similar to HGSOC histologically (Figure 1.2). Genetic profiling between grades is similar, suggesting that they are still a single tumour type (Tohill *et al.*, 2008).

Endometriosis has been shown to directly lead to EC in 15-32% of cases. *KRAS* and *ARID1A* mutations can appear in early endometriosis, with subsequent loss of *PTEN* shown to contribute to induction of invasive EC (Dinulescu *et al.*, 2005). *CTNNB1* and *PTEN* are the most commonly mutated genes (Catasús *et al.*, 2004). Mutations in *CTNNB1*, which codes for  $\beta$ -catenin, occur in 38%-50% of cases. These mutations are associated with low tumour grade, squamous differentiation and favourable outcome (Gamallo *et al.*, 1999). *PTEN* inactivation leads to activation of the pro-survival phosphatidylinositol 3 kinase (PI3K)-AKT signalling pathway, although the same effect is in some cases achieved through activation of *PIK3CA*, which codes for the p110 catalytic subunit of PI3K (Campbell *et al.*, 2004). *PTEN* is mutated in approximately 20% of ovarian ECs. *PTEN* mutations are also found in endometriotic cysts, providing further evidence for a precursor role (Sato *et al.*, 2000).

#### 1.1.2.5 Clear Cell Carcinoma

Clear cell carcinomas (CCCs) account for 10% of OCs. Presentation is often at stage I, with disease usually restricted to a single ovary. As with EC, there is a strong association of CCC with endometriosis, with such cases being associated with a better prognosis (Komiya *et al.*, 1999). As the name suggests, CCCs often appear as cells with a clear cytoplasm, although this phenotype is not restricted to just CCC, and can be seen in HGSOC and EC. Nuclei appear

eccentric, rounded and bulbous, and cells appear with multiple complex papillae with densely hyaline basement membranes (Figure 1.2).

CCCs possess mutations in *ARID1A* in approximately 50% of cases with consequent loss of the protein product, BAF250a (Wiegand *et al.*, 2010). In the same study, Wiegand *et al.* also found that *ARID1A* mutations can also be found in adjacent endometriosis, suggesting that this mutation may serve as an early step in transformation to CCC. CCCs are typically histologically positive for hepatocyte nuclear factor 1- $\beta$  (HNF1- $\beta$ ) and negative for WT1 and ER (Köbel *et al.*, 2009). HNF1- $\beta$  is a transcription factor which regulates glycogen synthesis and so may also play a role in CCC pathogenesis (Kato, Sasou and Motoyama, 2006).

CCCs are far less responsive to chemotherapy than HGSOC. This may be in part due to the fact that they are less proliferative and more genomically stable (Itamochi *et al.*, 2002).

### **1.1.3 Staging**

Following the recent developments in the theory that certain types of OC may originate from the fallopian tubes, The International Federation of Gynaecology and Obstetrics (FIGO) revised its staging criteria (Prat, 2014). This revision primarily sought to unify staging criteria for the ovary, peritoneum and fallopian tubes.

Stage I tumours are limited to the ovary, fallopian tube or peritoneum. Stage IA defines cases where tumours are present in a single ovary, and IB refers to presence in both ovaries, although this is rare (Ataseven *et al.*, 2016). In stage IC, tumour is present on the surface of the ovaries, possibly with a ruptured capsule, cytologically positive ascites, or positive peritoneal washings. Stage II tumours are limited to the pelvis and hold this designation regardless of origin. Uterine, fallopian or ovarian extensions are classed as stage IIA, and extensions to other pelvic regions are IIB.

Stage III tumours extend beyond the pelvic brim, either to the peritoneum or the retroperitoneal lymph nodes. Lymph node-only metastasis is designated as stage

IIIA1 (previously stage IIIC) and is associated with better prognosis (Baek *et al.*, 2008). Lymph node metastases can be identified using [18F]-fluorodeoxyglucose positron emission tomography (FDG-PET), with metastatic nodes defined by increased uptake of tracer, regardless of size. In the case of extrapelvic peritoneal implants, those microscopic in nature are classed as stage IIIA2, those macroscopic but  $\leq 2$ cm are stage IIIB, and those macroscopic and  $\geq 2$ cm are stage IIIC. HGSOE often presents in stage III (84%), particularly stage IIIC, with tumours often spread across the peritoneal wall, including involvement of organs such as the liver and spleen (Prat, 2012). Survival rates for debulking followed by chemotherapy vs chemotherapy followed by debulking appear to be similar, with successful primary debulking being the most important prognostic factor (Vergote *et al.*, 2010).

Stage IV includes distant metastases. This stage is subdivided into IVA, which refers to pleural effusions containing malignant cells, and IVB, which includes lymph node metastases outside of the abdominal cavity. Transmural bowel infiltration, umbilical deposit, and parenchymal metastases in the liver and spleen or elsewhere are also classified as stage IVB.

#### **1.1.4 Presentation and Diagnosis**

Early stage disease is often asymptomatic and can go unnoticed for many months or potentially years before presentation. Symptoms typically include abdominal pain and distension, bloating, back pain, constipation, diarrhoea, frequent urination, irregular menstruation, loss of appetite and fatigue, among others. The gastrointestinal symptoms are often mistaken for irritable bowel syndrome (IBS). As the mass around the ovary grows, it can lead to twisting of the fallopian tube, known as torsion, leading to further pain. Eventually fluid begins to accumulate in the form of ascites and growing tumours can lead to partial or complete blockage of the intestines.

Diagnosis begins with a physical examination, including pelvic examination, to feel for enlarged ovaries and/or presence of ascites fluid in the abdomen. Usually these initial tests will be performed if the patient's symptoms have persisted or worsened in a manner that seems inconsistent with IBS or related

ailments. If all of these factors give reason to suspect OC, then cancer antigen (CA) 125 levels in the blood will be measured (Bast *et al.*, 1981; Ledermann *et al.*, 2013). CA 125 is the protein product of the *MUC16* gene and is produced by many normal tissues, but is often elevated during OC, especially HGSOC. This is by no means a universal test however, as CA 125 levels are only elevated in 50% of stage I cases and 85% of advanced disease cases. CA 125 can also be elevated by non-gynaecological cancers such as breast, lung, colon and pancreatic, as well as non-malignant diseases such as endometriosis, ovarian cysts and pelvic inflammatory disease. If it is unclear at this point whether the cancer is of gynaecological or gastrointestinal (GI) origin, then additional measuring of carcinoembryonic antigen (CEA) or CA 19-9 can be used to differentiate, as these are higher in GI cancers, although neither CA125 nor CA19-9 is definitively diagnostic. The risk of malignancy index (RMI) is a combined index of serum level of CA 125, menopausal state and ultrasound findings (Jacobs *et al.*, 1990). These criteria can predict the risk of malignancy for adnexal masses with a positive predictive value of 77.7% (Bouzari *et al.*, 2011).

Besides blood tests, ultrasonography of the abdomen and pelvis is often performed. The purpose of this is to look for morphological features in an ovarian cyst, such as large lesions, multi-locular cysts, solid papillary projections and irregular internal septations, as well as ascites, which are all highly suggestive of OC. By this stage, a diagnosis can usually be suggested, although further scans in the form of a computed tomography (CT) scan and MRI can help assess the extent of the disease and aid surgical planning as well as identifying pleural effusions and other potential distant metastatic disease.

### **1.1.5 Ovarian Cancer Tumour Immunology**

The immune system forms a highly active part of the ovarian tumour microenvironment. While leukocyte infiltration forms a natural part of the anti-tumour immune response, there is now plenty of evidence to suggest that certain immune cell populations can be tumour-promoting (Cai and Jin, 2017; Zhang *et al.*, 2017).

Tumour associated macrophages (TAMs) form an important part of the microenvironment, and can be found as both M1 and M2 subtypes in HGSOC (Reinartz *et al.*, 2014). OC cells are known to recruit circulating monocytes, through a high expression of the chemotactic protein CCL2 (Negus *et al.*, 1995), which binds to the receptor CCR2, commonly found to be expressed by TAMs (Sica *et al.*, 2000). M1 macrophages are associated with a more tumour suppressive phenotype, and have been shown to transform into M2 macrophages following treatment with colony-stimulating factor-1 (CSF-1), which is upregulated by OC cells and associated with a negative outcome (Chambers *et al.*, 1997). OC cells can cause TAMs to upregulate mannose receptor (MR), which binds cellular mucins (including CA 125 and TAG-72), and promotes an immune-suppressive phenotype, in addition to the immunosuppressive molecule, PD-L1 (Allavena *et al.*, 2010). Elevated IL-6 levels in the ascites and tumours of OC patients is associated with increased TAM formation (Duluc *et al.*, 2007). Prognosis of cancer patients in general (and ovarian cancer in particular) has consistently been shown to be worsened in association with infiltrating TAMs, with TAM phenotype not appearing to matter (Zhang *et al.*, 2012).

It is now known that presence of CD3+ T cells within a tumour is correlated with better clinical outcome (Zhang *et al.*, 2003), tumour specific T cells and antibodies can be found in the blood of OC patients (Goodell *et al.*, 2006), and that T cells isolated from late-stage patients show specificity for and cytolytic activity against tumour cells (Santin *et al.*, 2001). CD8+ T cells expressing the  $\alpha$ E integrin subunit CD103 are associated with good prognosis and are suggested to directly contribute to anticancer killing (Sato *et al.*, 2005; Webb *et al.*, 2014; Komdeur *et al.*, 2016). Suppressor T cells (Treg) have been identified as negative prognostic factors in OC. These cells are distinguished as being CD4+, forkhead box P3 (FOXP3)+ and CD25+, and have been shown to shorten median survival in patients with a high ratio of Treg: CD8+ T cells (Sato *et al.*, 2005). Migration of Tregs into the microenvironment is promoted by CCL22, which binds to the CCR4 receptor present on Tregs (Landskron *et al.*, 2015). Tregs inhibit both CD8+ cell proliferation and release of IFN $\gamma$  and IL-2 (Curiel *et al.*, 2004).

Myeloid-derived suppressor cells (MDSCs) have been found to be present in the ascites, attracted by CXCL12, which is produced in a PGE2-dependent manner

(Obermajer *et al.*, 2011). One critical role of MDSCs is the production of IL-10, which is immunosuppressive and leads to a tumour-permissive microenvironment (Hart *et al.*, 2011).

Natural killer (NK) cells are another innate cell type, which are able to recognise and destroy cancer cells. Migration inhibitory factor (MIF) produced by tumours blocks NK cell cytotoxicity by downregulating the NK receptor NKG2D, which mediates the immune escape of OC (Krockenberger *et al.*, 2008). Likewise, the tumour protein B7-H6 binds to Nkp30 on the surface of NK cells, which triggers an anti-tumour response, with lower Nkp30 expression correlating with lower IFN $\gamma$  production and cytolytic activity (Pesce *et al.*, 2015). Interestingly, higher levels of B7-H6 have also been associated with cancer progression and metastasis (Zhou *et al.*, 2015). NK cells in the ascites have been shown to respond differently to IL-2 based on whether malignant cells are also present (da Silva *et al.*, 2017). In ascites where OC cells are present, NK cells are less responsive to IL-2, showing less degranulation. This suggests that in the ascites, OC cells are contributing to a suppression of anti-cancer immune responses.

NK cells have also been shown to recruit immature dendritic cells (iDCs) via the release of CCL3 and CCL4 (Wong *et al.*, 2013). NK cells encourage the maturation of DCs via CCR5, which leads to upregulation of CCL5, CXCL10 and CXCL9 on the surface of DCs. These markers allow DCs to attract and activate CD8 $^+$  T cells mediating their positive effects (Wong *et al.*, 2013).

### **1.1.6 Current Treatment Standards**

The cornerstone treatment for OC remains debulking surgery, followed by platinum-based chemotherapy. Surgery is typically performed first, and serves to remove as much tumour as possible, acquire samples for histological diagnosis and establish the FIGO stage. Surgery should include a total hysterectomy, bilateral salpingo-oophorectomy, tumour debulking, and omentectomy (Jayson *et al.*, 2014). Certain factors may affect resectability of tumours including upper abdominal disease, involvement of the porta hepatis, small bowel mesentery and diaphragm, extensive ascites, or spread beyond the abdominal cavity (Aletti *et al.*, 2006), as well as the patient's performance status and co-morbidities.

Laparoscopy may be done in advance of surgery in some cases to assess resectability.

If the patient is in poor condition or with extensive unresectable disease, it may be beneficial to treat first with neoadjuvant (pre-operative) chemotherapy to help reduce the size and quantity of any tumours. Percutaneous biopsies must first be taken to enable reliable histological diagnosis. In these cases, debulking should be done after three cycles of a six-cycle chemotherapy regimen. Evidence that providing chemotherapy before surgery does not have a negative impact on overall survival in stage III and IV patients has been provided in the recent EORTC55971 and CHORUS trials (Vergote *et al.*, 2010; Kehoe *et al.*, 2015).

Platinum-based chemotherapy agents have been the standard of care for first-line chemotherapy against OC since the late 70s (Young *et al.*, 1979). cis-dichlorodiammineplatinum(II) (cisplatin) was the first of these drugs to be used. Cisplatin works by cross-linking DNA, which causes DNA adducts to form, resulting in physical stresses and DNA damage, as well as an inhibition of DNA replication and repair. When cisplatin enters the cell, lower chloride content favours aquation of one of the Cl<sup>-</sup> groups, allowing it to subsequently bind to DNA bases covalently (guanine in particular). This allows the second Cl<sup>-</sup> group to undergo a similar process, thereby leading to the binding of DNA in two places. Attempts to replicate the crosslinked DNA results in damage, which activates the DNA repair machinery, but as repair cannot occur, apoptosis signalling becomes active and the cell eventually dies (Kelland, 2007).

Despite its effectiveness, cisplatin is notorious for its high nephrotoxicity, neurotoxicity, tinnitus and emetogenicity. For this reason, there has been a drive for development of safer analogues. The first of these, carboplatin (cis-diammine-[1,1-cyclobutanedicarboxylato]platinum(II)) entered the clinic in the mid-1980s (Harrap, 1985). The reasoning behind carboplatin was that a more stable dicarboxylate leaving group would reduce toxicity, which has been shown to be the case (Knox *et al.*, 1986). Carboplatin therefore works in the same way as cisplatin, with the leaving group affecting pharmacodynamics. Carboplatin is essentially devoid of nephrotoxicity, less toxic to the gastrointestinal tract and less neurotoxic. Carboplatin is dose-limited mainly by its myelosuppressive

effects. Carboplatin is now the standard treatment for OC over cisplatin worldwide (Jayson *et al.*, 2014).

In order to increase anti-tumour efficacy, carboplatin is now often given in combination with either paclitaxel or docetaxel (Ozols *et al.*, 2003; Vasey *et al.*, 2004), which are both taxanes. Taxanes work by disrupting microtubule function during M phase of mitosis. They do this by binding to and stabilising GDP-bound tubulin molecules, preventing them from depolymerising. This has the effect of blocking cell division, which can in turn lead to induction of apoptosis (Abal, Andreu and Barasoain, 2003).

### **1.1.7 New Therapies**

#### **1.1.7.1 Angiogenesis blockers**

Angiogenesis plays a key role the later stages of tumour development and metastasis, and has been identified as an important target for OC. Angiogenesis is a multi-factor process involving interactions with endothelial cells, blood platelets, macrophages/lymphocytes, fibroblasts (Markowska *et al.*, 2017). One of the best characterised pro-angiogenic pathways begins with the binding of members of the vascular endothelial growth factor (VEGF) family to VEGF receptors 1 and 2 on the surface of cells. This interaction can be blocked by the monoclonal IgG antibody Bevacizumab. Bevacizumab has now entered the clinic following several successful phase III trials for OC, in combination with carboplatin and paclitaxel (Burger *et al.*, 2011; Aghajanian *et al.*, 2012; Pujade-Lauraine *et al.*, 2012; Coleman *et al.*, 2015; Oza, Cook, *et al.*, 2015). The NHS England national cancer drug funds list currently recommends bevacizumab as a “1st line treatment of advanced (stage IIIc/IV) OC, suboptimally debulked either at primary or delayed primary (interval) surgery (including peritoneal and fallopian tube cancer) OR unsuitable for debulking surgery” (NHS, 2017).

Some small-molecule antiangiogenic drugs have now entered trials, including the tyrosine kinase inhibitors pazopanib and cediranib. Pazopanib targets VEGF and platelet-derived growth factor (PDGF) receptors and c-Kit, and cediranib targets VEGFR1-3 (Markowska *et al.*, 2017). Both drugs have been shown to increase progression-free survival (PFS) in patients with recurrent OC when given in

combination with standard treatment, although toxic side effects have been noted (Pignata *et al.*, 2015; Ledermann *et al.*, 2016; Reinthaller, 2016; Dinkic *et al.*, 2017). In addition to these, the fusion protein trebananib has also shown success in phase III trials (Monk *et al.*, 2014). Trebananib works by binding to the angiogenic signalling proteins Ang1 and Ang2, which inhibits their ability to bind and activate the Tie2 receptor. This offers an alternative to VEGF-dependent pathway blockers, to which tumours often become unresponsive (Mitamura *et al.*, 2017). A recent meta-analysis has solidified the evidence that anti-angiogenic drugs can improve PFS in OC, with bevacizumab and trebananib also showing an improvement in overall survival (Yi *et al.*, 2017).

### 1.1.7.2 PARP inhibitors

For patients with germline *BRCA1* and *BRCA2* mutations, poly(ADP-ribose) polymerase (PARP) inhibitors have now entered routine clinical practice. The PARP family encompasses 17 proteins, of which PARP1 and PARP2 are known to be involved in DNA repair. In cell lines with competent DNA damage responses, DNA repair can be carried out by one of several pathways. The BRCA proteins are involved in promoting the homologous recombination (HR) pathway in response to double strand breaks (DSBs). HR can become defective in BRCA-mutated individuals, which increases cellular reliance on alternative, overlapping pathways, such as non-homologous end-joining and single strand break (SSB) repair, mediated by PARP. PARP inhibition therefore reduces the cell's ability to rely on redundancy, and leads to an accumulation of lethal DNA damage (Yap *et al.*, 2011).

Olaparib was the first PARP inhibitor to be approved by both the FDA and EMA in 2014 following data from two phase II clinical trials showing that olaparib maintenance therapy significantly prolonged PFS survival, compared with placebo, especially in patients with BRCA-mutated OC (Ledermann *et al.*, 2012, 2014). Olaparib is also under investigation for combination with chemotherapy. A phase II trial showed that adding olaparib maintenance treatment following carboplatin and paclitaxel therapy increased PFS (Oza, Cibula, *et al.*, 2015). The ongoing phase III SOLO3 trial also aims to assess the efficacy of olaparib as an alternative to chemotherapy in BRCA-mutated patients with recurrent OC who

have failed two or more lines of chemotherapy (NCT02282020) whilst SOLO1 assesses the efficacy of olaparib in first-line treatment in patients with germline *BRCA1/2* mutations.

The two other PARP inhibitors that have been well-studied in OC are niraparib and rucaparib. Both drugs are orally taken and inhibit PARP1 and PARP2, with rucaparib also inhibiting PARP3. Niraparib has shown increased PFS in platinum-sensitive OC regardless of BRCA status, although those with BRCA deficiency see a greater benefit (Mirza *et al.*, 2016). This study led to approval of niraparib for maintenance therapy in patients with recurrent OC with at least a partial response to platinum by both the FDA and EMA in 2017. The efficacy of rucaparib has been proven in the ARIEL trials (NCT01891344, NCT01968213, NCT02855944), these studies have shown that rucaparib treatment improves PFS when used as a maintenance therapy, with *BRCA*-mutated and homologous recombination deficient patients seeing the greatest benefit (Coleman *et al.*, 2017; Swisher *et al.*, 2017). These studies have also helped show how loss of heterozygosity may be used to identify patients with *BRCA* wild-type platinum-sensitive OCs who might benefit from rucaparib.

### **1.1.7.3 Immune Checkpoint Inhibitors**

Ovarian tumours can present several mechanisms of immune evasion (as discussed earlier), which makes immunotherapy a valid line of investigation. Although a recent meta-analysis on six different studies showed that immunotherapy gave no significant clinical benefit (Alipour *et al.*, 2016), certain subsets of immunotherapy, such as immune checkpoint inhibitors, are beginning to show promise (Gaillard, Secord and Monk, 2016).

Checkpoint proteins, such as cytotoxic T-lymphocyte associated protein 4 (CTLA-4) and programmed cell death protein 1 (PD-1), function to protect the body against autoimmune activity on “self” tissues by attenuating T cell function (Gaillard, Secord and Monk, 2016). These proteins are often upregulated in cancer, with PD-1 expression shown to be negatively correlated with clinical outcome in OC (Hamanishi *et al.*, 2007). PD-1 is a cell surface receptor that becomes active when bound to the corresponding ligands PD-L1 and PD-L2

Several antibodies specific for CTLA-4, PD-1 or its ligands are currently in early development for use against OC.

Many checkpoint inhibitors are already approved for use in other cancers, which provides evidence for their safety. The majority of these therapies target PD-1 (pembrolizumab, nivolumab) or its ligands (durvalumab, atezolizumab, avelumab), with ipilimumab available for inhibition of CTLA-4 (Gaillard, Secord and Monk, 2016). The earliest trial using checkpoint inhibitors in OC was performed in 2015 with nivolumab for patients with platinum-resistant OC (Hamanishi *et al.*, 2015). In this phase II study, out of 20 patients, 40% experienced adverse events, with 10% experiencing severe events. While overall response was modest at 15%, this trial still represents a promising start for these treatments. Similar results were seen in a phase Ib, non-randomized, multicohort study for pembrolizumab in PD-L1-positive tumours, with objective response rate of 11.5% (Varga *et al.*, 2015).

#### **1.1.7.4 Metformin**

The anti-diabetic drug metformin has recently gained some attention for its proposed actions against cancer stem cells in OC. A study by Dilokthornsakul *et al.* (2013) showed that metformin significantly decreased the incidence of OC in type 2 diabetic patients. Pre-clinical studies show a potential anti-tumour and anti-proliferative effect of metformin in OC cells (Cantrell *et al.*, 2010; Rattan *et al.*, 2011). Several phase Ib/II studies are now in progress in order to assess whether addition of metformin to standard carboplatin/paclitaxel therapy yields clinical benefit (NCT02312661, NCT02437812, NCT01579812, NCT02122185).

## **1.2 Oncolytic Virotherapy**

### **1.2.1 Introduction**

Oncolytic viruses (OVs) are replication competent viruses that are able to infect, replicate selectively within, and kill malignant cells, whilst leaving healthy cells unharmed (Russell, Peng and Bell, 2012). During infection, new, mature virions are produced that can go on to infect neighbouring cells. This propagation of the therapeutic effect makes OVs unique to other forms of cancer treatment (Figure

1.3). Viruses also offer many other benefits that make them desirable tools for cancer therapy, such as the ability to exhibit tropism for particular cell types, high genetic manipulability and ability to engage the immune system.

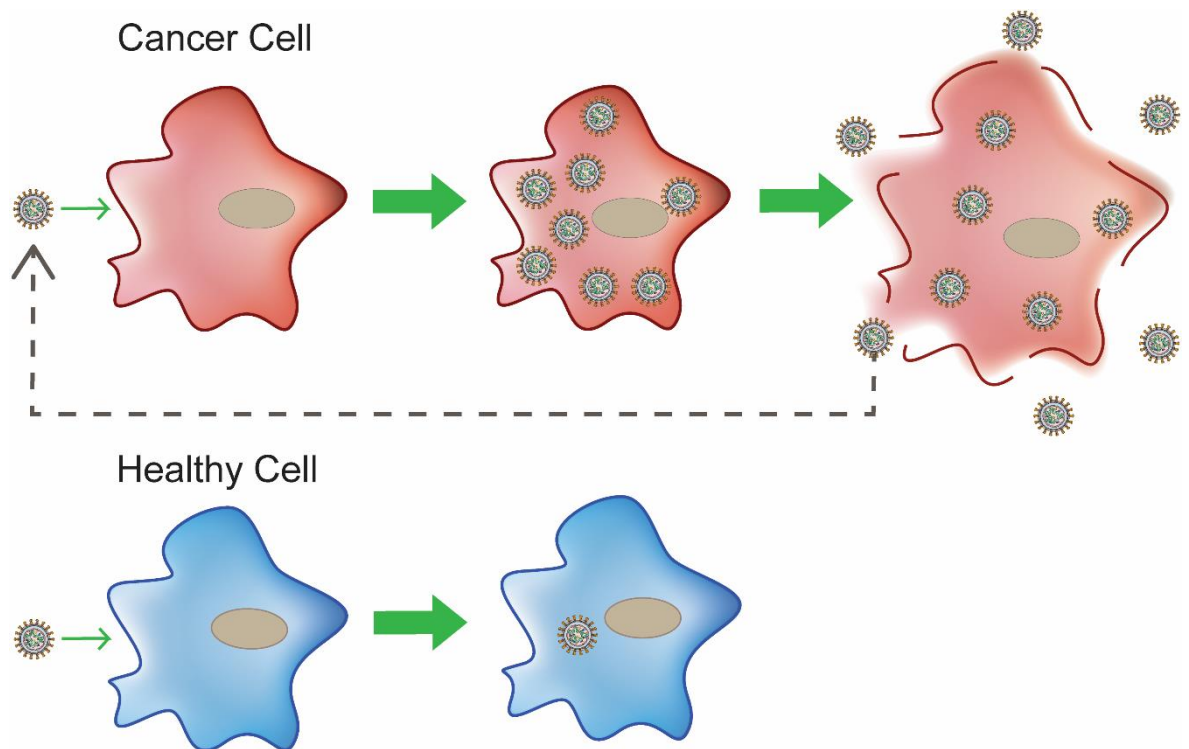


**Figure 1.3 Oncolytic virotherapy concept.** Oncolytic viruses (OVs) are replication competent viruses that can infect cancer cells selectively. Viruses may be able to infect healthy cells successfully, but productive infection will always be impaired. This property allows OVs to continue infecting nearby cancer cells, thereby propagating the therapeutic effect.

OVs exploit many viral properties that allow for targeting of appropriate cells. Some human viruses have natural tropism for tissues in which they normally cause disease, for example, human immunodeficiency virus (HIV), which naturally infects CD4<sup>+</sup> T-lymphocytes and can be used as a treatment for T-cell specific lymphoblastic leukaemias (Jeeninga *et al.*, 2005, 2006). Some viruses, including Newcastle disease virus (NDV), measles virus and reovirus, have a natural preference for replication within cancer cells, as many of the properties that promote successful tumorigenesis are also beneficial for viral replication. These include greater production of protein and replication of DNA, as well as cell cycle checkpoint abnormalities.

Viruses can be modified to infect cancerous tissues by making infection dependent on the presence of cancer-specific markers. Alteration of viral binding proteins represent one example of this, such as in measles virus where the haemagglutinin protein was modified, allowing it to bind epidermal growth factor receptor (EGFR) or insulin-like growth factor receptor (IGFR) (Schneider *et al.*, 2000). Viral replication can also be limited to certain tissues by placing viral genes under the control of tissue or cancer-specific promoters. This has been done with the adenovirus E1A protein, which was placed under control of the prostate-specific antigen (PSA) promoter, which meant that replication was only possible in prostate tumours (Y. Yang *et al.*, 2014). The same effect was achieved in HSV-1 by placing the essential viral gene ICP4 under translational control of the promoter for survivin, which is a commonly upregulated gene in glioma (Delwar *et al.*, 2016).

### **1.2.2 Oncolytic Viruses in Clinical Development**

There are currently three OV's that have gained clinical approval in various countries. The first of these was an unmodified strain of ECHO-7, known as Rigvir, which had been adapted to grow in melanoma cells. Rigvir was first approved for use in Latvia for melanoma therapy in 2004, and later approved for use in Georgia in 2015 and Armenia in 2016 (Chumakov *et al.*, 2012).

The second OV to be approved was H101, a strain of adenovirus that is deleted in the gene E1B55k. This virus has the same genetic make-up as dl1520 (ONYX-015), which was created independently. H101 has been approved in China for treatment of head and neck cancer since 2005 following a phase III randomized trial that showed intratumoral injection of H101 in combination with cisplatin plus 5-fluorouracil chemotherapy gave a significantly higher patient response rate than chemotherapy alone (Xia *et al.*, 2004; Garber, 2006). During normal infection, E1B-55k has many functions, including blocking p53 function; this has the effect of blocking apoptosis and enabling the continuation of cell cycling (Debbas and White, 1993). Removing this gene from adenovirus was initially thought prevent the virus from replicating in p53 wild-type cells, which were thus able to curtail infection (Harada and Berk, 1999; Nemunaitis *et al.*, 2000). However, it is now apparent that the tumour selectivity of viruses lacking E1B

55K stems from the loss of late viral RNA export that occurs in normal cells but remains intact in malignant cells (O'Shea *et al.*, 2004).

The third and most recently approved treatment is Talimogene Laherparepvec (T-VEC; also known as Imlygic, previously Oncovex<sup>GM-CSF</sup>). T-VEC is a multi-gene modified version of the JS-1 strain of HSV-1 that was approved by the US FDA in 2015 and by the EMA in 2016. T-VEC will be discussed in more detail later.

In addition to those viruses with full clinical approval, several other OV's have been granted orphan drug designation by the FDA (Table 1.1). These are agents that are granted special approval based on their potential to treat rare disorders. Reolysin is the T3D strain of reovirus, an RNA virus that naturally replicates preferentially in transformed cells (Hashiro, Loh and Yau, 1977; Duncan, Stanish and Cox, 1978), and is currently the only wild-type virus in late phase clinical development. A phase III trial in head and neck cancer comparing Reolysin plus carboplatin and paclitaxel chemotherapy with chemotherapy alone has recently been completed (NCT01166542). While final results are not yet available, preliminary results have shown significantly higher overall survival in the groups given Reolysin (Gong *et al.*, 2016).

**Table 1.1: Nationally approved and orphan drug designated oncolytic viruses**

Agent	Virus	Gene modification	Company	Disease	Status
<b>Oncolytic viruses granted full clinical approval:</b>					
T-VEC (Imlygic, talimogene laherparepvec)	Herpes Simplex Virus-1	$\gamma$ 34.5, $\alpha$ 47 deletion. GM-CSF insertion	Amgen	Inoperable stage IIIb to IV melanoma	Approved by the US FDA in 2015 and by the EMA in 2016
H101 (Oncorine)	Adenovirus	E1B-55k gene deletion	Shanghai Sunway Biotech	Head and neck cancer	Approved by the China SFDA in 2005
Rigvir	ECHO-7	None	RIGVIR	Melanoma	Approved in Latvia in 2004, Georgia in 2015 and Armenia in 2016
<b>Oncolytic viruses granted FDA orphan drug designation:</b>					
G207	Herpes simplex virus-1	$\gamma$ 34.5, UL39 deletion	Aettis, Inc.	Glioma	Designation since 2002
NTX-010	Seneca Valley Virus	None	Neotropix	Neuroendocrine tumours	Designation since 2008
DNX-2401	Adenovirus	Partial E1A deletion in Rb binding domain. RGD-4C insertion	DNatrix	Glioma	Designation since 2014
JX-594	Vaccinia Virus	Thymidine kinase deletion. GM-CSF insertion, LacZ insertion	Jennerex Biotherapeutics Inc.	Hepatocellular carcinoma	Designation since 2013
ONCOS-102	Adenovirus	$\Delta$ 24 deletion. GM-CSF insertion, serotype 3 AV knob protein replacement	Oncos therapeutics	Malignant mesothelioma, glioma and ovarian cancer	Designation since 2013
Reolysin	Reovirus	None	Oncolytics Biotech Inc.	Glioma, fallopian tube cancer, gastric cancer, ovarian cancer, pancreatic cancer	Designation since 2015

### 1.2.3 Oncolytic Viruses and Tumour Immunology

Although direct lysis of tumour cells by OV's does contribute to the overall anti-tumour effect, there is now substantial evidence that targeted infection of tumour cells with OV's has the potential to generate potent anti-tumour immune responses, both innate and adaptive. Virus-induced death has the benefit of combining the release and subsequent presentation of cellular damage-

associated molecular patterns (DAMPs) and tumour-associated antigens (TAAs) with virus-derived pathogen-associated molecular patterns (PAMPs). This provides the immune system with an array of potential antigens that can assist in mediating a sustained anti-tumour response (de Gruijl, Janssen and van Beusechem, 2015). The full effects of OV on the immune system are summarised in Figure 1.4.

As mentioned earlier, the immune cells that contribute to formation of the TME can be broadly categorised as either immunosuppressive or immunostimulatory. Suppressive phenotypes include Tregs, MDSCs, and M2-macrophages, while CD8<sup>+</sup> T cells, NK cells, DCs, and M1-macrophages all work to elicit an anti-tumour immune response. OVs can therefore mediate this switch in tumour microenvironment by inhibiting and depleting Treg cells and MDSCs, converting macrophage phenotypes, maturing DCs and recruiting NK and CD8<sup>+</sup> T cells. This can be achieved by the nature of OV replication, or by additional arming of OVs with immunostimulatory genes.

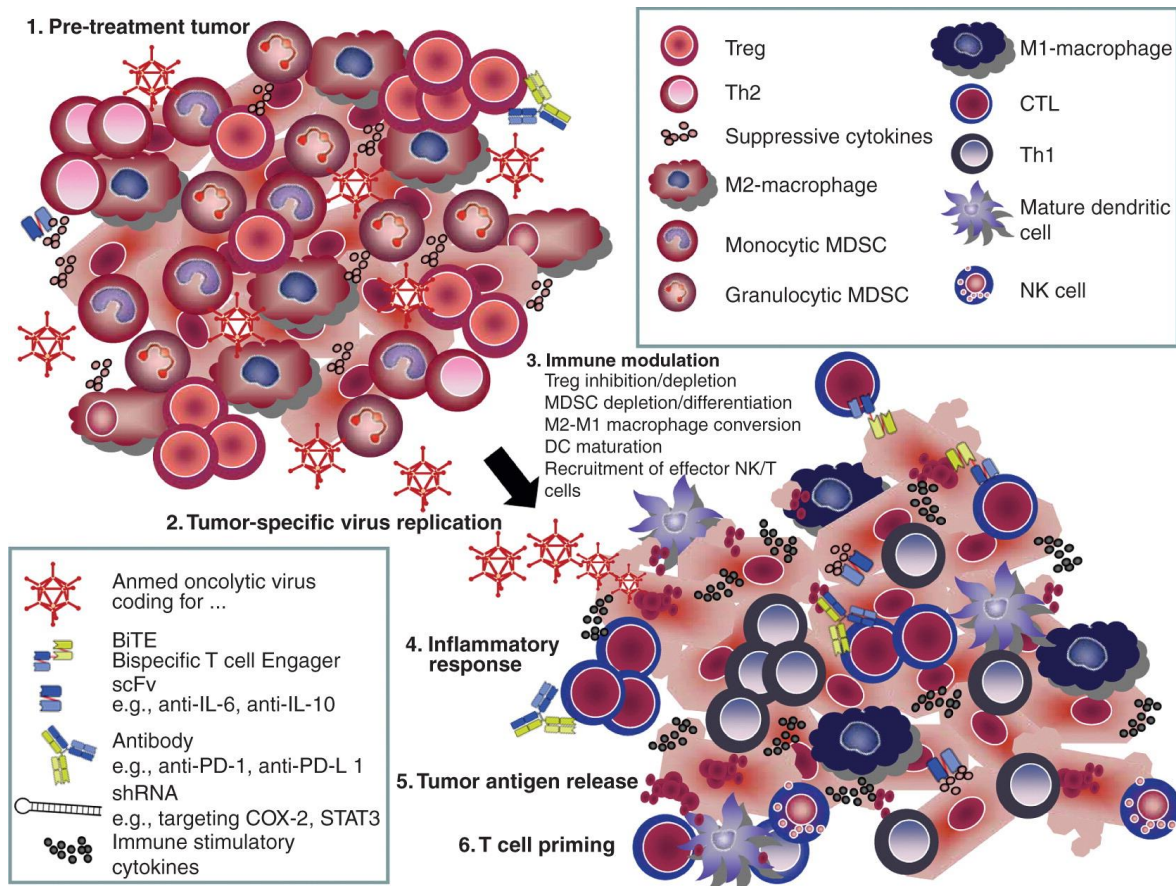


**Figure 1.4 Immune modulation of the tumour microenvironment by oncolytic viruses.** OV's have been consistently shown to be able to induce a beneficial modulation of the immune microenvironment. Beneficial modulations include inhibition or depletion of Tregs and MDSCs, conversion of TAMs from an M2 to M1 phenotype, promoting DC maturation and recruitment of effector NK and T cells. OV's can be armed to enhance this modulation with various anti-tumour and proinflammatory molecules such as antibodies, cytokines or BiTEs. Figure taken from *Expert Opinion on Biological Therapy* 2015 **15** 959-971.

Numerous beneficial TME changes have been demonstrated with various OV's. NDV was shown to lead to an infiltration of CD8<sup>+</sup> and CD4<sup>+</sup> effector cells in a murine model of B16 melanoma when injected intratumorally (Zamarin *et al.*, 2014). This effect was extended to distant tumour sites with the addition of CTLA-4 blockade. Mice were also significantly more protected against subsequent tumour challenge. Analysis of tumours from nude (T-cell defective) mice after incubation with The Coxsackie virus strain B3 (CVB3) showed accumulation of macrophages, DCs, granulocytes and NK cells, which are important for the outcome of the treatment (Miyamoto *et al.*, 2012). HSV-1 enhanced systemic tumour immunity for squamous cell carcinoma (Meshii *et al.*, 2013).

OVs can be armed with various anti-tumour cytokines in order to help guide the immune response. For instance, Ad5 strains expressing IFN- $\alpha$  showed increased tumour growth suppression and increases in survival in a hamster model of pancreatic cancer (LaRocca *et al.*, 2015). Addition of GM-CSF is a commonly-used method of TME modulation. In addition to the previously mentioned T-VEC, strains of VV and MV containing a GM-CSF transgene have also shown enhanced killing over non-GM-CSF variants as well as an increase in neutrophil and macrophage (VV only) infiltration (Grote, Cattaneo and Fielding, 2003; Parviainen *et al.*, 2015). Other examples of useful cytokines include IL-2, IL-12 and IL-18, whose inclusion within a number of oHSV vectors leads to increases in both anti-tumour efficacy and CD8<sup>+</sup> T cell infiltration and activation (Carew *et al.*, 2001; Fukuhara *et al.*, 2005; Derubertis *et al.*, 2007).

One hallmark of an immunosuppressive TME is the dampening of major histocompatibility complex (MHC) class I and II presentation of TAAs by both tumour cells and relevant antigen presenting cells (APCs). Several OVs, including VV, reovirus and MV have displayed an ability to promote DC maturation and subsequent presentation of antigens (Greiner *et al.*, 2006; Gujar *et al.*, 2010; Guillerme *et al.*, 2013). This process occurred in combination with a release of IFN- $\alpha$  in the case of MV and reovirus, as well as an additional release of IL-1 $\beta$ , IL-6, IL-12p40/70, IL-17, CD30L, CCL11, GM-CSF, KC, MCP-1, MCP-5, M-CSF, MIG, MIP-1 $\alpha$ , CCL5, TNF- $\alpha$ , VCAM-1, VSGF, CXCL-16, AXL, and MCP-2 for reovirus.

OVs are also useful in that they can utilise the bystander effect to kill cells not directly infected by them. One interesting example of this is via the use of bispecific T cell engagers (BiTEs). BiTEs consist of two linked single-chain variable antibody fragments (scFvs). The fragments have specificity for both the T cell receptor-signalling complex CD3 and a particular TAA (Iwahori *et al.*, 2015). This has the effect of linking T cells with tumour cells and mediating their tumour-specific activation. BiTEs can be expressed by OVs within tumours to accelerate the therapeutic effect (Scott *et al.*, 2018). Another proposed benefit of arming OVs with BiTEs is that BiTEs may act as immunological “decoys”, by redirecting the immune response away from virus infected cells thereby preventing premature clearance of virus. The first virus to be armed with a BiTE was a double-*tk*-deleted strain of VV, which was equipped with a BiTE targeting

EphA2 (Yu *et al.*, 2014). Other examples include an EGFR-targeting BiTE-expressing adenovirus (Fajardo *et al.*, 2017) and measles viruses (MV) encoding CEA- and CD20-targeting BiTEs (Speck *et al.*, 2018).

#### **1.2.4 Oncolytic Viruses and Clinical Ovarian Cancer Studies**

There have been numerous studies investigating the effect of various OV in ovarian cancer (Hartkopf *et al.*, 2011; S. Li *et al.*, 2012). In terms of clinical trials, there are three ongoing phase I/II studies for the use of MV. Two of these are exploring MV which possesses a gene encoding thyroidal sodium iodide symporter (NIS; NCT02364713 and NCT02068794), while one is investigating the addition of carcinoembryonic antigen (CEA; NCT00408590). No results are available yet for these studies. Other studies with VV strains have been started. One trial investigating the TK-deleted, GM-CSF-expressing strain JX-549 was withdrawn before completion (NCT02017678). Other phase I/II trials with GL-ONC1 - a strain possessing TK and haemagglutinin modifications, and p53MVA - a strain possessing a p53 insertion are both being investigated in patients with recurrent ovarian cancer (NCT02759588 and NCT02275039). In this case, the wild-type p53 expressed by p53MVA acts to elicit an immune response specific to cells expressing high levels of aberrant p53 (Song *et al.*, 2007, 2011).

Several adenovirus-based vectors are also in early clinical development.

Enadenotucirev is a chimera consisting of Ad11p/Ad3 strains being investigated in patients with recurrent platinum-resistant OC (NCT02028117).

Ad5.SSTR/TK.RGD is a virus possessing a TK insertion, which acts as a suicide gene, priming it for co-treatment with the drug ganciclovir (Kim *et al.*, 2012). A phase I study for this virus in a range of gynaecological cancers demonstrated its safety and efficacy (NCT00964756). In addition to this, disease was stabilised in several patients. Trials testing various replication-defective adenoviruses expressing wild-type p53 have been performed with little success (G.-X. Chen *et al.*, 2014). In these instances, viruses are designed more to act as gene-delivery vectors, aiming to restore p53 function to tumours. Ad5Delta24RGD contains both an *E1A* deletion and an addition of an integrin binding RGD-4C motif into the HI loop which enables it to bind integrins  $\alpha$ 8 $\beta$ 3 and  $\alpha$ 5 $\beta$ 1, thereby enhancing

its infectivity (Bauerschmitz *et al.*, 2002). This virus has undergone phase I testing for OC and shown to be well tolerated (NCT00562003).

Finally, there is one current phase II study assessing reovirus in combination with paclitaxel in patients with recurrent or persistent ovarian epithelial, fallopian tube, or primary peritoneal cancer (NCT01199263).

## **1.3 Herpes Simplex Virus 1**

### **1.3.1 Introduction and History**

Descriptions of genital lesions resembling herpes have been found as early as 3000 B.C. It was Hippocrates, however, who first used the Greek word *herpes* to describe certain bodily lesions. Literally meaning to “creep and crawl”, this word may well have been used to describe lesions that had resulted from numerous viral and non-viral sources. This trend continued throughout most of early history. It was Emile Vidal, in 1893, who was the first to recognise that genital herpes was infectious in nature. This discovery coincided with the discovery of viruses by Dimitri Ivanovski, who identified tobacco mosaic virus as a filterable infectious agent, far smaller than bacteria.

By 1913, Wilhelm Grüter had shown that herpes could be transmitted from human to rabbit and back again, forming the basis of the Grüter test, which became standard practice for diagnosis. For this, Grüter is widely sourced as the first to isolate HSV. Other milestones during the 20<sup>th</sup> century include the discovery that HSV travels through neurons by Ernest Goodpasture in 1925, the establishment of the theory of latency by Frank MacFarlane Burnet in 1939, and development of the first antiviral drug, acyclovir, in 1978.

Herpes viruses are now classified under the viral family *Herpesviridae*. There are nine herpesviruses that are known to infect humans, each having a “human-herpesvirus” designation 1-9 (Table 1.2). HSV-1 (HHV-1) occupies the subfamily known as *alphaherpesviridae*, along with HSV-2 and VZV (Davison *et al.*, 2009). A list of all currently known human herpes virus species can be found in Table 1.2 below.

**Table 1.2: Human herpes virus species**

Human Herpesvirus Number	Other Name	Subfamily	Major Associated Diseases
HHV-1	Herpes simplex virus-1 (HSV-1)	Alpha	Cold sores, genital warts
HHV-2	Herpes simplex virus-2 (HSV-2)	Alpha	Genital warts, cold sores
HHV-3	Varicella-Zoster Virus (VZV)	Alpha	Chicken pox, shingles
HHV-4	Epstein-Barr Virus (EBV)	Gamma	Infectious mononucleosis
HHV-5	Human Cytomegalovirus (HCMV)	Beta	Infectious mononucleosis, pneumonia
HHV-6A	Human Herpes Virus-6A	Beta	Linked to CNS disorders
HHV-6B	Human Herpes Virus-6B	Beta	Exanthema subitum
HHV-7	Human Herpes Virus-7	Beta	Exanthema subitum, acute febrile respiratory disease
HHV-8	Kaposi's Sarcoma-associated Virus (KSHV)	Gamma	Kaposi's Sarcoma and Multicentric Castleman's disease

Symptoms of HSV-1 infection consist of watery blisters forming on the skin or mucous membranes of the mouth or genitals, often preceded by a tingly or itchy sensation; lesions heal with a characteristic herpetic scab. These symptoms often go by the common names of 'cold sores', 'genital herpes', 'herpes' or 'genital warts'. Disease progression of herpes can be complicated by the latency stage of the virus life cycle. HSV-1 and HSV-2 often lie dormant, primarily in the ganglia of the trigeminal nerve in the face and in the sacral nerve in the pelvis. Sporadic re-emergence of the virus leads to 'outbreaks' and allows the virus to shed. HSV infection can be dangerous for immunocompromised people, such as those with AIDS or those undergoing chemotherapy. Rarely, HSV-1 infection can lead to severe disease such as encephalitis or keratitis.

### 1.3.2 Viral Structure

All Herpesviruses consist structurally of four main components: a core; capsid; tegument; and envelope (Figure 1.5). The core is a tightly-wound toroid structure of linear double-stranded DNA, which serves as the virus's genome. The capsid is an icosahedral protein structure surrounding the core, with a T=16 symmetry, consisting of 162 capsomeres. The envelope is a lipid bi-layer which

surrounds the capsid and contains several key proteins embedded within it, many of which act to mediate viral cell entry.

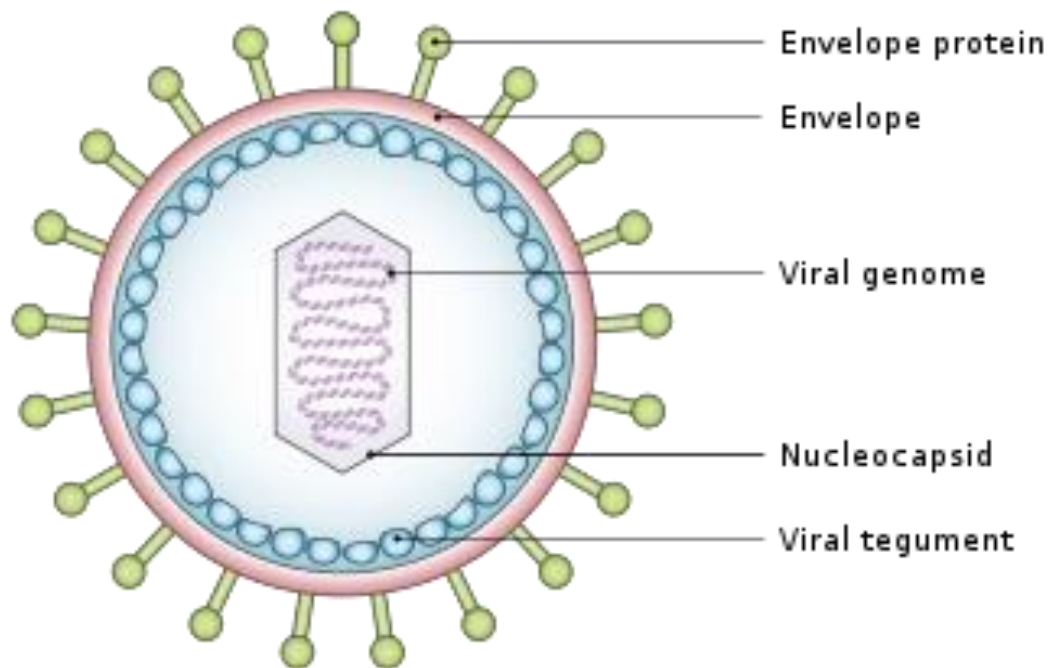


**Figure 1.5 Simplified structure of Herpesvirus virion.** All herpesvirus species consist of a double-stranded DNA genome, complexed within an icosahedral protein capsid. The viral tegument is a component that is unique to herpesviruses and exists as a layer between the capsid and the envelope. The tegument contains many proteins that assist in early entry processes within the life-cycle. The envelope contains many embedded glycoproteins that mainly assist in mediating viral entry.

Between the envelope and the capsid exists a semi-structured, proteinaceous layer called the tegument. So far, over 20 tegument proteins have been identified, with various roles mediating viral entry, replication and assembly. The largest tegument protein is VP1/2, which plays a key role in mediating capsid transport along microtubules (Sandbaumhüter *et al.*, 2013). Another tegument protein, VP16, is key in inducing transcription of immediate-early viral genes, and is proposed to act as a central tegument organisation protein (Vittone *et al.*, 2005). Viral particles tend to vary between 155 and 240 nm in diameter, with the capsid itself being 125 nm in diameter (Zhou *et al.*, 2000).

### 1.3.3 Viral Genome Organisation

The full genome sequence of HSV-1 strain 17 was first completed in 1988, which found the length to be 152,260 bp with a G+C content of 68.3% (McGeoch *et al.*,

1988). The current official length, last updated in 2016, stands at 152,222 bp (GenBank sequence accession number NC\_001806). The HSV genome consists of two covalently-linked sections, known as the long (L) and short (S) regions. Each of these regions consists primarily of a central unique portion ( $U_L$  and  $U_S$  respectively) that is flanked by inverted repeats. These repeats are labelled “a-c”, and arranged in a way so that  $ab$  and  $b'a'$  flank  $U_L$  and  $a'c'$  and  $ca$  flank  $U_S$  (Sheldrick and Berthelot, 1975; Wadsworth, Jacob and Roizman, 1975). The number of  $a$  repeats can vary between strains, as well as the number of repeated sub-sequences within each  $a$ , making the full genome length variable. The L and S sections of the genome can be found inverted relative to one another and therefore be found in four different configurations. Each configuration is found in roughly equimolar concentrations in any typical unit-length DNA population in wild-type virus-infected cells (Hayward *et al.*, 1975).

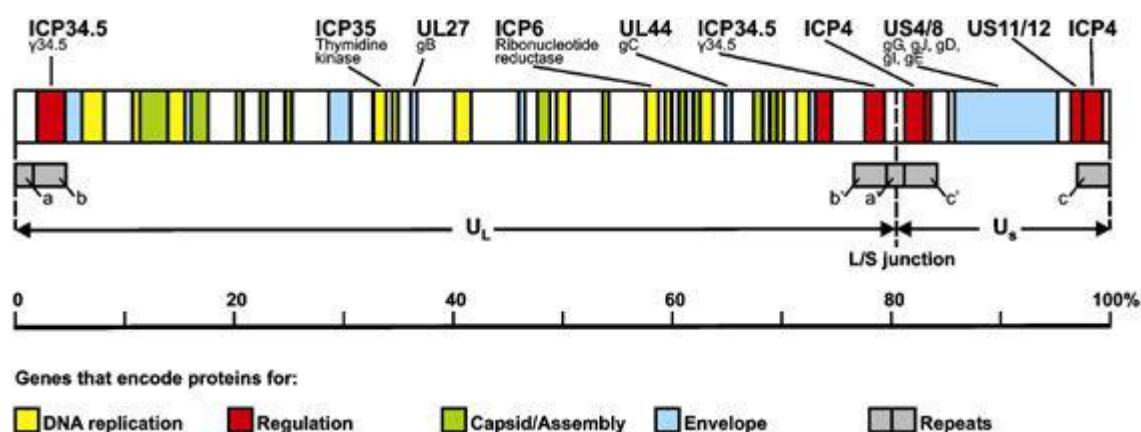


**Figure 1.6 Map of the HSV-1 genome.** Schematic representation identifies the key components of the HSV-1 genome. The genome consists of two main segments, L and S, which each contain repeat ( $R_L$ ,  $R_S$ ) and unique ( $U_L$ ,  $U_S$ ) regions. Genes are colour-coded by function, with the locations of some key genes shown above. Image taken from *Gene Therapy* 12, S170–S177 (2005).

There are currently >90 unique transcriptional units identified within the HSV-1 genome, with at least 80 of these coding for protein, and the vast majority of those coding for only a single protein. Therefore, the density of genes is roughly one gene per 1.5-2 kb of HSV DNA (McGeoch, Rixon and Davison, 2006). Genes are categorised broadly into either immediate early ( $\alpha$ ), early ( $\beta$ ) or late ( $\gamma$ ) genes (Honest and Roizman, 1975). The immediate early genes are typically involved in regulating expression of the early and late genes; early genes are responsible for regulating nucleotide metabolism, DNA synthesis and some surface glycoproteins; and late genes are almost entirely involved in producing

structural components of the virion. The genes *a0* and *a4* are found within the inverted repeat regions and so are present in two copies.  $\beta$  and  $\gamma$  genes are almost entirely within the unique regions, with the exceptions of *y34.5* and *ORF P*. Most genes have their own promoter, and introns occur in only a minority of genes. As an alphaherpesvirus, HSV-1 has a lower proportion of intron-containing genes than viruses of other subfamilies. A schematic overview of the structure of the HSV-1 genome is shown in Figure 1.6.

While the majority of the HSV-1 genome contains sequences relating to protein-coding genes, there are several important regions which code for RNAs that have roles outside of protein translation. The most recognised of these are known as the latency-associated transcripts (LATs) (Phelan, Barrozo and Bloom, 2017). LATs are long RNA fragments that have been strongly associated with inducing and maintaining the latency stage of HSV infection. However, their exact mechanisms are still under debate. Within the LAT region, several microRNA (miRNA) molecules have been identified, some of which have been shown to be important in the regulation of viral and host gene expression (Umbach *et al.*, 2008; Jurak *et al.*, 2010; Kramer *et al.*, 2011).

### **1.3.4 Viral Life Cycle**

#### **1.3.4.1 Cell Entry**

HSV-1 mediates cell entry via a series of direct interactions between envelope-embedded proteins within the virion and extracellular membrane proteins. These interactions work to mediate fusion of the viral envelope with the cell membrane in order to create a channel through which the viral tegument proteins and capsid can enter the cytoplasm. Three viral envelope glycoproteins are essential for cellular entry, which are called gD, gB and the heterodimer gHgL (Turner *et al.*, 1998). In addition to this, gC has been shown to contribute to cell entry but is not essential. The cellular membrane proteins that are responsible for permitting HSV-1 entry are 3-O sulphated heparan sulphate (3-O HS), herpesvirus entry mediator (HVEM) and nectin-1/2.

The entry process is initiated when gC and/or gB encounter heparan sulphate proteoglycans (HSPGs), which are most densely found on filopodia. If gC is not

present, then overall binding efficacy is reduced, but still functional. This initial process serves to hold the virion in place, allowing fusion to follow. Fusion can occur either on the exterior of the membrane or once the virion has been internalised within an endosome, with the likelihood of each dependent on cell type (Clement *et al.*, 2006). The fusion process is initiated by gD binding to the receptors above with gB and gHgL acting as fusogens to mediate the fusion of the viral and cellular membranes. On a molecular level, binding of gD to a receptor causes a conformational change in gD, which in turn alters the conformation of the gHgL complex, increasing its affinity for gB (Atanasiu *et al.*, 2007). The protein gB contains a spike region, which consists of a trimer of peptides, each possessing a movable arm region and a lipophilic fusion loop. The fusion loops are initially kept away from the outside of the virion by hydrogen bonds. When the affinity of gHgL for gB is increased, these hydrogen bonds are broken, allowing the arms to move and insert the fusion loops into the membrane of the cell (Clarke, 2015). Once the arms of gB are inserted, the membranes fuse, which allows the tegument proteins and capsid to enter the cell.

#### **1.3.4.2 Nuclear Trafficking**

Immediately after entry, the viral capsid becomes associated with a microtubule (MT)-dependent, minus end-directed motor, dynein (Sodeik, Ebersold and Helenius, 1997). This is the same process that HSV utilises in neurons, which allows it to travel impressive distances in both directions. The prevailing theory states that proteins of the outer tegument become detached from the capsid in order for it to bind microtubules, requiring the inner tegument to remain in place (Radtke *et al.*, 2010). Once the capsid reaches the centre of the cell, it docks with the nuclear pore complex (NPC) in a specific orientation, with one of its penton vertices facing towards the nuclear pore (Ojala *et al.*, 2000). Docking involves binding of capsid proteins to the NPC protein Nup358 and possibly Nup214 in a manner that is dependent on importin- $\beta$  (Copeland, Newcomb and Brown, 2009).

Uncoating of the viral DNA occurs through the capsid portal, which is formed by 12 copies of tegument protein UL6, allowing the DNA to travel through the

nuclear pore and into the nucleus (Newcomb *et al.*, 2001). The exact mechanism of this process is unclear, but it is thought that DNA is propelled through the NPC by pressure forces within the capsid (Liashkovich *et al.*, 2011). It also seems that uncoating is somewhat dependent on cleavage of the viral protein VP1/2 and an interaction between UL25 and Nup214 (Rode *et al.*, 2011).

#### **1.3.4.3 Replication**

Transcription, translation, replication and assembly all take place within the nucleus - during which, several large-scale structural changes take place. These include disruption of nucleolus, chromatin condensation and destruction of the nuclear lamina (Simpson-Holley *et al.*, 2005). Cellular processes become inhibited such as transcription (Jenkins and Spencer, 2001), splicing (Hardy and Sandri-Goldin, 1994), protein synthesis (Matis and Kúdelová, 2001) and cellular immune responses (Neumann *et al.*, 1997).

Immediate early genes are the first to be transcribed using the host RNA-polymerase II. This process requires the tegument protein VP16, which forms a complex along with the cellular Oct-1, HCF-1, LSD1, and the CLOCK histone acetyl transferase (Roizman, Zhou and Du, 2011). This complex works by selectively demethylating histones present in the  $\alpha$  region of the HSV genome, with similar processes taking place for the subsequent  $\beta$  and  $\gamma$  genes. The immediate early genes are: ICP0, ICP4, ICP22, ICP27, ICP47, and US1.5. Many of these have roles in transcribing the early and late genes, and some are involved in controlling cellular processes. ICP0 acts as a ubiquitin-ligase, and can tag cellular proteins for destruction such as interferon-inducible protein 16 (IFI16), which helps the virus evade the immune response (Orzalli, DeLuca and Knipe, 2012).

The  $\beta$  gene proteins are involved in viral genome replication, regulation of nucleotide metabolism, suppression of early  $\alpha$  genes, and activation of late  $\gamma$  gene. Examples of these include UL30, which acts as the viral DNA polymerase; UL23, a thymidine kinase which catalyses the formation of the nucleotide thymine; and US3, which is a multifunctional ser/thr kinase found to have roles

in apoptosis suppression, nuclear membrane rearrangement and capsid egress (Leopardi, Van Sant and Roizman, 1997; Mou, Wills and Baines, 2009).

After  $\beta$  genes become translated, replication of the viral genome can begin. There are two origin of replication sites within  $U_S$  (*oriS*) and one within  $U_L$  (*oriL*), where replication is initiated by ICP8 and UL9. ICP8 binds to free ssDNA, while UL9 unwinds it further. Following this, the proteins UL5, UL8 and UL52 bind and initiate their helicase-primase activities. UL30, the polymerase, copies the genome with help from a processivity factor, UL42. Some cellular replication proteins such as DNA ligase and topoisomerase II are also involved in the process, as well as the cellular chaperone protein heat-shock protein (HSP)90 (Weller and Coen, 2012). The viral proteins that are responsible for nucleotide metabolism are: thymidine kinase (UL23), ribonucleotide reductase (RR; UL39, UL40), deoxyuridine triphosphatase (UL50), uracil N-glycosylase (UL2), and alkaline nuclease (UL12). These proteins are important for viral DNA synthesis and repair because of viral inhibition of the corresponding cellular isoforms (Weller and Coen, 2012).

Genome replication involves first forming concatemeric DNA, which is subsequently divided into individual genomes. This was initially thought to be due to a simple rolling circle mechanism of replication, but more recent evidence suggests that this may not be possible. Numerous studies have shown that cellular DNA recombination mechanisms are highly active during HSV replication (Dutch, Bianchi and Lehman, 1995; Fu, Wang and Zhang, 2002) and may be a necessary part of replication and concatemerisation.

#### **1.3.4.4 Assembly and Egress**

Once replication has started, levels of  $\gamma$  genes begin to increase. These genes primarily code for structural proteins, such as the capsid proteins (UL38, UL35, UL18, UL19) and envelope glycoproteins (UL1, UL10, UL22, UL27, UL44, UL49A, UL53, US4, US6, US7, US8). In addition to these, there are also an array of tegument proteins and regulators of cellular function that are expressed within this group. One of the best-characterised is ICP34.5, which is coded for by the

gene *RL1*. ICP34.5 is a key protein involved in the inhibition of the cellular immune response and will be discussed in greater detail later.

Once the capsid proteins have been expressed, they begin to assemble into fully-formed capsids, entirely within the nucleus. Genomes are cleaved from their concatemers and packaged into the assembled capsids. From here, capsids travel across the nuclear membrane in a mechanism that is dependent on UL36 and UL37 (Sandbaumhüter *et al.*, 2013). The dual envelopment model suggests that virions first bud into the perinuclear space, which leads to the formation of a temporary envelope. Capsids then lose this primary envelope as they travel across the outer nuclear membrane into the cytoplasm. Tegument proteins and final envelopes are acquired by the budding of capsids into specialised vesicles which are thought to be produced by the Golgi or trans-Golgi network. This results in a double-enveloped capsid, with the inner membrane decorated with envelope proteins. The virion is then exocytosed by fusion of the outer membrane with the plasma membrane, leaving an external single-membraned particle (Owen, Crump and Graham, 2015).

A summary of all the major events during the HSV-1 life cycle is shown in Figure 1.7.

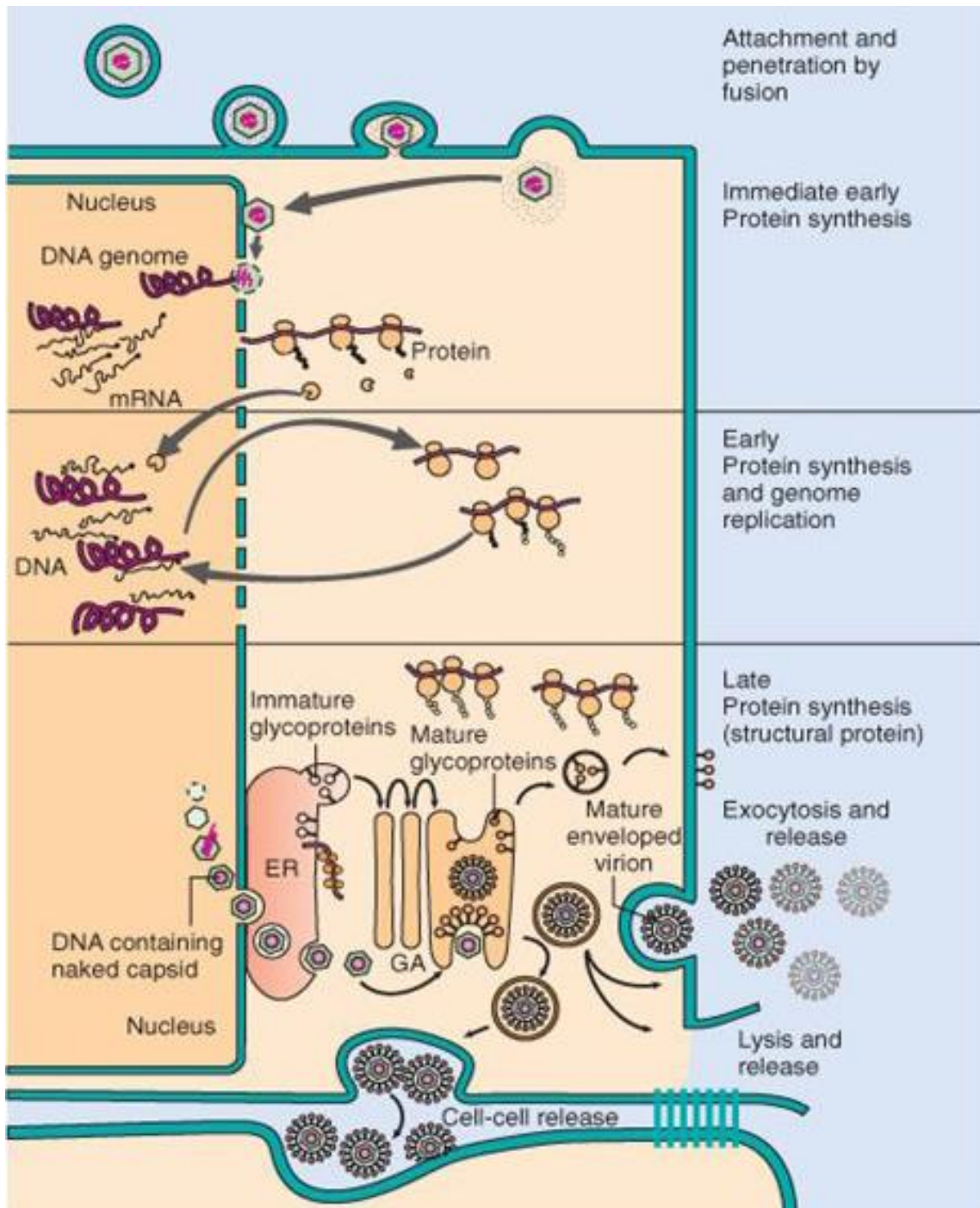


**Figure 1.7 Life cycle of HSV-1.** The life cycle of HSV-1 begins with attachment and fusion at the surface mediated by several HSV envelope glycoproteins. The virion uncoats, and the capsid is shuttled to the nucleus along microtubules. DNA is shuttled into the nucleus via nuclear pores and proteins are translated beginning with the immediate early, followed by early and then late genes. Capsid assembly occurs in the nucleus, with the capsid then traversing the nuclear membrane before becoming enveloped by the Golgi and packaged with tegument and envelope proteins. Virions are either exocytosed or released passively upon lysis. Image taken from *Elsevier. Murray: Medical Microbiology 7<sup>th</sup> Edition*.

### 1.3.4.5 Latency

Latent infection occurs when the virus enters a sensory neuron. It is currently thought that the architecture of these cells prevents the virus from entering a

lytic cycle. Selective application of virus to the distal portion of a neuron leads to a lower rate of lytic infection than when virus is added to the ganglion component (Hafezi *et al.*, 2012). This suggests that the greater distance the capsid must travel during neuronal infection affects its capability to infect lytically. This may be due to an inefficiency in transporting tegument proteins such as VP16 (Luxton *et al.*, 2005), which prevents  $\alpha$  genes from being transcribed due to histone-mediated epigenetic suppression (Lee, Raja and Knipe, 2016).

During latency, the viral genome resides within the nucleus of the neuronal cell, where it becomes organised into nucleosomes (Deshmane and Fraser, 1989). Most of the genome is transcriptionally repressed with the exception of the LAT, which suppresses lytic infection - although the exact mechanisms are still unclear (Phelan, Barrozo and Bloom, 2017). Physiological mechanisms can lead to cellular stress, which re-animates the virus from latency. Viral particles can travel back down the axon microtubules to the distal regions of the nerve and go on to shed and infect new cells and hosts.

## **1.4 Herpes Simplex Virus 1 as an Oncolytic Agent**

### **1.4.1 Introduction**

HSV-1 has become a popular agent for use as an oncolytic virus. Despite the pathogenicity of the wild type virus, many modified HSV-1 strains have now been developed that show high tumour selectivity and overall safety. HSV-1 has several characteristics that make it a desirable choice for cancer therapy. First, HSV-1 infects almost all cell types, due to the ubiquity of the receptors it uses for cell entry (Karasneh and Shukla, 2011). The virus has also been shown to have a natural preference for tumour cells due to the changes in receptor accessibility that occur during tumorigenesis. For instance, the entry mediator nectin-1 is not accessible in most normal cell types due to its presence as a component of the adherens junction complex, but becomes more accessible in cancer cells with decreased intracellular adherence (Yoon and Spear, 2002; Yu *et al.*, 2007).

HSV-1 also has a large genome, which includes several redundant genes, making modifications and insertions simple. The current standard method for making modifications to HSV-1 involves construction of a bacterial artificial chromosome (BAC) containing the entire genome, which can be amplified in *E.coli* and modified using standard molecular biology techniques (Bailer *et al.*, 2017). Constructing a BAC can be laborious; however, once one has been made for a virus of choice, the work need not be repeated. However, methods of mutation can also be inefficient and inaccurate. One method that may offer several advantages over BACs is CRISPR/Cas9. The Cas9 nuclease can induce targeted DNA double-strand breaks, guided by a user-defined ~20 bp guide RNA (gRNA) (Sander and Joung, 2014). This enables precise induction of mutations, usually small insertions/deletions (indels) that result in a frameshift premature stop codon. Alternatively, mutations can be substituted by providing a donor strand encoding a specific mis-sense mutation for the cell to repair with using HR. There are now a few examples of this technology being utilised for HSV and other large viruses (Bi *et al.*, 2014; Suenaga *et al.*, 2014; Lin *et al.*, 2016). CRISPR offers a much faster, less laborious and more precise method for inducing mutations than BAC-based methods and may soon become the standard of practice for certain types of modification. BACs still provide some advantages, as they can be combined with helper cell lines or viruses to produce non-replicating viruses (Bailer *et al.*, 2017). They may also be more efficient for large-scale gene insertions or deletions. A comparison summary of the two techniques is shown in Figure 1.8.

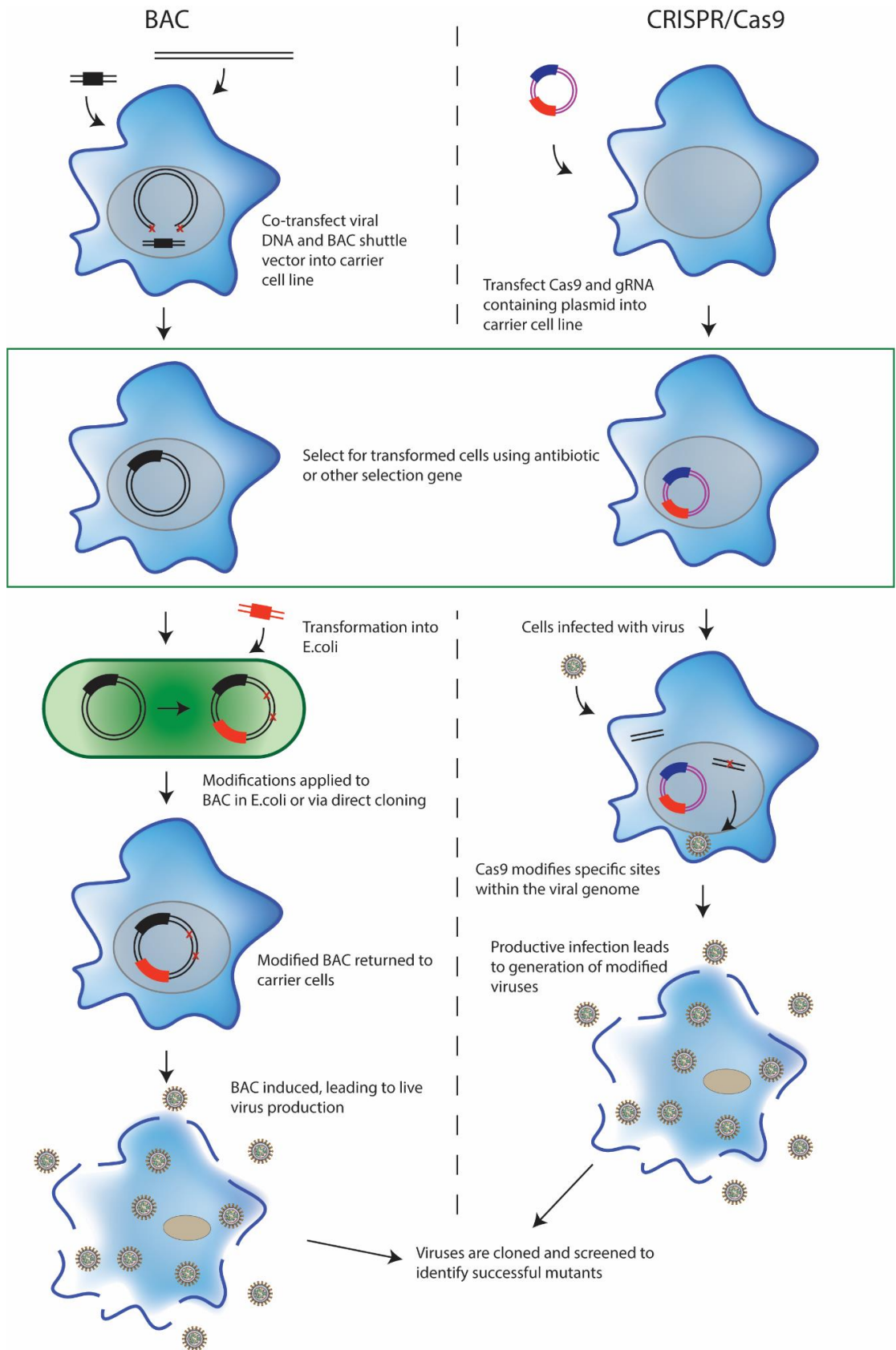


**Figure 1.8 Comparison of BAC and CRISPR methods for modification of large viruses.** BAC shuttle vectors allow for the circularisation of the viral genome. Cells bearing BACs must be selected for before isolating the BACs and inserting them into *E.coli* for amplification and applying modifications through homologous recombination or other molecular techniques. Viral production is subsequently induced in mammalian cells. CRISPR offers a simpler method for modification, requiring only a single transfection of cells

with a CRISPR plasmid, cells are selected for and infected with virus. The genomes of the incoming viruses are then selectively modified.

One other benefit of HSV-based oncolytics is the added safety that comes from having readily-available antiviral compounds such as acyclovir, in case of unexpected negative side-effects (De Clercq, 2004).

### 1.4.2 HSV-1716

Herpes simplex virus-1716 (HSV-1716) is an engineered variant of HSV-1, made by modification to the Glasgow strain 17+. HSV-1716 is rendered oncolytic due to a 759 base pair deletion in both copies of the *RL1* gene, which encodes ICP34.5 (MacLean *et al.*, 1991) (Figure 1.9). These *RL1*-deleted HSV variants represented the first generation of oncolytic HSV viruses.

Tumour selectivity of HSV-1716 was initially thought to be determined by interaction with the host immune protein kinase R (PKR) pathway. PKR recognises cellular double-stranded RNA (a by-product of viral infection) and in response, phosphorylates the alpha subunit of eukaryotic initiation factor 2 $\alpha$  (eIF-2 $\alpha$ ), inactivating it. This modification has the consequence of preventing protein translation within the cell, which includes translation of viral proteins, thereby protecting the host from further infection. ICP34.5 serves as one of HSV-1's tools for disarming this pathway, binding to and activating both protein phosphatase 1 $\alpha$  (PP1 $\alpha$ ) and eIF-2 $\alpha$  via the GADD34 homology domain. This bridges the two proteins, facilitating the reversion of the eIF-2 $\alpha$  phosphorylation and allows translation of viral mRNA (He, Gross and Roizman, 1997; Li *et al.*, 2011). HSV-1 strains deficient in ICP34.5 therefore have impaired replication in non-malignant cell types due to successful inhibition of protein translation by the cell. However, in Ras-transformed cells, PKR pathway activity has been shown to be inhibited (Mundschau and Faller, 1994), which presents one way in which replication of *RL1*-deleted HSV-1 progresses unimpeded in some tumour types. In addition, ICP34.5 binds to Beclin 1 in order to inhibit autophagy (Leib *et al.*, 2009; Gobeil and Leib, 2012), a process that is often dampened in malignant cells and may contribute to tumorigenesis (Kroemer, Mariño and Levine, 2010). Other mechanisms for ICP34.5 involving PI3K signalling (Sarinella *et al.*, 2006) and control of TANK-binding kinase 1-mediated signalling, which

mediates IRF3 phosphorylation and antiviral genes (Verpooten *et al.*, 2009) have been identified.

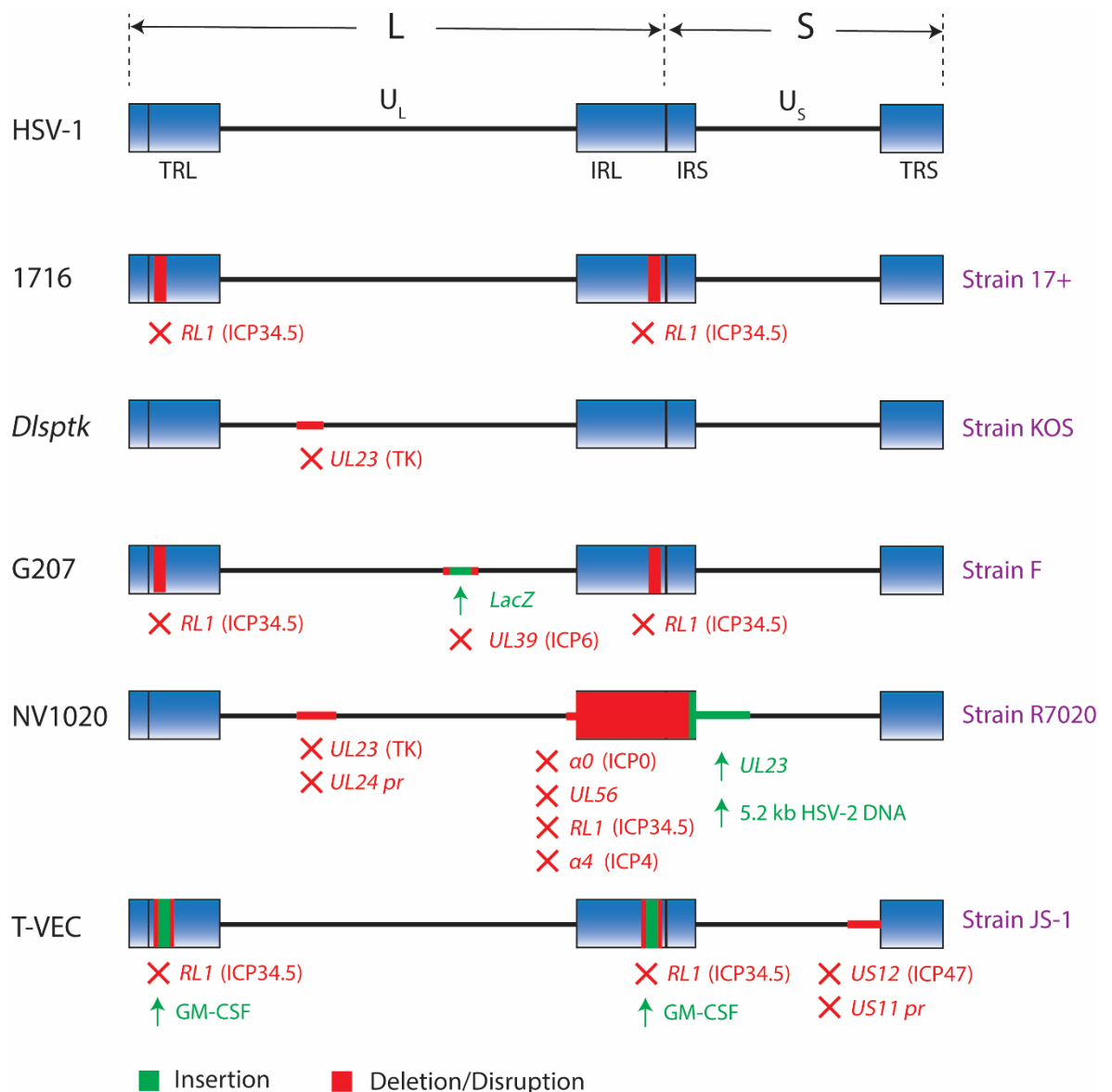


**Figure 1.9 Gene modifications of several oHSV strains.** A large number of modified oHSV strains have been developed, possessing mutations that allow for tumour selectivity and, in some cases, enhanced anti-tumour efficacy. Deletion of the *RL1* genes is a common trait among oHSVs due to the resulting attenuation of neurovirulence. Deletion of gene promoters can have the effect of reducing or removing gene expression and placing genes under other promoters can be used to control expression. A GM-CSF insertion within T-VEC helps to promote an anti-tumour immune response. The strains from which oHSVs are derived can also have a bearing on specificity and efficacy.

HSV-1716 has been shown to be non-neurovirulent when injected directly into the brains of mice (MacLean *et al.*, 1991; McKie *et al.*, 1998). In addition, the virus is unable to replicate in other primary tissues such as skin xenografts (Randazzo *et al.*, 1996). The same can be seen in other strains harbouring the

same mutation, such as R3616 and R4009, which have restricted replication at peripheral sites, and greatly reduced incidence of latency with no neurovirulence (Whitley *et al.*, 1993). Despite this restriction of virulence, HSV-1716 still replicates well in glioma cell lines (Bolovan, Sawtell and Thompson, 1994; McKie *et al.*, 1996), and leads to significant increases in survival when used for the treatment of glioma in mice (Kesari *et al.*, 1995; Lasner *et al.*, 1996).

So far three phase I clinical trials of HSV-1716 for the treatment of glioblastoma have been completed, all of which have shown no toxicity, shedding or reactivation from latency, although detection of virus in tumours is seen in some cases (Rampling *et al.*, 2000; Papanastassiou *et al.*, 2002; Harrow *et al.*, 2004). Other phase I/II trials have also been completed for the use of HSV-1716 to treat squamous cell carcinoma (Mace *et al.*, 2008) and malignant melanoma (MacKie, Stewart and Brown, 2001). In the squamous cell study, while no toxic effects were seen, no virus was detected in the tumours. In the melanoma study, presence of viral replication and tissue necrosis was noted in three of the five patients. More recent data from a phase I trial in children and young adults showed presence of anti-HSV immune responses, areas of necrosis and presence of HSV DNA in the serum (Streby *et al.*, 2017). One further trial for malignant pleural mesothelioma is currently underway (NCT01721018).

While no trials of HSV-1716 in OC have been performed, several preclinical studies have shown positive results. The first of these studies looked at the use of teratocarcinoma PA-1 cells as virus carriers in a mouse xenograft model (Coukos *et al.*, 1999). Treatment with HSV-1716 alone led to reduction of tumour volume and tumour spread and an increase in survival, with the use of carrier cells leading to further improvement. The first study to look at immune responses to HSV-1716 in ovarian mouse tumours found an upregulation of IFN- $\gamma$ , MIG, and IP-10 by the tumour cells, as well as a migration of NK and CD8<sup>+</sup> T cells (Benencia, Courrèges, Conejo-García, Mohamed-Hadley, *et al.*, 2005). Monocytes and dendritic cells were found to be responsible for some of this cytokine release. Later studies have also shown that HSV-1716 is capable of promoting dendritic cell maturation and presentation, and reverse the immune-suppressive phenotype of OC (Benencia *et al.*, 2008). The anti-angiogenic properties of HSV-

1716 in OC have also been assessed, showing that HSV-1716 has the ability to replicate within and kill primary and non-primary endothelial cells (Benencia, Courrèges, Conejo-García, Buckanovich, *et al.*, 2005).

### 1.4.3 Other Notable HSV-based Oncolytic Viruses

In addition to HSV-1716, several other first-generation oncolytic viruses involve modification of a single gene, to render the virus oncolytic. *Dlsptk* was the first oncolytic to harbour a mutation in the thymidine kinase (TK) gene (Martuza *et al.*, 1991)(Figure 1.9). TK catalyses the conversion of (deoxy)thymidine to (deoxy)thymidine monophosphate, a step that is crucial for the production of nucleotides needed for DNA replication (Kit, 1985). Possession of a viral TK gene boosts HSV replication, especially in non-dividing cell types. Loss of this gene, therefore, leads to preferential infection of rapidly dividing cell types, such as cancer cells. *Dlsptk* showed anti-cancer efficacy and reduced neurovirulence in glioma (Martuza *et al.*, 1991) and other brain tumour-types (Markert *et al.*, 1992). However, encephalitis was found to still be present at higher doses, which, in addition to the loss of susceptibility to acyclovir that comes with TK deletion, led to unacceptable safety concerns (Markert *et al.*, 1993).

The second generation of oncolytic HSVs started to incorporate more complex genetic alterations, to improve specificity, efficacy and safety. G207 is a double-mutant of HSV-1 that possesses similar deletions in the  $\gamma 34.5$  gene to HSV-1716, but also possesses a *LacZ* insertion within the *UL39* gene, which encodes ICP6 (Figure 1.9)(Mineta *et al.*, 1995). ICP6 forms the large subunit of the RR, required for deoxyribonucleotide synthesis (Street, 2016). Loss of this protein means that availability of DNA nucleotides is reduced in a manner similar to loss of TK. This improves the safety profile and reduces chance of reversion mutation (Mineta *et al.*, 1995). The safety of G207 has been proven in a number of phase I trials for the treatment of glioblastoma (Markert *et al.*, 2009, 2014), with no major toxicity at the doses used. One more recent study of a single patient, who was unresponsive to typical therapy even showed a dramatic increase in PFS (Markert *et al.*, 2015). There are current plans for a phase I trial using G207 alone or with single radiation dose in children with progressive or recurrent malignant supratentorial brain tumours (Waters *et al.*, 2017). G207 has held

orphan drug designation since 2002 (Table 1.1) (Bilsland, Spiliopoulou and Evans, 2016).

There now exist a number of oncolytic HSVs with more complex arrangements of modifications, which include exogenous gene insertions. NV1020 is an example of this type of virus. NV1020 is derived from the HSV-1 strain R7020 and was originally designed to be a HSV-2 vaccine (Meignier and Roizman, 1985). NV1020 contains numerous gene deletions that render it both safe and oncolytic, including one copy of each the diploid  $\alpha 0$ ,  $\alpha 4$ , and  $\gamma_{134.5}$  genes, which encode ICP0, ICP4, and ICP34.5, respectively; one copy of  $U_L56$ ; a 700 bp deletion spanning the TK locus and the promoter for  $U_L24$ ; an insertion of exogenous tk under control of ICP4 promoter, and; an insertion of a 5.2-kb fragment of HSV-2 DNA (Figure 1.9)(Kelly, Wong and Fong, 2008). Clinical trials with this virus have so far focused on adenocarcinoma of the colon, specifically in cases with hepatic metastases (Kemeny et al., 2006; Geevarghese et al., 2010). These studies have shown that NV1020 can stabilise liver metastases with limited toxic side-effects. It may also re-sensitise metastases chemotherapy and extend overall survival.

Arguably the best-known herpes-based OV, and indeed most famous OV in general is T-VEC. Like previously discussed viruses, T-VEC is based around a double *RL1* gene deletion, which renders the virus oncolytic (Figure 1.9). T-VEC originates from the strain of HSV-1 known as JS-1, which is a more potent clinical isolate, shown to induce more oncolysis than the laboratory 17+ strain (Hu *et al.*, 2006). In addition, T-VEC possesses an extra deletion in the gene encoding ICP47, which normally blocks antigen presentation in HSV-infected cells (Mohr and Gluzman, 1996). This deletion has the additive effect of placing the downstream *US11* gene under the control of the ICP47 immediate early promoter. This enhances tumour selective replication (Liu *et al.*, 2003). Finally, a transgene encoding GM-CSF is inserted in place of ICP34.5, under the control of the cytomegalovirus immediate early promoter. Expression of GM-CSF induces myeloid precursor cells to proliferate and differentiate into dendritic cells (DCs) at the site of infection, further amplifying the anti-tumour immune response (Toda, 2000).

Clinical development of T-VEC began with a phase I trial in 30 patients with multiple tumour types, where the tumours were accessible by injection, and who had failed prior therapy (Hu *et al.*, 2006). Treatment with T-VEC led to minor toxicities, which were mostly injection-site reactions. Disease stabilised in three patients. A further phase II study tested T-VEC in fifty patients with malignant melanoma (Senzer *et al.*, 2009). The overall response rate was 26%, with eight of these experiencing a complete response. One-year overall survival was 58%, or >90% for those who experienced a complete response. Following these successes, testing was expanded to a phase III, multi-centre, randomised-controlled trial for patients with injectable, unresectable melanoma (Andtbacka *et al.*, 2015). This study included GM-CSF treatment alone as a control. Durable response rate was significantly higher in T-VEC treated patients than those treated with injected GM-CSF alone. T-VEC treatment also gave longer median overall survival. T-VEC has now been approved by the FDA since October 2015 and the EMA since January 2016.

## **1.5 Cell Death**

### **1.5.1 Introduction to Death Modalities**

The field of cell death has changed rapidly over the past few decades, and as such, has suffered from the persistence of inconsistent and contradictory nomenclature. The Nomenclature Committee on Cell Death (NCCD) has proposed a number of guidelines to attempt to unify the theories and definitions currently in use (Kroemer *et al.*, 2009; Galluzzi *et al.*, 2012, 2015). Figure 1.10 illustrates an attempt to place all well-known death mechanisms into their various categories.

The first 'formal' classification of cell death types came shortly after the discovery of apoptosis as a form of 'programmed' cell death (Kerr, Wyllie and Currie, 1972) These early classifications were purely morphological, but still have relevance today. Type I cell death is apoptosis, which is characterised by cellular shrinkage, chromatin condensation (pykosis), nuclear fragmentation (karyorrhexis) and membrane blebbing, which consists of formation of cytoplasmic outgrowths, which eventually bud off to form apoptotic bodies

(Elmore, 2007). Type II cell death is referred to as 'autophagic cell death' (ACD). Autophagy is a catabolic cellular process for the degradation of cellular contents within lysosomes (Shimizu *et al.*, 2014). Autophagy is classically recognised as a pro-survival pathway that acts to degrade superfluous or damaged cellular components, although hyperactivation of autophagy can lead to cell death. Type III cell death, necrosis, was initially defined as death in the absence of Type I or II features (Clarke, 1990). Thought to be 'accidental', it was postulated that necrosis only came about from mechanical forces, elevated temperatures and pressures or treatment with detergents or extreme pH. This leads to a morphology that is defined by cytoplasmic swelling, rapid loss of membrane integrity, and organelle swelling and loss. The other broad characterisation built into these definitions is that apoptosis is a strictly tolerogenic process, while necrosis is highly immunogenic.

It is now recognised that these definitions are insufficient to describe the full range of death modalities that exist, and that several levels of operational, morphological, and molecular definitions are necessary. For instance, while a necrotic morphology can occur following physical processes, these characteristics can also result from a highly regulated series of molecular events (Galluzzi *et al.*, 2014; Chan, Luz and Moriwaki, 2015). Several instances also exist whereby apoptosis can promote an inflammatory immune response (Kroemer *et al.*, 2013)(Figure 1.10).

The latest NCCD guidelines suggest that cell death should first be designated as either 'accidental' (caused by physical/chemical/mechanical stresses) or 'regulated' (caused by distinct molecular mechanisms brought about by internal or external cellular signals). Further to this, 'programmed' cell death should be recognised as a subset of regulated death, whereby the death occurs as part of development or maintaining tissue homeostasis (Galluzzi *et al.*, 2015).

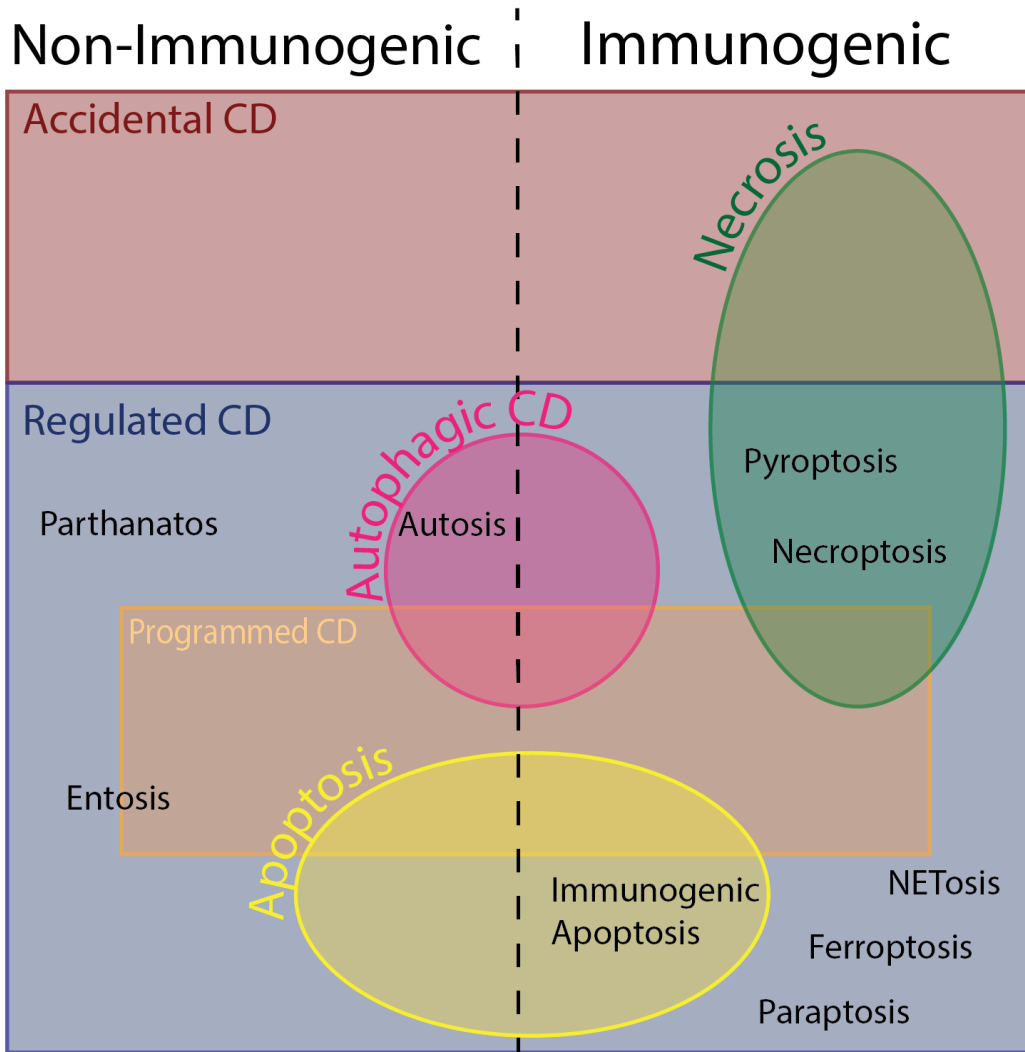


**Figure 1.10 Visual map of cell death modalities.** The earliest definition of cell death modalities divided death into three types, which were apoptosis, necrosis and autophagic cell death. Newer insights have identified new pathways. Some of these fall under the previous broad categories and some are entirely novel. Defining death as accidental, programmed or regulated is an important distinction. Immunogenic cell death types are gaining a lot of attention lately, many of the newly identified pathways fall under the heading of 'immunogenic'.

## 1.5.2 Apoptosis

### 1.5.2.1 Classical Apoptosis

The term apoptosis comes from the ancient Greek word meaning to 'fall off'. Apoptosis is still partly defined by the presence of morphological features mentioned previously. The molecular mechanisms of apoptosis, however, remain one of the most widely characterised of any cell death pathway and should be

used primarily to confirm whether apoptosis is taking place (Galluzzi *et al.*, 2012).

Apoptosis defines cell death that is dependent on the activity of caspases. Caspases are proteases that can cleave proteins (including other caspases) at aspartine residues (Thornberry and Lazebnik, 1998). Many caspases are expressed in their inactive, procaspase form, and become active upon cleavage by other caspases. This mechanism allows for rapid induction of cell death through a cascade-like amplification of signal (Elmore, 2007). Caspases -3, -6 and -7 are the executioner caspases. Activation of these proteins is seen as the 'point of no return', after which death of the cell will follow. The mechanisms that lead to executioner caspase activation can be divided broadly into the intrinsic and extrinsic pathways (Figure 1.11). Intrinsic pathway signalling is reliant on the mitochondria and is often triggered as a result of internal cellular stresses such as DNA damage. Extrinsic pathway signalling comes from signals received from the cell's environment and can involve a number of ligands and receptors. A third pathway, known as the perforin/granzyme pathway is unique to cytotoxic T-lymphocyte-mediated killing of antigen-expressing target cells.

The extrinsic pathway involves members of the tumour necrosis factor (TNF) receptor superfamily. These transmembrane receptors consist of extracellular cysteine-rich domains, and intracellular 'death domains' that are essential for transducing the signal to downstream proteins (Locksley, Killeen and Lenardo, 2001). Well-known ligand and receptor pairs that are involved in this pathway include TNF- $\alpha$ /TNFR1, TRAIL/TRAIL-R, FasL/Fas, Apo2L/DR4, Apo2L/DR5 and Apo3L/DR3 (Ashkenazi and Dixit, 1998). Binding of these ligands leads to the formation of a death-inducing signalling complex (DISC). The constituents of the DISC are dependent on the preceding ligand-receptor interaction. For instance, FasL/Fas binding leads to recruitment of the adaptor protein FADD (Wajant, 2002). TNF- $\alpha$ /TNFR1 binding leads to the recruitment of TRADD, which in turn recruits FADD and RIPK1. FADD can then recruit procaspase-8 through its death effector domain (DED), which causes it to auto-catalytically activate (Kischkel *et al.*, 1995). This can be inhibited by the protein c-FLIP, whose expression is controlled by the pro-survival NF $\kappa$ B pathway (Scaffidi *et al.*, 1999). This complex is also often referred to as complex IIa and is recognised as one of several

pathways that the cell can go down following TNF- $\alpha$  binding. Other potential pathways include necroptosis, which will be discussed later.

The intrinsic pathway is mediated by members of the B-cell lymphoma-2 (BCL-2) family, which receive input from various pathways within the cell. The proapoptotic proteins (BAX, BAK, Bcl-XS, Bad, Bid, Bik, Bim, Hrk, Bok) are responsible for promoting mitochondrial pore formation. BCL-2, BCL-XL BCL-W, Mcl-1, A1/ Bfl-1 are key anti-apoptotic proteins, which act to prevent mitochondrial pore complex formation and permeabilization (Zamzami *et al.*, 1998). Pore formation within the mitochondria allow for the release of apoptotic mediators, known as second mitochondria-derived activator of caspase (SMAC, also called DIABLO) and cytochrome c. This release allows cytochrome c to form what is known as the 'apoptosome', a complex that also consists of seven molecules each of cytochrome c, apoptotic protease-activating factor-1 (APAF-1), dATP and procaspase-9 (Hill *et al.*, 2004). Once formed, procaspase-9 becomes activated, and is able to cleave (and thus activate) executioner caspases, in particular caspase-3. SMAC is involved in a cross-talk mechanism with the intrinsic pathway by binding and inhibiting the cellular inhibitors of apoptosis (cIAP) proteins. These cIAPs are ubiquitinase proteins that can target members of the DISC, such as RIPK1, for degradation, thereby promoting cell survival (Deveraux *et al.*, 1998). SMAC works by inducing the self-ubiquitination and therefore degradation of cIAPs.

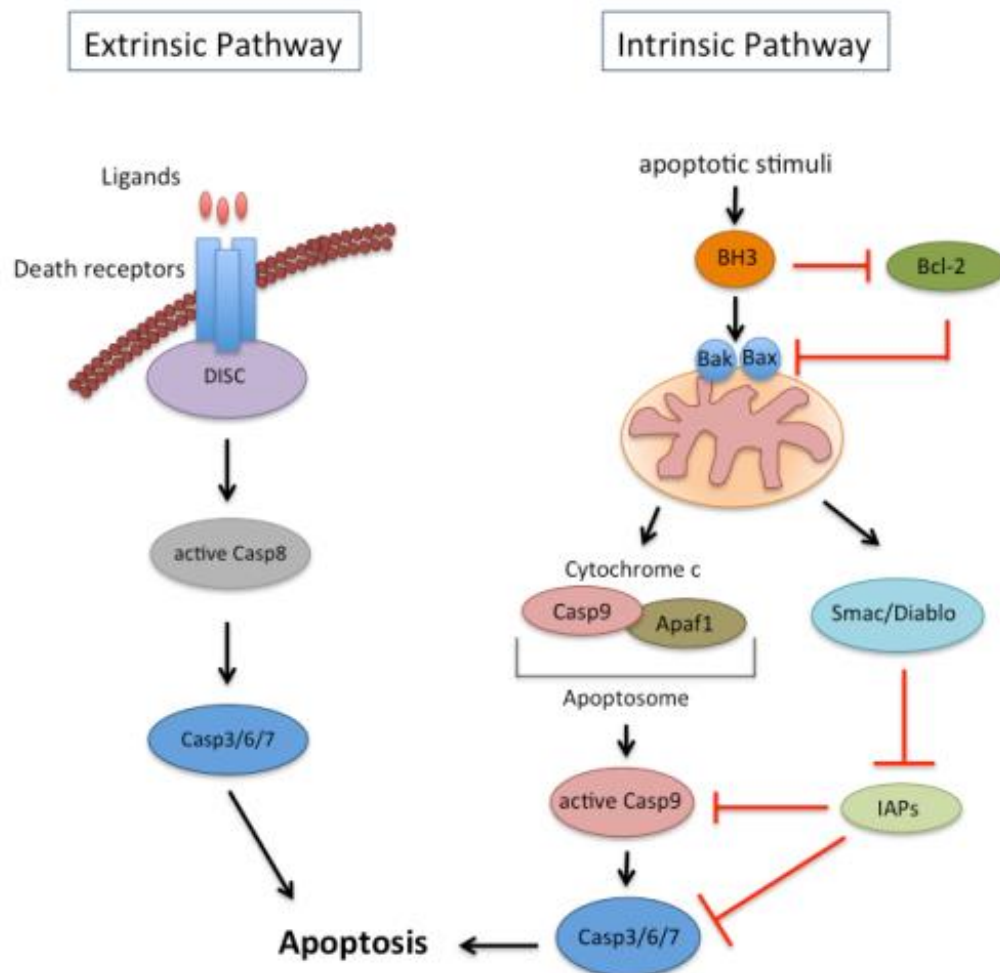


**Figure 1.11 Mechanisms of classical apoptosis.** Apoptosis consists of a highly regulated series of cellular events culminating in large-scale cellular modifications, degradation of DNA and organelles, and eventually death. Apoptosis can be induced (although not exclusively) via two main pathways. The extrinsic pathway is initiated by extracellular signals, including TNF- $\alpha$ , which activate membrane-bound receptors, leading to the formation of the DISC, which leads to caspase-8 activation and subsequent activation of the executioner caspases-3/6/7. Intrinsic death stimuli, such as DNA damage and other cellular stresses can activate members of the BCL-2 family of proteins. Members such as BH3, Bak and Bax promote death, whereas BCL-2 and others are pro-survival. Successful activation of Bak and Bax leads to formation of pores within the outer membrane of the mitochondria. This leads to release of cytochrome c, which forms the apoptosome with Apaf1 and caspase-9. This activates caspase-9 which goes on to activate the executioner caspases-3/6/7 in the same way as caspase-8. SMAC is also released from the mitochondria following pore formation and serves as an additional tool to promote apoptosis via blocking the anti-apoptotic IAP proteins. Figure made by Melanie Weigert.

Activation of either intrinsic or extrinsic pathways will lead into a common execution pathway. The execution pathway is mediated by the execution caspases-3, -6 and -7. Caspase-3 is seen as the main execution caspase, as it can be activated by either caspase-8, -9 or -10, feeding in from either of the three initiation pathways (Elmore, 2007). Caspase-3 causes the activation of the endonuclease caspase-activated DNase (CAD), by cleaving and releasing it from its inhibitor protein, ICAD (Sakahira, Enari and Nagata, 1998). CAD causes the

degradation and condensation of chromosomal DNA. Caspase-3 also affects actin organisation via the cleavage of gelsolin. Gelsolin is involved in promoting actin polymerisation by acting as a nucleus. However, when cleaved by caspase-3, gelsolin fragments then begin cleaving actin filaments, which results in large-scale structural alterations, loss of cell division and transport (Kothakota *et al.*, 1997).

In the final stages of apoptosis, cell fragments begin to be ingested by surrounding phagocytic cells. One of the well-recognised signals that initiate this is the externalisation of phosphatidyl serine (PS) that occurs in the later stages of apoptosis (Fadok *et al.*, 1992). PS is an anionic phospholipid that typically exists in high concentrations on the inner leaflet of the plasma membrane. During apoptosis, changes in membrane fluidity contribute to the externalisation of PS, which can be directly recognised by receptors on the surface of phagocytes (Fadok *et al.*, 2001).

#### **1.5.2.2 Immunogenic Apoptosis**

The first description of apoptosis proposed that it was, by definition, immunologically silent (Kerr, Wyllie and Currie, 1972). Decades later, there is now ample evidence that cells can die by an apoptotic phenotype, yet display signs of immunogenicity (Figure 1.10) (Heath and Carbone, 2001; Casares *et al.*, 2005). Immunogenic apoptosis (IA), therefore, broadly refers to a death modality that displays signs of apoptosis, such as caspase dependency, yet also shows signs of immunogenicity. Several hallmarks of ‘immunogenic cell death’, which seem to apply mostly to apoptosis, have been discovered (Green and Ferguson, 2009; Kroemer *et al.*, 2013). These include calreticulin (CAL), heat shock protein (HSP)70 and HSP90 exposure on the cell surface, and cellular release of high-mobility group box 1 (HMGB1) and adenosine triphosphate (ATP) (Figure 1.12). These molecules have all been shown to have numerous pro-inflammatory roles as signals to the immune system.

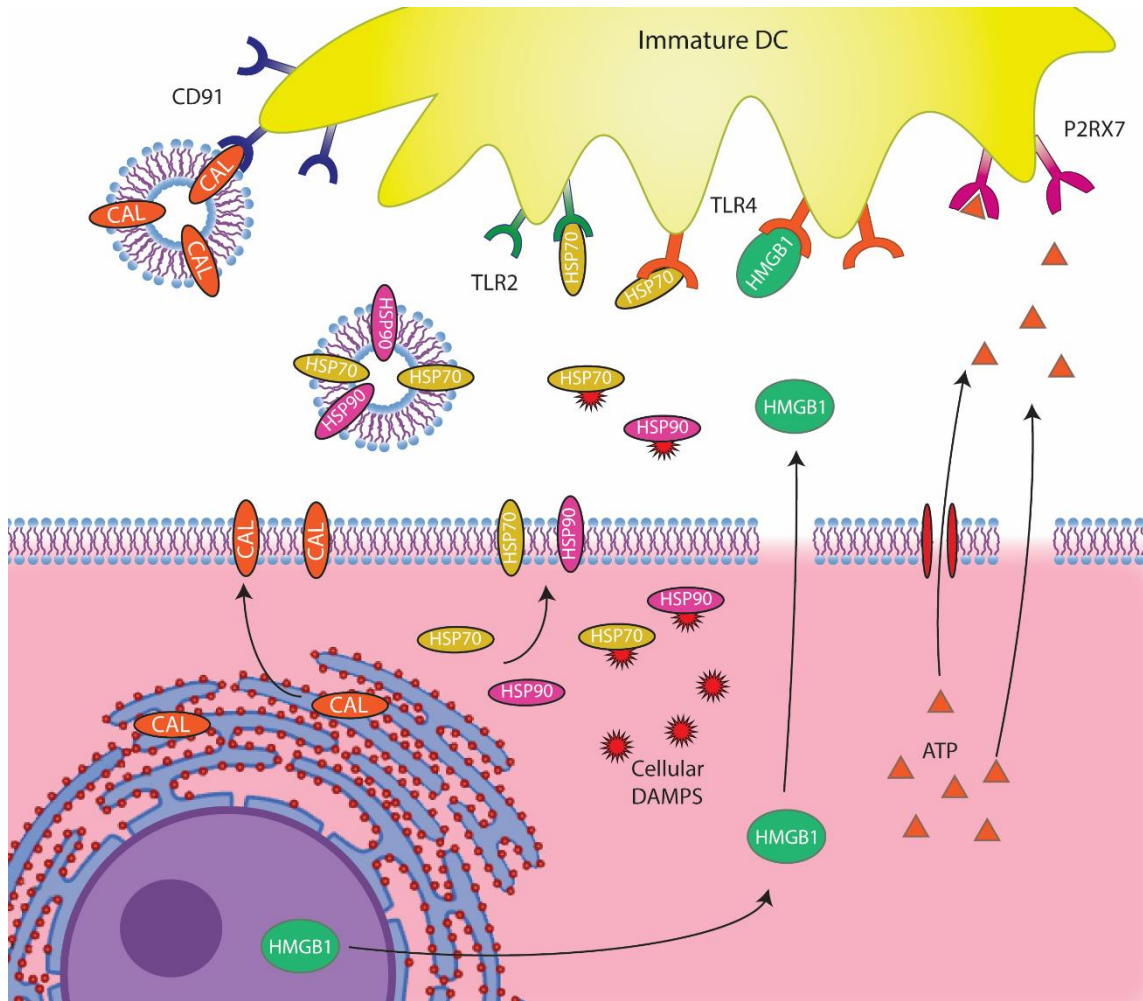


**Figure 1.12 Mechanisms of DAMP release from immunogenic apoptotic cells.** During immunogenic apoptosis (IA), various DAMPs are released from dying cells. HMGB1 typically resides within the nucleus, and during IA becomes released into the cytoplasm and subsequently exits via pores in the membrane. Once released, HMGB1 binds to TLR4 on DCs. ATP exists in a free form throughout the cytoplasm. During IA, ATP can exit the cell via pores or specialised cellular channels and act by binding to P2RX7 receptors. HSPs are chaperone proteins that act within the cytoplasm. HSPs first become inserted within the extracellular membrane and can then release freely into the cytoplasm or within extracellular vesicles. HSP70 has been shown to bind to TLR4. As chaperones, HSPs can assist in bringing other intracellular DAMPs into contact with immune cells. CAL is an ER protein that translocates to the extracellular membrane before being released in to vesicles which allows it to bind to CD91. All of these DAMPs work together to promote the action of DCs, among other cells, and generate a pro-inflammatory environment.

HSP70 and HSP90 are both chaperone proteins with intracellular and extracellular roles. Intracellularly, the proteins are known for their roles in inhibiting apoptosis. For instance, HSP70 can bind to death receptors and prevent DISC formation (F. Guo *et al.*, 2005), or limit CAD activity by regulating protein folding (Sakahira and Nagata, 2002), HSP90 can stabilise phosphorylated Akt, which leads to inactivation of the pro-apoptotic BAD and caspase-9 (Cardone *et al.*, 1998). During IA, HSPs translocate to the plasma membrane, where they are inserted and then released in a membrane-bound form, allowing them to interact with the immune system (Figure 1.12)(Vega *et al.*, 2008).

Released HSPs can act directly as chemokines by stimulating APCs. HSP70 for instance, can bind directly to TLR2 and TLR4, promoting NF $\kappa$ B signalling and IL-1, IL-6 and TNF release (Asea *et al.*, 2002). HSPs can also be released bound to other tumour/pathogen-associated molecules, thereby facilitating the recognition of these molecules by antigen presenting cells (Zhu *et al.*, 2016).

CAL is the most abundant protein in the endoplasmic reticulum (ER) lumen. During IA, CAL can become translocated to the outer cell surface (Obeid *et al.*, 2007). Certain anticancer agents have been shown to achieve this by caspase-8-mediated cleavage of the ER protein BAP31 and conformational activation of Bax and Bak (Panaretakis *et al.*, 2009). This process is not caspase-3 dependent and occurs before PS is exposed on the outside of the cell. CAL exposure determines immunogenicity of the cell by binding directly to immune receptors, including CD49, CD69, CD91, integrins and laminin. CAL acts as an 'eat-me' signal by binding to LDL-receptor-related protein (LRP) on the surface of CD91-positive cells, which includes macrophages and DCs (Figure 1.12). This has the effect of promoting the production of proinflammatory cytokines, such as IL-6 and TNF- $\alpha$ , as well as programming Th17 cell responses (Pawaria and Binder, 2011).

ATP is an important and abundant intracellular metabolite but has been shown to have equally important properties acting as an extracellular signal. Stresses such as mechanical distortion, plasma membrane damage, hypoxia, and exposure to cytotoxic agents can all result in ATP release, as well as programmed responses such as exocytosis of ATP-containing vesicles and secretion through various channels and transporters (Kroemer *et al.*, 2013). ATP release has been shown to be both caspase-dependent and independent in some cases. It can also act as a chemoattractant for macrophages and monocytes (Elliott *et al.*, 2009; Kronlage *et al.*, 2010). Kronlage *et al.* also showed that ATP may promote lamellipodial protrusions in macrophages. Other roles for ATP include stimulating DC maturation, and promoting expression of class II MHC molecules and the cytokines IL-1 $\beta$ , IL-18 and IL-12 (Granstein *et al.*, 2005; Idzko *et al.*, 2007). ATP has been shown to mediate some of these effects by binding to P2RX7 receptors (Figure 1.12), which can in turn activate caspase-1 and the NLRP3 inflammasome, leading to IL-1 $\beta$  and IL-18 release (Lin and Zhang, 2017).

HMGB1 is an essential nuclear protein and is the most abundant non-histone chromatin protein. HMGB1 can be released from cells during both active (IA) and passive (necrosis) processes. Active HMGB1 release first requires translocation of the protein to the cytoplasm (Figure 1.12). This process is JAK-STAT-dependent and involves hyperacetylation of residues within the nuclear localisation sequences (NLS) of HMGB1, facilitating its accumulation in the cytoplasm (Lu *et al.*, 2014). Release can occur secondary to this following exocytosis within vesicles or inflammasome mediated release (Gardella *et al.*, 2002; Lu *et al.*, 2012). HMGB1 exerts its extracellular effects by binding to a diverse range of receptors, including several toll-like receptors (TLRs) and receptor for advanced glycation end products (RAGE), among others (Yang *et al.*, 2015). The TLR4/MD-2 complex is key for mediating cytokine release from macrophages in response to HMGB1, which binds directly to MD-2 (Yang *et al.*, 2010). When it binds to RAGE, HMGB1 is endocytosed by the cell and can lead to induction of pyroptosis (Xu *et al.*, 2014). Other receptor interactions with HMGB1 can occur while it is associated with other molecules such as CXCL12 or nucleosomes (Urbonaviciute *et al.*, 2008; Schiraldi *et al.*, 2012).

### **1.5.3 Necrosis**

Following the recent shake-up of the cell death landscape, the terms ‘necrosis’, ‘necroptosis’, ‘programmed necrosis’ and ‘regulated necrosis’ have in some cases found themselves being used interchangeably but erroneously (see Figure 1.10). As mentioned previously, necrosis is a general cell death modality that is defined on the basis of cytoplasmic granulation, organelle and/or cellular swelling, leading to the eventual leakage of intracellular contents from the cell. Necrosis is always immunogenic, in that it induces a pro-inflammatory response. This can be due to both the natural effect of intracellular content release and the result of molecular signalling pathways leading up to death that promote cytokine production and release.

#### **1.5.3.1 Necroptosis**

The number of recognised regulated necrotic pathways is growing. The original ‘classical’ pathway of regulated necrosis to be discovered was necroptosis

(Vandenabeele *et al.*, 2010). Necroptosis was originally defined as a cellular response to a combination of drugs designed to bring about a specific series of events: TNF- $\alpha$ , SMAC mimetic and zVAD-fmk (carbobenzoxy-valyl-alanyl-aspartyl-[O-methyl]- fluoromethylketone). To be termed 'necroptosis', cell death must be caspase-independent, initiated by death receptors and dependent on the serine/threonine kinases RIPK1 and RIPK3 (Galluzzi *et al.*, 2012).

While several triggers of necroptosis are now known (Vanlangenakker, Vanden Berghe and Vandenabeele, 2012; Berghe *et al.*, 2014), the best-characterised pathway follows the binding of TNF- $\alpha$  to TNFR1 (Figure 1.13). As mentioned earlier, stimulation with TNF- $\alpha$  leads to the formation of complex I, consisting of the proteins TRADD, RIPK1, cIAP1 and 2, TNF receptor-associated factor 2 (TRAF2) and TRAF5. For necroptosis to occur, cIAPs need to become sufficiently depleted to counteract their anti-death effects. Autoubiquitination of cIAPs by SMAC or the class of drugs known as SMAC mimetics can achieve this. In addition to this, caspase-8 must be inhibited, which can occur following zVAD-fmk treatment or inhibition by viral proteins. When these conditions are met, the proteins RIPK1 and RIPK3 become associated with one another via direct interaction of their respective RIP-homotypic interaction motifs (RHIMs). This proximity allows for the proteins to auto- and transphosphorylate (Cho *et al.*, 2009), which leads to the formation of a filament-like complex known as the necrosome (J. Li *et al.*, 2012). Phosphorylation of RIPK1 can only take place once it has been deubiquitylated by cylindromatosis (CLYD) (Moquin, McQuade and Chan, 2013). This leads to the recruitment of the mixed-lineage kinase domain-like (MLKL) protein, a process that is dependent on the Ser-227 phosphorylation of RIPK3 (Chen *et al.*, 2013; McQuade, Cho and Chan, 2013). Once recruited, MLKL itself becomes phosphorylated on residues Thr357 and Ser358 by RIPK3 (Sun *et al.*, 2012). MLKL has been shown to form both trimers and following phosphorylation, which leads it to translocate to the plasma membrane to mediate necrosis effector mechanism (Cai *et al.*, 2014; X. Chen *et al.*, 2014).

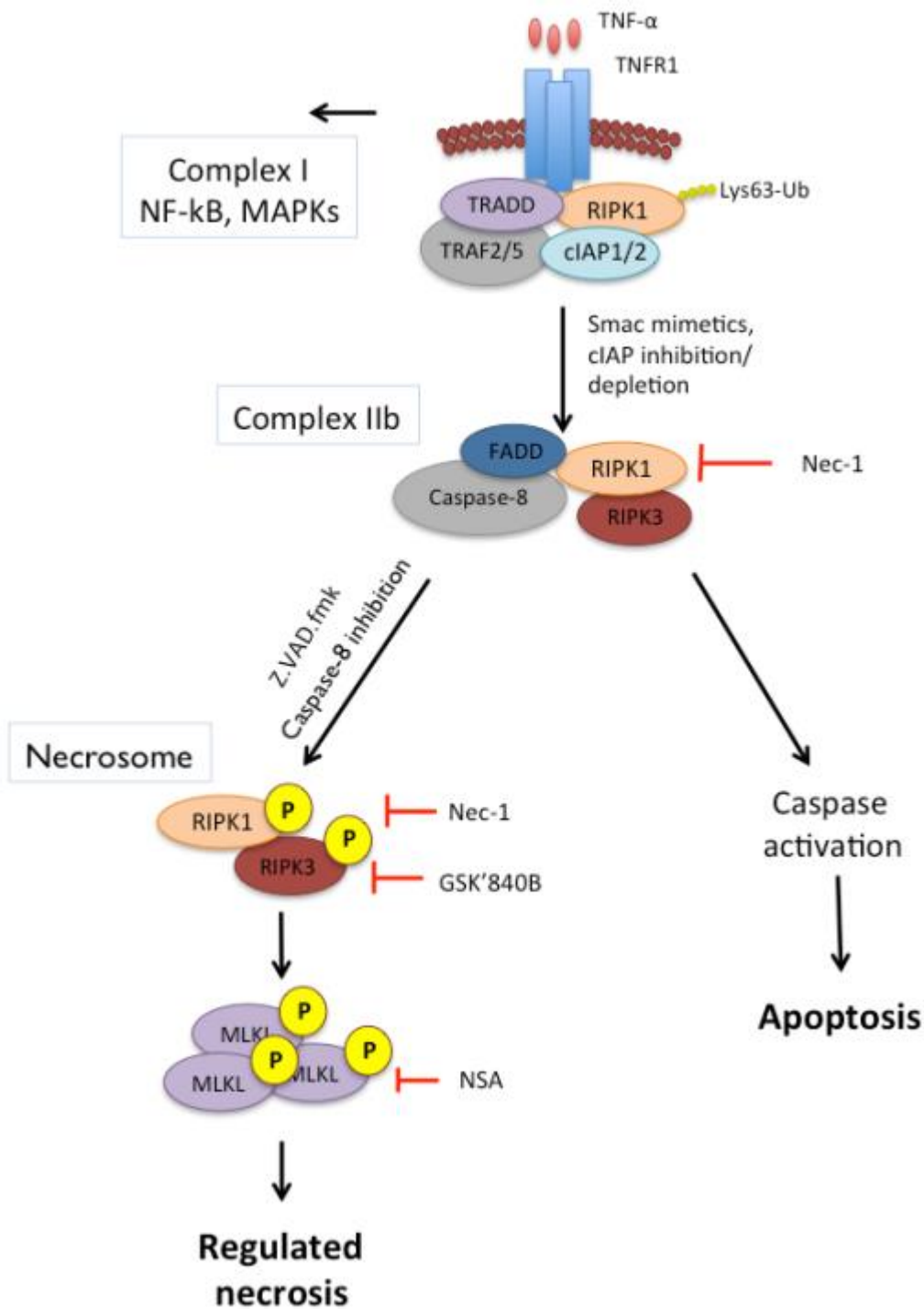


**Figure 1.13 Interconnected pathways of necroptosis and apoptosis.** Classical necroptosis signalling was first identified as a pathway resulting from binding of TNF- $\alpha$  to TNFR1. As shown previously, this leads to formation of a DISC, comprising of RIPK1, TRADD, TRAF2/5 and cIAP1/2. When cIAPs are depleted or inhibited, either by cellular SMAC or chemical homologues, A complex known as complex IIb is formed from RIPK1, RIPK3, FADD and caspase-8. At this point, the cell now has the option of committing to a necroptotic or apoptotic route. If caspase-8 remains activated, then apoptosis can occur via the extrinsic pathway. If caspase-8 becomes inhibited via chemical or viral mechanisms, then necrosome formation will occur, which consists of microfilaments comprised of RIPK3 and RIPK1. These proteins auto and trans phosphorylate, leading to the recruitment of MLKL. MLKL itself becomes phosphorylated by RIPK3, leading to oligomerisation and translocation to the membrane where it leads to death. Figure made by Melanie Weigert.

The precise mechanisms of MLKL action are still under debate. However, MLKL appears to be necessary for Na<sup>+</sup> and Ca<sup>2+</sup> ion influx, with the transient potential receptor (TRP) channel, TRPM7, under investigation (Cai *et al.*, 2014). Other theories argue that MLKL has a more direct membrane permeabilising mechanism mediated by the direct insertion of the four-helix bundle region of the protein into the plasma membrane (Su *et al.*, 2014). More recent evidence, however, suggests that MLKL may itself act as a novel type of ion channel, permissive to Mg<sup>2+</sup>, Na<sup>+</sup> and K<sup>+</sup> but not Ca<sup>2+</sup> (Xia *et al.*, 2016).

### 1.5.3.2 Pyroptosis

The term 'pyroptosis' was coined in 2000, describing a caspase-1 dependent form of necrosis induced by *Salmonella typhimurium* in macrophages (Brennan and Cookson, 2000). As a subtype of necrosis, pyroptosis is naturally immunogenic (Figure 1.10) Several more pathogen and non-pathogen inducers of this pathway have been identified, including myocardial infarction (Frantz *et al.*, 2003). TLRs and nod-like receptors (NLRs) are two mechanisms by which pyroptosis can be triggered. The best studied of these is the NACHT, LRR and PYD domains-containing protein 3 (NLRP3), which can respond to stimuli such as pore forming toxins, ATP, pathogenic DNA and UV damage (Mariathasan *et al.*, 2006; Feldmeyer *et al.*, 2007; Muruve *et al.*, 2008). NLRP3 associates with caspase-1 following activation, forming what is known as the inflammasome (Bergsbaken, Fink and Cookson, 2009). This leads to activation of caspase-1, which then acts as the death effector protein. Several downstream targets of caspase-1 do not contribute to death itself but can promote the inflammatory aspects of pyroptosis. The cytokines IL-1 $\beta$  and IL-18 are processed and released as a result of caspase-1 activation. IL-1 $\beta$  is a pyrogen that stimulates fever, migration of leukocytes into tissues and expression of other cytokines and chemokines. IL-18 induces IFN $\gamma$  production and promotes production of T cells and macrophages (Delaleu and Bickel, 2004). Release of these proteins is not dependent on cell lysis (Fink and Cookson, 2006). The effector mechanisms that lead to death following caspase-1 activation are still poorly understood. One known effector is gasdermin D (GSDMD), which is cleaved by caspase-1, enabling it to insert into the plasma membrane and form ion non-selective pores (Shi *et al.*, 2015; Chen *et al.*, 2016).

## 1.5.4 Autophagy

ACD was initially defined as cell death accompanied by large-scale autophagic vacuolisation (Schweichel and Merker, 1973). Macroautophagy (often and hereafter referred to as autophagy) is a physiological process that occurs in response to cellular stresses including starvation, mitochondrial damage, hypoxia and infection (Yin, Pascual and Klionsky, 2016). Autophagy exists as a mechanism for degrading long-lived proteins and organelles in bulk, as opposed to ubiquitination, which regulates short-lived proteins. Autophagy involves creation of double-membrane structures known as autophagosomes, which sequester material before fusing with lysosomes, whose contents mediate the degradation of material (Liu and Levine, 2015).

The Atg proteins mediate many stages of autophagy. The process begins when pre-existing organelles or newly synthesised lipids form isolation membranes (also known as phagophores) in a process that involves the ULK/Atg1 protein complex, which activates PI3K complex, subsequently recruiting more Atg proteins to the site of nucleation (Liu and Levine, 2015). Further vesicle development is governed by the protein Atg12 and a conversion of microtubule-associated protein 1A/1B light chain 3 (LC3)-I to LC3-II (Tanida, Ueno and Kominami, 2008). LC3 conversion is therefore a typical marker of autophagy.

### 1.5.4.1 Autophagic Cell Death

Circumstantial links between autophagy and cell death have been made historically over the last few decades (Kroemer and Levine, 2008). However, many now argue that these early reports of ACD lacked evidence linking the two processes. For death to be determined as ACD, evidence must now be provided that genetic inhibition of at least two autophagy components has a pro-survival effect (Galluzzi *et al.*, 2012; Liu and Levine, 2015). Using these criteria, several instances of ACD have been noted in mammalian systems wherein key apoptotic proteins have been disabled (Shimizu *et al.*, 2004, 2010; Pattingre *et al.*, 2005). Other instances note presence of ACD in apoptosis-competent cells, induced by p19ARF (Reef *et al.*, 2006), Ras (Elgendy *et al.*, 2011), and various other cytotoxic agents (Sharma *et al.*, 2014).

One distinct pathway of ACD, known as autosis, has been identified from death induced by treatment with a fusion protein consisting of 18 amino acids of Beclin-1 and 11 amino acids from the HIV Tat protein (Liu and Levine, 2015). This peptide acts by disrupting Beclin 1/GAPR-1 binding in the Golgi complex (Shoji-Kawata *et al.*, 2013). Further inducers of this pathway have been found to be starvation and hypoxia/ischaemia (Liu *et al.*, 2013). The unique features of autosis include focal plasma membrane rupture; focal concavity of the nucleus and ballooning of the perinuclear space; abnormal mitochondria, which become swollen and fragmented; and enhanced adhesion to the cellular substrate (Liu and Levine, 2015). The Na<sup>+</sup>-K<sup>+</sup>-ATPase pump has been shown to be a key autosis effector, with knockdown or inhibition of these protein leading to protection of cells against autosis (Liu *et al.*, 2013). How exactly this protein acts to bring about the cell's demise is yet to be uncovered. Na<sup>+</sup>,K<sup>+</sup>-ATPase has been shown to translocate to the perinuclear space and so may contribute to the swelling thereof (Galva, Artigas and Gatto, 2012). Na<sup>+</sup>-K<sup>+</sup>-ATPase has also been shown to have a role in cellular adhesion, and so it is possible that it mediates the enhanced adhesion seen in autosis (Contreras *et al.*, 1999).

Autophagy is closely linked with IA, due to its requirement as a precursor to ATP release (Kroemer *et al.*, 2013). Inhibitors of any essential autophagy protein will reduce levels of ATP release from dying cells (Michaud *et al.*, 2011). The exact mechanisms by which autophagy causes ATP release are still unclear.

### **1.5.5 Non-Classical Cell Death Modalities**

Ferroptosis is a form of RCD that is induced by intracellular perturbations such as severe lipid peroxidation. This process is dependent on generation of reactive-oxygen species and iron availability, hence the name (Stockwell *et al.*, 2017). Ferroptosis has a necrosis-like morphotype but occurs independently of necrosome components (Dixon *et al.*, 2012). Induction of ferroptosis results in the release of immunostimulatory DAMPS, which makes it immunogenic (Linkermann *et al.*, 2014; Kim *et al.*, 2016). Ferroptosis is under primary regulation of glutathione (GSH)-dependent enzyme glutathione peroxidase 4 (GPX4), which is an endogenous inhibitor of the process. The ferroptosis inducer erastin indirectly disrupts activity of GPX4, which contributes to ferroptotic

death (W. S. Yang *et al.*, 2014). Downstream of GPX4, accumulation of polyunsaturated fatty acids (PUFAs) can lead to their own fragmentation and ferroptosis, which is preventable by antioxidants such as ferrostatin-1 and liproxstatin-1 (Zilka *et al.*, 2017).

Parthanatos is a form of RCD that is driven by hyperactivation of PARP1 in response to severe DNA damage, oxidative stress, hypoxia, hypoglycaemia (Fatokun, Dawson and Dawson, 2014). Activation of PARP1 means an increase in cellular PAR production. This process causes a decrease in NAD<sup>+</sup> and ATP levels, although this does not contribute to death. PAR then directly binds to apoptosis-inducing factor (AIF), which facilitates its mitochondrial release and translocation to the nucleus. Here, AIF binds and activated migration inhibitory factor (MIF), a nuclease that causes large-scale nuclear degradation and death (Wang *et al.*, 2016). Hexokinase 1 (HK1) is another contributor to parthanatos that is activated by PAR, allowing it to inhibit glycolysis and cause cellular bioenergetic collapse (Andrabi *et al.*, 2014).

Entosis is a peculiar form of cell “cannibalism” that occurs between non-phagocytic cell types, where one cell engulfs the other, leading to its demise (Florey, Kim and Overholtzer, 2015; Krishna and Overholtzer, 2016). Engulfment has been shown to be dependent on cadherin 1 and catenin alpha 1, followed by actomyosin remodelling orchestrated by ras homolog family member A (RHOA) (Purvanov *et al.*, 2014; Wang *et al.*, 2015). Death of the endocytosed cell is somewhat dependent on autophagic proteins, which promote fusion of the cell with lysosomes (Florey *et al.*, 2011).

NETosis is a controversial form of cell death that appears to be, so far, restricted to haematopoietic cells (Q Remijsen *et al.*, 2011). NETosis was first characterised in neutrophils, where it was associated with the formation of large-scale neutrophil extracellular traps (NETs) (Brinkmann *et al.*, 2004). These NETs form from released chromatin and histone proteins that associate with granular and cytoplasmic proteins and are produced in response to microbial stimuli via TLRs. The mechanism of death is poorly understood, but thought to be dependent on formation of reactive oxygen species (ROS) (Quinten Remijsen *et al.*, 2011).

## 1.6 Immunogenic Cell Death and Oncolytic Virus Therapy

### 1.6.1 Oncolytic Viruses that Induce Immunogenic Cell Death

Numerous studies have made investigations into the presence of ICD under different oncolytic virus infection models, and in some cases, investigated the consequences this has on the surrounding immune environment. ICD appears to be present in many of the major virus species that have been utilised for oncolytic virotherapy.

Various adenovirus variants have been shown to induce markers of ICD. Ad5/3-hTERT-E1A-hCD40L, which is an Ad5/3 strain in which E1A expression lies under the transcriptional control of an hTERT promoter, and also encodes human CD40 ligand, was shown to induce HMGB1 release, CAL exposure and ATP release in endometrial carcinoma cells (Diaconu *et al.*, 2012). The full effect was only seen in cells that expressed the CD40 receptor, with those lacking the receptor only responding with HMGB1 release alone. This had the consequence of recruitment and activation of antigen-presenting cells and increased interleukin-12 production *in vivo*. Presence of macrophages and cytotoxic CD8<sup>+</sup> T cells was also noted in tumours. In an *in vitro* murine colorectal model, the virus Ad881 induced release of both HMGB1 and ATP in CT26 cells (Yamano *et al.*, 2016). This led to an increased vaccination effect when these cells were injected into mice who were then later challenged with tumour cells. We recently showed that the necroptotic protein RIPK3 played a role in cell death induced by the Ad5 virus strain dl922-947 (Weigert *et al.*, 2017). Expression of RIPK3 enhanced virus activity both *in vitro* and *in vivo*. However, blockage of RIPK1 and MLKL function was shown not to affect cell death.

An early study looking at VV showed presence of necrosis-like death, evidenced by HMGB1 release and PI staining (Z. S. Guo *et al.*, 2005). The strain used for this study was deleted in the serpin proteins SPI-1 and SPI-2, which have been shown to have roles in inhibiting apoptosis via interactions with cathepsin G (SPI-1) (Moon, Turner and Moyer, 1999) or Fas receptor, TNFR1, and IL-1 $\beta$ -converting enzyme-like enzymes (SPI-2) (Kettle *et al.*, 1997). A comprehensive investigation of cell death induced by *tk*-deleted VV in OC cells identified a strong role for

regulated necrosis (Whilding *et al.*, 2013). Here, necrotic morphology was identified by electron microscopy, as well as confirmation of a RIPK1/RIPK3/caspase-8 complex, with death attenuated following RIPK1 or MLKL blockade. This suggests that this mode of cell death is true necroptosis. HMGB1 release was also confirmed, proving that death had an immunogenic component. The VV strain JX-GFP possesses a GFP insertion within the *tk* locus, thus leading to a TK-deficient phenotype, but also contains an additional insertion of GM-CSF. The efficacy and immunogenicity of this virus was explored in melanoma cells (Heinrich *et al.*, 2017). Here, cells were shown to release HMGB1 upon death, with death also leading to an activation of both DCs and T cells when co-cultured. In the same study, a VV strain known as TG6002 was tested in the same setting. TG6002 possesses both TK and ribonucleotide reductase-encoding gene deletions in addition to the expression of the suicide gene FCU1. FCU1 encodes a protein which catalyses the conversion of 5-fluorocytosine (5-FC) into the toxic chemotherapeutic 5-fluorouracil (5-FU). TG6002 was shown to induce the same release of HMGB1 as JX-GFP and was also shown to induce CAL exposure when combined with 5-FC, but not alone.

Interesting evidence for the induction of ICD by Newcastle Disease Virus (NDV) was seen during infection of glioblastoma cells *in vivo* (Koks *et al.*, 2015). GL261 cells infected with NDV showed no signs of classic apoptosis, such as blebbing, PS externalisation and caspase-3 activation. There was a reduction in cytotoxicity seen during infection following treatment with the RIPK1 inhibitor necrostatin-1, which is suggestive of a necroptosis-like signalling pathway. NDV did induce membrane exposure of CAL and release of HMGB1 *in vivo*. However, no extracellular ATP was detected before death.

Other non-modified OVAs such as Parvovirus and Coxsackie virus have also shown presence of ICD. The strain CVB3 was shown to induce an apoptotic-dependent mode of cell death in non-small cell lung cancer cells based on inhibition with zVAD-fmk (Miyamoto *et al.*, 2012). Evidence of IA was proven due to presence of HMGB1 release, CAL exposure and ATP release *in vivo*. Intratumoral administration also showed an increase in recruitment of natural killer cells and granulocytes. An investigation into oncolytic parvovirus H-1 (H-1PV) in pancreatic ductal adenocarcinoma (PDAC) cells showed that the virus induced

HMGB1 release but not CAL exposure or ATP release (Angelova *et al.*, 2014). When used in combination with the apoptosis-inducing drug gemcitabine, H-1PV converted the subsequent death into an immunogenic form. This death coincided with IL-1 $\beta$  release which may suggest a role for pyroptosis, but this would need to be explored further.

### 1.6.2 Herpesviruses and Immunogenic Cell Death

Initial evidence for a link between herpesviruses and regulated necrosis was identified in murine CMV (MCMV), with its M45-encoded viral inhibitor of RIP activation (vIRA) (Upton, Kaiser and Mocarski, 2008). It is thought that cells have evolved a mechanism for inducing necrosis in response to viruses as a backup mechanism to eliminate pathogens that block caspase-8 signalling (Kaiser, Upton and Mocarski, 2013). DNA-dependent activator of interferon regulatory factors (DAI; also known as ZBP1 or DLM-1) is a cytosolic DNA sensor that induces type I IFN production (Takaoka *et al.*, 2007). More recently, a role for DAI in inducing regulated necrosis by direct binding to RIPK3 has been uncovered (Upton, Kaiser and Mocarski, 2008). This pathway of necrosis interaction is RIPK3-dependent but independent of RIPK1 and TRIF. The protein vIRA, an inactive homologue of the viral RR, has been shown to possess a RHIM (Figure 1.14), which enables it to directly bind and inhibit the complex formed between RIPK3 and DAI (Upton, Kaiser and Mocarski, 2012). This region of the protein also mediates inhibition of apoptotic death by a mechanism independent of caspase-8 (Guo *et al.*, 2015). Interestingly, the human CMV (HCMV) analogue of this protein, coded by *UL45*, is inactive (Patrone *et al.*, 2003). Instead, HCMV blocks necroptosis in a step that occurs post-MLKL phosphorylation, using a IE1-regulated gene product (Omoto *et al.*, 2015).

### Highly conserved region

mRIP1	518	KYT <b>IF</b> - NSSGI <b>QIGNHNYMDVG</b>
mRIP3	439	ALVFN - NCSEV <b>QIGNYNSLVAP</b>
mTRIF	679	PLI <b>TH</b> - HAQM <b>VQLGVNNHMWGH</b>
M45	51	YVR <b>IMNGVSGIQIGNHNAMSIA</b>
R45	63	YVKLS - GVS <b>GIQIGNSNVMSVA</b>
E45	33	RLSLQ - NVS <b>GLQIGNWNAMSIA</b>
ICP10	55	AYR <b>IS</b> - DSS <b>FVQCGSNCSMIID</b>
ICP6	64	SYR <b>IS</b> - DNN <b>FVQCGSNCTMIID</b>

**Figure 1.14 RIP-homotypic interaction motif sequences of cellular and viral proteins.** Many proteins have now been proven to possess a RIP-homotypic interaction motif (RHIM). These motifs show a high level of homology which allows them to bind with one another. Binding is dependent on a four-amino acid highly conserved region. Image adapted from *Trends Biochem Sci.* 2009 Jan;34(1):25-32.

HSV-1 and HSV-2 have been shown to regulate necrosis signalling via their respective RR proteins ICP6 and ICP10, both coded by *UL39* (Guo *et al.*, 2015). Although these proteins are analogues of MCMV's vIRA, both possess a distinct region within their RR domains that enable them to inhibit caspase-8 by binding directly to its DED (Dufour *et al.*, 2011). The RHIMs of these proteins are present in the N-terminal domain, which allows for direct binding to both RIPK1 and RIPK3 in both murine and human cells (X. Wang *et al.*, 2014; Huang, S. Wu, *et al.*, 2015). Interestingly, in murine cells, the complexes ICP6 forms with RIPK1 and RIPK3 lead to their activation and necrosis induction (Figure 1.15). In human cells however, this same interaction actually disrupts complex formation and leads to necrosis inhibition (Guo *et al.*, 2015). The caspase-8-binding properties of ICP6 and ICP10 leads to a sensitisation of cells to TNF- $\alpha$ -induced necroptosis. In human cells, this has no impact, as necroptosis is concurrently inhibited by the RHIM. This was shown to be altered, however, when a version of ICP6 containing a tetra-alanine substitution in the RHIM (mutRHIM) was overexpressed in human cells and complemented with a  $\Delta$ ICP6 mutant virus (Guo *et al.*, 2015). This had the effect of maintaining caspase-8 inhibition while removing the necroptosis blockade and sensitising cells to TNF- $\alpha$ .

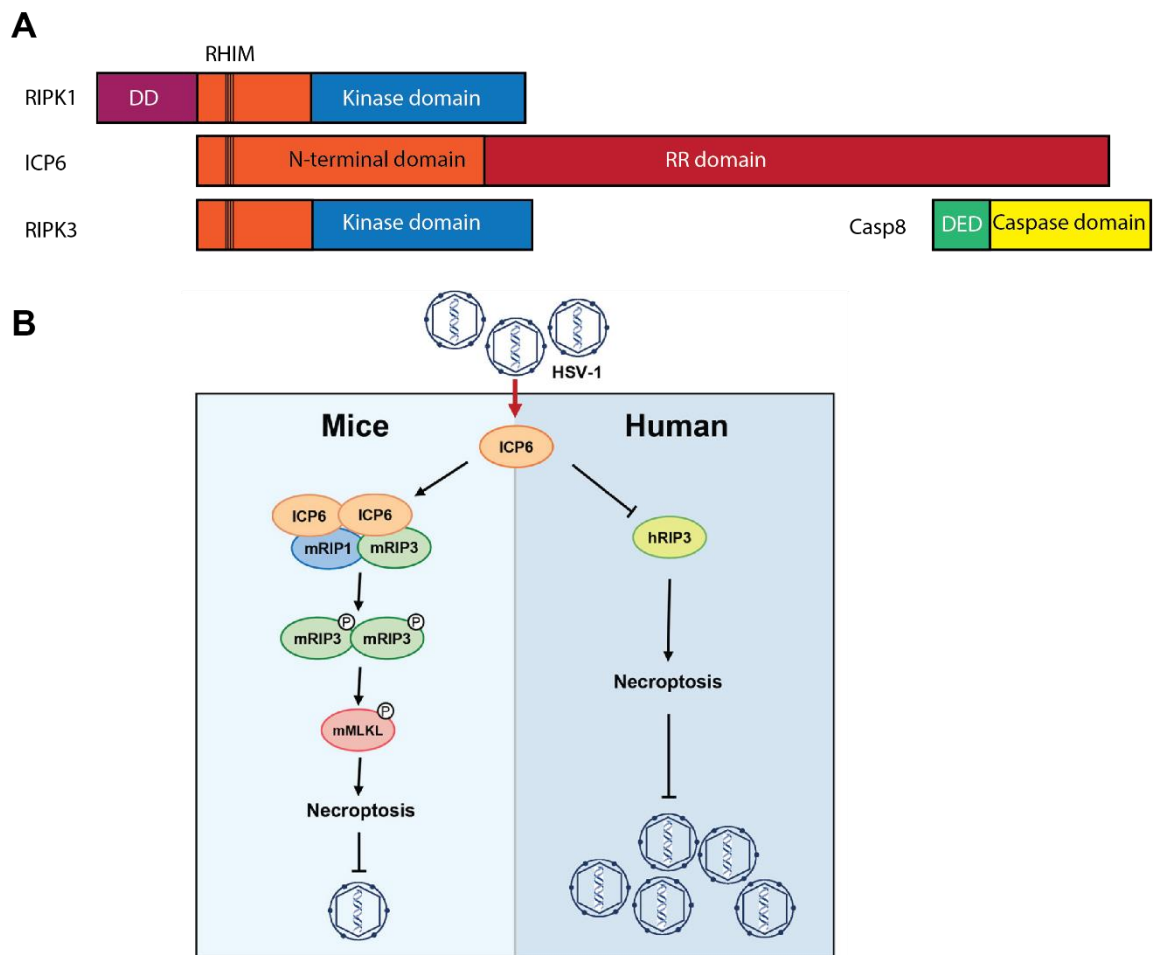


**Figure 1.15 Various cell death roles of HSV-1 ICP6.** (A) ICP6 possesses two domains, the N-terminal and RR domains. The RR domain has long been known for its role as the large subunit of the viral ribonucleotide reductase. Recent evidence has uncovered an alternative role for the RR domain as an inhibitor of caspase-8, mediated via its direct interaction with the death effector domain (DED). At the other end, the N-terminal domain binds to both RIPK1 and RIPK3 via the proteins' respective RHIMs. (B) The consequences of the interaction between ICP6 and RIPK1 and RIPK3 have been shown to differ between human and murine cells. In humans, ICP6 blocks RIPK1 and RIPK3 from interacting and therefore prevents their phosphorylation. In mice, ICP6 does the opposite by inducing phosphorylation and dimerization of RIPK3, which results in necroptosis. This dichotomy has the effect of more freely allowing HSV-1 to replicate in human cells. Image taken from *Cell Host & Microbe* 2015 17, 229-242DOI.

Evidence for induction of alternative modes of cell death have been demonstrated for oncolytic HSV-1 and HSV-2 in various models. Strains of these viruses lacking functional ICP0 or a nuclear localization sequence were assessed for their ability to induce IA in breast cancer cell lines (Workenhe *et al.*, 2014). The HSV-2 strains were shown to induce cleavage of caspase-3 and subsequently, cause HMGB1 release. In vivo, HSV-1 dICP0 showed a greater enhancement of immunogenic markers, such as elevated HSP70 expression compared with HSV-2 dICP0. This was shown to have a correlation with greater CD8+ T cell and APC infiltration. The PK domain of HSV-2 ICP10 contains a PK domain that has been shown to inhibit various death pathways (Perkins, Pereira and Aurelian, 2003;

Wales *et al.*, 2008). An oncolytic variant that contains a PK deficiency induced some evidence of apoptosis and pyroptosis in melanoma cells (Colunga, Laing and Aurelian, 2010). Death was dependent on cleavage and activation of caspase-3 and -7, and calpain, the latter of which has been shown to be a mediator of both apoptosis and necrosis (Cabon *et al.*, 2012). In addition, activated caspase-1, CD11b, and TNF- $\alpha$  were all also present, which is indicative of pyroptosis. Evidence for ICD induction by an HSV-1 RH2 strain in squamous cell carcinoma has emerged (Takasu *et al.*, 2016). RH2 is a recombinant virus formed by coinfection of Vero cells with strains R849 and HF, and possesses a  $\gamma$ 34.5 deletion (Takaoka *et al.*, 2011). All the classic signs of IA were present, including ATP and HMGB1 release and CAL exposure. Annexin-V/PI staining, PARP cleavage, and cell rescue following treatment with the pan-caspase inhibitor zVAD-fmk demonstrated presence of classical apoptosis as the driver of death. Further work on this system has shown that HSPs are present in the supernatant of infected cells as well as viral proteins, with extracellular matrix (ECM) components being released in smaller amounts (Tada, Hamada and Yura, 2018). This provides further evidence that induction of ICD is capable of altering the TME.

## **1.7 Aims of the Project**

### **1.7.1 Evaluate HSV-1716 as a treatment for ovarian cancer**

- Determine the ability of HSV-1716 to infect and kill ovarian cancer cell lines

### **1.7.2 Produce novel models for assessing ICP6 function**

- Produce lentivirus-modified cell lines expressing a range of ICP6 constructs with varying RHIM modifications
- Use CRISPR/Cas9 to create an ICP6-null strain of HSV-1716
- Use CRISPR/Cas9 to create an ICP6 RHIM-modified virus

### **1.7.3 Determine the role of immunogenic cell death during HSV-1716 infection**

- Assess the presence of various markers of immunogenic cell death following HSV-1716 infection
- Assess the presence of various markers of necrosis and the effect of blocking components of the necroptosis pathway following HSV-1716 infection

### **1.7.4 Determine the roles of ICP6 and RIPK3 in HSV-1716-induced immunogenic cell death**

- Investigate the effect of RIPK3 overexpression on HSV-1716-induced cell death
- Investigate the effect of ICP6-RIPK3 binding on HSV-1716-induced cell death and subsequent markers of immunogenic cell death

## 1.8 Hypothesis

Based on what is known on the current biology surrounding the potential for induction of immunogenic cell death and necrosis by HSV-1, I hypothesise the following: First, I predict that following HSV-1 infection of cancer cells, some immunogenic cell death is likely to be triggered, illustrated by evidence of some combination of ATP or HMGB1 release and CAL exposure. In regard to necroptosis, I predict that cell death will not be dependent on necroptotic signalling or the activities of the proteins RIPK3, MLKL or RIPK1. From what is known about the activity of ICP6, I predict that disruptive modification of the RHIM will have the effect of increasing necroptotic signalling during infection, which should result in greater viral induced killing of cancer cells and a more favourable immunogenic profile.

## **2 Materials and methods**

## 2.1 Cell and virus culture

### 2.1.1 Cell lines

All cell lines were cultured in T-75 flasks at 37°C, 95% humidity and 5% CO<sub>2</sub>. Almost all cell lines were maintained in Dulbecco's Modified Eagle medium (DMEM; Thermofisher, 12491-015) supplemented with 100 µg/ml Penicillin and 100 µg/ml Streptomycin (P/S) (Thermofisher, 105070-063), 5 µg/ml L-Glutamine (Thermofisher, 25030-181) and 10% heat inactivated foetal bovine serum (FBS; Thermofisher) with the following exceptions: JHOC5, 7 and 9 cells were grown in DMEM/F-12 1:1 with glutamine (Thermofisher, 11320-033), supplemented with 10% FBS, and 1x minimal essential medium (MEM) non-essential amino acids (NEAA; Thermofisher, 11140-035). A2780, OVTOKO, and OVMANA cells were grown in RPMI 1640 medium with added 100 µg/ml P/S, 5 µg/ml L-Glutamine and 10% FBS. NK92 cells were grown in MEM-α supplemented with 12.5% FBS, 12.5% horse serum (Thermofisher, 26050-070), 5 µg/ml L-Glutamine and 5 ng/ml IL-2 (added fresh with every medium change). These recipes are all hereby referred to as “complete medium” when appropriate, with full addition of supplements to be assumed unless otherwise stated, such as “serum-free medium”.

All human cell lines were authenticated by 16 locus STR analysis (LGC Standards) prior to use and intermittently over the course of the project. Vero cells were the only non-human cell lines used and as such, could not be authenticated. Vero cells were a gift from Dr Sheila Graham, University of Glasgow; HeLa-RIPK3 expressing cells and TOV21G MLKL CRISPR-edited cells were made using lentiviral transduction by Dr M. Weigert, University of Glasgow.

All cells were kept in frozen stocks in liquid nitrogen in FBS containing 10% Dimethyl Sulfoxide (DMSO; Fisher Sci, D/4120) and defrosted by thawing quickly in a 37°C water bath, before resuspending in 10 ml of complete medium. Cells were then centrifuged at 1200 rpm for 5 min to pellet, supernatant aspirated, and cells resuspended once more in complete medium before plating into flasks.

Passaging of cells was done by aspirating complete medium, washing once with phosphate buffered saline (PBS), and treating with 2X Trypsin EDTA

(Thermofisher, 15400-054) in PBS at 37° C for approximately 5 min. Cells were dislodged by firm tapping and resuspended in culture media.

Cells were routinely tested for presence of mycoplasma infection by the Beatson CRUK Centre Reagent Service, using the MycoAlert™ detection kit, (Lonza, LT01-118).

### **2.1.2 Viruses**

HSV-1716 is a genetically modified strain of HSV-1 and was received as a kind gift from Dr J. Connor, Virttu Biologics, Glasgow. HSV-1716 was stored in sodium lactate solution containing 10% glycerol and aliquoted to minimise freeze-thaw cycles.

## **2.2 Cell infection and drug treatment**

### **2.2.1 Infection**

To assess the effects of HSV infection on various cell lines, cells were plated at the stated seeding density and left for 24 h before addition of virus. The amount of virus used was calculated as a measure of multiplicity of infection (MOI) meaning number of viable plaque-forming units (see below) per cell. 10-fold serial dilutions were made in serum-free culture medium to give desired single or multiple MOIs for use. Medium was aspirated from cells and replaced with appropriate dilutions of virus in serum free medium. Plates were then left for 2 h before being re-fed with an equal volume of complete medium added on top and plates then left for the desired amount of time.

### **2.2.2 Drug treatment**

For experiments involving treatment of cells with drug, appropriate dilutions were made in complete medium and drugs were added either 24 h after cell plating if being used alone, or during re-feeding after cell infection when used in combination with virus. The working concentrations and source of various drugs are listed in Table 2.1.

**Table 2.1: List of drugs used with working concentrations and suppliers.**

Name	Working Conc*	Company	Cat #
TNF- $\alpha$	20 ng/ml	Peprotech	300-01A
LCL-161 (SMAC mimetic)	1 $\mu$ M	ChemieTek	CT-LCL161
zVAD-fmk	25 $\mu$ M	APExBIO	A1902
Necrostatin-1 (Nec-1)	100 $\mu$ M	Enzo life sciences	BML-AP309
Necrosulfonamide (NSA)	3 $\mu$ M (refed after 48 h)	Calbiochem	CAS 432531-71-0
GSK2791840B (GSK'840)	2 $\mu$ M	GlaxoSmithKline	-
Cisplatin	3-10 $\mu$ M	Accord Healthcare, Harrow, UK via Beatson West of Scotland Cancer Centre chemotherapy pharmacy	-

\* Unless otherwise stated

### 2.2.3 Transfection of siRNA

Working concentrations and time points for siRNA transfection were determined in cell lines of interest by treating at a range of siRNA concentrations and times and analysing samples by Western blot to check for protein knockdown.

For the assay,  $1 \times 10^4$  cells were seeded per well of a 24-well plate in antibiotic-free culture medium and left for 24 h to adhere. In one tube, 0.75  $\mu$ l (per well) of DharmaFECT 1 (GE Dharmacon) was added along with 300  $\mu$ l (per well) of OptiMEM. In another tube, the appropriate amount of siRNA was added with enough OptiMEM to make a final volume of 300  $\mu$ l (per well). These tubes were mixed gently by pipetting and left at room temperature for 5 min. Then the contents of both tubes were mixed and left at room temperature for 20 min. After this, an appropriate amount of antibiotic-free medium was added to give enough for a final volume of 1 ml per well, which was then added following aspiration of the current cell media. Cells were then left for typically 24 h before infecting with HSV-1716 in the usual manner. After infection, cell

viability was determined by MTT assay, described below. Protein was harvested from some wells for protein quantification by Western blot.

## **2.3 Cell Viability Assays**

### **2.3.1 MTT cytotoxicity assay**

Thiazolyl Blue Tetrazolium Bromide (MTT; Sigma) was used to assess cell viability after virus or drug treatment in flat cell culture. Once the desired end-point was reached, stock MTT (5 mg/ml) was added directly to cell supernatant to give a final dilution of 1:10 and then left at 37°C for 2 h. After 2 h, supernatant was removed from cells and a uniform volume of DMSO was added to all wells (0.5 ml for 24-well plate, 1 ml for 12-well plate, 2 ml for 6-well plate), and plates were shaken for approximately 5 min at room temperature before being read at 570 nm on a TECAN plate reader.

### **2.3.2 Sytox nuclear staining for NK cell co-culture**

To determine the cell-killing effects of co-culture with natural killer (NK) cells, TOV21G cells were seeded into 96-well plates at a density of 3000 cells per well in a volume of 100 µl and left for 24 h to adhere. Cells were then infected with virus as normal by aspirating medium and replacing with 50 µl of serum-free medium, left for 2 h, and then re-fed by supplementing the wells with a further 50 µl of complete medium. Eight hours post infection, NK-92 cells were added at a ratio of 10:1 (NK-92:TOV21G) in an additional 50 µl complete RPMI medium. Green Sytox Cyanine Nuclei Acid dye (Cat number 4632; Essen Bioscience, USA) was added at the cell infection stage at a final volume of 150 nM.

Plates were then loaded onto an Incucyte ZOOM imaging system for 75 h, with one 10x magnification image taken every hour per well. Data were extracted from images with a processing definition set using the IncuCyte Live Cell Analysis software. NK cell Sytox values were excluded from images using a two-dimensional surface area cut-off of 125 µm<sup>2</sup>. Using this, green object count per well data was generated. Total area under the curve (AUC) analysis was done on

green object counts over time using Graphpad Prism to summarise cell death data over the duration of the experiment.

## **2.4 HSV production, purification and titration**

### **2.4.1 Virus production**

Vero cells were seeded in 100 mm dishes with approximately  $1 \times 10^6$  cells or until the dishes appeared more than 80% confluent. For virus purification, 20 dishes were used per virus. If there was not enough input virus to infect 20 dishes, then preliminary rounds of bulking were first performed using smaller cell amounts. Input viruses were only used if from a known pure source originating from a single plaque or well of a TCID<sub>50</sub> plate. Cells were infected with virus in a final volume of 20 ml serum free medium at MOI of 0.1 if known. If MOI was not known, then amount of virus to add was estimated based on the source. After 2 h, medium was removed and replaced with 20 ml of complete medium. Dishes were left for approximately 2-3 days or until 100% cytopathic effect is seen in the cells (rounding up and beginning to detach). Cells were scraped with a cell scraper to detach into the medium. Cell suspensions were then mixed together in to an appropriate number of 50 ml centrifuge tubes and snap frozen in liquid nitrogen. At this point, samples were either thawed immediately at 37°C to continue or stored at -80°C until ready to proceed.

### **2.4.2 Virus Purification**

Once thawed, tubes were spun at 3000 rpm for 15 min and then supernatant passed through a 40 µm cell strainer to remove debris. Supernatant was then spun at 18,000×g on an Optima XPN-90 ultracentrifuge in Beckman Coulter Ultra-Clear centrifuge tubes to pellet virions. Supernatant was removed by aspiration and the remaining viral pellets were resuspended in 1-10 ml of filter sterilised TSG buffer. TSG buffer consists of 70% Solution A (150 mM NaCl, 1 mM Na<sub>2</sub>HPO<sub>4</sub>, 5 mM KCl and 30 mM Tris Base), 0.35% Solution B (200 mM MgCl<sub>2</sub> and 180 mM CaCl<sub>2</sub>) and 29.65% glycerol. Finally, virus samples were passed through a 0.45 µm filter to purify. Titrations of purified stocks were performed to ensure accurate calculation of MOI when used later.

### 2.4.3 Titration of viral stocks

Virus titres were determined by plaque assay. For this,  $2 \times 10^5$  Vero cells were plated per well of a 12-well plate. After 24 h, a series of 10-fold dilutions were made for each virus sample in serum free medium by adding 450  $\mu$ l medium to the current tube, adding 50  $\mu$ l of sample from the previous tube, vortexing and repeating. The dilutions chosen for plating were based on the expected titre. If titre could not be estimated, then 6 dilutions ranging from  $10^{-2}$ - $10^{-7}$  were used per sample. The medium was removed from the cells, replaced with 200  $\mu$ l of each dilution and left for one hour. After this, 2 ml of overlay warmed to 37°C was placed on top, which consisted of a 50:50 mixture of 1.2% Avicel RC-591(FMC), and 2X MEM (Invitrogen). Cells were then incubated for 72 h before removing overlay by tipping plates over a bucket containing Virkon and replacing with 3.7% paraformaldehyde (PFA) for 1 h to fix cells. PFA was removed and replaced with 0.2% crystal violet (Sigma Aldrich) for a further hour before washing in water and scoring. To score plates, dilutions containing approximately 20-100 plaques were selected and counted. Titres were calculated in terms of plaque-forming units (pfu)/ml and could be calculated by using the following formula:

$$\text{Titre (pfu/ml)} = \frac{\text{Average number of plaques at dilution}}{\text{Inoculum in ml} \times \text{Dilution factor}}$$

## 2.5 Cloning techniques

### 2.5.1 DNA extraction from cells and viruses

DNA was extracted from cells using the Qiagen DNeasy Blood & Tissue Kit (69504). For this, cells were typically seeded into 6-well plates at a density of  $1 \times 10^6$  cells per well and left for 24 h to adhere. Cells were then treated with the appropriate drug or virus combination as outlined above. Once ready, cells were washed once with PBS and trypsinised, before first resuspending in complete medium. After this, cells were centrifuged to pellet, and then resuspended in 200  $\mu$ l PBS. To this, 20  $\mu$ l proteinase k was added, before a further addition of 200  $\mu$ l Buffer AL. At this stage, samples destined for viral DNA analysis were

heated at 56°C for 10 min to encourage capsid degradation before proceeding. Next, an addition of 200 µl 100% ethanol was made, followed by further mixing. This mixture was transferred to a DNeasy Mini spin column and centrifuged at >6000×g for 1 min. Several washes were performed by repeating this process, first with 500 µl of Buffer AW1, then with 500 µl Buffer AW2. DNA was eluted into 30 µl water by pipetting onto the membrane and centrifuging for 1 min.

For DNA extraction from pure virus concentrates, an appropriate volume of virus sample was diluted to a final volume of 200 µl with PBS before proceeding as outlined above. If the required volume of virus stock exceeded 200 µl, then volumes of all other reagents were increased correspondingly.

### **2.5.2 Polymerase chain reaction for amplification of DNA fragments**

PCR amplification of DNA was used as a step for both creation of expression plasmids and diagnostic analysis of experiments. Most PCR reaction samples were made using a final concentration of GoTaq Green Mastermix (1X) (Promega, M712), 1 µM forward and reverse primers and 50 ng DNA, with optimisation performed if necessary. Components were mixed in individual reaction tubes and run on an Applied Biosystems Verti thermocycler. Cycling conditions were typically 2 min at 95°C, then 35 cycles of [30 s at 95°C; 30 s at 58°C; 60 s at 72°C], and 5 min at 72°C.

### **2.5.3 Restriction enzyme digestion of DNA**

Restriction enzyme digestion of plasmids and DNA fragments was performed for both diagnostic analysis and construction of new plasmid constructs. All restriction enzymes were purchased from New England Biosciences (NEB) and used following the manufacturer's instructions. A typical 50 µl reaction consisted of 1 µg (for visualisation on gel) or 5 µg (for gel purification) of DNA, 1 µl restriction enzyme and 5 µl 10X buffer. The recommended buffers for single digests were used, and double digests were done based on the NEB double digest finder (<http://tinyurl.com/zf4yypr>). Enzymes used are shown in Table 2.2.

**Table 2.2: List of restriction enzymes used with buffer and supplier**

<b>Enzyme</b>	<b>Buffer</b>	<b>Manufacturer</b>
BbsI	2.1	NEB
BspHI	CutSmart	NEB
EcoRI	2.1	NEB
HindIII	2.1	NEB
SpeI	CutSmart	NEB
XbaI	CutSmart	NEB
XhoI	Cutsmart	NEB

### **2.5.4 Ligation**

Ligations were performed using a Rapid DNA Ligation kit version 10 (Roche, 11635379001). A 3:1 ratio of insert to vector DNA was typically used but optimised as necessary. In addition to DNA fragments, 10 µl of 2X annealing buffer and 1 µl of T4 ligase were added together with water to make a total reaction volume of 20 µl. Tubes were incubated at room temperature for 5 min, before either freezing at -20°C or directly using by diagnostic digestion or transformation.

### **2.5.5 TA ligation of PCR products into pCR TOPO 2.1 vector**

In order to sequence a DNA fragment, or for easy addition of restriction sites, PCR products were flipped into a pCR TOPO 2.1 vector (Invitrogen, K450002) by TA overhang ligation. The TOPO vector is pre-cut with thymidine overhangs, each bound to a molecule of topoisomerase. When combined, this enzyme recognises adenine overhangs left by the PCR reaction and recombines the fragments into a complete plasmid. To perform this reaction, 0.5-4 µl of PCR or gel extracted product was added to a 0.2 ml tube alongside 1 µl of provided salt solution and 1 µl of TOPO vector. The mixture was incubated at room temperature for 5-30 min and then directly transformed into TOP10 competent *E.coli* using the following protocol.

## **2.5.6 Separation and visualisation of DNA fragments on agarose gel**

Sizes of DNA fragments amplified by PCR were visualised by separation on an agarose gel. Gels were made by dissolving 2 g of agarose (Melford, M1200) in 200 ml of TAE buffer (40 mM Tris pH 7.8, 20 mM glacial acetic acid, 1 mM EDTA in dH<sub>2</sub>O) to give a concentration of 1%. Agarose was heated in short bursts in a microwave until fully dissolved and left to cool slightly for 10 min at room temperature before addition of 4 µl ethidium bromide (1:50,000 dilution) (Sigma Aldrich, E1510) to visualise DNA. Gels were poured and set in a Sub-Cell GT Cell, (Bio-rad, 1704402). PCR product (typically 5 µl) was loaded into the gel wells directly in GoTaq solution alongside a 1 kb Plus DNA Ladder (Invitrogen, 01787), which was loaded at a 5:1 ratio with Blue/Orange Loading Dye (Promega, G1881). Gels were run in a tank containing 1X TAE buffer at 100 V for approximately 60 min and imaged using ChemiDoc MP, (Bio-rad).

If bands were to be excised for purification, then gels were made at a concentration of 0.7% agarose, more PCR product was added, and gels were run at 25 V overnight for more discrete bands.

## **2.5.7 Gel extraction and purification of DNA**

DNA was extracted from gels using a QIAquick gel extraction kit (Qiagen, 28706). First DNA bands were visualised on a UV transilluminator, and bands of appropriate sizes cut out using a sterile scalpel and placed in Eppendorf tubes. Weights of the gels were measured, and QG buffer was added at a 3:1 ratio v/w and heated at 50 °C until melted. One volume isopropanol was then added and mixed before placing in a spin column. Columns were spun with DNA being caught by the membrane. Columns were then washed once each with buffers QE and PE respectively and eluted in to nuclease free water.

## **2.5.8 Determination of nucleic acid concentration**

DNA or RNA concentration was measured using a Nanodrop 2000 spectrophotometer (Thermofisher). Samples were used if the 260/280

wavelength ration was between 1.8 and 2.0 and the 260/230 ratio was greater than 1.7.

### **2.5.9 Transformation of competent *E.coli***

Circularised DNA plasmids were amplified by growth in transformed TOP10 chemically competent *E.coli* cells (Invitrogen, C404010). Tubes of cells were thawed on ice, then either used directly or split between two Eppendorfs to use for two different samples. Per tube, 2 µl of DNA was added and mixed gently by flicking, before being left on ice for 30 min. After this, tubes were heat pulsed by leaving in a 42°C water bath for 45 s. Tubes were then left on ice for at least 2 min to cool down and then mixed with 200 µl of the kit-provided SOC medium and incubated for 1 h on a shaker at 37°C. Between 20 and 200 µl of this was then added to agar plates based on estimated efficiency and incubated overnight at 37°C until colonies were formed. Agar plates were supplemented with either kanamycin or ampicillin, based on the antibiotic resistance gene in the plasmid being transformed.

### **2.5.10 Mini and Maxi preparation of DNA from *E.coli***

Transformed *E.coli* colonies were grown further by inoculation of tubes containing 4-5 ml of Lennox broth (LB) (Invitrogen, 12780-052) with supplemented antibiotic. LB consisted of 10 g/l peptone-140, 5 g/l yeast extract and 5 g/l NaCl, made up in dH<sub>2</sub>O and autoclaved before use. Inoculated tubes were cultured at 37°C overnight in a shaking incubator at 225 rpm. After this, cells were either pelleted by centrifugation for Mini-prep or used to further inoculate 200 ml of LB plus antibiotic for Maxi-prep.

For Mini-preps, tubes were centrifuged at 1120×g for 5 min, LB was aspirated, then plasmid DNA extracted using a Qiagen 8000 Robot and quantified using a Biophotometer 6131 (Eppendorf). At this point, presence of desired sequence was either confirmed by diagnostic restriction enzyme digestion or Sanger sequencing with an appropriate primer. All Mini-prep processes and sequencing was performed by at the Molecular Technology Service, CRUK Beatson CRUK Institute.

For Maxi-preps, conical flasks containing 200 ml of inoculated LB were incubated overnight at 37°C on a shaking incubator at 225 rpm. Broth was then decanted into a 250 ml conical flask and centrifuged at 2000 rpm (rotor JS 4.2) for 15 min. Medium was then aspirated and plasmid extracted by Maxi-prep at the Molecular Technology Service, CRUK Beatson CRUK Institute.

## **2.6 Creation of ICP6 expressing cell lines by lentiviral transduction**

### **2.6.1 Creation of lentiviruses from plasmid constructs**

Lentiviral plasmids containing cDNA for various ICP6 constructs were received as a kind gift from Prof E. Mocarski, Emory University (Table 2.3). Plasmids were prepped and purified using the protocols above before transfection into 293T cells in order to produce lentiviruses. Transfection was done in 10 cm plates, wherein  $2 \times 10^6$  cells were seeded and left for 24 h. Plasmids were added together in the amounts shown below in one tube with 1.5 ml of Opti-MEM and vortexed. In another tube, 45  $\mu$ l of Lipofectamine™ 2000 was added to the remaining 1.5 ml of Opti-MEM and mixed gently. Tubes were left at room temperature for 5 min before the two tubes were combined to give a plasmid/Lipofectamine™ mix and left for a further 20 min for micelles to form around the DNA. Medium from the 293T cells was then aspirated and replaced with 5 ml antibiotic-free medium. The Opti-MEM mix was then added on top and left for 16 h overnight. After this, medium was replaced with 10 ml complete medium. After another 32 h, supernatant was harvested, spun to remove debris, and stored at -80°C or used immediately. Lentivirus reagent quantities are summarised in Table 2.4.

**Table 2.3: ICP6-expressing plasmid information and naming.**

Plasmid Name	Insert	Vector
pLV-ICP6_FL	Flag tagged Full length ICP6	pLV-EF12-MCS-IRES-Puro
pLV-ICP6 (mutRHIM)	Flag tagged Full length ICP6 with AAAA substitution in place of RHIM aa 75-78	pLV-EF12-MCS-IRES-Puro
pLV-ICP6 ( $\Delta$ 1-243)	Flag tagged ICP6 deleted in the first 729 nucleotides	pLV-EF12-MCS-IRES-Puro
pLV-ICP6 (244-629)	Flag tagged ICP6 deleted in the first 729 nucleotides and last 1524 nucleotides	pLV-EF12-MCS-IRES-Puro

**Table 2.4: Lentivirus reagent quantities for cell line transduction.**

Component	Amount
pLV-cDNA vector	9 $\mu$ g
Gag-Pol + Rev expression vector (psPAX; Addgene)	6 $\mu$ g
VSV-G expression vector (pCMV-VSV-G; Addgene)	3 $\mu$ g
<b>Total plasmid DNA</b>	<b>18 <math>\mu</math>g</b>
Lipofectamine™ 2000	45 $\mu$ l
Total Opti-MEM	3 ml

## 2.6.2 Transduction of cell lines with lentiviruses

Target cells were grown in 6-well plates at a density that allowed for 25-50% confluence at time of transduction. Lentiviral stocks were thawed and mixed with polybrene to give a final concentration of 5  $\mu$ g/ml. Medium from cells was aspirated and replaced with approximately 3 ml lentiviral supernatant. The next day, supernatant was removed and replaced with 2 ml complete medium. After 48 h of transduction, puromycin was added in fresh complete medium at a

concentration of 1 µg/ml and cells were monitored until complete death was seen in the untransduced control well.

### **2.6.3 Dilution cloning of ICP6 cells**

Once selected for, transduced cells were expanded until presence of ICP6 could be confirmed by Western blot. Once confirmed, fresh cells were dilution cloned. First, a cell suspension was made and diluted using serial dilutions to form a total volume of 40 ml containing 400 cells. Of this, 200 µl was then dispensed into each well of a 96-well plate to give an average dilution of 2 cells per well. After a few days, wells were manually checked by microscope to identify wells with single colonies. These were later trypsinised and expanded before being checked for ICP6 expression by Western blot.

## **2.7 CRISPR/Cas9 gene editing of HSV-1716.**

### **2.7.1 Guide design**

Three gRNA sequences were designed to target three separate sites within the RHIM domain of ICP6, using the online <http://crispr.mit.edu/> tool.

### **2.7.2 Transfection**

Vero cells were plated in 6-well plates at a density of  $1 \times 10^5$  cells/well and transfected with a px459 plasmid containing the Cas9 gene and the guide RNA sequence of interest. Cell media was changed 24 h following transfection. After 48 h, media was replaced to contain 2.5 µg/µl puromycin and left for a further 48 h, or until significant cell death was seen in untransfected wells. After this, two control wells were trypsinised and counted in order to calculate an MOI of 1. Cells were infected in 1 ml serum-free medium for 2 h and then supplemented with a further 1 ml of complete medium. After 48 h, cells were removed by scraping and kept suspended in medium, before being snap-frozen in liquid nitrogen and thawed in a 37°C water bath three times.

### **2.7.3 Isolation of viral clones**

Vero cells were plated at a density of  $1 \times 10^4$  cells/well in 200  $\mu$ l in 96-well plates. Serial dilutions of the virus clonal pool were made across the plates to give a total of 6 dilutions of 12 replicates per plate. Four plates were used per guide to give a total of 48 replicates per dilution. The plates were incubated at 37°C for 2-5 days until full cytopathic effect was seen in most wells. Plates were scored to determine which wells had been infected by a single viral particle and these wells were isolated by pipetting to dislodge cells and freeze-thawing three times in liquid nitrogen.

### **2.7.4 Screening for gene edited viral clones**

Clones were first screened for presence of ICP6 protein expression by infecting Vero cells with 5  $\mu$ l of virus for 24 h, harvesting protein and staining on an immunoblot for ICP6. To identify clones which contained mutations conferring no effect on protein expression, the surveyor assay was used. This involved mixing equal quantities of mutant and wild type DNA, amplified by primers spanning a 300 bp segment of the gene surrounding the target site. These were then denatured at 95°C for 10 min and allowed to hybridise by cooling gradually to 25°C. Afterwards, 400 ng of sample was mixed with 1  $\mu$ l of nuclease and enhancer and left on ice for 1 h. The nuclease causes double strand breaks at regions that contain a mismatch, which can be visualised on an agarose gel.

## **Sequencing**

PCR fragments that were amplified previously were cloned into pCR-TOPO 2.1 plasmids by mixing 0.5-2  $\mu$ l of DNA with 1  $\mu$ l of enzyme in a 5  $\mu$ l reaction and leaving for 5 min at room temperature. These sequences containing plasmids were transformed into TOP10 chemically competent *E.coli*, which were then Mini-prepped and sequenced in house by Sanger sequencing.

## 2.8 Quantitative PCR

### 2.8.1 Viral replication

Cells were seeded at a density of  $1 \times 10^5$  per well in 6-well plates and left for 24 h to adhere. Cells were then infected with HSV-1716 at MOI 1 in serum free medium, refed with complete medium after 2 h. At 0, 8, 16, 24 and 48 h post infection, DNA was extracted using the Qiagen blood and tissue kit as described. A standard curve of purified HSV-1716 DNA was used to determine viral copy number. For this, DNA was extracted from purified viral stocks using the Qiagen blood and tissue kit, with concentration determined by Nanodrop. The following equation was used to calculate viral genome copy number from DNA concentration:

$$\text{Copy number (molecules)} = \frac{C \times N_A}{(L \times 660) \times 10^9}$$

Where:  $C$  = concentration of DNA in ng

$N_A$  = Avogadro's constant ( $6.0221 \times 10^{23}$ )

$L$  = length of DNA in bp (152,000 for HSV-1716 genome)

660 = average mass of 1bp in g/mole

$10^9$  = conversion of ng to g

Appropriate dilutions of viral DNA were then made to form a standard curve spanning  $1 \times 10^8$ - $6.4 \times 10^3$  genome copies. For the PCR reaction, 50 ng of DNA was added to each well of a 96-well qPCR plate (Bio-Rad) along with 18  $\mu$ l of master mix, giving a final concentration of 1X Bio-Rad universal probes, 900 nM forward primer, 900 nM reverse primer, and 250 nM corresponding fluorophore-tagged probe. Nuclease-free water was added to make up reaction volumes to 20  $\mu$ l. Plates were run with the cycling parameters described in Table 2.5.

**Table 2.5: Standard qPCR cycling conditions.**

Temperature	Time
50 °C	2 min
95 °C	3 min
<b>40 cycles of the following:</b>	
95 °C	10 s
60 °C	60 s

## **2.8.2 RNA extraction for RT-PCR from cells**

RNA from cells in culture was extracted using the Qiagen RNeasy Plus mini-kit (74106). Cells were seeded in a 6-well plate at a density of  $1 \times 10^6$  cells/well and left for 24 h to adhere. Cells were washed once with PBS and trypsinised before being resuspended in buffer RLT containing 1%  $\beta$ -mercaptoethanol ( $\beta$ -ME). Equal volume of 70% ethanol was then added to the samples. This is then transferred to an RNeasy Mini spin column, where it was spun at  $8000 \times g$  for 1 min. Columns were washed by adding buffer and centrifuging  $8000 \times g$  for 1 min. Washing was performed first with buffer RW1, before an on-column DNase digestion was performed using 80  $\mu$ l of the prepared DNase solution at room temperature for 15 min. One further wash was performed with RW1, followed by two washes with buffer RPE. RNA was eluted into 30  $\mu$ l of RNA/DNase-free water, aliquoted and stored at  $-80^\circ\text{C}$ .

## **2.8.3 Complementary DNA (cDNA) generation**

For standard RT-PCR, cDNA was generated using the High-Capacity cDNA Reverse Transcription Kit (Applied Biosystems, 4368814). For this, 1  $\mu$ g of RNA was diluted into a total of 10  $\mu$ l per sample. RT 2X master mix was prepared by combining RT Buffer, dNTP Mix, RT Random Primers, and MultiScribe™ reverse transcriptase, diluted to 2X concentrations. 10  $\mu$ l of master mix was added to each 10  $\mu$ l sample to give a total reaction volume of 20  $\mu$ l. Samples were run on an Applied Biosystems Veriti 96-well thermocycler under the conditions described in Table 2.6.

Table 2.6: cDNA generation thermocycler conditions.

	Step 1	Step 2	Step 3	Step 4
Temperature (°C)	25	37	85	4
Time	10 min	120 min	5 min	∞

## 2.8.4 qPCR following reverse transcription

The qPCR protocol outlined above for 'Viral Replication' was used, following cDNA generation.

## 2.8.5 RT<sup>2</sup> Profiler array

The RT<sup>2</sup> Cytokines and Chemokines array (Qiagen, PAHS-150ZE) was used to determine differences in transcript levels of 84 cytokines and chemokines between HSV-1716 and HSV-3D7 infected cells. Cells were seeded in a 6-well plate at a density of  $1 \times 10^6$  cells/well and left for 24 h to adhere. Cells were infected following the standard protocol. RNA from cells was extracted using the Qiagen RNeasy Plus mini-kit. RNA was only used if it had a A260:A230 ratio of greater than 1.7 and a A260:A280 ratio of 1.8 to 2.0. In addition to this, RNA samples were required to have an RNA integrity number (RIN) of greater than 7

Synthesis of cDNA for the array was done using the RT<sup>2</sup> First Strand Kit (Qiagen; 330401). For this, a genomic DNA elimination step was first performed by mixing 800 ng of sample RNA per array (one sample per 384-well plate array) with 2  $\mu$ l Buffer GE, then making up to a final volume of 10  $\mu$ l with nuclease-free water. This mix was incubated for 5 min at 42 °C and then immediately transferred to ice. For the reverse transcription, a mastermix was prepared containing Buffer BC3, Control P2, RE3 Reverse Transcription Mix as per manufacturer's instructions, and then added in a 1:1 ratio with the 10  $\mu$ l sample from the previous step. This was incubated at 37 °C for 60 min, followed by a 95 °C incubation for 5 min to stop the reaction.

For the PCR, samples prepared in the previous steps were mixed with the 2X RT<sup>2</sup> SYBR Green Mastermix and water to give a final volume of 1300  $\mu$ l per sample. Of this, 10  $\mu$ l was dispensed into each well of the array plate before sealing the

plate with the provided cover and centrifuging for 1 min at 1000×g. The programme was run on an Applied Biosystems 7500 Fast Real-time PCR System consisting of the parameters described in Table 2.7.

**Table 2.7: RT<sup>2</sup> cytokine and chemokine profiler array cycle conditions.**

Cycles	Duration	Temperature
1	10 min	95 °C
40	15 s	95 °C
	1 min	60 °C

## 2.9 Protein expression levels

### 2.9.1 Preparation of whole cell lysates

To extract protein from cultured cells,  $1 \times 10^6$  cells were typically seeded in 6-well plates and left for 24 h before treating. When ready, cells were trypsinised, centrifuged at 1200 rpm for 5 min to pellet, and lysed in RIPA buffer (150 mM NaCl, 10 mM Tris pH 7.8, 1 mM EDTA, 1% Triton X-100, 0.1% SDS) with freshly added protease inhibitor cocktail (Roche) at a concentration of 1 tablet per 10 ml and 1% phosphatase inhibitor (Sigma; P5726). Samples were then centrifuged at 15000 rpm for 20 min at 4 °C to remove cellular debris and transferred to a new 1.5 ml Eppendorf tube.

### 2.9.2 Determination of protein concentration

Protein concentration was measured by Bradford assay, whereby 5 µl of sample was diluted in 45 µl of PBS to create a 1:10 dilution. Protein standards were made by dissolving a known mass of bovine serum albumin (BSA; Sigma) in water and diluting to make concentrations ranging linearly from 0-0.5 mg/ml. Wells of a 96-well plate were loaded with 10 µl of either standard or diluted sample, with 200 µl of working Bradford (Bio-rad; 1:5 dilution in dH<sub>2</sub>O) solution on top. Plate was left for approximately 5 min at room temperature to allow colour change to form, before being read at 595 nm on a TECAN microplate reader.

### **2.9.3 Preparation of polyacrylamide gels**

Gels were prepared using the Bio-rad Mini-Protean tetra Handcast System and consisted of 8% polyacrylamide (National Diagnostics, EC-890), 375 mM Tris HCL pH8.8 (Sigma), 0.1% SDS, 0.1% ammonium persulphate (APS) and 0.06% tetramethylethylenediamine (TEMED; Sigma) for the resolving portion and 5% polyacrylamide, 125 mM Tris HCL pH6.8, 0.1% SDS, 0.1% APS and 0.1% TEMED for the stacking portion. The above preparations were made up in dH<sub>2</sub>O in the order stated and mixed gently before pipetting into casts, one gel portion at a time, allowing approximately 20 min for setting of the resolving gel before adding stacking gel on top with well comb. Gels were either used immediately or stored at 4° C in dH<sub>2</sub>O.

### **2.9.4 Preparation of samples**

To prepare protein samples for separation sodium dodecyl sulphate polyacrylamide gel electrophoresis (SDS-PAGE), lysates were diluted to a concentration typically ranging from 0.5-1 µg/µl (depending on the amount of protein available) in lammeli buffer (300 mM Tris-HCL, 10% SDS, 50% glycerol, 20% B-ME, 3.7 mM bromophenol blue) and boiled at 95° C for 10 min. Samples were cooled to room temperature before running.

### **2.9.5 SDS-PAGE and Western blotting**

Of the boiled sample, 20 µl was loaded per well of the gel, alongside 8 µl of prestained protein standards (Novex) and run at 120 V for approximately 90 min, or until good separation at the target molecular weight was seen. Running buffer consisted of 20 mM Tris HCL, 190 mM Glycine, and 0.1% SDS made up in qH<sub>2</sub>O. After separation, proteins were transferred to a nitrocellulose membrane (Amersham) by wet blotting using a Bio-rad Mini-Protean Tetra Transfer System. Transfer buffer consisted of 20 mM Tris HCL, 190 mM Glycine, and 20% methanol made up in qH<sub>2</sub>O. Sponges, filter papers and nitrocellulose membranes were soaked in transfer buffer, before assembly of a sandwich, consisting of one sponge, one filter paper, gel, membrane, filter paper and sponge. At each point of assembly, a roller was used to ensure removal of air bubbles. The assembled

sandwich was placed into the transfer cassette, into the tank with 1 L of transfer buffer and an ice pack, and run at 100 V for 60 min.

### **2.9.6 Antibody staining**

After membrane transfer, membranes were blocked by incubating for 1 h at room temperature in 5% (w/v) non-fat milk (Marvel) made up in TBST buffer (150 mM NaCl, 20 mM Tris Base, 0.1% Tween20, pH7.6). After blocking, membranes were washed briefly in TBST before incubating with primary antibody diluted in TBST, either for 1 h at room temperature or overnight at 4°C. Membranes were then washed three times for 5 min with TBST before incubation with HRP-conjugated secondary antibody made up in TBST for 1 h at room temperature. Membranes were washed again, three times for 5 min and then developed for detection by removing the liquid from the membrane and adding a 1:1 mixture of ECL (GE Healthcare, RPN2106) or ECL prime (GE Healthcare, RPN2232) detection reagent on top. Chemiluminescence was detected on a Bio-rad Chemidoc, with exposure time varying based on intensity of signal.

### **2.9.7 Co-immunoprecipitation**

To prepare cell lysates for co-immunoprecipitation (CoIP),  $1 \times 10^6$  HeLa-RIPK3 cells were seeded in a 100 mM dish and left for 24 h to adhere. Cells were either mock infected, or infected with either HSV-1716, HSV-3B1, HSV-3D7 at MOI 1 in 15 ml of serum-free medium, and re-fed 2 h later with complete medium. After 24 h, media was removed from cells and transferred labelled 50 ml falcon tubes. The cells were washed once with 20 ml PBS, which was subsequently removed and added the same tubes, and treated with 3 ml trypsin per plate for approximately 5 min at 37°C. Trypsinised cells were dislodged by gently tapping the side of the dish, and resuspended in 10 ml of complete medium, before being added to the same falcon tubes. Collection of all medium and washes was done to ensure any floating or dead cells were still harvested.

Tubes were spun at 1200 rpm for 5 min to pellet cells, resuspended in 10 ml PBS and spun again under the same conditions to pellet again. The pellet was then resuspended in 1 ml of Nonidet-P40 buffer (10 mM Tris pH8.0, 150 nM NaCl, 1%

Nonidet-P40) with freshly added protease inhibitor cocktail (Roche) at a concentration of 1 tablet per 10 ml and 1% phosphatase inhibitor (Sigma; P5726) and left to lyse on ice for 15 min. Lysates were spun at 14000 rpm for 20 min at 4°C to pellet debris and transferred to fresh 1.5 ml Eppendorf tubes.

Protein concentration was measured by Bradford assay as described previously and used to calculate the necessary dilutions needed to prepare 0.5-1 mg protein in 500 µl of Nonidet-p40 buffer. For this, 3 µg of the desired antibody was added directly and the tubes incubated on a rolling wheel at 4°C for 2 h. Afterwards, 15 µl of magnetic beads (Dynabeads Pan Mouse IgG; Invitrogen) were added to each sample and incubated for a further 2 h at 4°C on a shaker. Immunoprecipitation was then performed using a magnetic rack to separate the magnetic bead-bound material from the supernatant. Supernatant from this initial pull-down was kept and beads were resuspended in 500 µl Nonidet-P40 buffer to wash. Three of these washes were performed in total before finally suspending beads in 20 µl of lammeli buffer. Samples were heated at 95°C for 10 min to denature proteins and their interactions, before a final precipitation of the magnetic beads and transfer of supernatant to a new 1.5 ml Eppendorf. Protein samples were then analysed by following the above SDS gel and Western blot protocols. A list of all antibodies used for Western blotting and CoIP can be found in Table 2.8.

Table 2.8: List of antibodies and suppliers used.

Primary antibodies				
	Origin	Supplier	Catalogue number	Dilution in TBST for immunoblot
Anti-human RIPK1	Mono-rabbit	Cell Signalling Technology	8737	1:1000
Anti-human RIPK3	Poly-rabbit	Novus	NBP2-24588	1:200
Anti-human MLKL	Mono-rat	EMD Millipore	MABC604	1:1000
Anti-human $\beta$ -actin	Mono-mouse	Sigma	a1978	1:5000
Anti-HSV1	Poly-rabbit	Dako	B0114	1:3000
Anti-ICP6	Poly-rabbit	Described, Conner et al., 1993	-	1:1000
Secondary antibodies				
Anti-rabbit	Poly-goat	Dako	P0448	1:3000
Anti-mouse	Poly-goat	Dako	P0447	1:3000
Anti-rat	Poly-rabbit	Dako	P0450	1:3000
CoIP antibodies				
	Origin	Supplier	Catalogue number	Amount used ( $\mu$ g)
Anti-human RIPK3	Mono-mouse	Santa Cruz	Sc-374639	3
IgG control	Mono-mouse	Abcam	ab37355	3

## 2.9.8 Fluorescent antibody detection array

To analyse the levels of an array of chemokines following viral infection,  $1 \times 10^6$  of either TOV21G, HeLa-Lzrs or HeLa-RIPK3 cells were seeded into each well of a 6-well plate for 24 h. After this, cells were infected with either HSV-1716 or HSV-3D7 at MOIs of 2 (TOV21G) or 2.5 (HeLa), giving a final volume of 2 ml/well. After 16 h, supernatants were harvested while simultaneously treating cells with MTT to determine viability. Supernatants were spun at 1200 rpm for 10 min to pellet any debris and then immediately frozen at  $-80^\circ\text{C}$  until needed.

Once conditions were found which led to similar levels of cell death, supernatants were defrosted at room temperature and tested for presence of chemokines using a Raybio C-Series Human Chemokine Antibody Array C1 (AAH-CHE-1). For this, the array chip was equilibrated to room temperature, and then blocked with 100  $\mu$ l blocking buffer for 30 min at room temperature. Blocking buffer was then aspirated and replaced with 100  $\mu$ l of each sample for 2 h at room temperature. The chip was then washed with each of the wash buffers provided for 2 min, three times and incubated with 70  $\mu$ l biotin-conjugated anticytokines for 2 h at room temperature with gentle rocking. After a repeat wash, 2 ml of HRP-streptavidin was added to each well and incubated for 2 h at room temperature. After a further set of washing, 70  $\mu$ l of streptavidin-fluor was added to each well and incubated for 2 h in the dark before more of the same washes. The chip was then removed from its casing and rinsed with dH<sub>2</sub>O, before leaving to air dry in a laminar flow hood. Once dry, the chip was packaged and sent to be read with an Innopsys' InnoScan® using cy3 or "green" channel (excitation frequency = 532 nm).

## **2.10 Flow cytometry**

### **2.10.1 Cell surface expression of Calreticulin**

To analyse the surface expression of calreticulin following virus or drug treatment,  $8 \times 10^5$  cells were first seeded in to a 6-well plate and left for 24 h to adhere. Cells were infected or treated as described earlier for 1-24 h before fresh collection of samples for flow cytometry.

First cell medium was removed and placed in a 14 ml Falcon tube. Cells were then washed with PBS and trypsinised, with all resulting waste fluid being added to the same tube. Each subsequent wash was made by spinning cells at 1200 rpm for 5 min, aspirating supernatant and resuspending cells. Cells were washed once in protein containing FACS buffer (PBS, 2% calf serum, 1 mM EDTA, 0.1% sodium azide) before being transferred to a 5 ml round bottom polystyrene FACS tube (Falcon; 352054). FACS buffer was removed and cells were resuspended in 100  $\mu$ l FACS buffer, before adding 10  $\mu$ l of buffer containing 500 ng of PE-conjugated CAL or isotype control antibody. Samples were left to incubate for 30

min at 4°C, then were washed once with protein-free FACS buffer before being resuspended in the same buffer containing a 1:1000 dilution of Zombie Violet™ viability dye. This was incubated for 10 min at 4°C. Samples were then washed once in protein-containing FACS buffer, fixed in 3.7% PFA for 5min at room temperature, washed once more in FACS buffer before analysing by flow cytometry.

### **2.10.2 Annexin V/Zombie Violet staining for determination of cell death**

For this,  $8 \times 10^5$  cells were seeded in a 6-well plate before receiving virus or drug treatment as described. First cell medium was removed and placed in a 14 ml Falcon tube. Cells were then washed with PBS and trypsinised, with all resulting waste fluid being added to the same tube. Each subsequent wash was made by spinning cells at 1200 rpm for 5 min, aspirating supernatant and resuspending cells. Cells were washed with protein-free FACS buffer, before suspending in a 1:1000 dilution of Zombie Violet™ Viability dye, which was incubated for 10 min at 4°C. After this, cells were washed with protein-containing FACS buffer once and then once with 1X Annexin V binding buffer (Biolegend; 422201). Cells were then resuspended in 100 µl of 1X Annexin V binding buffer, with 5 µl of FITC-conjugated Annexin V added on top and left to incubate for 15 min at room temperature. After this, cells were washed again in binding buffer, and fixed by suspending in 3.7% PFA for 5 min at room temperature. One more wash in binding buffer was done before analysis by flow cytometry.

### **2.10.3 Analysis by flow cytometry**

Samples were analysed on a BD FACSVerse™ system. Cell debris was gated out based on FSC-A and SSC-A values. Doublets were removed by plotting FSC-A against FSC-H. In the case of the CAL assay, Zombie Violet™ staining was used first to eliminate dead cells before taking measurements. Data was analysed using FlowJo™ 10 software. A list of flow cytometry antibodies can be found in Table 2.9.

**Table 2.9: List of flow cytometry antibodies used with suppliers**

Name	Fluorophore	Origin	Supplier	Catalogue number	Quantity
Anti-Calreticulin	PE	Mouse FMC75 IgG1	Enzo Life Sciences	ADI-SPA-601PE	500 ng/test
Annexin V	FITC	-	Biolegend	640906	450 ng/test
Zombie Violet™ viability dye	-	-	Biolegend	423113	1:1000 dilution

## 2.11 Transmission Electron Microscopy

TOV21G cells were grown in T-75 flasks at a density of  $5 \times 10^6$  for 24 h before treating or infecting following the protocols outlined above, using 7.5 ml serum-free medium, then re-feeding 2 h later with complete medium. Cells were treated for 48 h before washing once with PBS, and then fixed with a 2.5% glutaraldehyde, 0.1 M sodium cacodylate buffer for 1 h at 4°C. Cells were scraped off the surface off the flask and suspended in 0.1 M sodium cacodylate with 2% sucrose, then spun to pellet. The pellet was then washed three times for 5 min in the same buffer, making sure to keep the pellet intact each time. All future washes were performed by aspirating and replacing the liquid carefully, keeping the pellet intact. The remaining steps were performed either by, or with substantial help from Margaret Mullin, University of Glasgow. Samples were post-fixed in 1% osmium tetroxide, 0.1 M sodium cacodylate for 1 h at room temperature. Samples were washed three times in distilled water for 10 min before staining with 0.5% aqueous uranyl acetate for 1 h in the dark. Two more washes were performed in distilled water for 1 min each before beginning a dehydration series. For this, pellets were placed in solutions containing 30%, 50%, 70%, and 90% ethanol respectively in ascending order and for 10 min each. Four washes were then performed in absolute ethanol, followed by three 5 min washes in propylene oxide. Samples were then left in 1:1 propylene oxide: araldite/epoxy812 resin overnight for the propylene oxide to evaporate. Samples were then transferred to pure araldite/epoxy812, with 2-3 changes made throughout the day, before leaving overnight. Once in a final set of resin,

samples were added to flatbed moulds and sealed in by polymerising the resin with a 60°C incubation for 48 h. Sections of about 6070 nm width were cut using a LEICA Ultracut UCT and DIATOME diamond knife at an angle of 6°. Sample sections were picked up on 100mesh formvar coated copper grids then contrast stained with 2% Methanolic Uranyl Acetate for 5 min, followed by Reynolds Lead Citrate for 5 min.

Images were taken on a FEI Tecnai T20 (Zeiss, UK) at an accelerating voltage of 200 kV, using the GATAM Digital Imaging system.

## **2.12 Luminescence detection of ATP release**

ATP release following HSV-1716 or HSV-3D7 infection was measured using a luminescence-based assay kit (Abcam, ab113849). For this,  $2 \times 10^4$  TOV21G cells were seeded per well of a 96-well plate and left for 24 h to adhere. Cells were then infected with a range of MOIs for HSV-1716 and HSV-3D7 in a volume of 50 µl serum-free medium, and then refed with 50 µl complete medium 2 h later. Infected cells were incubated for 48 h before assessing ATP release. For this, 90 µl of supernatant was harvested from each well and deposited into the corresponding well within a 96-well opaque white plate. A standard curve dilution series of purified ATP was made in complete medium ranging from 10 pM-10 µM. Of each standard dilution, 90 µl was also added to the new white plate. To each of these wells, 50 µl of substrate solution was added. The plate was then covered and placed in a PHERAstar luminometer, where it was shaken for 5 min and left to dark adapt for 10 min before determining luminescence. In parallel, cell viability was determined by MTT on the cells remaining in each well.

## **2.13 Statistical analyses**

Statistical tests were performed using Graphpad Prism software. Unless otherwise stated, all data points plotted represent mean values from technical repeats  $\pm$  standard deviation (SD). In some cases, individual biological repeats

are displayed as dot plots, which include individual data points as well as mean  $\pm$  SD.

Exact statistical tests used are stated in each case. Student's two-way t tests were used when comparing two conditions alone. When comparing a set of means in a single group, one-way ANOVA was performed. In order to control the Type I error rate, statistical significance was determined by doing a multiple comparisons test with an appropriate correction method. For comparing all means in a set with each other, Tukey correction was applied; for comparing every mean with one control mean, Dunnett's correction was applied; for any other selected subset of means, Sidak correction was used. If two or more groups of data were to be compared, a two-way ANOVA was used. In all instances, cut offs for statistical significance were as follows: \*,  $p < 0.05$ ; \*\*,  $p < 0.01$ ; \*\*\*,  $p < 0.001$ ; \*\*\*\*,  $p < 0.0001$ . Gaussian distribution was assumed in all tests.

In instances where two sets of data were correlated, correlation coefficients are given, denoted by  $r$ . Linear regressions were also performed in tandem to display a line of best fit. Values for  $r$  were interpreted with the following boundaries: 0, no linear relationship;  $\pm 0.3$ , a weak linear relationship;  $\pm 0.5$ , a moderate linear relationship;  $\pm 0.7$ , a strong linear relationship;  $\pm 1$ , a perfect linear relationship.

### **3 Basic observations of HSV-1716 in cancer cells**

### 3.1 Introduction

To begin investigating the specifics of HSV-1716 infection in OC cells, it was first important to perform some basic characterisation experiments to determine the efficacy of HSV-1716 as a potential treatment for OC. For this, viral replication and killing was assessed in a range of cancer cell lines.

In 2013, Domcke *et al.* assessed the suitability of a range of commonly used OC cell lines as models of HGSOC. Many of the cell lines that appear in this thesis were assessed in the study (OVCAR4, COV31G, JHOC5, OVTOKO, OVMANA, SKOV3, IGROV1, A2780, TOV21G). It was shown that some of the most cited cell lines (including SKOV3, IGROV1 and A2780) are in fact genomically unlike HGSOC primary tumours, due to lack of characteristic mutations in genes such as *TP53*, abnormally high copy-number alterations, and/or presence of hypermutated phenotypes (IGROV1). OVCAR4 and COV318 cells were shown to be highly representative of HGSOC, with both possessing mutations in *TP53*, and COV318 possessing an additional *CCNE1* amplification. TOV21G cells were found to be more representative of CCC, which was the histological designation given at the time of isolation. These cells possess a mutation in *ARID1A*, which is found in approximately 50% of CCCs, but are also hyper-mutated. This information will have to be carefully taken into consideration when analysing the clinical relevance of any findings outlined in this thesis.

There have been a number of preclinical studies involving the use of HSV-1716 in OC (Coukos *et al.*, 1999; Benencia, Courrèges, Conejo-García, Buckanovich, *et al.*, 2005; Benencia *et al.*, 2008). However, none of these has assessed the killing capabilities of the virus across such a large panel of ovarian cell lines, or in a panel that has been as well characterised.

In addition, some basic experiments concerning the sensitivity of OC cells to necroptosis were performed. These experiments serve as a foundation for the cell death experiments to come and help to identify particular cell lines that may have desirable properties.

## 3.2 HSV-1716 replicates within human ovarian cancer cells

To assess the infectious properties of HSV-1716 in OC cells, a panel of established OC cell lines was infected with HSV-1716 at an MOI of 1 and incubated for 24 h before extracting protein from the samples and analysing by immunoblot (Figure 3.1a). Blots were stained under these conditions using a polyclonal anti-HSV antibody. The presence of staining was evident in all cell lines tested under these conditions, suggesting that HSV-1716 could successfully infect and produce protein in these cell lines. The intensity of staining did not appear to vary greatly between lines, suggesting that their permissiveness to viral protein production was similar.

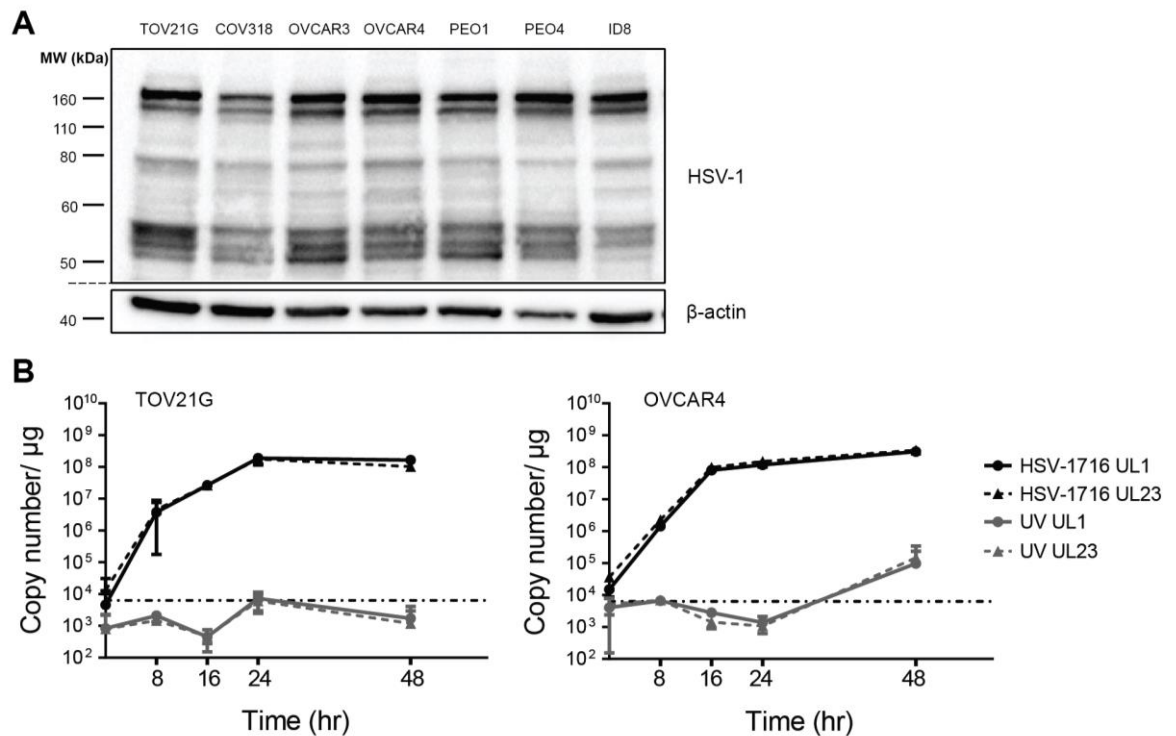


**Figure 3.1 Replication of HSV-1716 within ovarian cancer cells.** OC cell lines were infected with HSV-1716 at an MOI of 1 and left for 48 h before harvesting lysates for immunoblot, stained for either HSV protein or  $\beta$ -actin. (B) TOV21G (left) or OVCAR4 (right) cells were each infected with either live or UV-inactivated (UV) HSV-1716 at MOI 1 and left for 8, 16, 24 or 48 h before extracting cellular DNA. Quantitative PCR was performed to determine number of HSV genome copies per  $\mu$ g of total DNA, following use of one of two primers targeting genes UL1 and UL23. Dotted line represents the lower limit of detection based on lowest standard curve concentration. Data points are represented as mean  $\pm$  SD. MW, molecular weight; kDa, kilodaltons; hr, hour;

To further demonstrate that HSV-1716 was capable of replication within OC cells, two cell lines from this panel, TOV21G and OVCAR4 were infected with HSV-1716 at an MOI of 1 for up to 48 h to observe genome replication (Figure 3.1b). For this, whole cell DNA was extracted at 8, 16, 24 and 48 h time points and qPCR was performed using primers for two distinct genome regions, which corresponded to the viral genes UL1 and UL23. UL1 encodes glycoprotein L, which resides within the external lipid bilayer of the virion and is crucial for viral entry. UL23 encodes a thymidine kinase that catalyses the conversion of thymidine to thymidine-5'-phosphate. Distinct genome regions were chosen to illustrate that replication of the entire genome was taking place, and not just certain regions. In both cell lines, HSV-1716 was shown to increase in genome copy number after 8 h of infection, with copy number continuing to increase up until 24 h. After 24 h, in TOV21G it plateaus, and in OVCAR4 the increase continues until 48 h at least. In comparison, cells infected with HSV-1716 that had been inactivated by exposure to UV light showed almost no replication above baseline. The entire life cycle of wild-type HSV-1 infection is 18-20 h (Knipe *et al.*, 2014), so the fact that genome copy numbers were seen to remain at high levels and even increase past 48 h suggests that multiple rounds of replication and infection are taking place. There was no difference in copy number seen using either primer set, suggesting that the whole viral genome is replicated evenly. This provides further strong evidence that HSV-1716 is able to replicate within OC cells.

### **3.3 HSV-1716 kills both continuous and primary human ovarian cancer cells**

To assess the oncolytic properties of HSV-1716 in OC cells, a panel of established OC cell lines was infected with HSV-1716 at a range of MOIs for 96 h, before cell viability was determined by MTT assay. The purpose of this experiment was to assess whether infection with this virus led to the death of cancer cells, thus proving the virus's therapeutic potential in OC. HSV-1716 was able to cause complete death of most cell lines within the range of MOIs and time frame tested (Figure 3.2). The cell lines that were most sensitive to HSV-1716 infection were JHOC9 (IC<sub>50</sub>: 0.01) and TOV21G (IC<sub>50</sub>: 0.02), while the least sensitive were

UWB1.289 (IC<sub>50</sub>: 2.4) and PEO1 (IC<sub>50</sub>: 3.2). Cell lines therefore had quite a broad range of sensitivities. These cell lines represented distinct OC backgrounds, including both high-grade serous and clear cell carcinoma lines. Although the two most sensitive cell lines were both of clear cell carcinoma lineages, the other clear cell carcinoma cell lines OVTOKO, OVMANA and JHOC5 each had relatively high IC<sub>50</sub> values (0.88, 2.4 and 2.1 respectively). It is therefore not possible to speculate from these results whether HSV-1716 has a preference for either cancer type.

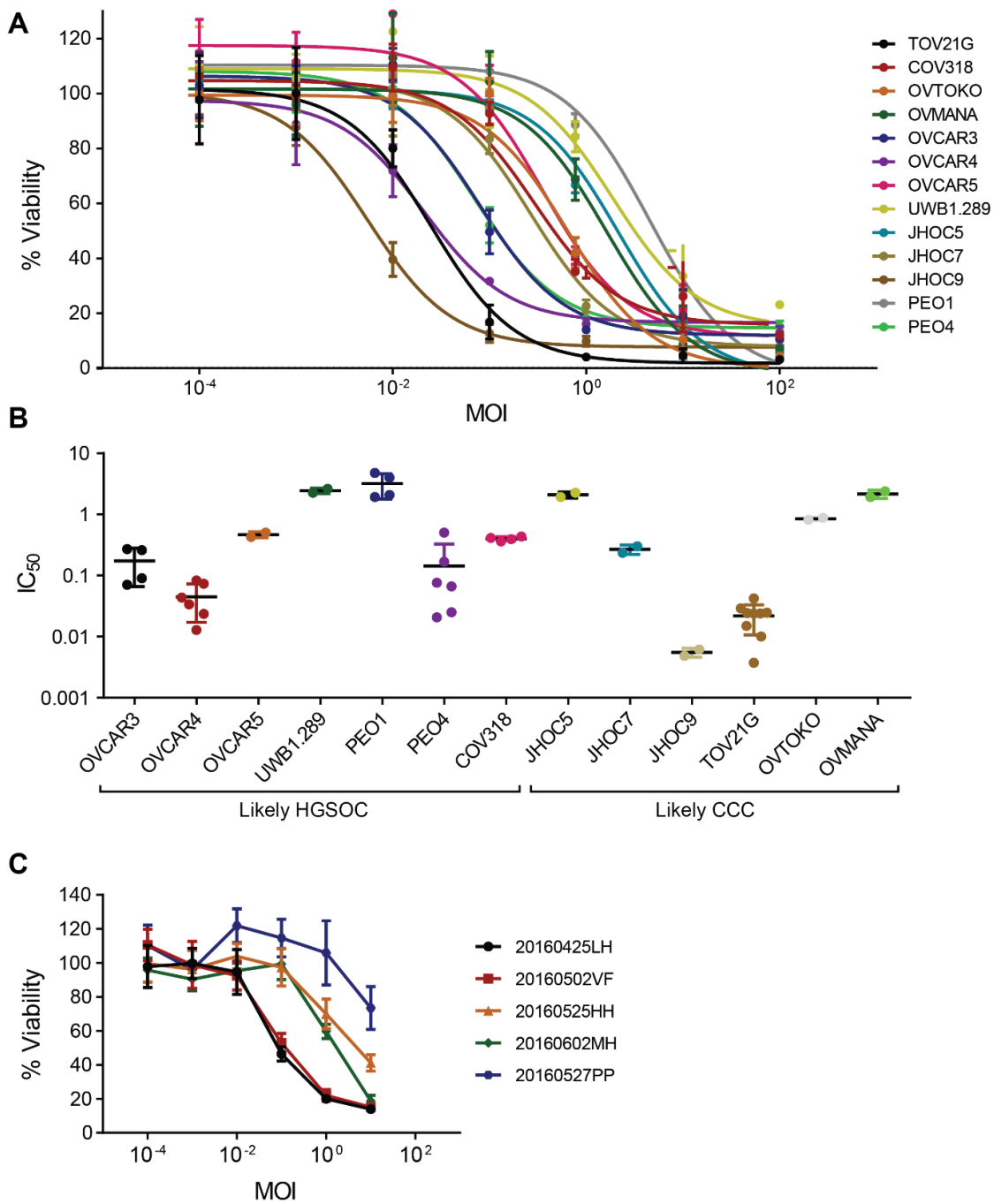


**Figure 3.2 HSV-1716 killing of primary and established ovarian cancer cell lines.** (A-B) Several OC cell lines were infected with HSV-1716 for 96 h at a range of MOIs before cell viability was determined by MTT assay. 'A' shows dose-response data from selected experiments, plotting mean  $\pm$  SD; curves were calculated using Prism's 'sigmoidal dose-response' function. 'B' shows pooled  $IC_{50}$  values from multiple experiments. (C) A selection of primary OC lines derived from patient ascites were infected with HSV-1716 at a range of MOIs for 96 h. Data points are represented as mean  $\pm$  SD.  $IC_{50}$ , half-maximal inhibitory concentration; MOI, multiplicity of infection.

Primary OC cells were obtained from the ascites of patients after they had been drained. Ascites fluid was centrifuged to pellet the cells, which were then cultured briefly before experimentation. Overall, five different primary cell cultures were infected with HSV-1716 at a range of MOIs and left for 96 h before

determining cell viability. HSV-1716 was able to successfully kill to some degree in all cells, with a roughly similar range of sensitivity as the cell lines (Figure 3.2). 20160527PP was by far the least sensitive cell line, while 20160425LH and 20160502VF were both the most sensitive.

### **3.4 Susceptibility of ovarian cancer cell lines to necroptosis**

In order to select suitable cell lines for experiments investigating effect on programmed necrosis, it was first necessary to assess the capacity for classical programmed necrosis induced by TSZ (TNF- $\alpha$ , SMAC mimetic, zVAD.fmk) within these cells.

Firstly, expression of major necrosome components, namely, RIPK3, RIPK1 and MLKL, was assessed by immunoblot (Figure 3.3). The purpose of this experiment was to determine both the ubiquity of expression of these proteins in OC cell lines, and to correlate expression with necrotic capacity. Interestingly, most cell lines appeared to express all the necessary components to some degree. Every cell line showed some RIPK1 expression, the highest being OVCAR4, and the lowest being OVMANA and COV318. MLKL expression was present in all cell lines; however, expression in COV318 was too low to reliably tell apart from background staining and so may not have been present at all. RIPK3 offered the greatest variation in expression across cell lines, yet all seemed to express it to some degree, with the lowest expression being in OVCAR5 cells and the highest in OVCAR4 and TOV21G. This ubiquity in RIPK3 expression is interesting, as it has previously been shown that the majority of cancer cell lines express no RIPK3 (Koo *et al.*, 2015). In this paper, over two thirds of the 60+ cancer cell lines tested expressed no RIPK3, which was shown to be due to methylation-dependent silencing of *RIPK3*. None of the cell lines tested here appears in the panel shown in the paper, so a direct comparison is not possible.

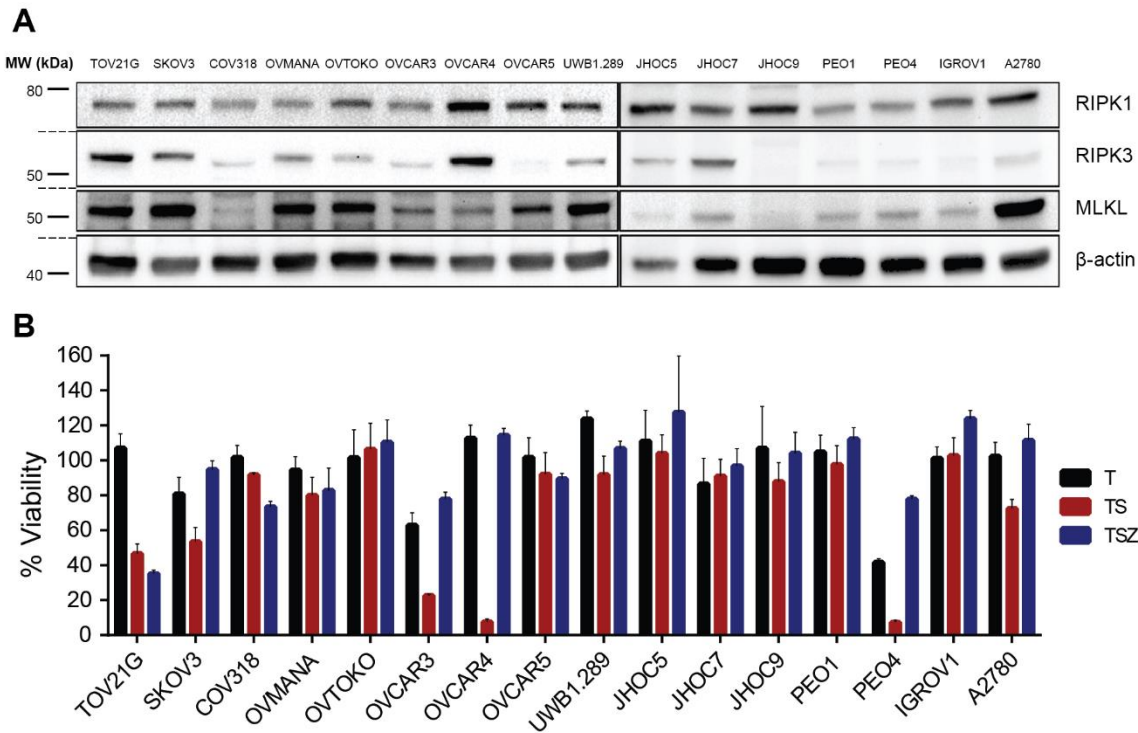


**Figure 3.3 Assessing the necroptosis-competency of ovarian cancer cell lines.** (A) Lysates were taken from several untreated OC cell lines and assayed by immunoblot for the necrosome proteins RIPK1, RIPK3 and MLKL. (B) Ability of OC lines to undergo necroptosis was determined by treatment with either T, TS or TSZ for 48 h, with viability determined by MTT assay. Mean cell viabilities are plotted from selected experiments  $\pm$  SD. MW, molecular weight; kDa, kilodaltons; T, TNF- $\alpha$ ; S, SMAC mimetic; Z, zVAD-fmk.

To assess the functional necroptotic potential of the OC cell panel, each cell line was treated with TNF- $\alpha$ , SMAC mimetic and zVAD-fmk - TSZ (Figure 3.3). By using different combinations of these three drugs, it is possible to induce cell death via a number of different pathways. In some cells, treatment with TNF- $\alpha$  alone can be enough to trigger cell death following the binding of TNF- $\alpha$  to TNFR1. This process is enough to cause the formation of complex I, which is a precursor to both apoptotic and necrotic forms of cell death (Vanlangenakker, Vanden Berghe and Vandenabeele, 2012). At this point, cIAP proteins are able to halt any further progression of death through their interaction with TRAF2 and TRAF5. Inhibition of cIAPs by ubiquitin/proteasome-mediated degradation induced by proteins such as SMAC therefore can allow the process of death to continue. Several SMAC mimetic drugs are available to mimic this process, and can help promote the induction of cell death when used in conjunction with TNF- $\alpha$ . The type of cell death caused by this combination can be either apoptotic or necrotic. Therefore, in order to induce a necrotic form of cell death specifically, caspases must also be inhibited. This can be done using a pan-caspase inhibitor such as zVAD-fmk. Therefore, by using all three drugs in

combination (known as TSZ), necrosis can be triggered. It was this precise combination of treatments that first identified the classical necroptotic pathway.

In the cell lines tested, a range of sensitivities to the TSZ combination were seen. OVTOKO, UWB1.289, PEO1, IGROV1 and JHOC5 showed no sensitivity at all to any combination of TSZ. OVCAR4 and PEO4 showed apoptotic cell death, whereby cell death is seen in the presence of TNF- $\alpha$  and SMAC mimetic, but addition of zVAD-fmk reversed this completely (Figure 3.3b). TOV21G and COV318 were the only cell lines that appeared to show any capacity for classical necroptotic cell death, with amount of cell death increasing or remaining the same when zVAD-fmk was added. Of these, TOV21G was by far the more sensitive, with a mean viability of 35% under TSZ treatment, compared to 73% for COV318.

Interestingly, this shows that expression of necroptotic machinery does not appear to guarantee, nor correlate with susceptibility to necroptosis. COV318 displayed marginal sensitivity to necroptosis despite having the lowest expressions of RIPK3 and MLKL, and OVCAR4 had the most marked resistance to necroptosis despite showing the highest expression of RIPK3. As the most necroptosis-sensitive cell line, TOV21G was subsequently used for the majority of experiments.

### **3.5 Assessing the characteristics of a RIPK3 over-expression model in HeLa cells**

To further probe the effect of necroptosis during HSV-1716 infection, an isogenic pair derived from HeLa cells was received as a gift from Dr M. Weigert in the host lab (Weigert *et al.*, 2017). Earlier studies have also confirmed that HeLa cells categorically lack any RIPK3 expression (H. Wang *et al.*, 2014; Schmidt *et al.*, 2015). Here, several HeLa-RIPK3 over-expressing clones were assessed for expression of RIPK3 and the impact of this on necroptosis. Three RIPK3-expressing clones were selected and compared to the empty vector control line, HeLa-Lzrs, as well as the parental wild-type cells (Par; Figure 3.4). Initially,

RIPK3 expression was determined by immunoblot. No expression was seen at all in the HeLa-Lzrs cells as expected. In all three clones expressing the RIPK3 vector, clear bands were seen following RIPK3 staining. No clear difference in quantity of RIPK3 staining was visible in this image. To further determine whether this expression system had any impact on other elements of the necrosome, two clones - HeLa-D2 and HeLa-E4, were compared to parental and HeLa-Lzrs cells for expression of RIPK3, RIPK1 and MLKL. When comparing parental cells to HeLa-Lzrs control, similar levels of each protein were seen with loading control levels of  $\beta$ -actin taken into account. Slightly higher levels of MLKL do appear to be present in the HeLa-Lzrs cells compared to parental cells (Figure 3.4b), but it is hard to determine the significance of this.

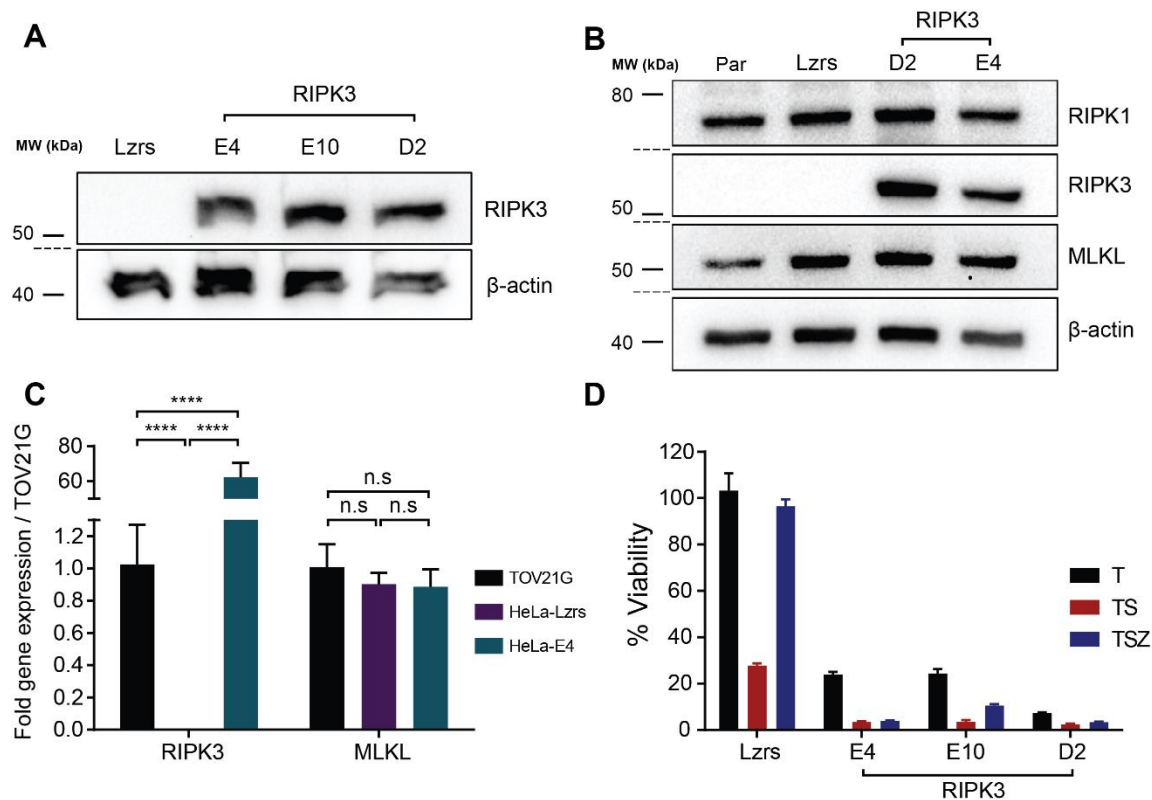


**Figure 3.4 Assessing the characteristics of a HeLa-RIPK3 over-expression model.** HeLa cells that have been transduced to express RIPK3 were received as a gift and assessed to determine their protein expression and necroptotic characteristics. **(A)** Whole cell lysates from untreated cells were obtained and probed for RIPK3 expression by immunoblot. **(B)** Untreated lysates from a selection of clones were probed by immunoblot for additional necroptotic proteins and compared to unmodified, parental (Par) cells. **(C)** DNA samples were extracted from untreated TOV21G and HeLa cells and analysed by RTqPCR to determine mRNA levels of RIPK3 and MLKL. Statistical significance was determined by two-way ANOVA (Sidak's multiple comparisons test). \*\*\*\*  $p < 0.0001$ , n.s., not significant. **(D)** Cells were treated with various combinations of TNF- $\alpha$  (T; 20 ng/ml), SMAC mimetic (S; 1  $\mu$ M) and zVAD-fmk (Z; 25  $\mu$ M) for 48 h before determining cell viability by MTT assay. MW, molecular weight; kDa, kilodalton.

RTqPCR was also performed on TOV21G, HeLa-Lzrs and HeLa-E4 cells. TOV21G was used as a positive control, as it has been shown previously to express these genes. Results in Figure 3.4c show these data, presented as fold-change compared to TOV21G. As expected, levels of RIPK3 mRNA were virtually undetectable in the HeLa-Lzrs cells ( $4.3 \times 10^{-4} \times$  TOV21G expression). In comparison, levels present in HeLa-E4 cells were much higher (62 $\times$ ) than TOV21G. In terms of MLKL expression, no significant difference was seen between HeLa-Lzrs and HeLa-E4, which indicates that over-expression of RIPK3 does not interfere with MLKL expression. In addition, levels of MLKL mRNA did not differ between either of the HeLa lines and TOV21G.

To show that RIPK3 expression has the potential to alter cellular capacity to undergo necroptosis, the HeLa cell lines were treated with varying combinations of TSZ (Figure 3.4d). As shown already, treating cells with a combination of TNF- $\alpha$  and SMAC mimetic enables cells to undergo cell death via the TNFR1 pathway, which can result in either apoptosis or necroptosis. Upon addition of zVAD-fmk, cells with a propensity to undergo necroptosis will see little rescue or no rescue from cell death, whereas death in cells that lack this ability will see complete rescue from death. In Figure 3.4d, HeLa-Lzrs cells can be seen to match the latter phenotype, with a drastic decrease in cell death following TS exposure that is nearly completely rescued after addition of zVAD-fmk. In contrast, all HeLa-RIPK3 lines see marked reductions in cell viability following all drug combinations. Crucially, there is little (E10) or no (E4, D2) rescue from cell death following addition of zVAD-fmk. Interestingly, there is also a large drop in cell viability following TNF- $\alpha$  treatment alone when comparing HeLa-RIPK3 cells to HeLa-Lzrs.

Taken together, these results indicate that HeLa-Lzrs and HeLa-RIPK3 clones (E4 in particular) represent a true isogenic cell pair, with no visible off target effects on other components of the necrosome. Any subsequent differences seen between these cells can therefore reliably be assumed to result from the presence or absence of RIPK3.

## 3.6 Discussion

In this chapter, I have shown that HSV-1716 can infect and kill a large number of established and primary OC cell lines. HSV-1 has presented itself as an ideal candidate for the development of oncolytic viruses, in part, due to its ability to infect and replicate within a large number of cell types (Karasneh and Shukla, 2011). One of the main reasons for this limited selectivity is the ubiquity of entry receptors across host cell types (Tiwari *et al.*, 2005, 2006; Choudhary *et al.*, 2011). While there are limited data on the presence of viral entry receptors in OC cells, molecules such as heparan sulphate proteoglycans are known to be near-ubiquitous (Fuster and Esko, 2005). There is also evidence that HVEM is upregulated in OC cells compared to benign ovarian tissues, which provides the possibility that OC cells could be particularly permissive to HSV-1 (Zhang *et al.*, 2016).

While entry mediators for HSV are commonplace, the ability of the virus to replicate effectively within a cell is far more relevant to its clinical efficacy. Tumour selectivity of HSV-1716 is determined by the double-*RL1* deletion, which encodes ICP34.5. While the potential mechanisms for how ICP34.5 deletion can influence tumour selectivity have been described, it is now clear that the exact mechanisms are likely to be multifactorial and are also likely to differ between cell types. It is therefore still important to fully characterise the replicative and cell killing abilities of HSV-1716 in this system.

While studies with HSV-1716 in OC cells have been performed, these have in some cases focused on cell lines that are not typical of specific OC types, such as A2780, SKOV3 (Coukos *et al.*, 2000) or ID8 (Benencia, Courrèges, Conejo-García, Mohamed-Hadley, *et al.*, 2005). The reasons behind the unsuitability of the first two lines has been discussed. The murine cells, ID8, have also proven to be less representative of HGSOC than previously thought. Our lab has previously shown using whole exome sequencing that the original ID8 cells possess no mutations in any of the genes commonly altered in HGSOC (*Trp53*, *Brca1*, *Brca2*, *Nf1*, *Rb1*), or any other OC subtype (Walton *et al.*, 2016). For these reasons, it is important to characterise HSV-1716 in the most relevant OC cell lines available.

In a small range of OC cell lines infected with HSV-1716, anti-HSV staining was demonstrated in all lines after 24 h. The entire life cycle of HSV-1 in permissive tissue culture cells has been shown to be approximately 18-20 h (Knipe *et al.*, 2014). This provides strong evidence that HSV-1716 can successfully replicate within all cells tested, as the only HSV antigens detectable at this stage should be from replicating virus. In two selected cell lines, TOV21G and OVCAR4, HSV-1 viral DNA copies were shown to increase with time in comparison to UV inactivated virus. This provides further evidence that HSV-1716 is capable of replicating within these cells.

After 24 h in TOV21G cells, levels of viral DNA following UV-inactivated virus infection appear to rise above the defined lower limit of detection of 6400 genomes/ $\mu$ g DNA. This number was determined as the highest dilution of purified HSV-1716 DNA used in the standard curve, below which a reliable inference of copy number from Ct value was not possible. This means that for any values above this value can be interpreted with a reasonable level of reliability. Values below the lower limit of detection, however, cannot be reliably assessed. Such measurements may represent true zero values or may just be too low to detect. This is a problem that can arise when trying to prove an expected value to be zero using a technique that does not allow for absolute zero measurements. In the instance of UV-inactivated virus replication, there may be some low levels of replication occurring due to live virions left over from an incomplete inactivation process, or that low reliability in measurements at such low levels of DNA has led to this discrepancy. Further experiments shown later in this thesis (Figure 4.9) using plaque assays as a measure of viral replication consistently showed no plaques in any samples infected with UV-inactivated virus, which suggests that these viruses may well be fully inactivated.

HSV-1716 killed all OC lines at MOIs ranging from 0.005 to 4. It also showed dose-dependent killing effects in all primary cell lines tested too. However, many of these primary lines were not as sensitive as the cell lines. This provides some strong evidence that HSV-1716 could be an effective agent for treatment of OC in a situation where infection of primary tumours is successful.

While assessing the sensitivity of cell lines to TSZ, only TOV21G was shown to behave in a way typical of necroptosis-sensitive cells. This was despite most cell lines displaying some level of RIPK3 expression. I have already mentioned how cell lines have been commonly shown to lose RIPK3 expression due to selective methylation (Koo *et al.*, 2015). However, little previous work has been done characterising the necroptotic expression of OC cell lines (McCabe *et al.*, 2014). In this one study, OVCAR3, OVCAR4 and OVCAR5 cells were all shown to express some level of RIPK3, with OVCAR3 expressing the most. This, in part, matches with the results shown here, with the exception that OVCAR4 were the most highly-expressing line. The lines IGROV and SKOV3 both were shown to lack any expression of RIPK3 in the McCabe *et al.* paper, which directly contradicts the results shown here. A possible reason for these discrepancies may be that different primary antibodies were used for the detection of RIPK3 between this study and the one cited, which illustrates a major problem with using antibodies in biomedical research.

The McCabe *et al.* study also showed that OVCAR3 were sensitive to necroptosis, shown by treatment with IAPa (equivalent to SMAC mimetic) and zVAD.fmk, while results here showed clearly that OVCAR3 had an apoptotic phenotype. Another possible explanation for these differences could be a mismatching in cell samples. However, all cell lines used in this study were validated by STR sequencing.

Use of the isogenic HeLa-RIPK3 pair will provide valuable insights into the role of RIPK3 during HSV-1716 infection in subsequent chapters. HeLa cells were initially isolated from an unusually aggressive form of cervical cancer (Gey, Coffman and Kubicek, 1952). Any results derived from these cells cannot therefore be extrapolated to the disease of ovarian cancer. As a result, the work of this thesis will primarily focus on unravelling the core machinery of cell death and its role in HSV-1716 infection.

RIPK3 expression was shown to be exclusive to the clones that were transduced with *RIPK3*-encoding lentiviruses, and not the empty vector-containing HeLa-Lzrs cells. This was shown by both immunoblot and RTqPCR. It should be noted that complete lack of mRNA expression can never be reliably confirmed using

quantitative PCR methods due to the limits on sensitivity at lower concentrations. Results here were expressed as fold change in comparison to TOV21G cells using the  $\Delta\Delta C_t$  method, from which, levels of RIPK3 mRNA in HeLa-Lzrs were found to be 0.00043 $\times$  that of TOV21G. Functionally, it is likely that this value can be considered as essentially zero. In addition, RIPK1 and MLKL expression was found to be the same between HeLa-Lzrs and HeLa-E4 cells by immunoblot, and MLKL the same by PCR, suggesting that no effect on other members of the necrosome complex have resulted from this modification.

HeLa-RIPK3 cells were all found to be more sensitive to treatment with TNF- $\alpha$  alone than HeLa-Lzrs, which requires addition of SMAC mimetic to induce any death at all. This suggests that the presence of RIPK3 can by-pass the need for cIAPs to be depleted for death to proceed. This lies in contrast to TOV21G cells, which requires presence of both T and S for death to occur. The fact that RIPK3 transcript levels are >60 $\times$  higher (and protein levels visibly higher) in HeLa-E4 cells compared to TOV21G may account, at least in part, for this difference. HeLa-E10 cells appeared to be unique among the RIPK3 clones in that they could be partially rescued from cell death by addition of zVAD-fmk, albeit far less than was seen with HeLa-Lzrs (increase in % cell viability of 69 vs 7 for HeLa-E10). This implies that some apoptotic signalling is still responsible for death following TS exposure in these cells in a way that cannot be switched to necrosis following caspase inhibition. This introduces an interesting question about the ability of cells to switch seamlessly between these types of cell death within a population, and whether the percentage of death attributable to either apoptosis or necrosis is fixed or variable dependent on conditions.

Based on the overall similarity of the HeLa-RIPK3 cell lines, many of the proceeding experiments were performed in just one line, HeLa-E4, for simplicity. In these experiments, HeLa-E4 is denoted as simply “HeLa-RIPK3”.

## **4 Creation of ICP6 modified Virus and Cell Lines**

## 4.1 Introduction

As mentioned in Chapter 1, recent evidence has arisen that suggests that ICP6 may play a key role in HSV-1 mediated cell death through its interactions with RIPK1 and RIPK3. In murine cells, ICP6 forms complexes with RIPK1 and RIPK3, leading to their activation and necrosis induction (Huang, S. Wu, *et al.*, 2015). However, in human cells, this same interaction disrupts complex formation and leads to necrosis inhibition. Further evidence suggested that ICP6 mediated these interactions via its RHIM, which is present in the N-terminal portion of the protein (Guo *et al.*, 2015). In the latter study, Guo *et al.* were able to show that, by modifying the RHIM of ICP6 in an ICP6-expressing cell line system, sensitivity to necroptosis was increased when cells were complemented with an ICP6 null virus.

In this chapter, I sought to confirm the hypothesis that in a similar system, an ICP6-null HSV-1716 could trigger necroptosis when complemented with a RHIM deficient version of ICP6. I also sought to take this one step further, by creating a RHIM-deleted version of HSV-1716 itself.

## 4.2 Creation of ICP6 modified viruses using a CRISPR/Cas9- based system

### 4.2.1 Developing a CRISPR/Cas9 gene-editing technique for viruses

Despite the now commonplace nature of the use of CRISPR/Cas9-based techniques for the editing of mammalian cell lines, this technique has still yet to be used routinely in the alteration of large viruses such as HSV-1. For small viruses, such as hepatitis C virus, simple methods for gene editing already exist, as entire virus genomes can be cloned into plasmids. For larger viruses, genomes have typically been edited by relying on homologous recombination, or cloning entire genomes into BACs (Post and Roizman, 1981). Both of these techniques are laborious, time-consuming and, in some cases, require addition of additional genes for selection purposes, which then need to later be removed or risk

interfering with cellular processes during amplification. CRISPR, much like in cells, offers a faster, more efficient and convenient way to edit genes in large viruses.

To date, little has been published on the use of this technique in HSV-1 (Bi *et al.*, 2014; Suenaga *et al.*, 2014; Lin *et al.*, 2016). Therefore, in order to utilise CRISPR for the editing of HSV-1716, I had to devise my own technique based on the available expertise in the host lab (Walton *et al.*, 2016, 2017)(Figure 4.1).

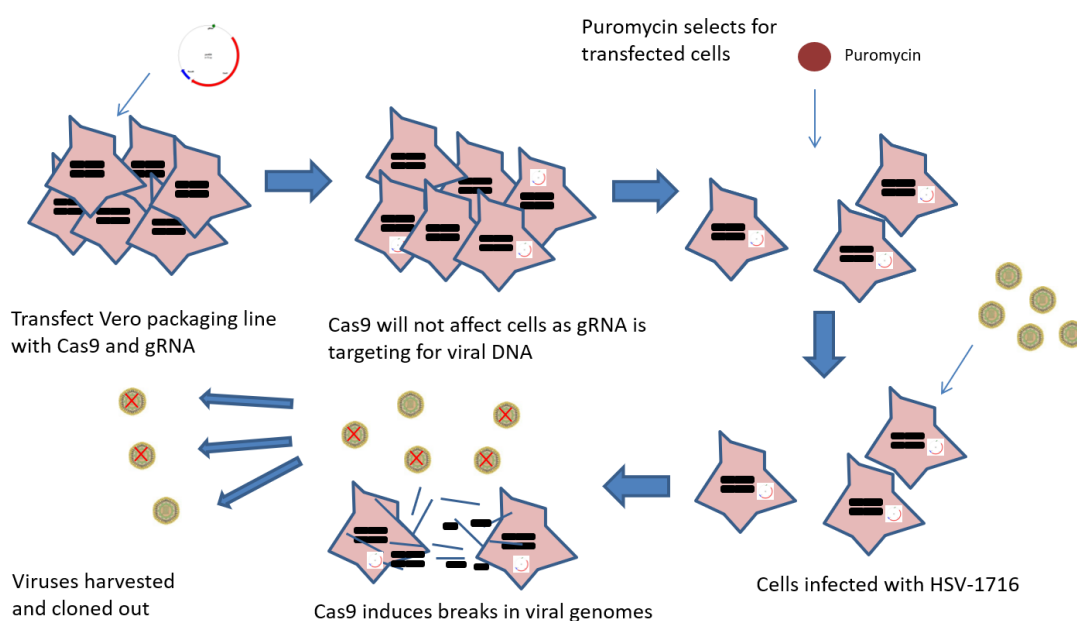


**Figure 4.1 CRISPR-based method for HSV genome editing.** An outline of the method devised for editing the ICP6 gene of HSV-1716. Vero packaging cells were transfected with a px459 plasmid containing the *Cas9* gene, a gRNA element corresponding to the RHIM of ICP6, and a puromycin resistance gene. Plasmid-containing cells were then selected for with puromycin before infecting with HSV-1716 at an MOI of 1 for 48 h. Resultant viruses were collected and dilution cloned into 96 well plates containing Vero cells. Clones were screened for gene alterations by a combination of immunoblot, PCR for fragment size comparison and Surveyor assay.

In standard CRISPR/Cas9 editing of cell lines, cells are transfected with a single plasmid containing *Cas9*, which induces double strand breaks in the DNA. The plasmid also contains a gRNA scaffold, into which the corresponding DNA sequence of interest can be inserted. There is typically also a eukaryotic antibiotic resistance gene, such as puromycin resistance, that can be used for transient selection of successfully transfected cells.

To see whether puromycin resistance could be used to select for cells in the presence of HSV-1716, it was important to first determine whether puromycin had any effect on HSV-1716 replication, which might affect efficiency. For this, TOV21G-pLV cells were used, which are TOV21G cells that had been stably transfected with a plasmid containing a puromycin resistance gene, and so could be treated with puromycin without negative effect on viability. TOV21G-pLV cells were infected with HSV-1716 and left for two hours before refeeding with medium containing puromycin. After 48 h, DNA was taken from cells to observe changes in viral genome copy number in response to puromycin.

As can be seen in (Figure 4.2), addition of 2.5  $\mu\text{g}/\text{ml}$  puromycin significantly reduced the number of total viral genome copies from 11.1 to  $4.65 \times 10^6/\mu\text{g}$  DNA (averaged across gene regions). This was equivalent to a reduction in genome copies by a factor of 1.72. I decided that despite a significant drop in virus replication in the presence of puromycin, the reduction was small enough to continue to use puromycin as the method of selection.

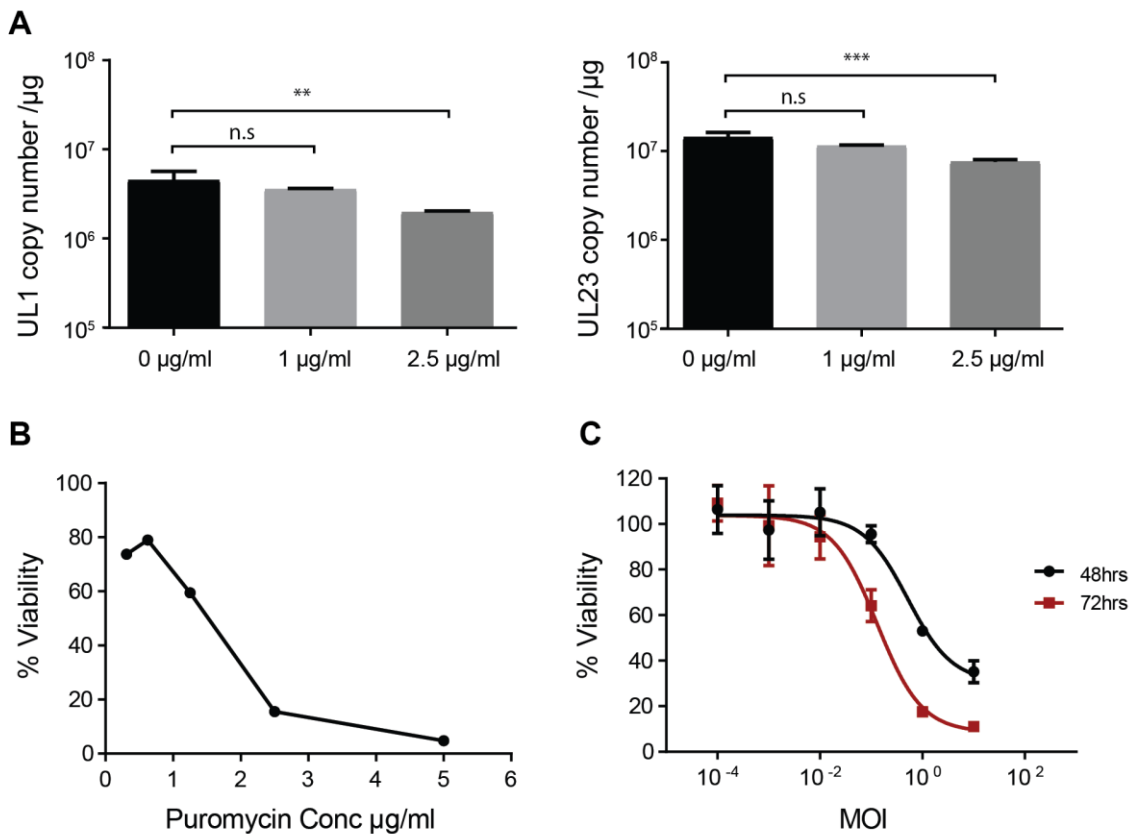


**Figure 4.2 Assessing the suitability of puromycin and Vero cells for CRISPR gene editing of HSV-1716.** (A) TOV21G-pLV cells were infected with HSV-1716 at an MOI of in the presence of puromycin for 48 h before analysing viral DNA levels by qPCR targeting two HSV genes, UL1 (left) and UL23 (right). Mean copy number / $\mu\text{g} \pm \text{SD}$  are plotted. Statistical significance was determined by one-way ANOVA (Dunnnett's multiple comparisons test). \*\*  $p < 0.01$ , \*\*\*  $p < 0.001$ . (B) Vero cells were treated with a range of puromycin concentrations for 48 h before cell viability was determined by MTT assay. (C) Vero cells were infected with HSV-1716 at a range of MOIs for 48 or 72 h with cell viability determined by MTT assay. MOI, multiplicity of infection; n.s., not significant.

Next it was important to determine the suitability of the Vero cell line as a packaging line for the CRISPR protocol. Vero cells are one of the standard cell lines for the production of HSV-1 particles for a variety of applications including standard culture, vaccine and oncolytic virus production (Morgan, 2007). For this reason, it was preferable to use this cell line for the production of CRISPR-edited viruses, in order to maintain as much similarity as possible to previous virus generations. First, the sensitivity of Vero to puromycin was determined by analysing cell viability after 48 h of treatment. Cell viability decreased in an expected dose-dependent fashion, with 5  $\mu\text{g/ml}$  being enough to cause near complete death, and 2.5  $\mu\text{g/ml}$  resulting in a cell viability of approximately 15%. Therefore, I concluded that puromycin was a suitable selective agent for use

with Vero cells, with 2.5 µg/ml being chosen as the dose to proceed with for the experiment.

Finally, a dose-response experiment was performed in Vero with HSV-1716 to determine the sensitivity of Vero cells to infection. It has previously been shown that Vero cells are susceptible to infection with HSV-1 (Elion *et al.*, 1977; Roehm *et al.*, 2016; Abdoli *et al.*, 2017), but it was important to choose an appropriate MOI that would cause a high enough number of virus particles to be released without inducing complete cytotoxicity. As shown in Figure 4.2, HSV-1716 shows dose-dependent and time-dependent cytotoxicity. The conditions chosen for subsequent experiments were MOI 1 for 48 h. Once the conditions for the experiment were selected, the CRISPR was performed as outlined in the methods.

#### **4.2.2 Design of Guide Sequences**

The two goals of the ICP6 CRISPR experiment were first, to create a virus completely lacking ICP6 expression for use in a complementation experiment with ICP6 expressing cell lines, and second, to create a virus containing a specific in-frame RHIM-deleted form of ICP6 to observe the effect of loss of the RHIM alone.

Achieving the first of these goals simply required design of a guide targeted to a locus close to the beginning of the gene. This ensures that a successful frameshift indel would result in no functional protein expression. Luckily, the RHIM sits just 218 nt downstream from the start codon, making it a suitable location to target for both goals. Achieving the second goal required targeting of the RHIM itself and either relying on the spontaneous generation of an in-frame mutation or supplying a donor strand to create the exact mutation needed. Only the first of these strategies was needed, and thus no donor strand was used.

To create a CRISPR plasmid specific to the region of interest, suitable sequences for the creation of guide RNAs were chosen using two online programmes: <http://crispr.mit.edu> and <http://chopchop.rc.fas.harvard.edu>. Both programmes use algorithms to choose sequences surrounding a region of interest

that meet the criteria for a guide RNA, such as being adjacent to an appropriate protospacer adjacent motif (PAM) (which for Cas9 is 5'NGG, where N is any nucleotide). In addition, the programmes recommend sequences that are not likely to lead to off-target effects elsewhere in the genome. Unfortunately, at the time of writing this thesis, the genome of HSV-1 is not available for use with either of these algorithms. To bypass this, all chosen sequences were crosschecked for any potential off-target binding against the HSV-1 strain 17 genome using the program SnapGene. Guides were also selected based on sequences that were rated highly in both program. Each program ranks potential guides by their predicted binding affinity and potential for off-target binding. Three guides were chosen and cloned into px459 (see Figure 4.3)

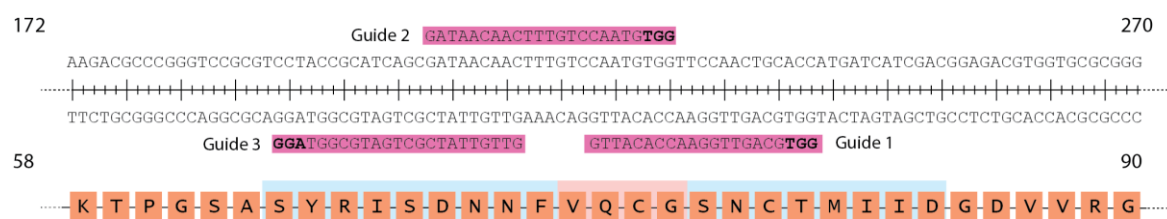


**Figure 4.3 CRISPR guide sequences used for ICP6 gene editing.** The three guides that were designed for editing of ICP6 were chosen following selection by the programs 'chopchop' and crispr.mit.edu. The necessary 'NGG' sequence for each guide is shown in bold. The RHIM is highlighted on the corresponding amino acid sequence in blue, with the four-amino acid highly conserved region in red.

### 4.2.3 Isolating and identifying CRISPR viral clones

After performing the CRISPR procedure, clones were isolated by performing dilutions in a 96-well plate. Once isolated, clones were screened for presence of an appropriate mutation in four stages. First, DNA extracted from infected Vero cells was amplified by PCR using primers spanning a 354 bp region either side of the RHIM. Samples were electrophoresed on an agarose gel to identify any samples with large deletions (approximately 100 bp or more). PCR lanes from part of this screen are shown in Figure 4.4a, which shows a selection of clones that were modified using two of the three guides. However, none of the selected clones harboured any large deletions. Next, an immunoblot was performed to

observe changes in functional protein expression. Here, the same viral clones were used to infect Vero cells, followed by extraction of protein 24 h later. Samples were analysed for the presence of both ICP6 and pan-HSV proteins. Using this method, three ICP6-null clones were identified - 1C5, 3B10 and 3B1. Despite lack of ICP6, productive HSV-1 infection was still evident, as pan-HSV staining was still present. To identify any clones that may still be expressing a near full-length form of ICP6, but had still undergone CRISPR-mediated mutation, a surveyor assay was performed.

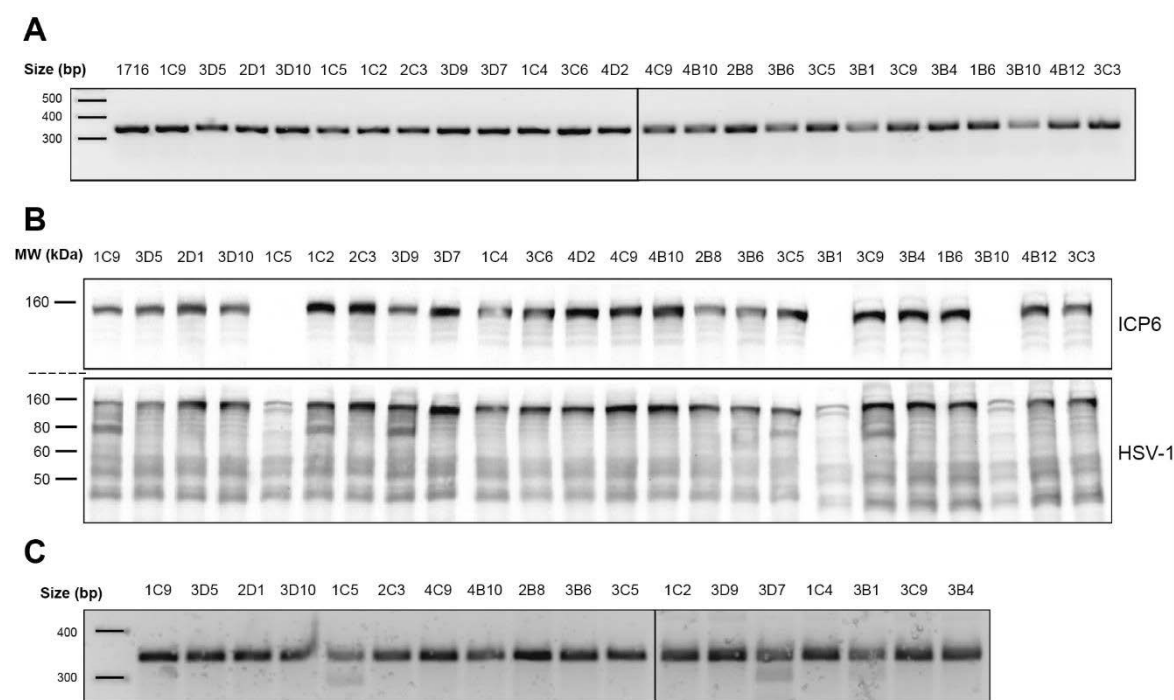


**Figure 4.4 Isolation of CRISPR-edited viral clones.** (A) Initial screening of extracted DNA from isolated clones by PCR. Samples were acquired following infection Vero cells with an untitred volume of virus for 24 h. Primers spanning a 354 bp region flanking the RHIM of ICP6 were used to identify any large deletions within the gene. (B) Further screening for presence of whole ICP6 protein and HSV-1 proteins was performed by immunoblot following infection of Vero cells with an untitred volume of virus for 24 h. (C) Samples from 'A' were further analysed using surveyor assay, to observe presence of mismatches between WT and clone DNA. MW, molecular weight; kDa, kilodalton; bp, base pairs.

The surveyor assay works by mixing PCR products from a sample of unmodified DNA with the test DNA in a 1:1 ratio. The mixture is then denatured and re-annealed, which allows the formation of hybrid duplexes. At this point if the samples differ in sequence at all, then there will be mismatches within the duplexes. These mismatches can be recognised by the addition of the Surveyor nuclease, which will cleave the duplex if it detects them. These cleavages are

identifiable as additional bands at molecular weights lower than the full product on gel electrophoresis.

The results of this screen can be seen in Figure 4.4c. Here, a selection of the same clones from the previous screens were analysed and compared to the clones known to contain mutations, which served as positive controls. There are faint extra bands visible below the main band for the clones 1C5, 3D7 and 3B1. Of these, the only new identification was 3D7. This clone expressed full length ICP6 by immunoblot but was still indicated to contain some form of mutation.

To confirm the presence of mutations in the four identified clones, Sanger sequencing was performed on the region spanning the expected location of mutations. For all the clones, distinct changes in DNA sequence around the region of the RHIM were noted (Figure 4.6). As expected, the mutations seen in the viruses 1C5, 3B1 and 3B10 were all frameshift indels resulting in premature stop codons. In 1C5, a 2 bp deletion was identified in base pairs 225-226, which lies within the 4-amino acid highly conserved region of the RHIM. For both 3B1 and 3B10, a single adenine insertion was identified between amino acids 222 and 223. This meant that 3B1 and 3B10 were genetically identical. This may have occurred by chance or mean that two viruses from the same CRISPR-modified cell had become isolated separately. For this reason, 3B10 was excluded from further experiments.

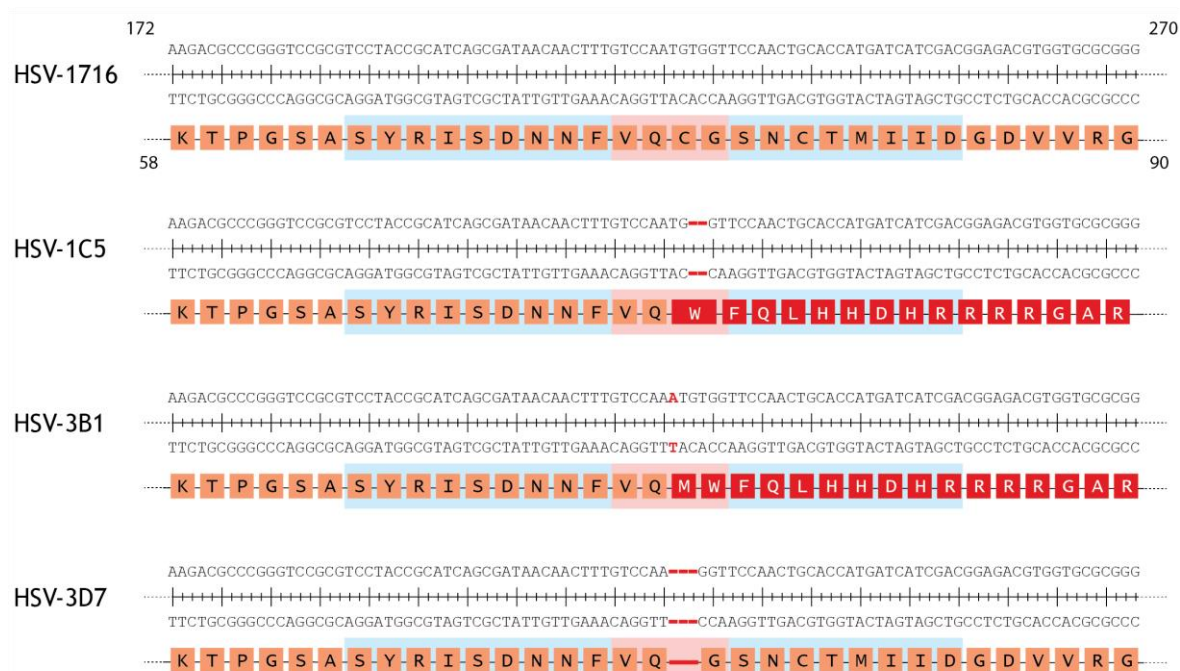


**Figure 4.5 Illustration of nucleotide changes in ICP6 virus mutants.** Three clones were isolated containing successful gene alterations in ICP6. The clones 1C5 and 3B1 both possessed frameshift mutations that resulted in gross changes in amino acid sequence downstream of the site of mutation (shown in red). Nucleotide deletions are illustrated with red dashes, with insertions shown in red bold. In the case of HSV-3D7, a complete three base-pair deletion was seen within the highly conserved region of the RHIM, resulting in complete loss of the corresponding cytosine amino acid, with no further changes in the downstream sequence.

The sequence data obtained from the clone 3D7 identified a 3 bp in frame deletion spanning amino acids 223-225. This mutation also sits within the 4-amino acid highly-conserved region. This finding fits perfectly with the data from the Surveyor assay and immunoblot, which suggested that any mutation that 3D7 contained would not result in a premature stop codon. This deletion therefore has the functional effect of deleting one cysteine amino acid from the RHIM, with the remainder of the protein translating correctly. The fact that the ICP6 staining for 3D7 appears normal, suggests that the deletion does not affect the ability of the rest of the protein to fold correctly.

### 4.3 Creation of a range of ICP6-modified cell lines

To observe the effect of a range of mutations affecting the RHIM of ICP6, TOV21G and OVCAR4 cells were transfected with plasmids encoding various modified ICP6 open reading frames. Guo *et al.* have previously noted a change in response to TSZ and HSV-1 infection following modifications within the N-

terminal domain of ICP6, and the RHIM in particular. They showed that when the cells contained a version of ICP6 lacking in a RHIM, there was greater sensitivity to TSZ than in those expressing a full version of ICP6. RHIM mutant cells were also more sensitive to infection with an ICP6-null virus.

To determine the effect of these same mutations in the context of HSV-1716 infection, we received the same plasmid constructs as used by Guo *et al.* as a kind gift. Specifically, the constructs received were: ICP6(1-1137), hereby referred to as “ICP6(FL)””; ICP6(1-1137, *mutRHIM*), hereby referred to as “ICP6(*mutRHIM*)””; ICP6( $\Delta$ 1-243) and ICP6(244-629). All of these constructs were tagged with a Flag sequence and are summarised in Figure 4.6. These constructs were transduced into both TOV21G and OVCAR4 cells using a lentivirus vector.

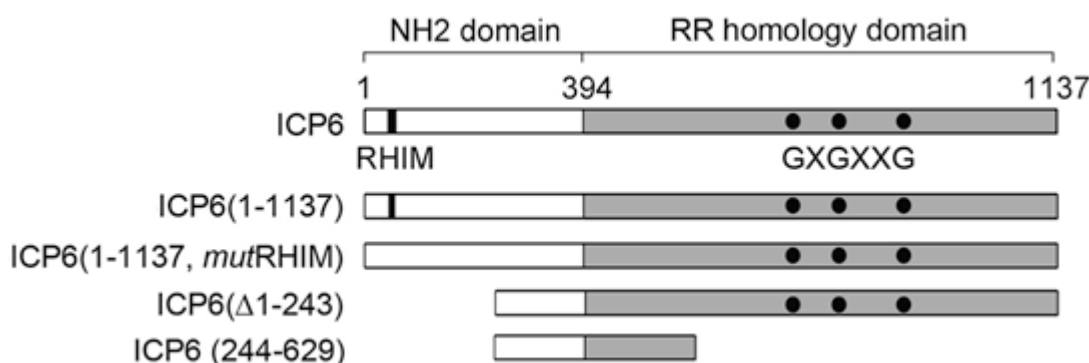


**Figure 4.6 Schematic representation of ICP6 mutant constructs overexpressed in TOV21G and OVCAR4 cells.** Various constructs based on HSV-1 ICP6 were put into both TOV21G and OVCAR4 cells. All constructs contained flag sequences at the N-termini. Different constructs were altered in different ways that affected the presence of either the RHIM, the C-terminal domain or both. ICP6(1-1137, *mutRHIM*) contains a tetra-alanine substitution within the four-amino acid highly-conserved region of the RHIM, which negates its action. ICP6( $\Delta$ 1-243) achieves the same effect by deleting the entire first 243 amino acids from the protein. The GXGXXG site illustrated on the C-terminal domain represents the nucleotide binding region required for ribonucleotide reductase activity. Figure adapted from *Cell Host Microbe* 2015 Feb 11;17(2):243-51.

To confirm the presence of the desired proteins, immunoblots were performed for each set of transduced cell lines (Figure 4.7). ICP6 staining was seen in all cell lines transduced with some construct of ICP6, but no staining was seen for cells transduced with the lentivirus backbone alone (pLV). For ICP6(FL) and ICP6(*mutRHIM*) constructs, staining was seen at the known ICP6 molecular weight of 124 kDa. For the constructs ICP6( $\Delta$ 1-243) and ICP6(244-629), which were truncated, bands were seen at the predicted lower molecular weights of ~100 kDa and ~43 kDa respectively.

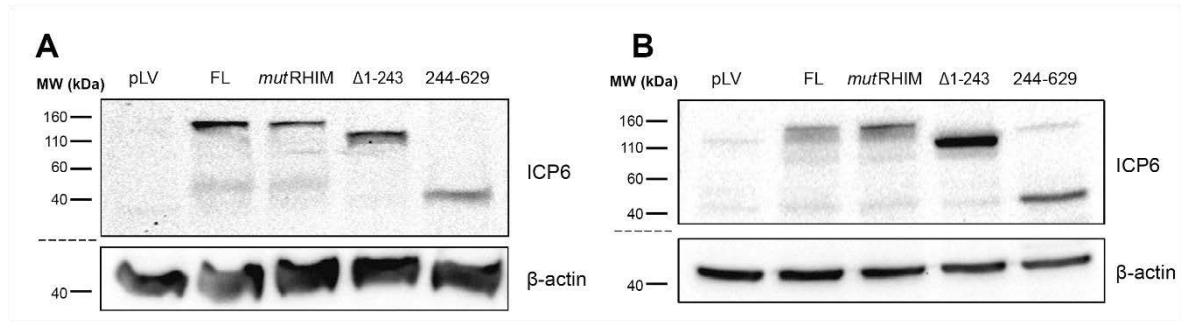


**Figure 4.7 Visualisation of ICP6-expressing cell lines by immunoblot.** TOV21G (A) and OVCAR4 (B) cells were stably transduced with various ICP6 constructs using a lentivirus-based system. Shown here are the resulting immunoblots from untreated cell lines showing staining with an ICP6 antibody. MW, molecular weight; kDa, kilodalton.

#### 4.4 Effect of ICP6 RHIM on sensitivity to TSZ

Guo *et al.* showed that expression of full length ICP6 in HT-29 cells reduced death induced by TSZ treatment. However, when ICP6 lacking a functional RHIM was expressed, sensitivity to TSZ was restored. I sought to determine if this effect was also seen in OC cell lines.

TOV21G cells were evaluated in these experiments because they were the only cells sensitive to TSZ-induced necroptosis (Figure 3.3). Upon treatment with TSZ, TOV21G-pLV behaved much the same as the parental TOV21G cells in that a large drop in cell viability to 47% was seen following TS treatment, which was decreased further to give a viability of 35% when treated with the full TSZ (Figure 4.8a). In comparison, viability of TOV21G-ICP6(FL) was 81% when treated with TSZ, suggesting that the presence of full-length ICP6 had afforded protection from necrosis induction. In contrast, when TOV21G-ICP6(*mut*RHIM) was treated with TSZ, sensitivity was restored to the same level as TOV21G-pLV. As the only difference between the ICP6 sequence of the FL and *mut*RHIM constructs is the presence of a AAAA substitution in place of the highly conserved region of the RHIM, it is clear that a functional RHIM is crucial for the mechanism of protection from necrosis by ICP6. A similar sensitivity was seen in TOV21G-ICP6( $\Delta$ 1-243) cells, but to a lesser extent, with a significantly higher viability still than TOV21G-pLV. This indicates that by removing the entire N-terminal domain, some, but not all sensitivity to TSZ can be restored.

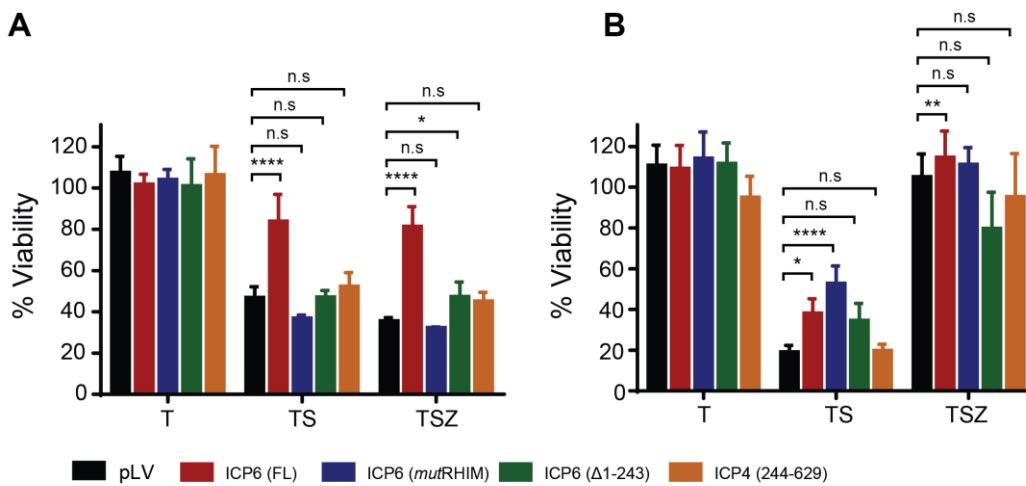


**Figure 4.8 Susceptibility of ICP6-expressing cell lines to TSZ treatment.** TOV21G (A) and OVCAR4 (B) cells were treated with varying combinations of the drugs TNF- $\alpha$  (T; 20 ng/ml), SMAC mimetic (S; 1  $\mu$ M) and zVAD-fmk (Z; 25  $\mu$ M) for 48 h before determining cell viability by MTT assay. Mean cell viabilities from single experiment are plotted  $\pm$  SD. Statistical significance was determined by two-way ANOVA (Dunnett's multiple comparisons test). \*  $p < 0.05$ , \*\*  $p < 0.01$ , \*\*\*\*  $p < 0.0001$ ; n.s, not significant.

It is interesting that removing this entire domain protects less than simply modifying the RHIM. It could be that there are other regions within the N-terminal domain that are able to interact with part of the necroptotic machinery in some way, possibly facilitating necroptosis.

When the same experiment was performed in OVCAR4 cells, as expected, OVCAR4-pLV cells showed high levels of cell death following TS treatment that was entirely protected against following further addition of zVAD-fmk (Figure 4.8b). In contrast to the TOV21G cell lines, there was a smaller, albeit still significant rescue effect from cell death induced by TS in the OVCAR4 FL, *mutRHIM* and  $\Delta$ 1-243 lines compared to pLV alone. There was no significant change in cell death, however, in the OVCAR4-ICP6(244-629) line compared to pLV alone. This effect fits well with the hypothesis outlined by Guo *et al.* because the C-terminal domain of ICP6 contains a caspase 8 binding domain, which results in an inhibition of caspase 8 function. All constructs that contained this domain were able to offer some level of protection against TS-induced apoptosis. Interestingly, there did seem to be an extra level of protection given by the *mutRHIM* construct, compared to FL, which is not present in the  $\Delta$ 1-243 construct.

## 4.5 Effect of CRISPR-mediated ICP6 mutations on viral activity

### 4.5.1 Effect on viral replication

Replication ability of the viruses HSV-3B1, HSV-1C5 and HSV-3D7 was analysed in TOV21G cells by plaque assay and compared to HSV-1716. The plaque assay uses viral killing as a basis for measurement of viral titre and so detects whole, viable virus particles. This method, therefore, provides an alternative estimation of viral replication than qPCR, which only measures genome copies. TOV21G cells were infected with each virus at MOI 1, and harvested 8, 16 and 24 h thereafter (Figure 4.9).

Both  $\Delta$ ICP6 viruses were shown to have impaired growth compared to HSV-1716. Area under the curve (AUC) analyses of replication curves were performed to enable statistical comparison between samples. At 24 h, HSV-3B1 showed a significant decrease in AUC compared to HSV-1716 from  $5.4 \times 10^5$  to  $1.5 \times 10^5$  (pfu/ml) $\times$ min (72%;  $p=0.0002$ ). HSV-1C5 showed a smaller decrease in AUC to  $1.8 \times 10^4$  (pfu/ml) $\times$ min (67%;  $p=0.0004$ ), compared to HSV-1716. However, there was no significant difference between HSV-3B1 and HSV-1C5. It is expected that we would see the same replication in these two viruses as they are phenotypically identical. HSV-3D7 performed similarly to HSV-1716, with an AUC of  $4.4 \times 10^5$  (pfu/ml) $\times$ min, which was not significantly different from HSV-1716 (Figure 4.9).

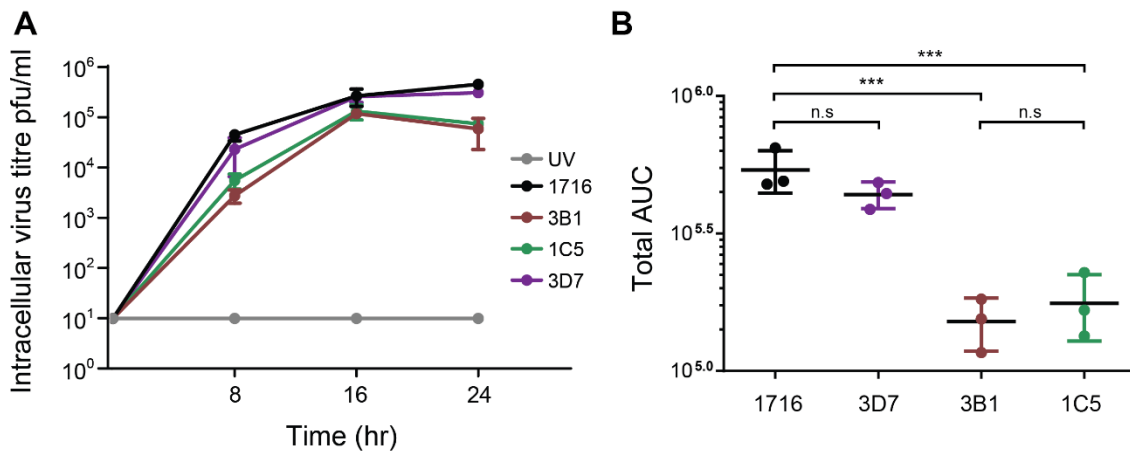


**Figure 4.9 Replication of ICP6-modified viruses in TOV21G cells.** TOV21G cells were infected with each strain of HSV at an MOI of 1 and left for either 8, 16 or 24 h before permeabilising cells and extracting total whole virus for titration determination by plaque assay. 10<sup>1</sup> represents the lowest number of viruses detectable due to dilution factors and so any samples for which plaques were not seen are represented as this value. A replication curve demonstrating viral titre for each time point for a single experiment is shown in 'A'. Here, mean titres are plotted  $\pm$  SD. Separate area under the curve (AUC) analyses were done for each repeat experiment to enable statistical comparison between viruses (B). Individual data points are plotted alongside the means  $\pm$  SD. Statistical significance was determined by one-way ANOVA (Tukey's multiple comparisons test). \*\*\*  $p < 0.001$ ; n.s, not significant.

Therefore, the presence of complete ICP6 appears to be important for viral replication. This is not surprising, as ICP6 was initially identified as a viral ribonucleotide reductase (RR), which catalyses the production of deoxyribonucleotides from ribonucleotides. This is a major step in allowing the virus to replicate efficiently, especially in non-proliferating cells. A virus with a similar genotype, known as G207, has been created previously (Mineta *et al.*, 1995). G207 contains the same  $\gamma$ 34.5 deletion as HSV-1716, but on an HSV-1 strain R3616 background. G207 also contains an *E.coli lacZ* gene in place of the *UL39* gene, which encodes ICP6 (Figure 1.9). Total loss of ICP6 is thought to have a disproportionately large effect on the ability of the virus to replicate in normal cell types, due to the lower abundance of free nucleotides. The presence of a double deletion also makes the virus safer for use as an oncolytic agent due to the decreased likelihood of a double reversion mutation. The data shown here, and in studies performed with G207, show that ICP6 is not necessary for viral replication, but complete ICP6 deletion significantly impairs replication.

The fact that HSV-3D7 showed highly similar levels of replication to HSV-1716 suggests that the single amino acid deletion within the RHIM has had no effect on the RR function of ICP6. This is expected as HSV-3D7 appears to still produce visibly-full-length protein by western blot.

#### **4.5.2 Effect on viral killing**

To determine the effect of these mutations on virus-induced cell death, the viruses were used to infect a number of immortalised and primary OC cell lines, with resulting cell viability measured by MTT assay. In TOV21G cells, HSV-3B1 and HSV-1C5 were both significantly restricted in their ability to cause cell death, requiring higher MOIs to achieve similar levels of killing as HSV-1716 (Figure 4.10a). This restriction in killing ability could be due to the reduced replication of the virus. As would be expected, cell killing induced by HSV-3D7 infection was seen to be no different than HSV-1716, as in this virus, the RR domain is still functionally intact. Interestingly, in OVCAR4 cells there appeared to be no difference in cell death between any of the viruses (Figure 4.10b).

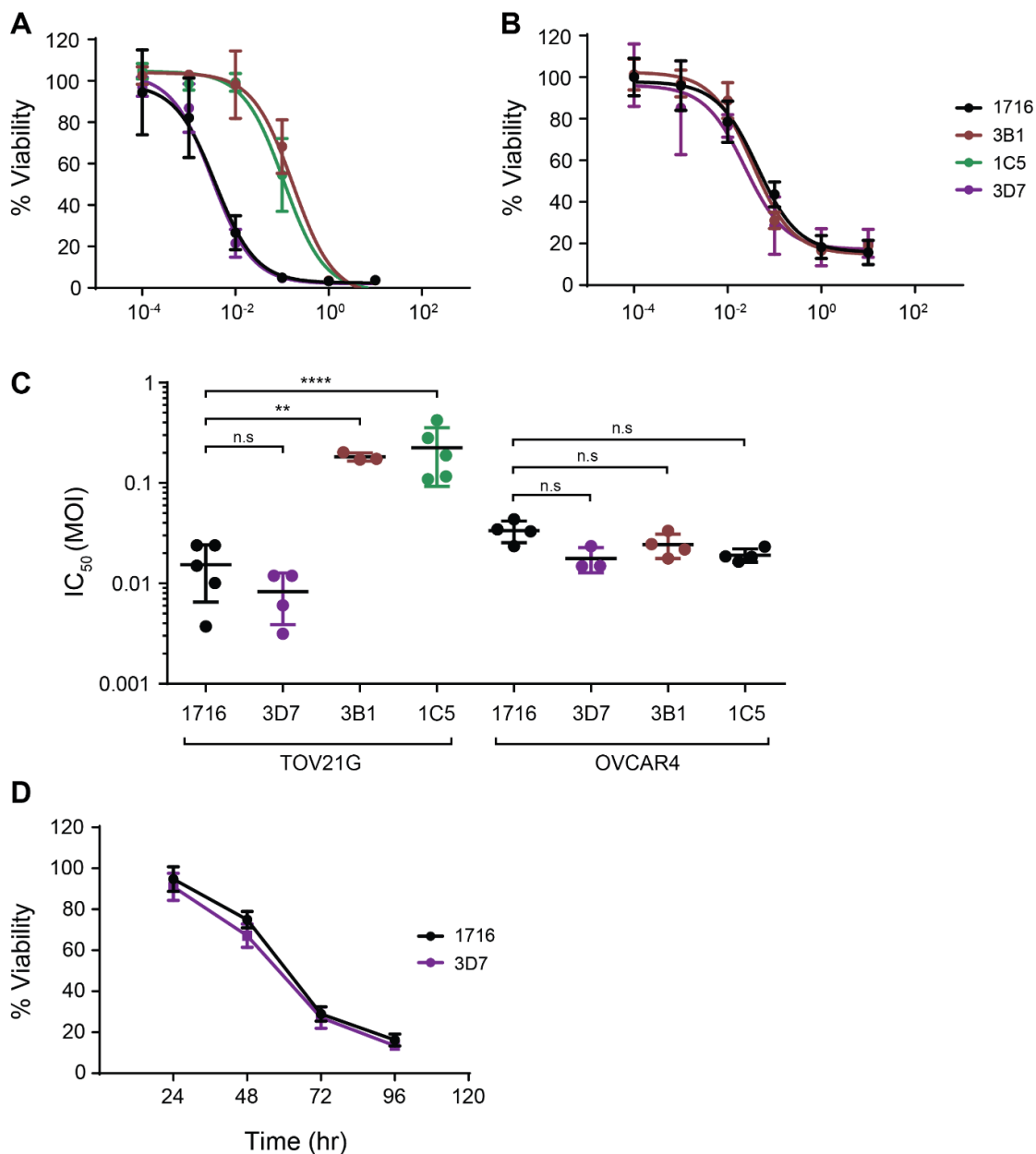


**Figure 4.10 Effect of CRISPR-mediated ICP6 alterations on viral killing in cell lines.** (A-C) TOV21G and OVCAR4 cells were infected with either HSV-1716, -3D7, -3B1, or -1C5 at a range of MOIs for 96 h before determining cell viability by MTT assay. 'A-B' show dose-response data from a single experiment in TOV21G (A) and OVCAR4 (B) cells, and 'C' shows pooled  $IC_{50}$  values from multiple experiments. Statistical significance was determined by one-way ANOVA (Sidak's multiple comparisons test). n.s, not significant; \*\*,  $p < 0.01$ ; \*\*\*\*,  $p < 0.0001$ . (D) TOV21G cells were infected with HSV-1716 or HSV-3D7 at MOI 1 and left for 24, 48, 72 or 96 h before determining cell viability by MTT assay.

When primary cancer cells were infected with the viruses, a similar mixture of effects was seen. In the lines 20160503VF and 20160425LM, much like in TOV21G cells, lower levels of cell killing were seen with HSV-3B1 and HSV-1C5 when compared with HSV-1716 (Figure 4.11). In 20160525HH however, there seemed to be no difference in killing between any of the viruses, as was seen with OVCAR4.

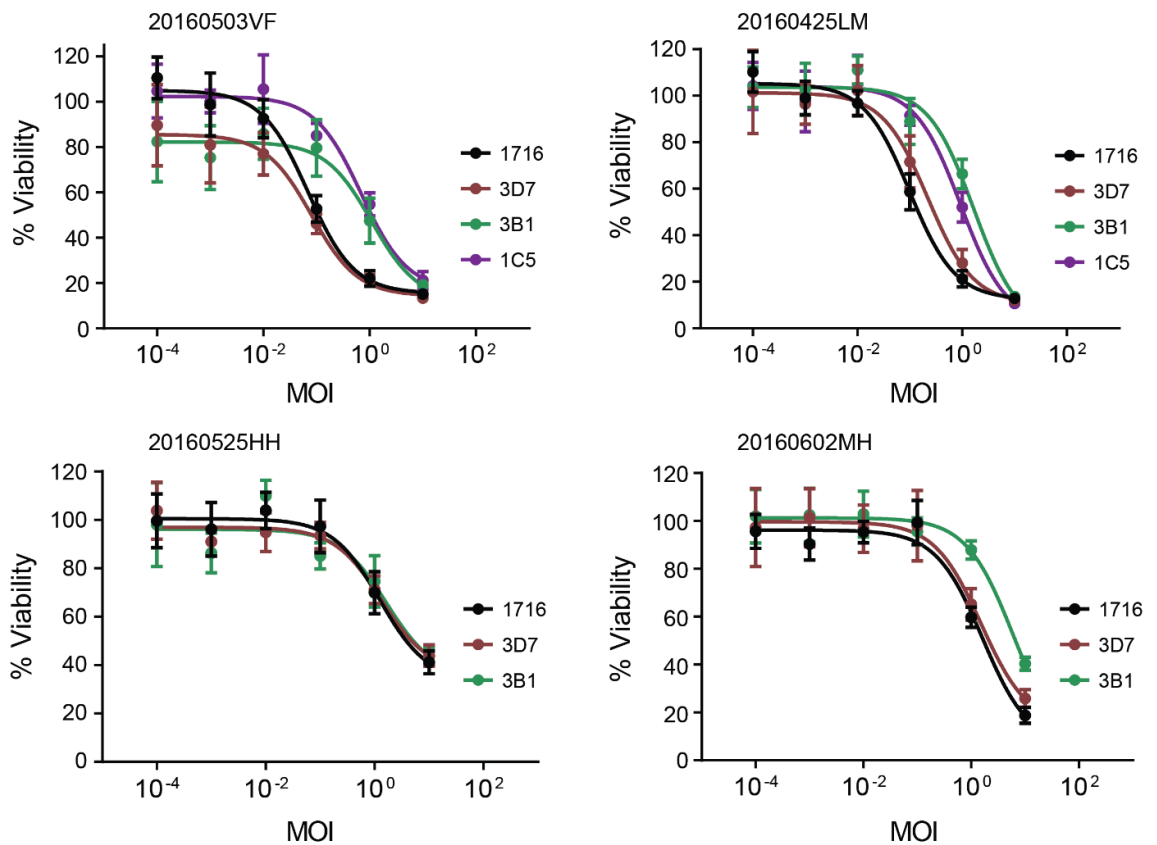


**Figure 4.11 Effect of CRISPR-mediated ICP6 alterations on viral killing in primary OC cells.** Primary OC cells isolated from the ascites of patients were infected with either HSV-1716, -3D7, -3B1, -1C5 at a range of MOIs for 96 h before determining viability by MTT assay. Dose-response data from selected experiments are shown.

Modification of the RHIM of ICP6 is predicted to affect the ability of the protein to bind to and inhibit RIPK3. The result of this is expected to be a greater amount of necroptotic signalling and necrotic death. So far, these results show that amount of overall cell death remains largely unchanged in the presence of this modification. This could mean that a single amino acid deletion in this location is not sufficient to significantly affect RIPK3 binding. Alternatively, it could be that disrupting this interaction does not affect overall quantity of cell death but may still be having other effects on cell signalling, type of death, and the consequences of this.

### 4.5.3 Effect on RIPK3 binding

It has been shown that ICP6 and RIPK3 are able to interact via their respective RHIMs, and it is thought to be this interaction that leads to inhibition of necrosis by preventing RIPK3 phosphorylation and subsequent MLKL activation (Guo *et al.*, 2015). It was therefore important to prove that by altering the RHIM in ICP6, we had subsequently altered its ability to interact with RIPK3.

To achieve this, a RIPK3 coimmunoprecipitation (CoIP) on HeLa-RIPK3 cells infected with either HSV-1716 (WT ICP6), HSV-3D7 (RHIM modified) or HSV-3B1 (ICP6 deleted) virus was performed (Figure 4.12). HSV-1716 was used as a positive control as a virus that should produce ICP6-RIPK3 binding and HSV-3B1 was used as a negative control as a virus that produces no ICP6 at all, while HSV-3D7 was the virus to be tested.

Before this could be performed, a time course experiment was set up to optimise the chance of capturing a protein interaction (Figure 4.12a). For this, protein was extracted from HeLa-RIPK3 and TOV21G cells at 4, 8, 16 and 24 h following infection with HSV-1716. ICP6 and RIPK3 expression was examined by immunoblot. As expected, ICP6 expression increased gradually throughout the course of infection, with initial expression first visible at 8 h p.i for both TOV21G and HeLa cells. RIPK3 expression remained fairly constant throughout the course of infection, more so for TOV21G than HeLa-RIPK3 cells, where RIPK3 expression decreased slightly as infection progressed. Expression of RIPK3 in the HeLa-RIPK3 cells is much higher overall than in TOV21G cells, even considering decrease in expression over time. For this reason, HeLa-RIPK3 cells were chosen as the cell line to use for the CoIP, due to a greater chance of capturing an interaction. In addition to this, 24 h was chosen as the appropriate time point for the same reason.

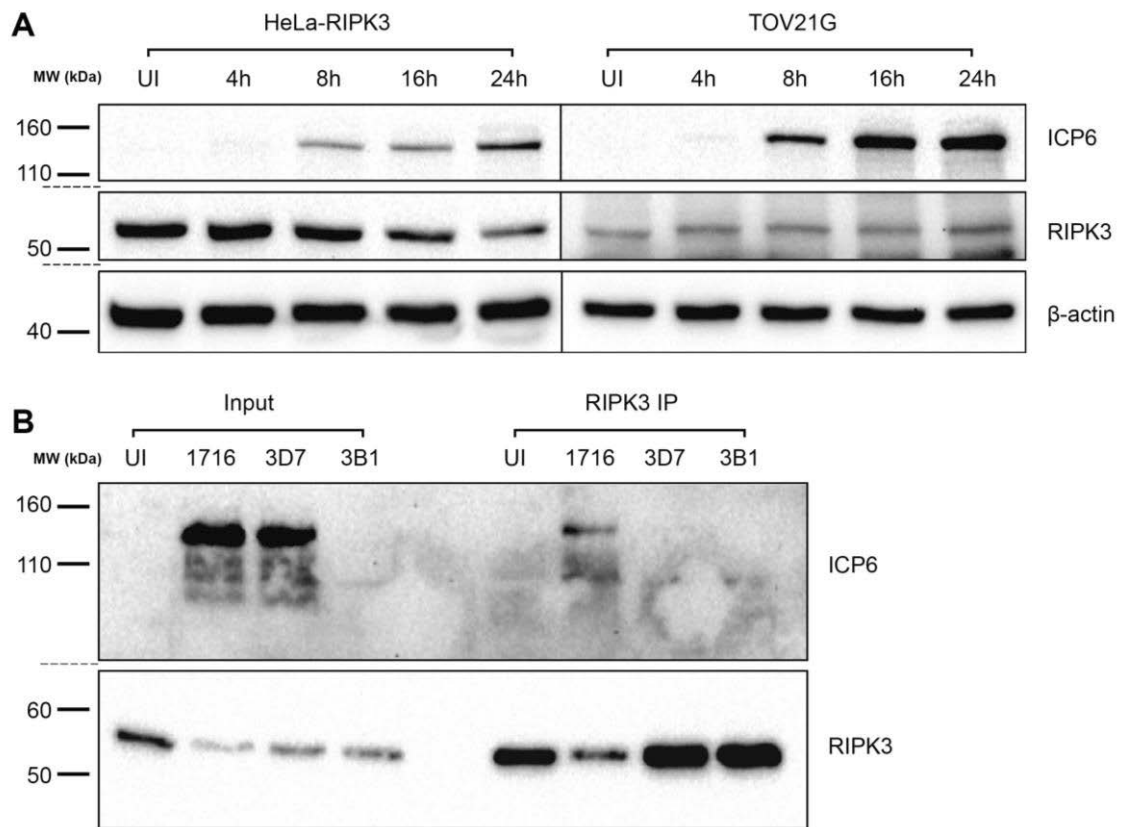


**Figure 4.12 Co-immunoprecipitation of ICP6 and RIPK3 in HSV-infected cells.** (A) HeLa-RIPK3 or TOV21G cells were infected with HSV-1716 at an MOI of 1 and left for 4, 8, 16 or 24 h before extracting whole cell lysate for immunoblot staining against ICP6 and RIPK3. (B) HeLa-RIPK3 cells were infected with either HSV-1716, -3D7 or -3B1 at an MOI of 1 for 24 h before harvesting lysates and precipitating out RIPK3 with a specific monoclonal antibody. Input samples and the precipitated products were compared by immunoblot for presence of ICP6 and RIPK3 pull-down. UI, uninfected; MW, molecular weight; kDa, kilodalton.

Figure 4.12b shows the result of the CoIP of RIPK3 in HeLa-RIPK3 cells infected with HSV-1716 or HSV-3D7 for 24 h. ICP6 expression is clearly seen in the lysate of cells infected with both HSV-1716 and HSV-3D7, but not HSV-3B1, as expected. However, when RIPK3 is precipitated, ICP6 is only detectable in the HSV-1716 and not HSV-3D7 samples. This proves that while full-length ICP6 is still produced by HSV-3D7, the interaction with RIPK3 is absent, indicating that loss of a single RHIM domain amino acid in HSV-3D7 is sufficient to disrupt the interaction with RIPK3. Based upon the data of Guo *et al.*, the expected consequence of this would therefore be that more necrosis signalling is able to take place, as a key block to necrosis in human cells has been removed.

## 4.6 Complementation of $\Delta$ ICP6 HSV-1716 with ICP6 expressing ovarian cancer cells

In order to recreate a system of viral infection, the ICP6 expressing TOV21G cells were infected with both  $\Delta$ ICP6 viruses, HSV-3B1 and HSV-1C5. In theory, this should create a complementary effect allowing us to understand the impact of RHIM function of HSV-1716 induced cell death. Consistently, there was seen to be a difference in sensitivity to cell death between the cell lines. Addition of ICP6(FL) appears to cause a slight reduction in sensitivity to cell death compared to pLV alone. Killing was decreased further in ICP6( $\Delta$ 1-243) cells and even further in the ICP6(*mut*RHIM). If a full complementation effect was being seen, we would expect addition of ICP6(FL) protein into the cells to improve cell killing, restoring it to wild-type levels, as this should mimic standard HSV-1716 infection. This is not the case, however, suggesting that constant expression of ICP6 does not have the same effect as in normal viral infection. This makes interpreting the results seen here difficult. The further inhibition of cell death seen when a functional RHIM is absent, suggests that in this system, the RHIM may have an important role in promoting cell death of some kind.

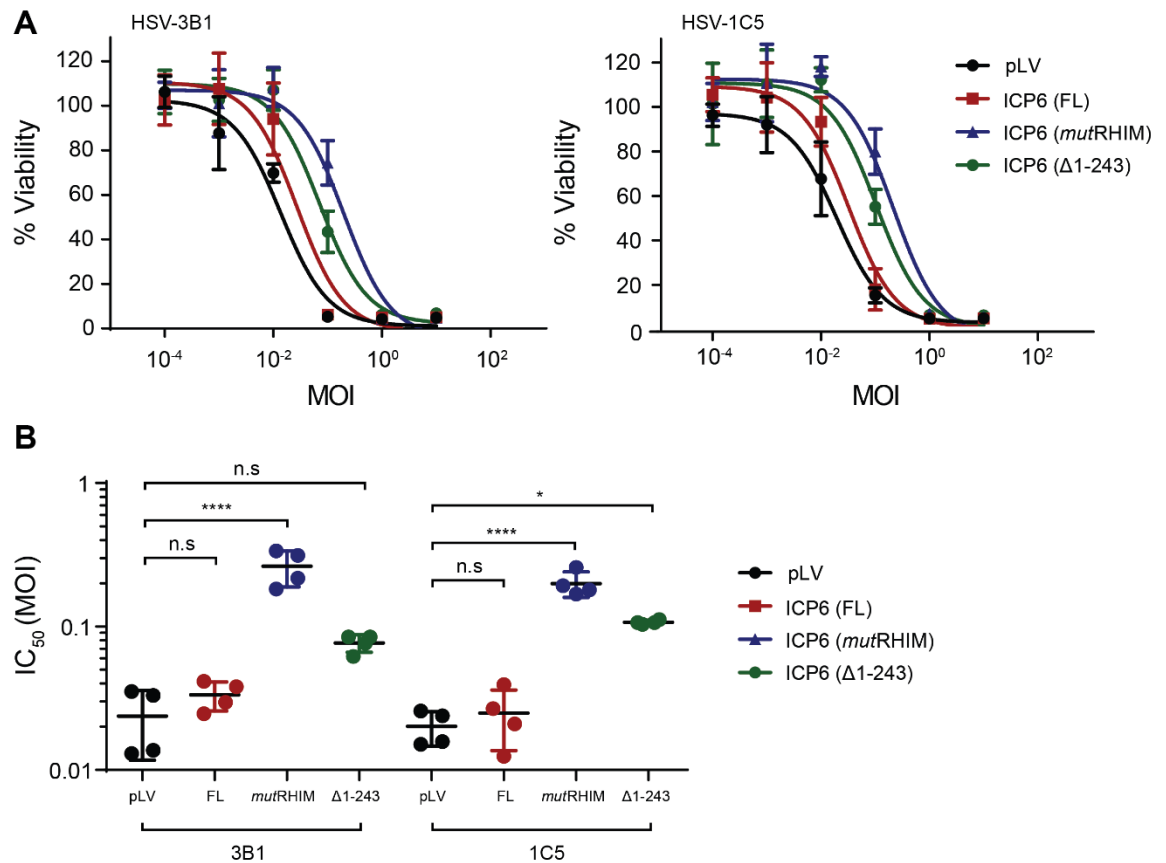


**Figure 4.13 Complementations of ICP6-null viruses with ICP6-expressing cells.** TOV21G cells that had been transduced to express various forms of the viral ICP6 protein were infected with either HSV-3B1 or HSV-1C5 at a range of MOIs for 96 h before determining cell viability by MTT assay. 'A' shows dose response data from a single experiment, with 'B' showing pooled IC<sub>50</sub> values taken from multiple repeat experiments. In both cases, mean viability or IC<sub>50</sub> is plotted  $\pm$  SD. Statistical significance was determined by one-way ANOVA (Tukey's multiple comparisons test). \*  $p < 0.05$ , \*\*\*\*  $p < 0.0001$ ; n.s, not significant; MOI, multiplicity of infection; IC<sub>50</sub>, half-maximal inhibitory concentration.

## 4.7 Discussion

In this chapter, I have described the creation and characterisation of both a range of ICP6-altered viruses and ICP6-expressing cell lines. To successfully alter the genome of HSV-1716, it was first necessary to devise a modified CRISPR-based method tailored to large viruses. Developing efficient methods for genome editing of large viruses is necessary not just for the creation of oncolytic viruses, but also other gene therapy vectors as well as standard investigative virology. Genomes of smaller viruses such as adeno-associated virus or HIV are easily edited as entire genomes can be cloned into single plasmids. For larger viruses, however, construction of large BACs is necessary, which can be time-consuming and laborious. CRISPR therefore presents itself as a potential useful technology for this use. Another downside to the use of BACs is the fact that drug selection

genes need to be placed within the genome of the virus, as opposed to CRISPR where selection of cells takes place prior to viral infection. This can lead to undesirable changes in viral behaviour.

At present, there are still relatively few studies that have described the use of CRISPR in HSV (Bi *et al.*, 2014; Suenaga *et al.*, 2014; Lin *et al.*, 2016). In the first study, Suenaga *et al.* included the *CD8* gene as a selection marker for cells successfully transfected with the CRISPR plasmid (pX330 backbone). Cells were then treated with magnetically-labelled anti-CD8 antibody and separated out from the rest of the population by magnetic-activated cell sorting (MACS). In this thesis, selection of successfully transduced cells was instead made with the inclusion of a puromycin resistance gene, included as part of the pX459v2 plasmid construct. This offered a simpler and less time-consuming method of cellular selection, which also has the benefit of not requiring expensive specialist MACS equipment. Bi *et al.* demonstrated the first use of donor strands to create an insertion of a GFP gene within the *tk* locus. This enabled two ways in which successfully targeted clones could be identified quickly through screening, either by simple microscopy for presence of GFP-tagged cells or by selection with acyclovir, which only targets viruses that are TK-competent. While these methods allow for simple validation of the protocol, these types of selection cannot be used in all situations. One reason being that GFP may interfere with known or currently unknown cellular processes (Jensen, 2012).

In this study, out of 24 clones screened, four were found to have undergone successful gene editing events, giving an efficiency rate of approximately 15%. While this is a small sample size, these figures do suggest that this method can achieve reasonably levels of efficiency of gene editing. The method of selection that I have described therefore has the benefits of being simple, while still avoiding any potential interference from selection genes and maintaining a practical level of efficiency.

Another concern with CRISPR technology is that of off-target DNA-editing effects (Zhang, 2015). This has shown to be a bigger problem in human cells than in the relatively few studies in viruses. This is likely partly due to a larger human genome, which increases the probability of similarities between sites. It may

also be that the shorter timeframe over which viruses are exposed to the CRISPR machinery reduces the likelihood of off-target events. One of the more recent studies showed that when guides were chosen that exclusively aligned to one region (as was done in this study), occurrence of off-target events was reduced below the detection limits of deep sequencing (Lin *et al.*, 2016).

Of the four clones that were isolated, one was shown to possess a two bp deletion, one a three bp deletion, and two a two bp insertion. Of the three guides designed, only two were eventually used. The clones 1C5 and 3D7 were both isolated from a procedure using guide 1, while 3B1 and 3B10 were from a procedure using guide 2. The fact that 3B1 and 3B10 were both found to be identical could therefore be the result of two progeny from a single HR event becoming cloned out separately. It could also be that the same mutation event occurred twice. Mutations made with guide 1 were remarkably precise, spanning only a 4 bp region. Reliable conclusions about precision cannot be drawn from such small sample sizes however.

When assessing replication and killing, clones possessing a total loss of ICP6 were shown to replicate and kill less effectively than HSV-1716 and HSV-3D7 in TOV21G cells. As discussed, this is likely due to the loss of RR activity, which is important for producing free nucleotides for replication. These findings illustrate the importance of probing different regions of proteins for their varied functions and taking these into consideration when making oncolytic vectors. It has been suggested that the RHIM may play an important role in suppressing necroptosis in human cells (Guo *et al.*, 2015). If creating a virus that can optimally induce necroptosis is indeed a therapeutically beneficial goal, then altering ICP6 in such a way that modifies RHIM activity while maintaining the RR domain may be desirable. This same approach should be taken with other multifunctional proteins in HSV or other viruses, as the benefits of removing whole genes may be inferior to modifying select regions. This discussion also ties in to the problem of how to best balance efficacy with safety and specificity. As mentioned, ICP6 is commonly targeted as a means of rendering a virus safer and/or more specific for cancer cells (Mineta *et al.*, 1995; Fukuhara *et al.*, 2005). The replicative costs of deleting this gene must also be weighed up against the benefits of greater safety.

In OVCAR4 cells, loss of ICP6 showed no effect on viral killing. Continuing with the RR hypothesis, it could be that in certain cell lines, free nucleotides are abundant enough to maintain a high level of replication despite RR deficiency. This illustrates that data from different cell lines need to be interpreted carefully. It could mean that, in these cells, the benefits of removing the entire *RL1* gene are higher than selective RHIM manipulation. However, as OVCAR4 cells are not susceptible to death by necroptosis, further investigation into the effect of this is not possible.

The ColP results shown here demonstrate that a small in-frame deletion of a single amino acid within the highly conserved region of the RHIM is sufficient to prevent the interaction between ICP6 and RIPK3. This experiment was performed in the HeLa-RIPK3 overexpression model, which presents certain problems for interpretation. Firstly, higher than typical levels of RIPK3 may lead to non-specific binding patterns to proteins such as ICP6. Conversely, it could be argued that this fact would make the contrasting lack of binding seen with HSV-3D7 more compelling.

Lentivirus based expression systems were used to transduce TOV21G and OVCAR4 cells with various ICP6 constructs (Figure 4.6). These overexpression systems can be useful for comparing the effect of binary presence or absence of a protein. However, when used to compare several different protein constructs to one another, certain considerations need to be noted. Achieving similar levels of protein expression between cell lines is important. Here, levels of expression were compared by western blot, which offers a semi-quantitative estimation of overall protein concentration, assuming that the ICP6 antibody binds with equal affinity. This could mean that small biological differences between cell lines may be due to this factor. Another issue with multiple comparisons is the risk of insertion within different sites of the genome due to the unselective nature of lentiviruses. One must also consider whether to isolate clones for each genotype before comparison. This increases the number of potential comparisons but can provide greater evidence of an effect due to the expressed protein. One issue with clones, however, is the risk of amplifying heterogeneities within the wild-type cell population. Clones may behave differently to one another due to this fact, instead of due to the protein of interest. Maintaining transduced cells as

heterogeneous pools can therefore be a benefit by keeping differences in expression levels, insertion sites and heterogeneity averaged out over the populations. Clones were not made for these cell lines.

In TOV21G cells, response to TSZ was shown to match the results seen with Guo *et al.* Expression of full-length ICP6 leads to a strong significant rescue from TSZ-induced necroptosis. Presumably, this is because the RHIM of ICP6 is successfully blocking RIPK3 activation. This provides some evidence that the necroptotic machinery of TOV21G cells must operate in a way that is functionally similar to the HeLa-RIPK3 line, in which the CoIP was performed. As with the HeLa-RIPK3 system, however, special consideration must be taken as to the reliability of this kind of protein expression. It may be that the higher level of ICP6 protein seen here is more likely to lead to binding and inhibition than during the course of typical viral infection. None of the cell lines expressing constructs lacking a functional RHIM (*mutRHIM*,  $\Delta$ 1-243 and 244-629) were shown to have similar levels of rescue than that of native ICP6, supporting the theory that the RHIM is directly involved in this process. Some significant rescue over the vector control line for the  $\Delta$ 1-243 and 244-629 lines was seen however. These constructs both contain deletions of the first 243 amino acids of the protein. This could mean that other regions within the N-terminal domain, outside of the RHIM, also have roles concerning sensitivity to necrosis, or it may be that differing expression levels between the cell lines is responsible for the slight difference.

In OVCAR4 cells, no change in cell death was seen between cell lines in response to TSZ, with the exception of OVCAR4-ICP6( $\Delta$ 1-243). Some significant changes were also seen between the ICP6(*mutRHIM*) and pLV cells in response to TS, which should have the effect of inducing apoptosis, as caspase-8 remains uninhibited (Chen, Yu and Zhang, 2016). Explaining these changes is difficult given the information available on this system. RIPK1 has been shown previously to have roles in promoting both apoptosis and cell survival following TNF- $\alpha$  stimulation (Gentle *et al.*, 2011; Jin *et al.*, 2016). RIPK1 can become ubiquitinated in a process mediated partly by cIAP1 and cIAP2, which leads to NF- $\kappa$ B activation and promotion of cell survival. RIPK1 can also associate with the proteins FADD and Caspase-8 in what is known as complex IIa, which leads to

apoptosis. This could mean that the RHIM or other regions within the N-terminal domain of ICP6 may interact with either of these processes.

Complementation of ICP6-expressing cell lines with ICP6-null HSV-1716 was designed to recreate the effect of ICP6-mutant viruses. In this system, gene modifications can be made in plasmids using simple molecular biology techniques before reconstitution into lentiviruses and transduction in cell lines. Overall, this system is simpler and less laborious than the current BAC standard for editing viruses themselves. In this instance, lentivirus-ready plasmids were given as a kind gift from the Mocarski lab, which added to their convenience.

Paradoxical results were seen when ICP6-null virus-infected TOV21G-ICP6 lines were assayed for cell viability. Patterns of activity were shown to be the same between the two viruses, confirming their phenotypic similarity. Addition of full-length ICP6 had no effect on viability, whereas  $\Delta 1-243$  and *mutRHIM* cells were less sensitive to viral killing (significant difference between pLV and  $\Delta 1-243$  was only seen for 1C5). Given the results seen following TSZ treatment, we would expect to see an inhibition of viral killing in the cells expressing ICP6. The fact that we did not see this suggests that either RIPK3 activation is not necessary for viral killing or the RIPK3 inhibition that is taking place is not sufficient to affect cell death. It's also important to understand the effect that the addition of a functional RR domain is having here, too. It could be that loss of killing resulting from RIPK3 binding is counteracted by gain of killing from RR ability. The real comparison therefore is that of ICP6(FL) and ICP6( $\Delta 1-243$ )/ICP6(*mutRHIM*). Disruption of the RHIM here seems to inhibit the ability of the virus to kill. This goes against the theory that an uninhibited RIPK3 should be free to trigger necrosis, leading to more cell death. It may therefore be the case that unknown pro-survival roles of RIPK3 and RIPK1 maybe be taking precedence over necrosis induction. Viral infection consists of a much more complex series of interactions with the cell than TSZ treatment, and so it is possible to see contradicting results.

The suitability of this model must also be taken into consideration. Expressing high levels of ICP6 constitutively is unlikely to mimic the cellular environment of viral infection. Protein production and regulation during infection is a tightly

orchestrated series of events, so potential unknown interactions between other viral proteins and the variance in their levels over time must be considered. For this reason, we chose to focus more heavily on the CRISPR-derived RHIM-modified virus, HSV-3D7 for future experiments. This virus contains a RHIM modification that differs from the one contained within the ICP6(*mutRHIM*) cell lines, but this modification was still shown to be sufficient to abolish ICP6-RIPK3 binding.

## **5 Understanding the Role of Immunogenic Cell Death in HSV-1716 infection**

## 5.1 Introduction

Immunogenic cell death broadly describes any type of death that has the ultimate effect of inducing some form of immune system reaction. An exact nomenclature for immunogenic cell death types has yet to be entirely agreed upon. The markers of 'immunogenic cell death' defined by Kroemer *et al.* are calreticulin exposure, ATP and HMGB1 release (Kroemer *et al.*, 2013). As this is not strictly the only type of cell death that is immunogenic, this type of death has also been referred to as immunogenic apoptosis (Vandenabeele *et al.*, 2016). It is also important to note that certain aspects of this are not limited to apoptotic death, with markers such as HMGB1 and ATP release having been seen in otherwise 'necrotic' cell systems (Whilding *et al.*, 2013; Newton and Manning, 2016). Other types of cell death that have been shown to be immunogenic are necrosis and pyroptosis and some forms of autophagy-induced cell death (Galluzzi *et al.*, 2012, 2014; Pasparakis and Vandenabeele, 2015). These modes of death all represent distinct non-apoptotic processes and so should not be bundled together with immunogenic apoptosis. 'Necroptosis' is another label that is sometimes used clumsily. Necrosis is itself a type of immunogenic cell death, with necroptosis being a specific subset of this. Necrosis is defined by primarily visual and markers such as cell swelling and membrane permeabilization seen by TEM. To characterise cell death as being necroptotic, one must prove that formation of the necrosome complex, consisting of RIPK1, RIPK3, MLKL, FADD and caspase-8 is occurring.

To characterise the type of cell death following infection with HSV-1716 and HSV-3D7, markers of different types of ICD were analysed. The goal of these experiments was to establish answers to the following questions: Does HSV-1716 induce a form of immunogenic cell death in cancer cell lines? Does disruption of the interaction between ICP6 and RIPK3 alter the mode of cell death caused by the virus? The second question was addressed by comparing the difference in markers of cell death following HSV-1716 and HSV-3D7 infection.

## 5.2 Markers of immunogenic apoptosis following HSV-1716 or HSV-3D7 infection

### 5.2.1 Extracellular calreticulin exposure

CAL is the most abundant protein present in the ER lumen. In response to induction of immunogenic cell death, a portion of this CAL is transported to the cell membrane within vesicles that are exocytosed, resulting in its expression on the outside of the cell. This phenomenon can be observed using flow cytometry by staining non-permeabilised cells. CAL is an important marker of immunogenic apoptosis mainly because of its ability to act as an “eat-me” signal by binding to CD91 on the surface of macrophages and DCs, which leads to phagocytosis of the CAL-exposing cell (Basu *et al.*, 2001; Obeid *et al.*, 2007; Chao *et al.*, 2010).

To determine whether CAL is exposed following HSV-1716 treatment, TOV21G cells were infected for 1, 4 and 24 h before analysis by flow cytometry (Figure 5.1). At no time point did cells show any sign of extracellular CAL increase compared to baseline. This suggests that CAL does not translocate to the membrane during HSV-1716 infection, and that cells are therefore not subject to the immunogenic consequences that such a translocation entails. As a positive control, TOV21G cells were fixed before being treated with Triton-X, a membrane permeabilising detergent, for 5 min. These cells showed a distinct increase in CAL staining intensity, suggesting that this protein is still present within the cells.

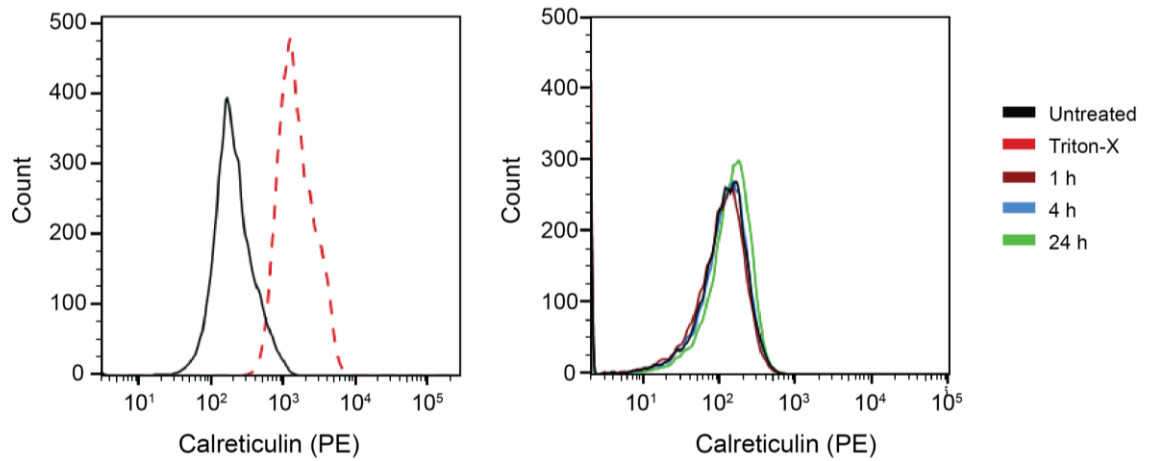


**Figure 5.1 Calreticulin release from HSV-1716-infected cells.** TOV21G cells were infected with HSV-1716 at MOI 1 and left for 1, 4 or 24 h before suspending cells into FACS buffer and staining with a PE-conjugated CAL antibody and Zombie Violet viability dye. Samples were then analysed by flow cytometry. Zombie Violet staining was used to exclude already dead cells, leaving histogram plot data here for CAL.

### 5.2.2 HMGB1 release

HMGB1 is a chromatin-associated non-histone protein that is universally expressed (Kroemer *et al.*, 2013). HMGB1 can be released from cells both actively and passively and so has become a hallmark of both immunogenic apoptosis and necrosis (Scaffidi, Misteli and Bianchi, 2002; Andersson and Tracey, 2011). HMGB1 is a relevant marker of ICD due to its role in directly stimulating the innate immune system, through binding to and stimulating receptors such as TLR4 and CD24.

HMGB1 release was assessed by immunoblot on samples from cells that had been infected with virus at MOI 1 for 16 h. Supernatant from these samples was then concentrated. The volumes of these concentrates were then measured, and the samples diluted until all samples were of equal volume.

HMGB1 present intracellularly, as measured by immunoblot in whole cell lysates, was unchanged across all conditions, with the exception of HSV-1716-infected HeLa-RIPK3 cells, in which levels were slightly lower (Figure 5.2). In TOV21G cells, HMGB1 was present in the supernatant following HSV-1716 and HSV-3D7 infection but not in uninfected cells, indicating that HSV-1716 cytotoxicity in TOV21G cells demonstrates at least one immunogenic component. There was no difference in HMGB1 release seen between HSV-1716 and HSV-3D7 infected cells,

suggesting that disruption of ICP6-RIPK3 binding has no effect on HMGB1 release.

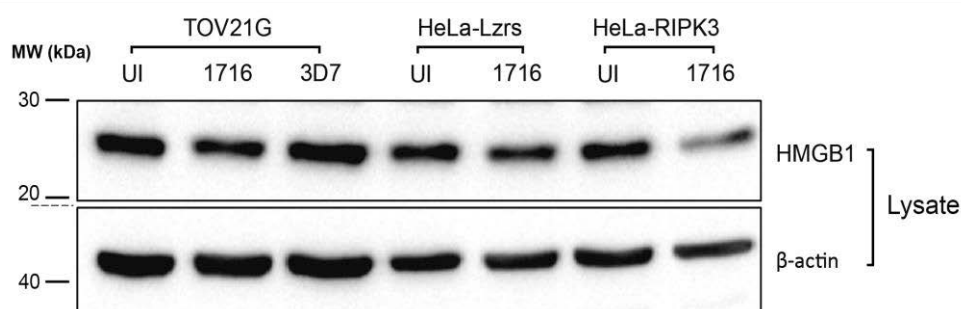


**Figure 5.2 HMGB1 release following HSV-1716 and HSV-3D7 infection of TOV21G and HeLa cells.** TOV21G and the HeLa cell isogenic RIPK3 pair were each infected with either HSV-1716 or HSV-3D7 for 16 h before lysates were taken and supernatants were harvested and concentrated. Samples were then prepared and stained for HMGB1 and  $\beta$ -actin by immunoblot. MW, molecular weight; kDa, kilodalton; UI, uninfected.

In the HeLa-RIPK3 overexpression model, HMGB1 levels were also shown to increase following infection of HeLa-Lzrs cells with HSV-1716. In comparison to TOV21G, HeLa-Lzrs cells appear to have higher levels of basal HMGB1 release, which reaches higher overall levels following infection. The difference in levels between infected and uninfected is also much greater in the HeLa, suggesting a greater overall sensitivity to ICD. It is possible, however, that the limit of detection of this assay is too small to determine a more pronounced change in release.

Interestingly, in the HeLa-RIPK3 cells there is greater basal release of HMGB1 compared to HeLa-Lzrs, indicating that expression of RIPK3 alone can force cells to undergo cellular release with no external stimulus. As HMGB1 can be associated with both necrosis and IA, it is not possible to determine from these data alone which mode of death is being activated. As expected, when HeLa-RIPK3 cells are infected with HSV-1716, levels of HMGB1 increase further. It is not clear, due to the semi-quantitative nature of this blot, whether the increase following HSV-1716 infection is greater in HeLa-RIPK3 cells, or whether this just represents higher basal levels in both infected and uninfected cells. This provides further evidence to the theory that overexpression of RIPK3 can drive cells down a necrosis-like pathway, that is possibly further affected by HSV-1716.

$\beta$ -actin staining was present in the concentrated supernatants, which was unexpected. Levels of this did not seem to change across conditions as drastically as HMGB1, with levels appearing lower in uninfected lysates.

### **5.2.3 ATP release**

ATP release is the third major DAMP released in association with IA. ATP, along with other nucleotides, is also commonly associated with non-specific release following necrosis (Dosch *et al.*, 2018). TOV21G cells were infected with either HSV-1716 or HSV-3D7 at the selected MOIs of 0.03, 0.3 and 3 and incubated for 48 h before harvesting supernatants to determine ATP concentration. ATP concentration was determined using a luminescence-based assay which relies on the chemical reaction of ATP with D-Luciferin. Cell viability was determined by MTT assay in parallel to confirm the presence and magnitude of cell death that was occurring.

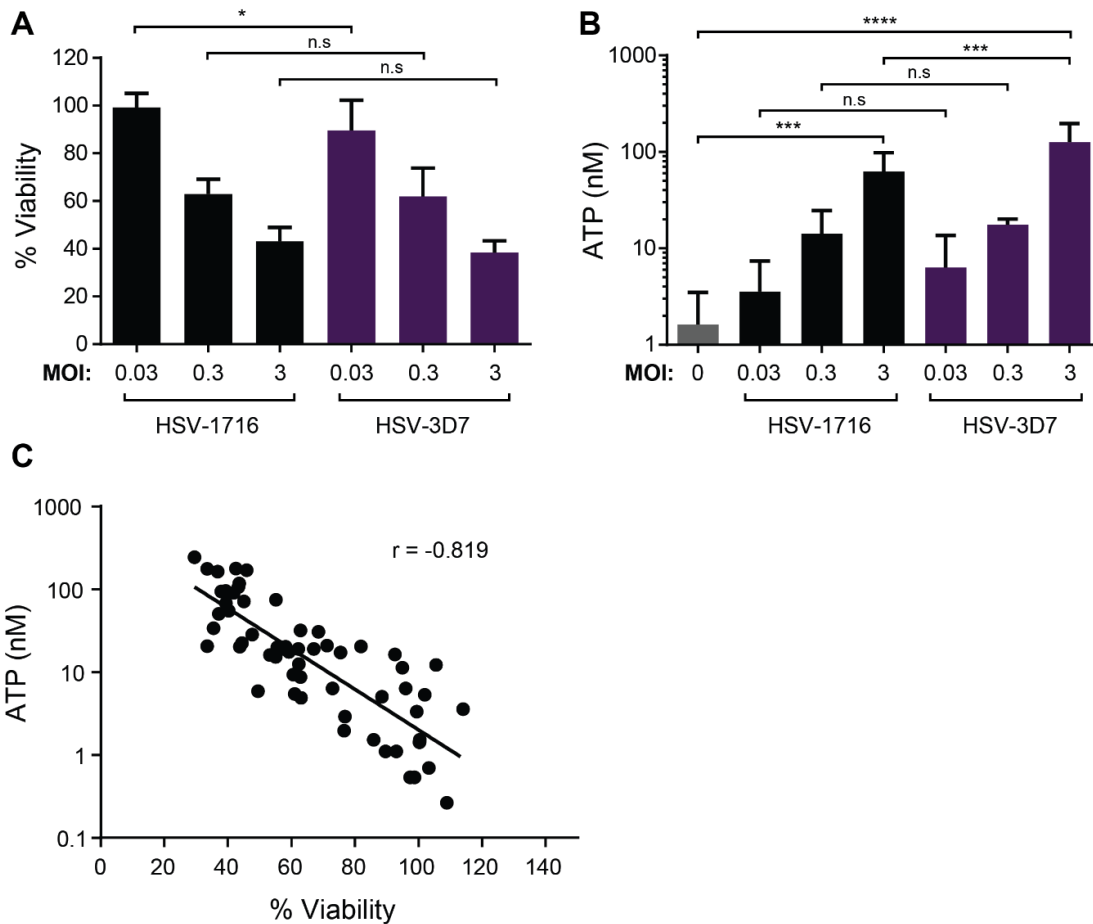


**Figure 5.3 Release of ATP from HSV-1716 and HSV-3D7 infected cells.** TOV21G cells were infected with HSV-1716 or HSV-3D7 at a range of MOIs for 48 h before determining cell viability by MTT assay. In parallel, supernatants from infected cells were harvested, with ATP concentration determined by luminescence-based assay. 'A' shows % cell viability following infection, 'B' shows parallel ATP supernatant concentrations. Mean values from a single experiment are plotted  $\pm$ SD. Statistical significance was determined by one-way ANOVA (Sidak's multiple comparisons test (A), Tukey's multiple comparisons test (B)). n.s, not significant; \*,  $p < 0.05$ ; \*\*\*,  $p < 0.001$ ; \*\*\*\*,  $p < 0.0001$ . (C) ATP concentrations and cell viability measures are correlated for individual data points, with  $r$  value displayed. Line of best fit based on linear regression is also shown.

When comparing % cell viabilities, no significant difference in death was seen between HSV-1716 and HSV-3D7 at the MOIs of 0.3 and 3 (Figure 5.3a), which mirrors what has previously been seen when comparing death caused by these two viruses (Figure 4.10). There was, however, a marginal significant increase in mean death at the 0.03 MOI (99.2 vs 90.0,  $p = 0.042$ ). Similar levels of death allow for easy comparison of the parallel ATP release.

In Figure 5.3b, ATP release can be seen to clearly increase as MOI increases. Statistically significant change compared to uninfected cells can only be seen in cells infected with MOI 3 of both viruses (HSV-1716, 63 vs 1.6,  $p = 0.0006$ ; HSV-3D7, 126 vs 1.6,  $p < 0.0001$ ). Comparison between other MOIs and uninfected were not significant (annotation not shown).

When comparing differences in ATP release between the two viruses, again, a statistically significant higher level of release was seen following HSV-3D7 infection compared to HSV-1716 - at MOI 3 only (126 vs 63,  $p=0.0003$ ). This difference is important as it is seen at an MOI for which levels of cell death appear to be the same.

To gain further confirmation that ATP release is a phenomenon that occurs following HSV infection, all individual values for cell viabilities were correlated against ATP release and plotted along with a line of best fit (Figure 5.3c). A strong negative linear relationship was seen between the two measures ( $r=-0.819$ ).

#### **5.2.4 Response to inhibition of caspase-8**

Caspases are a group of cysteine-proteases that have become known largely for their roles in promoting and executing apoptosis (Elmore, 2007). Executioner caspases require cleavage by other proteases in order to become activated for apoptotic purposes. Classical apoptosis stems from two inter-connected pathways, known as the intrinsic and extrinsic pathways. Caspase-8 is involved towards the end of the extrinsic pathway and caspase-9 is involved toward the end of the intrinsic. Both caspases-8 and -9 are able to proteolytically cleave the key executioner caspase-3, which activates it, allowing it to initiate many of the physiological effects of apoptosis. The compound zVAD-fmk is able to block all caspase subtypes, although it does have higher affinities for some over others (Yang *et al.*, 2004; Yee *et al.*, 2006). It is also able to promote necroptotic cell death via its inhibition of caspase-8, which aids in the formation of the necrosome complex (Vandenabeele, Vanden Berghe and Festjens, 2006).

To determine the role of apoptosis in HSV-1716 and HSV-3D7-induced cell death, cells were infected with either virus at a range of MOIs and treated with the pan-caspase inhibitor zVAD-fmk (25  $\mu$ M) for 96 h, before measuring viability by MTT assay (Figure 5.4). The purpose of this experiment was to see if inhibition of caspases had an effect on viral-induced cell death. If a decrease in cell death is seen with zVAD-fmk, then that death is likely apoptosis-dependent; if no change

in cell death, or an increase in death is seen, then that death is not apoptosis-dependent.

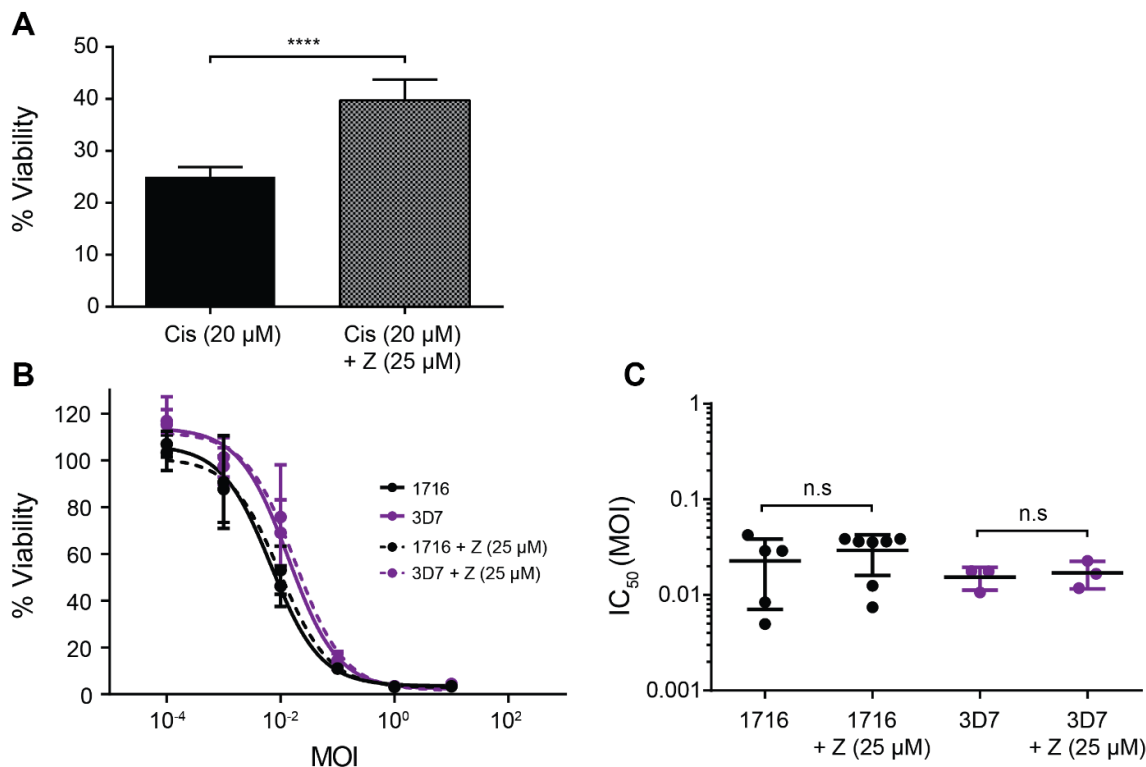


**Figure 5.4 Effect of caspase inhibition on HSV killing in TOV21G cells.** (A) TOV21G cells were treated with either cisplatin (Cis) alone or in combination with zVAD-fmk (Z) at concentrations of 20 μM and 25 μM respectively and left for 48 h before determining cell viability by MTT. Significance was determined by unpaired, two-tailed t test; \*\*\*\*,  $p < 0.0001$ . (B and C) TOV21G cells were infected with either HSV-1716 or HSV-3D7 at a range of MOIs and left for 2 h before refeeding with either untreated media or media containing zVAD-fmk (final conc, 25 μM). After 96 h, cell viability was determined by MTT assay. 'B' shows dose-response data from a single experiment, while 'C' shows pooled IC<sub>50</sub> data from several repeat experiments, with significance determined by Tukey's one-way ANOVA multiple comparisons test: n.s, not significant. MOI, multiplicity of infection; IC<sub>50</sub>, half-maximal inhibitory concentration.

Before this experiment could be performed, a positive control experiment was first necessary to see if 25 μM zVAD-fmk was sufficient to protect against apoptosis in TOV21G cells. Earlier experiments have shown that this concentration of zVAD-fmk is sufficient to entirely rescue certain cells from TS-induced apoptosis (OVCAR4, Figure 3.3; HeLa-Lzrs, Figure 3.4), however, addition of zVAD-fmk in TOV21G only promotes necroptosis following TS treatment.

Cisplatin is a well-known inducer of apoptosis, which acts by cross-linking DNA. This leads to activation of the DNA-damage pathway, which involves proteins such as ATR, p53, p73, and mitogen-activated protein (MAP) kinases, culminating

in induction of apoptosis (Tanida *et al.*, 2012). Here, TOV21G cells were treated with 20  $\mu\text{M}$  cisplatin with and without 25  $\mu\text{M}$  zVAD-fmk (Figure 5.4). In the cisplatin-only condition, there was a significant reduction in viability to 25%, which was partially rescued by zVAD-fmk to give a mean survival of 39% ( $p < 0.0001$ ). This demonstrates that 25  $\mu\text{M}$  zVAD-fmk is sufficient to cause some level of caspase inhibition.

In contrast to cisplatin, when TOV21G cells were infected with either HSV-1716 or HSV-3D7 in the presence of zVAD-fmk, no significant change in cell death was seen when compared to either virus alone (HSV-1716,  $p=0.8$ ; HSV-3D7,  $p=1.0$ ). This shows that caspases alone are not necessary for the induction of cell death by HSV-1716. There was also no effect on cell death when the same cells were infected with HSV-3D7. This shows that modification of the RHIM of ICP6 does not lead to any increase in reliance on apoptosis. It has been shown that a region within the RR domain of ICP6 is capable of binding to and inhibiting caspase 8 (Dufour *et al.*, 2011). This is thought to prevent the virus from inducing apoptosis. As no modifications to this domain are present in HSV-1716 or HSV-3D7, it makes sense that adding in additional caspase blockade would do nothing to affect cell death induced by either virus.

## **5.3 Markers of general necrosis following viral infection**

### **5.3.1 Annexin V/ Zombie Violet staining**

TOV21G cells were infected with either HSV-1716 or HSV-3D7 for 24-72 h and assayed for phosphatidylserine (PS) exposure and pore formation by flow cytometry. PS is a naturally occurring phospholipid that sits within the plasma membrane. During the initial stages of apoptosis, PS becomes exposed on the outer cell membrane. Outer membrane PS exposure can be detected by Annexin V (AV), a protein that binds to PS in the presence of  $\text{Ca}^{2+}$  ions. AV that is conjugated to a fluorophore such as fluorescein isothiocyanate (FITC) or phycoerythrin (PE), can be detected by flow cytometry. AV is typically used in conjunction with a membrane-impermeable nuclear stain, which can detect pore formation and therefore act as a viability/membrane integrity dye, such as propidium iodide (PI) or Zombie Violet (ZV), which is a dye that works similarly

to PI, but differs in that it retains fluorescence following fixation, and so is more easily utilised for virus experiments.

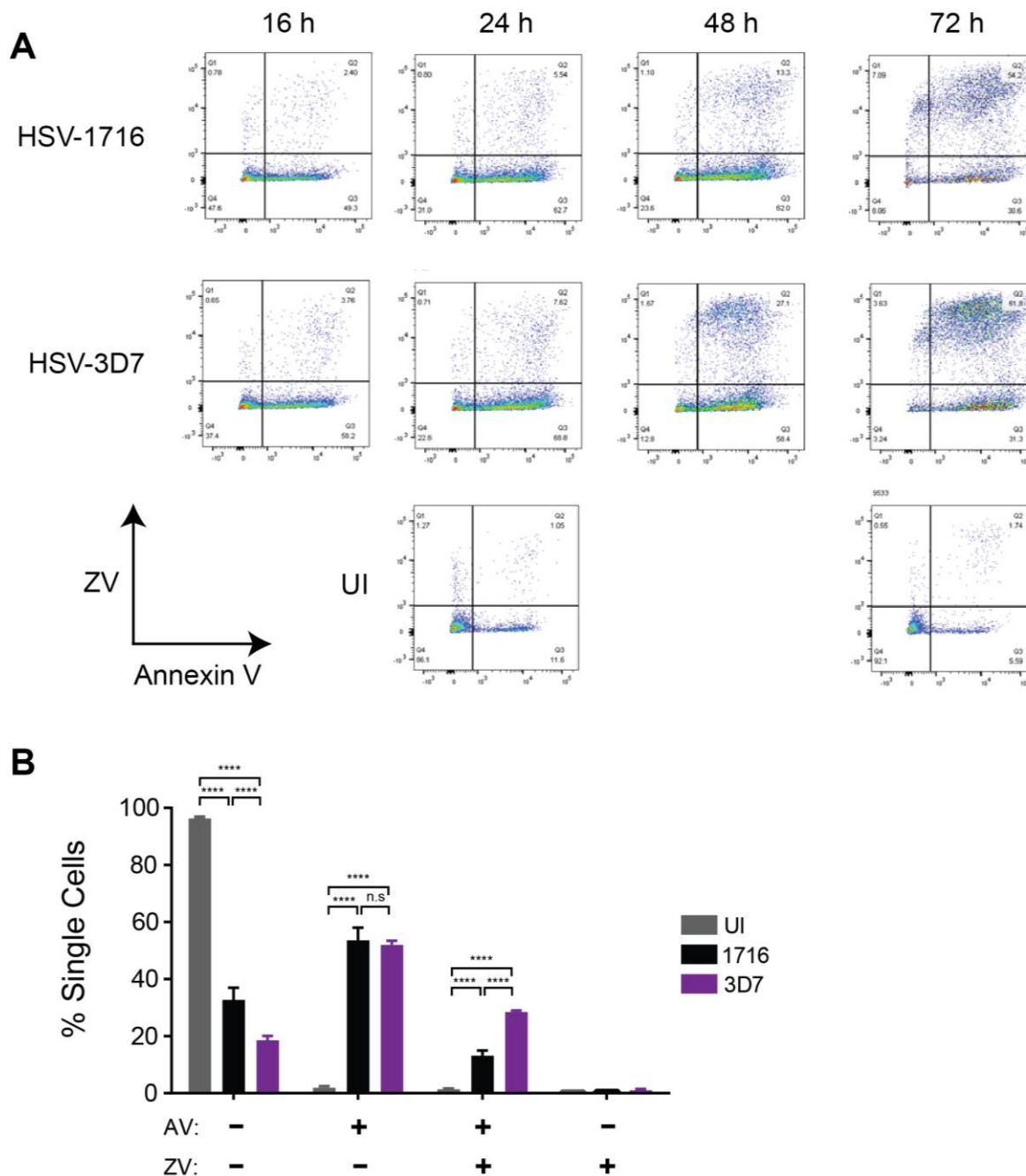


**Figure 5.5 Effect of HSV-1716 and HSV-3D7 infection on Annexin V exposure and pore formation.** TOV21G cells were infected with either HSV-1716 or HSV-3D7 at an MOI of 1 for either 16, 24, 48, or 72 h before being trypsinised and suspended in FACS buffer, and then subsequently stained for either FITC-conjugated Annexin V (AV) or Zombie Violet (ZV) nuclear viability dye. Cells were then fixed, and data obtained using a flow cytometer. (A) Individual dot plots of staining intensity for both AV and ZV are shown here. Cell doublets were first gated out based on forward and side scatter, and then cut-offs for a positive stain were made based on unstained samples (not shown). (B) Values from repeat experiments at the 72 h time point were pooled and plotted as a bar plot to calculate statistical differences. Statistical significance was determined by two-way ANOVA (Dunnett's multiple comparisons test). \*\*\*\*  $p < 0.0001$ ; n.s, not significant. UI, uninfected.

Combining AV with a nuclear stain is an established method for monitoring the time course of apoptotic and necrotic death. In apoptotic cells, a period of positive AV staining is seen before the emergence of membrane pores, which indicates secondary necrosis; cells dying by a primarily necrotic form of cell death will display pore formation in conjunction with AV staining (Rieger *et al.*, 2011). The purpose of this experiment was to assay for the presence of necrosis and apoptosis in dying cells infected with HSV-1716 or HSV-3D7.

TOV21G cells infected with either virus display what appears to be a period of positive AV staining before ZV staining becomes positive, which is suggestive of an apoptotic mechanism. However, staining of cells observed at 72 h, show a significantly higher proportion of double positive AV+ZV+ (late necrotic) cells in the HSV-3D7 infected population ( $p < 0.0001$ ) compared to HSV-1716, while proportions of AV+ZV- (apoptotic) cells show no significant difference. This means that there are a greater portion of permeabilised cells following HSV-3D7 infection, which could mean that, despite similar levels of early apoptosis and similar levels of overall cell death, HSV-3D7 is inducing an altered mode of cell death that leads to greater cell permeabilization, such as necrosis.

### **5.3.2 Visual evidence of necrosis by TEM**

To understand the visual aspect of the cell death process in both HSV-1716 and HSV-3D7-infected cells, electron micrograph images were taken following infection of TOV21G cells in culture at an MOI of 1 for 48 h (Figure 5.6-Figure 5.9). As a positive control for a classic necrotic phenotype, one set of cells was treated with TSZ for 48 h. Multiple images were taken at two different magnifications to observe gross cell morphology, mitochondrial morphology and presence of whole virions. Figure 5.6 shows uninfected control cells - cells appear elongated with a diameter of approximately 8  $\mu\text{m}$ . Nuclei are large, taking up much of the cell, but appear in tact with a well-defined electron-dense nuclear membrane and visible nucleoli. Some filopodia are also visible along the flanks of the cells. Mitochondria can be seen in the more magnified images and appear unperturbed, with regular cristae. The diameter of the mitochondria is approximately 400-600 nm.

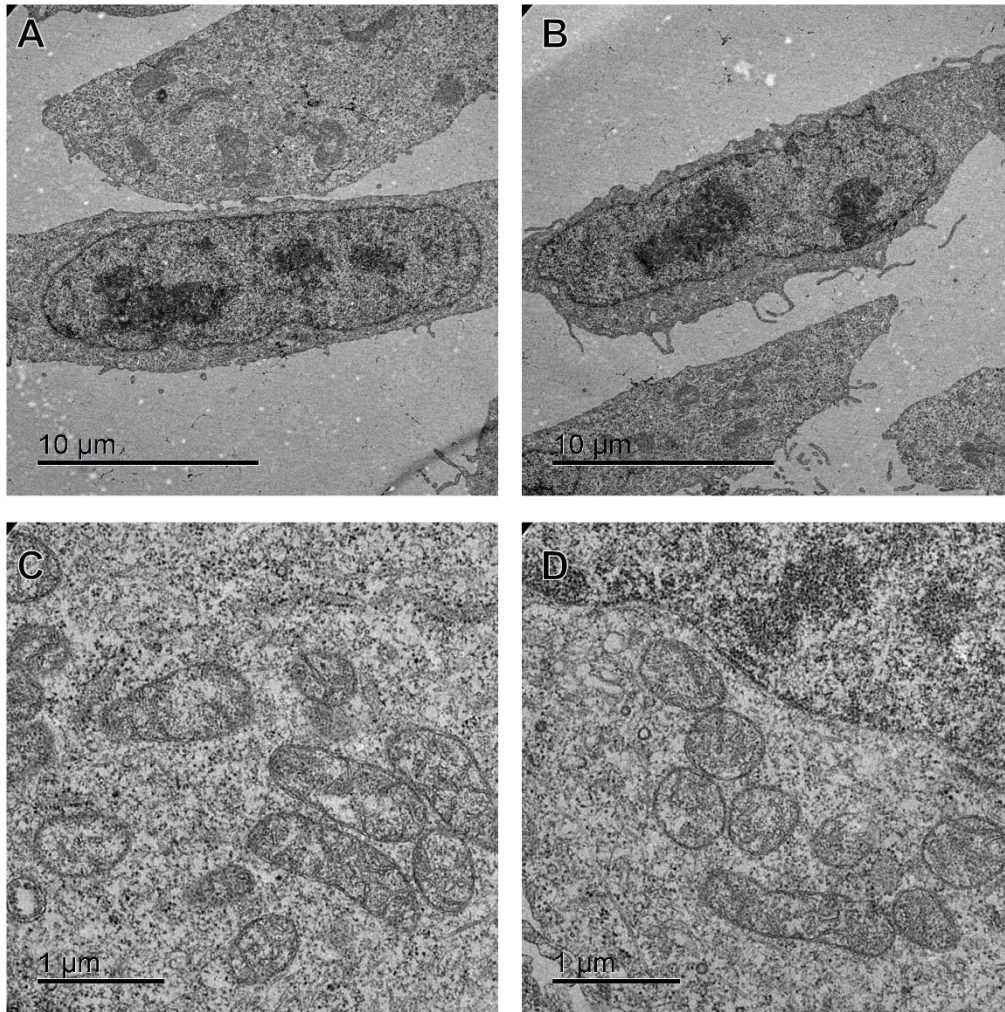


**Figure 5.6 Electron micrograph images of uninfected TOV21G cells.** (A-B) Low magnification images of uninfected TOV21G cells. Cells take on an elongated shape with in-tact nuclei and cell membranes. (C-D) Higher magnification image of mitochondria, which appear in-tact with regular cristae. Scale bars are shown in the bottom left of each image.

Upon treatment with the necroptosis-inducing combination TSZ, cellular morphology begins to change drastically (Figure 5.7). Both cytoplasmic and nuclear swelling begin to occur. Cellular diameter appears to be approximately 10-20  $\mu\text{m}$ . Occurrence of pore formation in the plasma membranes of dying cells was seen (Figure 5.7; indicated by red arrows). Together these indicate a largely necrotic morphology. Higher magnification analysis of the mitochondria shows a slightly swollen and more deformed morphology than those of uninfected cells. Diameters of these mitochondria are larger on average ranging from 400 nm to 1 $\mu\text{m}$ .

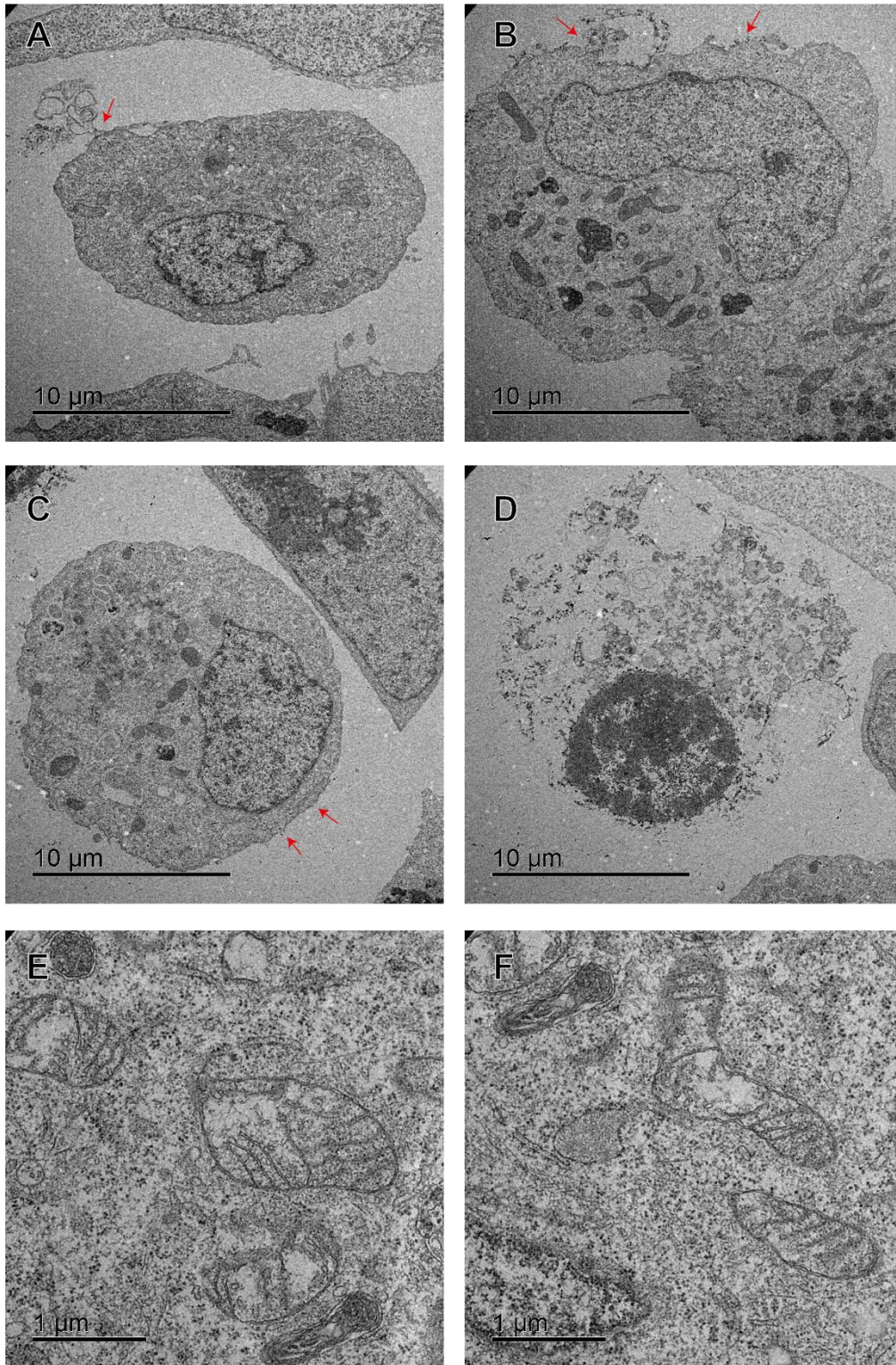


**Figure 5.7 Electron micrograph images of TOV21G cells treated with TSZ.** (A-D) Low magnification images of whole cells following treatment with TSZ. Cells are showing typical signs of death and necrosis, illustrated by enlarged, swollen cytoplasm and nuclei, and loss of membrane integrity (red arrows). A later stage necrotic cell is shown in panel D, in which cellular contents have become released into the extracellular space and the nucleus has begun to degrade. There is a distinct lack of budding, chromatin condensation or vacuolisation, which would be indicative of apoptosis. (E-F) Higher magnification of mitochondria, showing swollen and deformed morphology.

When cells were infected with HSV-1716, broadly similar morphology changes were seen in comparison to TSZ treatment. Many cells were swollen and enlarged, with evidence of loss of plasma membrane integrity and cellular spillage (Figure 5.8a-b). There were instances of what appear to be more apoptotic cell morphologies (Figure 5.8c). This consisted of cellular shrinkage and condensation of the nuclear chromatin, accompanied by large-scale cellular vacuolisation and membrane 'budding'. Cells with this kind of phenotype were relatively less abundant compared to the more necrotic types. In HSV-3D7-infected cells, similar necrotic morphologies were noted in most cells.

Some small, regularly-sized spherical structures were seen in both HSV-1716 and HSV-3D7-infected cells (Figure 5.8d, Figure 5.9d), but not in uninfected or TSZ-treated cells. The diameters of these structures was approximately 120 nm for both viruses (SD=10), which corresponds with the known diameter of the HSV capsid, 125 nm (Knipe *et al.*, 2014).

In both HSV-1716 and HSV-3D7-infected cells, distinct mitochondrial changes were seen, which differed from those seen in TSZ-treated cells. The mitochondrial diameters were between 170 and 340 nm, much smaller than in both uninfected and TSZ-treated cells. This change appeared in combination with a more electron-dense appearance, and in some cases, appearing elongated or fused with one another.

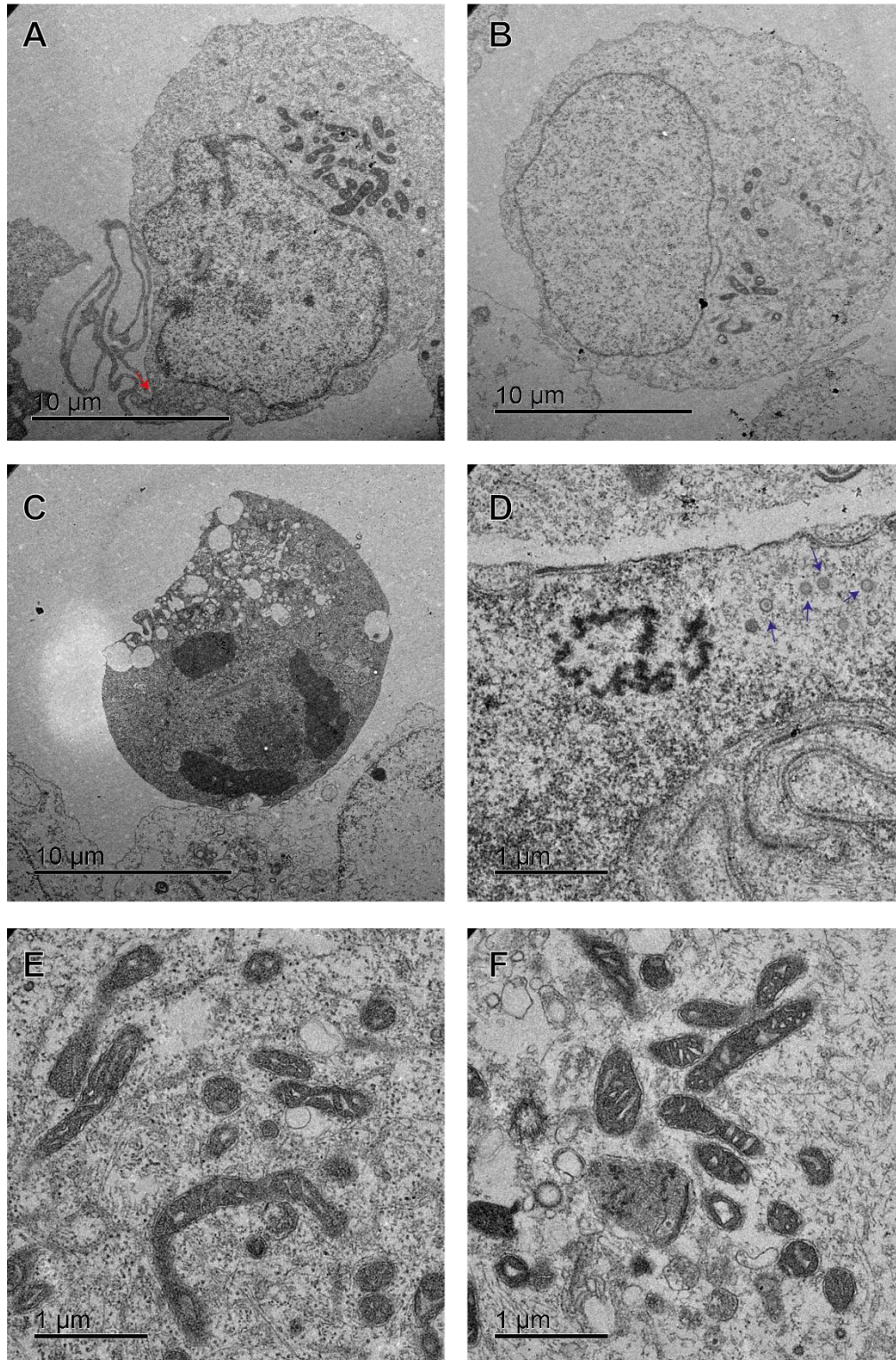


**Figure 5.8 Electron micrograph images of TOV21G cells infected with HSV-1716.** (A-C) A selection of low magnification images of whole cells infected with HSV-1716. Panels A and B show classically necrotic cell morphologies, consisting of swollen cytoplasm and nuclei, and loss of membrane integrity (red arrow). In panel C, a more apoptotic phenotype is apparent, with chromatin condensation, mass vacuolisation and membrane budding. (D) Evidence of whole virions is denoted by the blue arrows. (E-F) higher magnification images of mitochondria show a distinct electron dense and condensed phenotype.

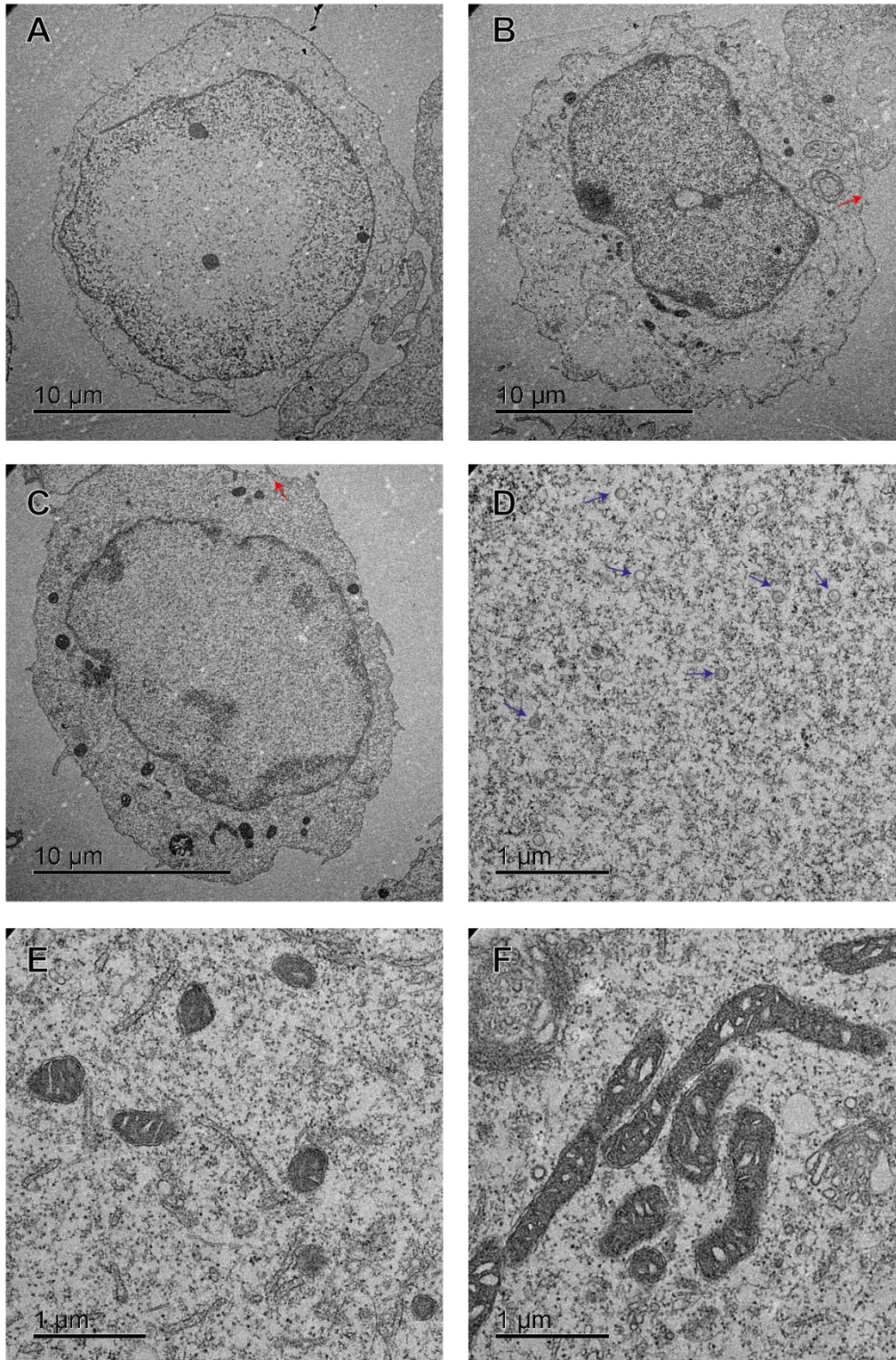


**Figure 5.9 Electron micrograph images of TOV21G cells infected with HSV-3D7.** (A-C) A selection of low magnification images of whole cells infected with HSV-3D7. Classically necrotic cell morphologies, consisting of swollen cytoplasm and nuclei, and loss of membrane integrity (red arrows) are displayed. (D) Evidence of whole virions is denoted by the blue arrows. (E-F) higher magnification images of mitochondria show a similar electron dense and condensed phenotype to HSV-1716.

## 5.4 Markers of necroptosis following viral infection

### 5.4.1 Phosphorylation of MLKL

MLKL is the downstream effector protein of the necroptosis pathway and is recruited and phosphorylated by RIPK3 at residues Thr357 and Ser358. MLKL then forms trimers and translocates to the plasma membrane, where it has been shown to act as a  $Mg^{2+}$  ion channel in the presence of  $Na^+$  and  $K^+$  (Xia *et al.*, 2016). Overall calcium ion influx is recognised as a major downstream event of MLKL activation which may be linked to its channel function. Membrane rupture then eventually leads to cell death (Hildebrand *et al.*, 2014). Phosphorylated MLKL (pMLKL) can therefore be used as a marker for the presence of necroptosis.

TOV21G cells were infected with either HSV-1716 or HSV-3D7 for 24 h, before assaying for the presence of pMLKL by immunoblot. Treatment with TSZ was used as a positive control for necroptosis induction and was also given 24 h before cells were lysed. Under basal conditions, some pMLKL was apparent in the cells, which was increased following TSZ treatment. However, no increase in pMLKL staining was seen when TOV21G cells were infected with either HSV-1716 or HSV-3D7. This suggests strongly that that HSV-1716 does not induce classical programmed necrosis identical to TSZ treatment in these cells, and also provides evidence that prevention of the binding of ICP6 and RIPK3 is not sufficient alone to drive cells down this specific pathway.

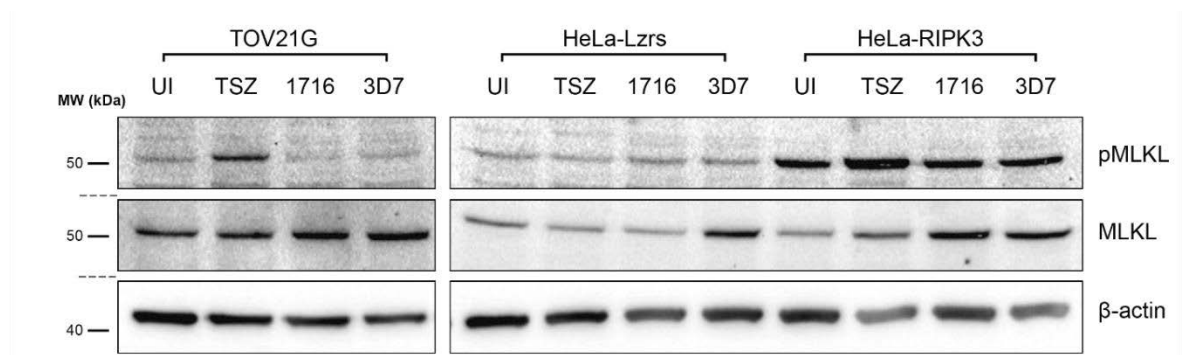


**Figure 5.10 Phosphorylation of MLKL following HSV-1716 or HSV-3D7 infection of cancer cells.** TOV21G, HeLa-Lzrs and HeLa-RIPK3 cells were infected with either HSV-1716 or HSV-3D7 or treated with TSZ for 24 h before harvesting cell lysates and determining presence of MLKL or phosphorylated MLKL (pMLKL) by immunoblot. UI, uninfected; MW, molecular weight; kDa, kilodaltons.

In HeLa-Lzrs cells, similar levels of basal pMLKL were seen to TOV21G in untreated cells. In these cells however, treatment with TSZ was not sufficient to lead to an increase in pMLKL staining. I have already shown that HeLa-Lzrs cells are incapable of dying in response to TSZ treatment due to their lack of RIPK3 expression. When infected with either virus, pMLKL levels also remained unchanged from the uninfected control. This would be expected based on what is already known - that necroptosis is only possible in the presence of RIPK3

Interestingly, some differences were seen when comparing HeLa-Lzrs to HeLa-RIPK3. In HeLa-RIPK3 cells, basal levels of pMLKL staining were much higher. This implies that presence of RIPK3 alone is enough to cause cells to undergo some level of necroptotic signalling without any other stimulus beyond cell culture medium. This same effect was seen when looking at HMGB1 release, serving as further evidence that RIPK3 is perhaps able to self-activate at high expression levels. As expected, when HeLa-RIPK3 cells were treated with TSZ, pMLKL expression increased further, similar to that seen in TOV21G and in keeping with the critical role of RIPK3 in determining sensitivity to necroptosis. When these cells were infected with either HSV-1716 or HSV-3D7 however, no change in pMLKL was seen over basal expression. This suggests that the presence of high levels of RIPK3 does not permit HSV-1716 to kill with greater induction of necroptosis. However, the amount of necroptosis activation is still higher than comparative infection of HeLa-Lzrs cells. Whether presence of RIPK3 and HSV-1716 infection in combination can have useful additive effects in terms of immune system activation, will be interesting to explore.

#### **5.4.2 Response to necrosome inhibitors**

TOV21G cells were infected with either HSV-1716 or HSV-3D7 for 96 h in the presence of various inhibitors of necroptosis (Figure 5.11). These inhibitors each target one component of the necrosome machinery, with necrostatin-1 (Nec-1) being an inhibitor of RIPK1, GSK'840 an inhibitor of RIPK3 and necrosulphonamide (NSA) an inhibitor of MLKL (Degterev *et al.*, 2005; Sun *et al.*, 2012; Rodriguez *et al.*, 2016). The purpose of this was to determine whether any of these proteins alone were crucial for cell death induced by either virus.

Before investigating the effect of viral infection, TOV21G cells were first treated with TSZ in combination with each of the three drugs (Nec-1: 100  $\mu$ M, GSK'840: 20  $\mu$ M, NSA: 3  $\mu$ M) for 48 h to confirm that the doses used were sufficient to induce cell death (Figure 5.9a). As seen previously, treatment with TS was enough to reduce cell viability in TOV21G cells to 44%. Addition of zVAD-fmk had no significant effect on cell death ( $p=0.49$ ). This TSZ-induced necroptosis was completely reversed by addition of either Nec-1, GSK'840 or NSA, with viabilities rising significantly to >99% for each ( $p<0.0001$  in all cases).

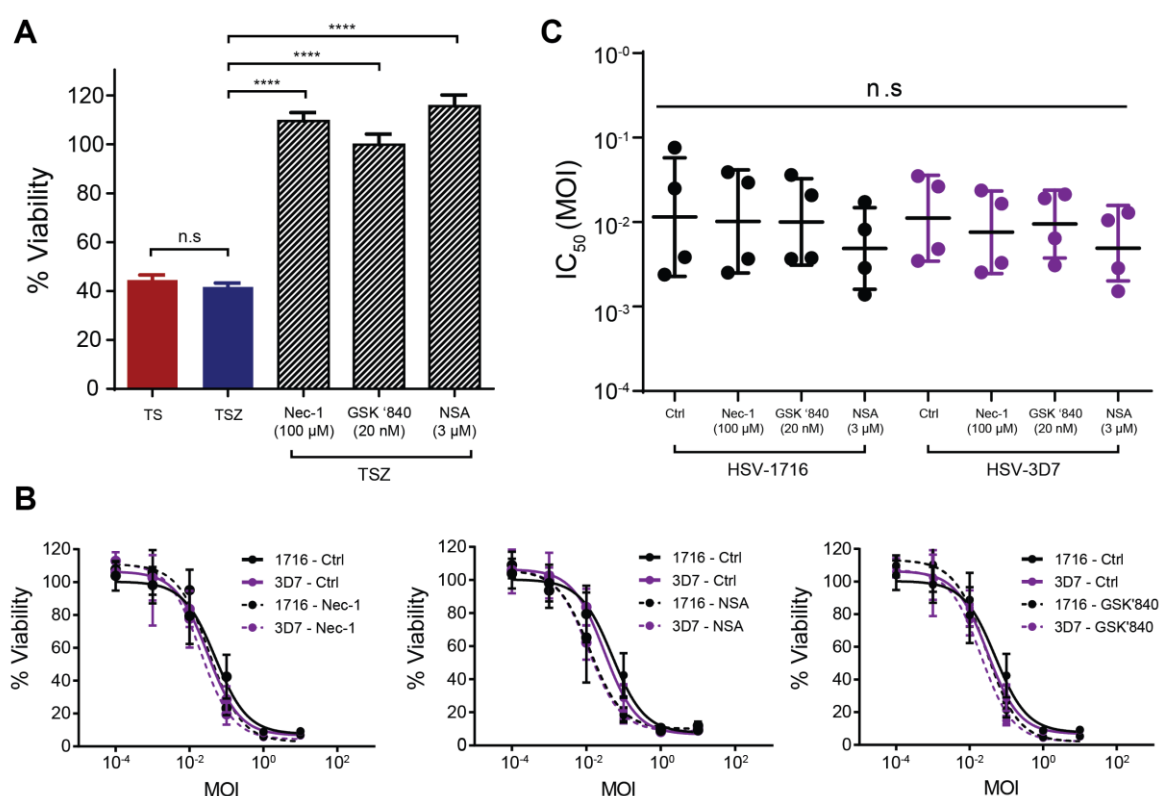


**Figure 5.11 Effect of pharmacological necrosome inhibition on HSV-1716 and HSV-3D7-induced cell death.** (A) TOV21G cells were treated with various combinations of TNF- $\alpha$  (T; 20 ng/ml), SMAC mimetic (S; 1  $\mu$ M), zVAD-fmk (Z; 25  $\mu$ M), Nec-1 (100  $\mu$ M), GSK '840 (20 nM) and NSA (3  $\mu$ M) for 48 h before determining cell viability by MTT assay. Statistical significance was determined by one-way ANOVA (Dunnett's multiple comparisons test). \*\*\*\*  $p<0.0001$ , n.s, not significant. (B) Cells were infected with either HSV-1716 or HSV-3D7 at a range of MOIs for 2 h, before refeeding with either Nec-1 (100  $\mu$ M), GSK '840 (20 nM) or NSA (3  $\mu$ M) and leaving for another 96 h. Cell viability was then determined by MTT. Dose-response data from single experiments are shown in B, while pooled IC<sub>50</sub> values from multiple experiments are showed in C. Statistical significance was determined by one-way ANOVA (Tukey's multiple comparisons test). n.s, not significant. Nec-1, necrostatin-1; NSA, necrosulfonamide; IC<sub>50</sub>, half-maximal inhibitory concentration; Ctrl, control (no drug); MOI, multiplicity of infection.

The same compounds and doses were then tested during the course of 96 h viral infection for both HSV-1716 and HSV-3D7 (Figure 5.11b-c). No significant changes in IC<sub>50</sub> were seen when RIPK1, RIPK3 or MLKL were inhibited in either HSV-1716

or HSV-3D7. IC<sub>50</sub> values remained constant around the value of 0.01. These results are further evidence to the fact that HSV-1716 does not induce classical necroptotic cell death in TOV21G cells. These results also further show that HSV-3D7 does not behave differently to HSV-1716 in terms of necroptotic signalling, despite lack of binding to RIPK3.

### **5.4.3 Response to short interfering RNA knockdown of RIPK3 and MLKL**

To further investigate the role of RIPK3 and MLKL in HSV-1716-induced cell death, and to confirm results seen pharmacologically, short interfering RNA (siRNA) knockdown of these proteins during viral infection was performed. Preliminary experiments showed that RIPK3 was optimally knocked down by 24 h with 10 nM of RIPK3 siRNA in TOV21G cells. This knockdown was shown to be sustained for at least 72 h before beginning to increase. Cells were therefore transfected with either RIPK3 or scrambled sequence (Scr) siRNA for 24 h before infecting with HSV-1716 and left for a further 48 h. Viability was then measured by MTT assay. To confirm that protein was still knocked down at endpoint, cell lysates were taken from cells treated with each siRNA and stained for RIPK3 by immunoblot. At 72 h post-treatment, RIPK3 levels were still shown to be reduced. Despite this, at both MOIs tested there were no significant differences in death between cells with WT and knocked-down RIPK3. This would appear to fit with the results seen in the previous section, which suggests that RIPK3 is not necessary for HSV-1716-induced cell death.

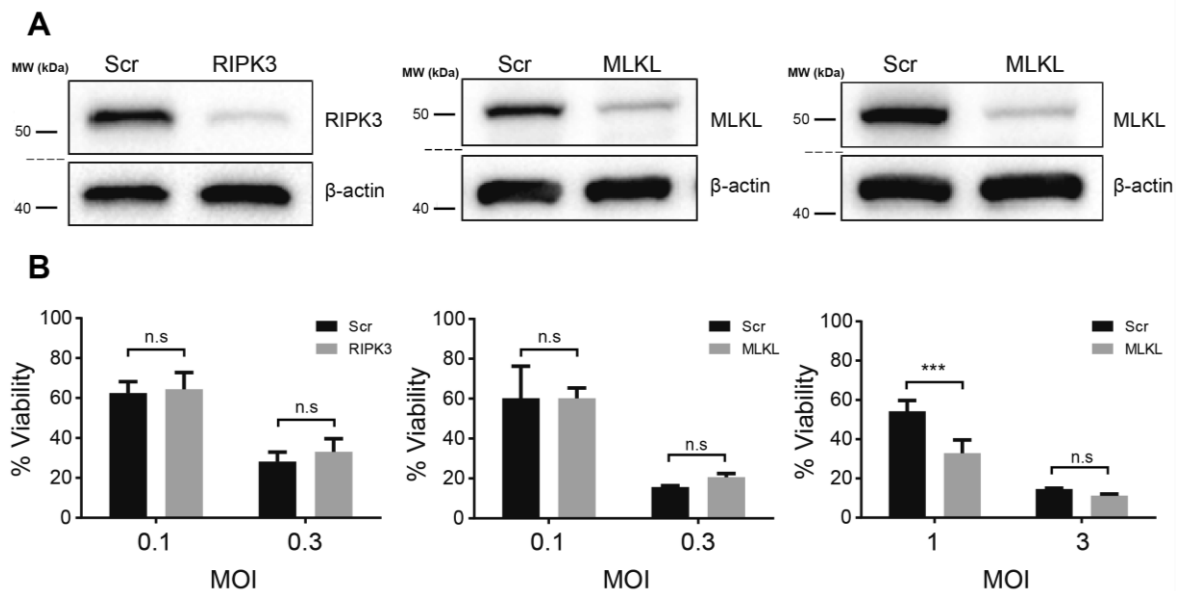


**Figure 5.12 Effect of siRNA knockdown of RIPK3 and MLKL on HSV-1716-mediated killing.** TOV21G (left, middle) or HeLa-Lzrs (right) cells were treated with equimolar amounts of either scrambled (Scr), anti-RIPK3 or anti-MLKL siRNA for 24 h, infected with HSV-1716 and then left for a further 48 h, before harvesting lysates for immunoblot or determining cell viability by MTT. Quantities and duration of siRNA exposure were determined by assessing protein expression at different concentrations and time points. 'A' shows endpoint lysates taken after 72 h of siRNA treatment, stained for the proteins of interest. 'B' shows cell viabilities at two MOIs for each of the two conditions. Statistical significance was determined by two-way ANOVA (Sidak's multiple comparisons test). \*\*\*  $p < 0.001$ ; n.s., not significant. MW, molecular weight; kDa, kilodaltons; MOI, multiplicity of infection.

The same experiment was performed in TOV21G cells with siRNA targeting MLKL. In this instance, a 5 nM concentration of siRNA was used per condition with infection taking place after 24 h and analysis of cell viability at 72 h. Here, the immunoblot shows that MLKL was also highly knocked down, although to a lesser degree than RIPK3. As with RIPK3, no significant change in cell death was seen following infection at either MOI, although a small increase in viability was seen at MOI 0.3. This may be evidence that when cells are lacking in MLKL, cell death is more difficult to induce. As the change in death seen is so small and not significant, this argument is not too convincing. Regardless of whether MLKL may play a small role in HSV-1716-mediated death, it is clear that MLKL is not essential for death to occur.

The same MLKL siRNA was used in HeLa-Lzrs cells determine whether cell death mechanics differ in a cell line that produces high levels of MLKL and lacks expression of RIPK3. These cells were treated with the same anti-MLKL siRNA regimen as TOV21G, but at a higher siRNA concentration of 30 nM, which produced a similar level of MLKL knockdown. Surprisingly, there was a significant

increase in killing when MLKL was knocked down, shown for both MOIs that were tested. Viability decreased from 54% to 33% in cells infected with MOI 1 and from 15% to 11% in cells infected with MOI 3. Such a change in death suggests that presence of MLKL is actually detrimental to HSV-1716 killing in this system.

#### 5.4.4 Effect of RIPK3 overexpression on HSV-1716 and HSV-3D7-induced cell death

To further investigate the role of RIPK3 in HSV-1716-induced cell death, RIPK3-overexpressing HeLa cells discussed earlier (Figure 3.4) were infected with either HSV-1716 or HSV-3D7 for 96 h and assessed for changes in cell viability by MTT assay (Figure 5.13). Individual RIPK3-expressing clones (E4, E10 and D2) were each compared in addition to the empty-vector control line, HeLa-Lzrs. Both viruses were found to kill all cell lines at the range of MOIs tested ( $10^{-4}$ - $10^2$ ). Overall, HeLa cells were much less sensitive to viral infection than many of the OC lines investigated previously. In addition to this, the comparative change in cell death is higher over a narrower range of MOIs, with viability changing greatly between the MOIs of  $10^0$  and  $10^1$ .

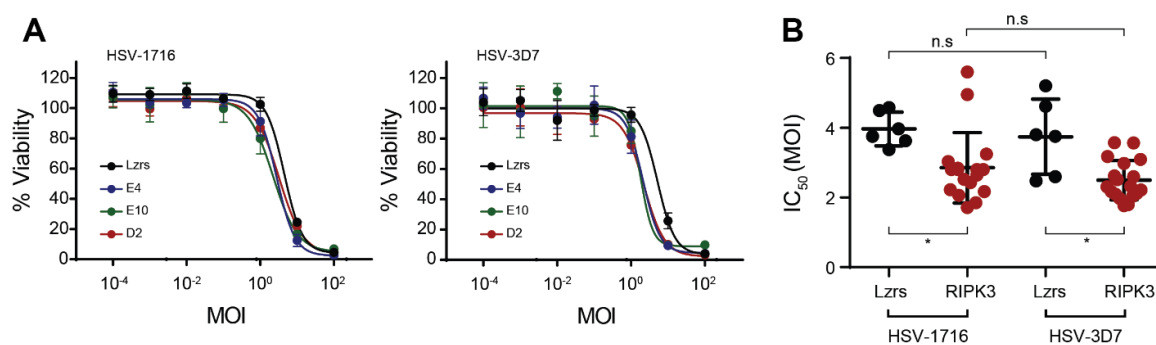


**Figure 5.13 Effect of RIPK3 overexpression on HSV-1716 and HSV-3D7-induced cell death.** HeLa cell clones that have been transduced with either empty vector (Lzrs) or RIPK3-expressing (E4, E10, D2) lentiviruses were infected with either HSV-1716 (left) or HSV-3D7 (right) and left for 96 h before determining cell viability by MTT. 'A' shows dose-response data from a single experiment for all RIPK3 genotypes. 'B' shows data for pooled  $IC_{50}$  values from all experiments, whereby RIPK3-overexpressing clones have been pooled into a single dataset. Statistical significance was determined by one-way ANOVA (Tukey's multiple comparisons test). \*,  $p < 0.05$ ; n.s., not significant; MOI, multiplicity of infection;  $IC_{50}$ , half maximal inhibitory concentration.

Sensitivity to death appears to be higher in the RIPK3-expressing cell lines compared to HeLa-Lzrs, in the case of both HSV-1716 and HSV-3D7 infection. No noticeable difference in sensitivity can be noticed between RIPK3-expressing genotypes. In order to determine the significance of these changes,  $IC_{50}$  values

from multiple repeat experiments were taken and compared together. To gain greater statistical power, data from the separate RIPK3 genotypes were pooled. A significant decrease in average IC<sub>50</sub> value was seen in the RIPK3-expressing cells compared to Lzrs when infected with HSV-1716 (4.0 vs 2.9;  $p=0.031$ ). A similar decrease could also be seen between the two cell types when infected with HSV-3D7 (3.7 vs 2.5;  $p=0.012$ ). Despite this, no difference in killing between the two viruses could be determined in either HeLa-Lzrs or HeLa-RIPK3 cells ( $p = 0.964$  and  $0.571$  respectively).

#### **5.4.5 Effect of Genomic MLKL Knock-Down on Viral Killing**

To confirm the effect of a more permanent disruption to MLKL expression than siRNA can provide, MLKL-modified TOV21G cells were acquired from previous work done in the host lab (Weigert *et al.*, 2017). These cells were made using CRISPR/Cas9 gene-editing technology but were only found to possess heterozygous loss of MLKL, resulting in reduced MLKL expression, but not total loss. To confirm MLKL reduction, lysates from untreated MLKL-modified clones, F9 and D6, were taken and compared for MLKL expression against parental MLKL cells by immunoblot. As expected, levels of MLKL were shown to be highly reduced, despite similar levels of  $\beta$ -actin loading control.

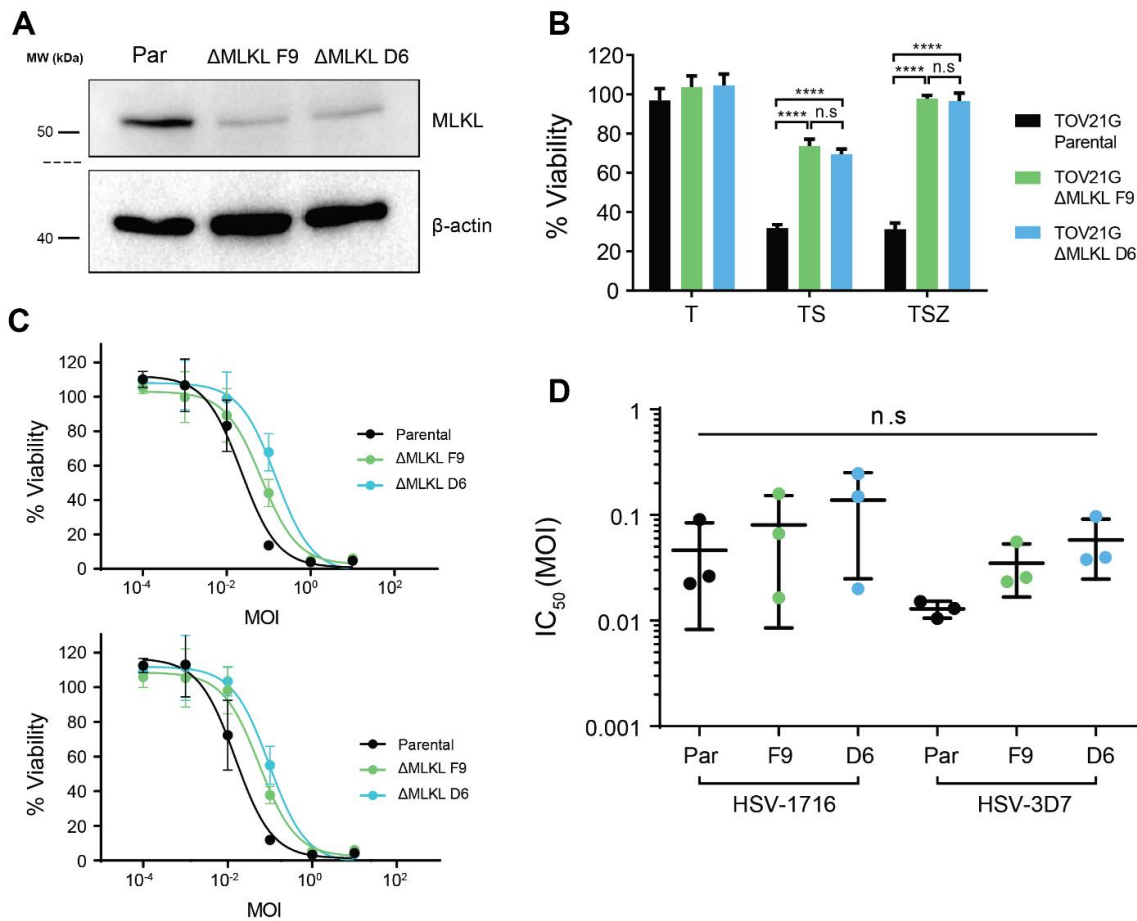


**Figure 5.14 Effect of Genomic Knockdown of MLKL on HSV-1716 and HSV-3D7-mediated killing.** (A) Lysates from untreated TOV21G (parental and ΔMLKL) cell lines were harvested and assayed by immunoblot for presence of MLKL protein. (B) Each of the TOV21G cell lines were treated with a combination of either TNF-α (T; 20 ng/ml), SMAC mimetic (S; 1 μM) and zVAD-fmk (Z; 25 μM) for 48 h before determining cell viability by MTT assay. Mean viabilities are plotted ± standard deviation (SD). Statistical significance was determined by two-way ANOVA (Tukey's multiple comparisons test). \*\*\*\*  $p < 0.0001$ ; n.s, not significant. (C and D) TOV21G (parental and ΔMLKL) cells were infected with HSV-1716 or HSV-3D7 at a range of MOIs and left for 96 h before determining cell viability by MTT assay. 'C' shows dose-response curves from a single experimental repeat, showing HSV-1716-infected cells on top and HSV-3D7-infected on the bottom (mean viabilities ± SD). 'D' shows pooled individual IC<sub>50</sub> values from multiple experiments with bars representing means ± SD. Statistical significance was determined by one-way ANOVA (Sidak's multiple comparisons test). MW, molecular weight; kDa, kilodalton; IC<sub>50</sub>, half-maximal inhibitory concentration; MOI, multiplicity of infection.

To determine the effect of this phenotypic change on the ability of the cells to undergo necroptosis, cells were treated with either T, TS or TSZ and assessed for cell viability. As expected, parental cells showed a large, significant reduction in viability to 31% following either TS or TSZ treatment, indicating induction of necroptosis. In comparison, clones F9 and D6 experienced a much smaller reduction in viability to only 74% and 64% respectively ( $p < 0.0001$ ), with no significant difference between the clones. In the TSZ conditions, F9 and D6 both showed an even greater rescue from death, with viabilities returning to 98% and

97% respectively ( $p < 0.0001$  vs parental). The heterozygous loss of MLKL therefore lead to a complete rescue from TSZ-induced necroptosis.

When compared for their ability to be killed by HSV-1716 or HSV-3D7 after 96 h of infection, MLKL-modified cells showed limited differences to the parental cell line. In HSV-3D7-infected cells, no significant differences were seen across any of the cell lines when  $IC_{50}$  values were compared across multiple experiments. For cells infected with HSV-1716, no change was seen between the  $IC_{50}$  averages either. Despite this, there does appear to be a trend towards inhibition of cell death following MLKL depletion. A further statistical test was performed after pooling the two clones to give a by-genotype analysis by t test. Following this, however, there was still no significant shift in  $IC_{50}$  seen in these cells.

## **5.5 Effect of ICP6-RIPK3 binding on response to TNF- $\alpha$**

Disruption of the interaction between ICP6 and RIPK3 alone appears to have no effect on cell death, as demonstrated by identical cell viabilities of various cell lines following infection with HSV-1716 and HSV-3D7 (Figure 4.10-Figure 4.11). Here, the effect of additional treatment of infected cells with TNF- $\alpha$  was investigated. For this, HeLa-RIPK3 cells were infected with either HSV-1716 or HSV-3D7 at MOI 10 and left for 2 h before refeeding with 10 ng/ml TNF- $\alpha$  and left for 24 h before determining cell viability by MTT assay.

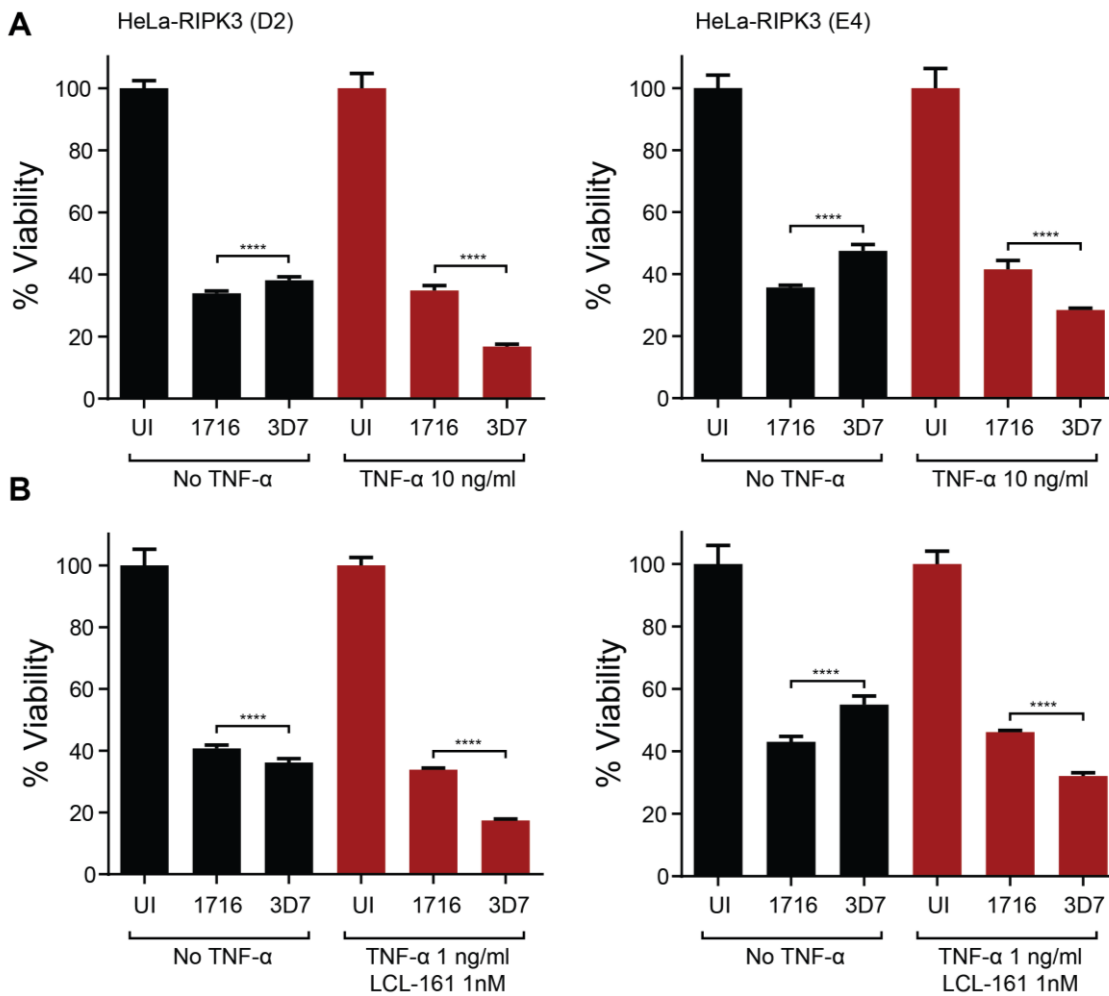


**Figure 5.15 Effect of co-treatment of HeLa-RIPK3 cells with virus and TNF- $\alpha$  on cell death.** (A) HeLa-RIPK3 cells (clones D2 and E4) were infected with HSV-1716 or HSV-3D7 at an MOI 10 for 2 h before refeeding cells with complete media containing TNF- $\alpha$  alone to give a final concentration of 10 ng/ml. (B) HeLa-RIPK3 cells (clones D2 and E4) were infected with HSV-1716 or HSV-3D7 at an MOI 10 for 2 h before refeeding cells with complete media containing TNF- $\alpha$  and LCL-161 (SMAC mimetic) to give final concentrations of 1 ng/ml and 1 nM respectively. Cells were then left for 24 h before determining cell viability by MTT assay. Cell viabilities are calculated as a percentage of untreated cells. In the case of drug treatment, viability is plotted as a percentage of uninfected, drug-treated cells. Mean cell viabilities are plotted  $\pm$  SD. Statistical significance is determined by one-way ANOVA (Sidak's multiple comparisons test). \*\*\*\*,  $p < 0.0001$ ; UI, uninfected.

In both of the HeLa cell lines tested, cell viability was significantly higher for HSV-3D7-infected cells than HSV-1716 (E4, 48% vs 36%,  $p < 0.0001$ ; D2, 38% vs 34%,  $p < 0.0001$ ). Conversely, when 10 ng/ml TNF- $\alpha$  treatment was provided in addition to viral infection, cell viabilities (relative to TNF- $\alpha$  alone) became much lower in the HSV-3D7-infected cells compared to HSV-1716 (E4, 29% vs 42%,  $p < 0.0001$ ; D2, 17% vs 35%,  $p < 0.0001$ ).

Next, I explored whether this effect could be modulated by the addition of SMAC mimetic, which I have shown increases the level of cell death in HeLa-RIPK3

cells (Figure 3.4). Concentrations of both T and S were modified to find a concentration that induced about 50% death (not shown) - 1 ng/ml and 1 mM respectively. The same pattern of cell death changes was seen under these conditions as for T alone, with the exception that a slightly higher level of death was seen in HSV-3D7-infected HeLa-RIPK3 (D2) cells was seen compared to HSV-1716 (36% vs 40%,  $p < 0.0001$ ). However, a much larger decrease in comparative cell viability was seen when these cells were treated with the drug combination (17% vs 34%,  $p < 0.0001$ ), indicating that the increased sensitivity to death stimulation remains. In the HeLa-RIPK3 (E4) line, a very similar pattern was seen to treatment with T alone, with cell viability appearing higher in HSV-3D7-infected cells in the absence of drug (55% vs 43%,  $p < 0.0001$ ). In the presence of TS, death was increased in the HSV-3D7-infected cells to give relatively higher levels of death than HSV-1716 (32% vs 46%,  $p < 0.0001$ ). Together, these results demonstrate that HSV-3D7-infected cells appear to have a much larger sensitivity to treatment to further death stimulus in the form of TNF- $\alpha$ .

## 5.6 Discussion

Some markers of immunogenic apoptosis were noted following HSV-1716 infection of TOV21G cells, namely HMGB1 and ATP release. CAL exposure was not seen following infection at the 1, 4 and 24 h time points tested. CAL exposure is an early process that occurs before PS exposure (Obeid *et al.*, 2007). Determining appropriate time points over the long replication cycle of a virus is therefore difficult. PS exposure was shown to already begin increasing at the earliest time point tested here at 16 h, suggesting that the window for CAL exposure would exist sometime before this. The results shown here are a representation of several repeat experiments. Other data not shown assessing later time points such as 12 and 16 h also showed no evidence of CAL. Other studies looking for CAL exposure following virus infection find evidence of this as late as 96 h post-infection (Koks *et al.*, 2015). By this time however, HSV-1716-infected TOV21G cells are long dead. I am therefore confident that no CAL exposure takes place during HSV-1716 infection. CAL is an ER protein ubiquitously expressed across cell types. However, to confirm the activity of the

antibodies, a sample of cells were permeabilised with Triton-X before staining. This control confirmed the validity of the method.

HMGB1 release was observed following HSV-1716 infection in both TOV21G and HeLa cells. This was the first evidence showing that HSV-1716-induced cell death has at least one immunogenic aspect. HMGB1 levels were determined by immunoblot of concentrated cell supernatant. Supernatants were concentrated by a factor of approximately 45, with parallel samples measured and diluted appropriately to ensure equal concentrations. This method had to be relied on to ensure loading uniformity.  $\beta$ -actin was still stained for as a control and appeared to be present in the supernatant alongside HMGB1. This correlates with a form of cell death displaying high membrane permeability.  $\beta$ -actin was still present in the supernatant of uninfected cells, probably due to basal cell turnover. Levels of  $\beta$ -actin did increase in the supernatant during infection, which is why it cannot be considered as a true loading control. Interestingly, release of HMGB1 did appear to increase by a relatively larger amount compared to  $\beta$ -actin, which suggests a more active or permissive mechanism of release.

The two hypotheses tested in the HMGB1 experiment were that HSV-3D7 would show greater HMGB1 release than HSV-1716, and that in HSV-1716-infected cells RIPK3 expression would result in greater release also. In the first instance, both viruses were shown to cause similar increases in levels of HMGB1 in the supernatant, suggesting that the ability of ICP6 to bind RIPK3 has no bearing on its release. HMGB1 is passively released from injured cells upon membrane permeabilization, and so has been described as both a marker of IA and necrosis (Kroemer *et al.*, 2013). No studies so far have shown a molecular link between RIPK3 and HMGB1 release beyond simple increases in membrane permeability resulting from necroptosis. Therefore, it is reasonable to suggest that similar levels of death resulting from either virus lead to similar levels of HMGB1 release. It could be that changes in levels of RIPK3 signalling, as a result of ICP6 binding, lead to different molecular consequences, despite the same overall membrane permeability and subsequent death being seen.

The second of these hypotheses is that RIPK3 overexpression leads to greater HMGB1 release, which has shown to be true. In addition to this, RIPK3

overexpression appears to lead to an increase in HMGB1 present in the supernatant even without further stimulation. Levels of RIPK3 seen in this system are much higher than native levels in any of the OC cell lines observed in this study. This could mean that overexpression of RIPK3 to this degree is able to have some form of 'overdrive' effect, whereby cells are forced down a necroptotic route without any outside stimulus. Due to the semi-quantitative nature of immunoblotting, it is hard to say whether this effect is entirely responsible for the additional increase in HMGB1 release seen following HSV-1716 infection in HeLa-RIPK3 cells, or whether some level of synergism exists between viral-induced death pathways and necroptosis.

A strong negative correlation was seen ( $r=-0.819$ ) between ATP release and cell viability following infection with either HSV-1716 or HSV-3D7, suggesting that cell death leads to release of ATP from the cell. ATP release is associated with both IA and necrosis, yet it is unclear which mechanism is driving this release. This phenomenon does provide a second line of evidence that cell death following HSV-1716 infection is immunogenic in nature. Interestingly, ATP release was significantly higher following HSV-3D7 infection than for HSV-1716 in the MOI 3 condition. Cell viability in these conditions was in fact ~5% lower for HSV-3D7 compared to HSV-1716, although this difference was not statistically significant ( $p=0.52$ ). In addition, no statistically significant difference in ATP release was seen at any other MOI. While the results shown here are from a single experiment, similar trends were seen in other repeats. It is therefore hard to say with certainty that ATP release is comparatively higher at equal levels of cell death for HSV-3D7 compared to HSV-1716. It would certainly be reasonable to postulate that a decrease in ICP6-RIPK3 binding, leading to increased RIPK3 activation, could lead to a higher proportion of cells in a population dying by necrosis and, therefore, releasing more ATP into the supernatant.

TOV21G cells infected with either HSV-1716 or HSV-3D7 saw no change in death upon addition of the pan-caspase inhibitor zVAD-fmk. To confirm the appropriate concentration to use, cisplatin treatment was used as a positive control for apoptosis. Cisplatin is a well-known inducer of apoptosis, although it is possible that the mechanisms of apoptosis induction differ from those that may be employed by HSV-1716. A rescue effect seen in the presence of zVAD-fmk should

confirm that apoptotic mechanisms are totally blocked. Despite this, viability was only restored to 40% upon zVAD-fmk addition, implying that the pathway of death employed by cisplatin was not completely blocked and therefore, may involve other mechanisms. However, more complete blockage of death seen using the concentrations used here in other cell types suggest that a high level of caspase inhibition is taking place. It does therefore seem that while caspases may still play some role in HSV-1716-induced necrosis, they are not a primary requirement for death that can be circumvented. HSV-3D7 likewise showed no change in its ability to induce death when caspases were inhibited, suggesting that disruption of the RIPK3-ICP6 interaction does not alter the virus's reliance on apoptosis.

Combining annexin V staining with a membrane-impermeable dye such as propidium iodide, 7-AAD or, in this case, Zombie Violet is an established way to determine the apoptotic and necrotic portions of a cell population (Degterev *et al.*, 2014). AV+ staining is a hallmark of early classical apoptosis (Vanags *et al.*, 1996; Rimon *et al.*, 1997). The ZV+ cell populations are those which have become permeabilised, and can represent either true necrotic cells, or apoptotic cells that are entering the later stages of death and thus have become permeabilised. This is why the AV/PI assay often has limited usefulness in diagnosing cell death modalities, due to the high interconnectedness of these pathways. It is particularly important to pay attention to the timescales over which changes in cell staining occur. Initial PS exposure, followed by late cell permeabilization is characteristic of apoptosis, whereas direct permeabilization in combination with PS exposure is characteristically necrotic. In this case, frequencies of AV+ cells and AV+/ZV+ cells appeared to rise in concert over time, which would suggest that necrosis and apoptosis may be occurring simultaneously. Ultimately, this assay is of limited use unless the cell type in question adheres strictly to the established dogma. While one explanation for the increase in AV+/ZV+ cells in HSV-3D7-infected samples could be that more necrosis is taking place, it is also possible that flow cytometry is just a more sensitive method for determining cell death compared to the MTT assays used elsewhere in this study. Either way it is hard to conclude the meaning of this difference considering the contradicting data on immunogenic cell death.

To give a visual representation of the processes that occur following infection with HSV-1716 or HSV-3D7, or with TSZ treatment, electron micrograph images were taken of TOV21G cells. Electron microscopy has remained a gold-standard procedure for distinguishing apoptosis from necrosis, with each process being largely defined by the morphological features seen with this type of analysis. Necrotic cells undergo rapid membrane permeabilization, cell hydration and swelling, and organelle disruption. Nuclei also remain well-preserved in the early stages of death (Burattini and Falcieri, 2013). In comparison, apoptotic cells experience a decrease in cell size; fluid loss and cytoplasmic condensation; and convolution of nuclear and cellular membranes. Chromatin condenses and forms cup-shaped masses beneath the nuclear envelope in the early stages, with cellular fragmentation happening later. Many of the hallmarks of necrosis were shown to occur following treatment with all of the tested death stimuli for 48 h. One example of an apoptotic cell was found for HSV-1716 infection, but not for HSV-3D7 or TSZ treatment. Making conclusions about the relative abundance of apoptotic or necrotic cells is not possible with TEM, as a qualitative method. It is therefore possible, or perhaps likely, that cells undergoing apoptotic cell death were also present in the other samples. The images shown in the results were chosen to give a representative view of the types of dying cell that were identified in the experiment. Image quality for TEM can vary, partly due to variations in the sample preparation process. As a result, the images shown here are somewhat less detailed than those shown in other studies (Krysko *et al.*, 2008; Burattini and Falcieri, 2013), which limits the ability to distinguish more comprehensive changes in organelle structure.

Identification of what appeared to be viral capsids was noted in cells infected with either HSV-1716 or HSV-3D7, but not other samples. As mentioned, clarity in these images is low and so picking out such small objects at these magnifications is difficult. The objects identified here are also few and sparsely distributed, which is not what would be expected during a productive viral infection (Le Sage and Banfield, 2012; Wild *et al.*, 2015). The lack of temporal information given by this technique must also be considered. It may be that the cells observed here are too early in the infection cycle to catch large scale virion production and release. Of course, some cells within the same sample may

progress through the cell death process at different speeds, in which case, identifying the right processes becomes a matter of luck and persistence.

Abnormalities in the mitochondria were seen following the various treatments, with TSZ leading to enlarged, swollen mitochondria, and either virus leading to condensed, elongated mitochondria. This condensed structure has been previously noted following HSV-1 infection in oligodendroglial cells (Bello-Morales *et al.*, 2005), and is well-known to be associated with a highly metabolically active state, typical of viral infection (Hackenbrock, 1966, 1968). Crucially, it seems that structural changes following HSV-3D7 infection do not differ in any noticeable way to HSV-1716 infection, with both viruses seeming to already kill via a visually necrotic mechanism.

In order to determine the response of downstream necroptosis signalling to HSV-1716 and HSV-3D7 in TOV21G and HeLa cells, a pMLKL immunoblot was performed on cell lysates. MLKL is the key downstream regulator of necroptosis, and pMLKL has been well-described as a marker of necroptosis induction (Sun *et al.*, 2012; Linkermann, Kunzendorf and Krautwald, 2014). In the necrosis competent cell lines TOV21G and HeLa-RIPK3, levels of pMLKL were expected to be higher following HSV-3D7 infection than for HSV-1716. No increase in pMLKL was seen for either virus in either cell line. This means that HSV-1716 does not appear to be able to induce necroptosis even in necroptosis-competent cell lines. It also means that the disrupted ICP6-RIPK3 interaction resulting from the HSV-3D7 genotype makes no difference to this either. In line with what has been shown in other experiments, pMLKL levels increased following TSZ treatment in TOV21G and HeLa-RIPK3 cells, but not HeLa-Lzrs controls, which confirms that both these cell lines are necroptosis-competent. Interestingly, basal pMLKL levels were higher in HeLa-RIPK3 cells compared to HeLa-Lzrs, which coincides with the hypothesis that overexpressed RIPK3 can 'overdrive' cells down a necroptotic pathway without further stimulus.

Further careful analysis is needed for this experiment, again, due to the semi-quantitative nature of immunoblot. However, pMLKL staining remains as one of the only true biomarkers for this process. This is primarily because necroptosis is defined by its signature activation of the proteins RIPK1, RIPK3 and MLKL.

Therefore, direct analysis of these proteins is the only way to properly confirm its activation.

Further probing of the necroptosis pathway was achieved with targeted inhibition or knockdown of each of the individual necrosome components. The drugs Nec-1, GSK'840 and NSA are all well described for their ability to inhibit RIPK1, RIPK3 and MLKL respectively (Su *et al.*, 2016). To confirm their effects at the concentrations tested in these cells, their abilities to rescue cells from TSZ-induced necroptosis was confirmed. However, no effect on cell death was seen when cells were infected with either HSV-1716 or HSV-3D7. This appears to provide more evidence to the hypothesis that necroptosis is not an active process during HSV-1716 infection. Not only this, but it seems that none of the individual components of the necrosome plays a key role in the death process. This is an important distinction because both RIPK1 and RIPK3 have been shown to have proapoptotic or even pro-survival roles in certain circumstances (Ichim and Tait, 2015). In addition to this, it is important to consider that pharmacological inhibition of these proteins determines only the role of their kinase function. It has been shown that induction of apoptosis following RIPK3 activation occurs in a kinase-independent manner that requires RIPK1, FADD and caspase-8. Therefore, if RIPK3 was having a proapoptotic effect in this system, then pharmacological inhibition would not help determine that.

To help discern further whether necrosome proteins have any role in HSV-1716 killing, siRNA knockdown was performed in both TOV21G and HeLa cells for RIPK3 or MLKL. Immunoblots were used to confirm that successful knockdown had taken place over the optimised time scale tested. In TOV21G cells no significant change in killing was seen when RIPK3 was knocked down, fitting with the limited role RIPK3 has appeared to have in previous experiments. A small non-significant increase in cell viability of ~5% was seen in one MOI for MLKL knockdown in TOV21G cells. The fact that this change occurred in only one MOI condition, and that the change was so small makes it seem likely that MLKL knockdown had no true functional effect on HSV-1716 killing. More convincing changes were seen following MLKL knockdown in HeLa-Lzrs cells. In these cells however, a further decrease in viability was seen following knockdown. This suggests that loss of a key death protein is actually driving further death, which

is counter-intuitive to what is known about MLKL. There have been reports that MLKL may play a role in promoting cell survival in some cases, particularly cancer (Liu *et al.*, 2016); whether or not this is what is occurring here is unclear. As can be seen in the immunoblots, in all cell lines and conditions, complete knockdown of protein was never achieved. This illustrates one of the key disadvantages of siRNA as a method: it is often impossible to completely deplete levels of a protein target to zero. In many cases, large-scale knockdown may be sufficient to see a dose-dependent effect. In other instances, low levels of residual protein may be sufficient to maintain high levels of activity. In recent years, opting instead for permanent, absolute knockout with CRISPR/Cas9-based methods has proven to be more effective, reliable and convenient. The siRNA experiments performed here were done prior to the establishment of standardised CRISPR protocols within our lab.

Further examination of the effect of RIPK3 in HSV-1716-induced cell death was explored with the HeLa-RIPK3 over-expression system. Overexpression of RIPK3 led to a significant increase in cell death following infection. From what has been uncovered so far, this data seems to tie in to the theory that high RIPK3 expression sensitises cells to further death stimuli, including viral death. This correlates well with the greater HMGB1 release seen following viral killing in HeLa-RIPK3 cells. Given that no change in pMLKL levels occur in these cells during infection, it seems that despite additional death, necrosis may still not be the sole driver. This information continues to suggest that high-RIPK3 cells may be more sensitive to death by any means, including the predominantly non-necrotic death mode induced by HSV-1716. Additionally, there was no difference in cell killing between HSV-1716 and HSV-3D7 in either HeLa-Lzrs or HeLa-RIPK3 cells. This mirrors what was seen in the RIPK-expressing TOV21G cells and suggests that even when RIPK3 is present in very high levels (Figure 3.4), a disruption in ICP6-RIPK3 interaction is not alone sufficient to drive cells down an increased necrotic pathway. It is worth noting the magnitude of the differences in  $IC_{50}$  is relatively small (1.1 and 1.2 pfu/ml for HSV-1716 and HSV-3D7 respectively), with variability in measurements sometimes obscuring the change. Nonetheless, the difference is still of significance to this study.

Following CRISPR/Cas9-based gene editing of MLKL within TOV21G cells, the effect of having a more permanent knock-down of the gene could be explored. As mentioned, the MLKL-modified cell clones were received from previous work done in the lab. The clones were both shown to contain heterozygous mutations within the MLKL gene locus (not shown), which resulted in a reduced expression. This means that these experiments suffer from the same major drawback as those done with siRNA, in that small amounts of residual MLKL may have noticeable effects. One major benefit of having stably-edited cells is that expression remains at a constant level, allowing for longer experiments and improving consistency of results between experiments. When cells were treated with T, TS or TSZ and compared for their susceptibility to killing, both clones were markedly more resistant to death by TS or TSZ than the parental line, with the latter having almost no effect on cell viability. It is interesting that viability was so different between TS and TSZ treatment for the clones, when it rarely differs in the parental line. Resistance to the addition of the caspase inhibitor, zVAD-fmk is an indicator that death is operating on a primarily necroptotic basis. This suggests that when MLKL is depleted, death can still occur via an apoptotic route induced by TS. This could indicate that in parental cells, TS stimulation typically causes a combination of apoptotic and necroptotic outcomes, which gets switched to pure necroptosis following the addition of zVAD-fmk. It could also mean that death following TS exposure is purely apoptotic and becomes switched to a purely necroptotic pathway following addition of zVAD-fmk.

Overall, the TSZ experiments in MLKL-modified cells prove that despite incomplete knock-out, these cells are still wholly resistant to necroptosis. This is important when interpreting the following experiments involving viral infection. Here, no overall change in average  $IC_{50}$  was seen between the cells infected with either HSV-3D7 or HSV-1716, but an overall trend towards inhibited death was seen. This means that cells expressing less MLKL died less than those with full expression. It may be that MLKL contributes to overall cell death caused by HSV-1716, but this is hard to conclude. This would suggest that any such effect is independent of MLKL kinase activity, as evidenced from a lack of effect following NSA treatment.

To further probe the relationship between ICP6-RIPK3 binding and sensitivity to necroptosis, HSV-1716 and HSV-3D7-infected HeLa-RIPK3 cells were treated additionally with TNF- $\alpha$  and assessed for cell death. Remarkably, in both of the lines tested, HSV-3D7 was much more sensitive to additional treatment with TNF- $\alpha$ , as evidenced by a greater drop in cell viability than HSV-1716-infected cells. This fits perfectly with the notion that disruption of the interaction between ICP6 and RIPK3 can fundamentally change the ability of RIPK3 to activate and induce necroptotic death. Additional treatment with SMAC mimetic gave the same pattern of behaviour but did not seem to amplify any necrotic effect. This is hard to compare directly as much lower concentrations of the drugs needed to be used when added in combination. Overall, HeLa-RIPK3 cells are exceptionally sensitive to the TS drug combination, yet treatment with either T alone or TS is enough to induce higher levels of cell death when RIPK3 is free to activate.

This matches with the other data shown in this study that shows HSV-1716 and HSV-3D7 to induce similar levels of cell death and necrosis under most conditions. It seems clear that presence of uninhibited RIPK3 is not sufficient to lead to increased levels of necrosis alone and that additional stimuli are required to drive cells down this pathway. It will therefore be interesting to explore further the effect of TNF- $\alpha$  treatment on these other necroptotic markers.

## **6 Immune system responses to HSV-1716 and HSV-3D7 infection**

## 6.1 Introduction

How HSV-1716 and HSV-3D7 interact with the immune system is one of the key questions concerning this project. The main benefit of inducing immunogenic cell death is the subsequent ability to engage and activate the immune system, ideally in a way that is beneficial for cancer clearance. I have shown so far that HSV-1716 can induce some form of immunogenic cell death through the increase of HMGB1 and ATP release; however, no necrotic signalling appears to be present during the course of infection. The mutation present in HSV-3D7 is sufficient to reverse the binding of ICP6 to RIPK3, which is expected to increase necrotic signalling, but this has not been shown to be the case so far. It may still be possible that this change in interaction can lead to changes in cytokine and chemokine regulation and release independently of necrosis. This chapter will explore both the capability of HSV-1716 to act on the immune system as an oncolytic virus and also any further changes to this that may exist due to the mutation present in HSV-3D7.

## 6.2 Cytokine and chemokine regulation following viral infection

### 6.2.1 mRNA regulation

Measuring mRNA levels for various cytokines is a useful method for determining regulation of these genes under certain conditions. RNA extracted from uninfected TOV21G cells, or those infected with HSV-1716 or HSV-3D7 was analysed using the Qiagen RT2 profiler array to assess changes in cytokine and chemokine mRNA regulation (Figure 6.1). When comparing HSV-1716 infected cells over uninfected, 29 genes were significantly (fold-change  $\geq 2$ ,  $p < 0.05$ ) upregulated, and 4 genes were significantly downregulated. The most highly upregulated genes were adiponectin (*ADIPOQ*; log<sub>2</sub>(14.5)-fold), interferon- $\gamma$  (*IFNG*; log<sub>2</sub>(12.9)-fold), interferon gamma-induced protein 10 (*CXCL10*; 2<sup>13.2</sup>-fold) and interleukin-17F (*IL17F*; log<sub>2</sub>(14.2)-fold). The most significantly downregulated gene was TNF Receptor Superfamily Member 11b (*TNFRSF11b*).

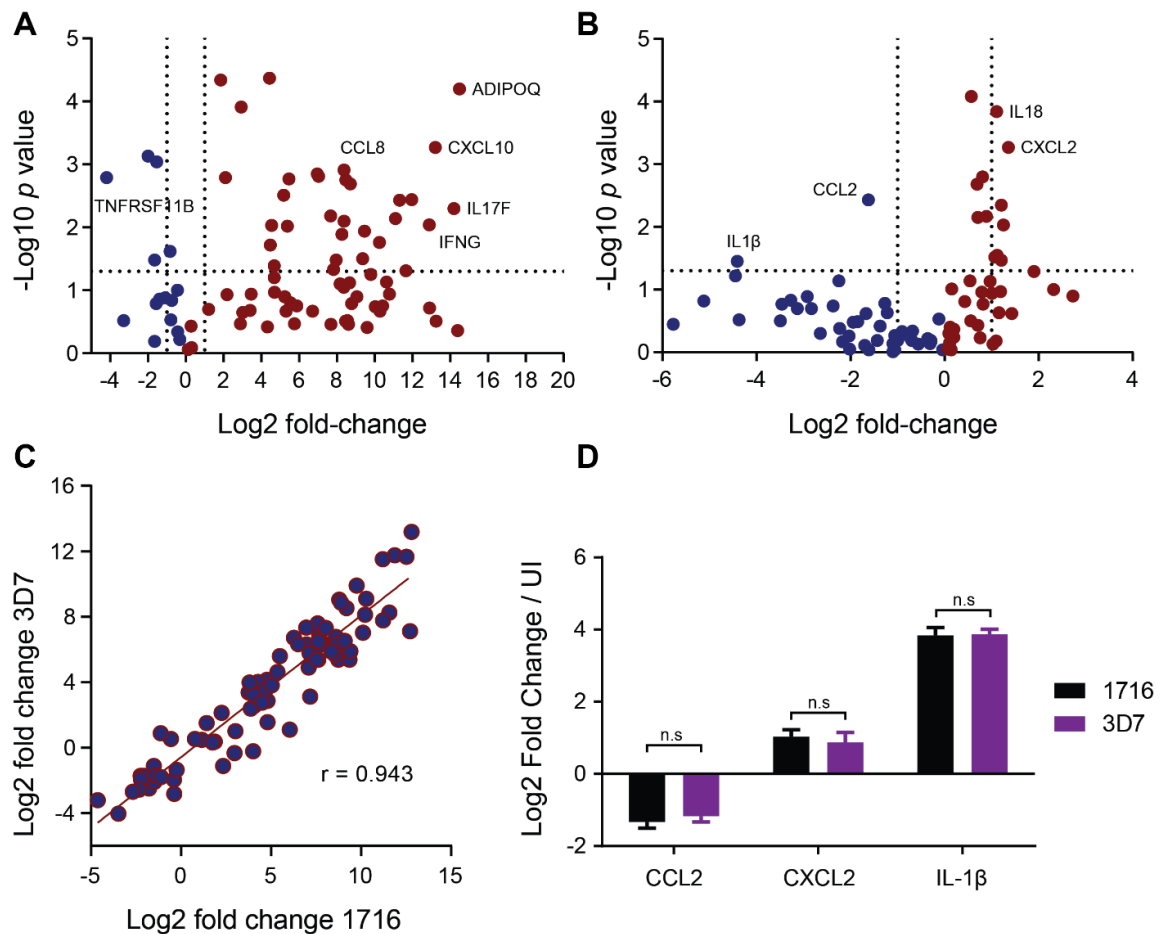


**Figure 6.1 Effect of HSV-1716 or HSV-3D7 infection on cytokine and chemokine regulation.** TOV21G cells were infected with either HSV-1716 or HSV-3D7 at an MOI of 1 for 24 h before suspending cells and harvesting cellular RNA. Cellular RNA samples were then analysed using an RTqPCR-based cytokine/chemokine array for 80 different genes. (A) mRNA levels in HSV-1716-infected cells are plotted against uninfected cells as a volcano plot, with  $p$  value and fold-change cut-offs shown as dotted lines (0.05 and 2 respectively). Selected chemokines are labelled. (B) mRNA levels in HSV-3D7-infected cells are plotted against HSV-1716-infected cells as a volcano plot. (C) Fold change values for both HSV-1716 and HSV-3D7-infected cells over uninfected are plotted against each other and correlated. (D) Selected cytokines that showed significant differences in 'B' were quantified in individual RTqPCR assays under the same infection conditions. Statistical significance determined by two-way ANOVA (Sidak's multiple comparisons test). n.s., not significant; UI, uninfected.

When comparing differences between cells infected with HSV-1716 or HSV-3D7, only 8 genes were shown to be significantly different between the conditions, with the majority of these differences being of a much lower magnitude than shown in the previous figure, with all being less than 4-fold upregulated and only one (IL1 $\beta$ ) becoming more than 4-fold downregulated. Despite this, three of these genes, CCL2, CXCL2 and IL-1 $\beta$ , were individually analysed by qPCR to confirm the difference between the viruses, where it was found that there was no significant difference in cytokine expression between HSV-1716 and HSV-3D7 ( $p$  values = 0.31, 0.47 and 0.79 respectively). Most interestingly, IL1 $\beta$  expression was now 2<sup>3.8</sup>-fold upregulated by both viruses as opposed to 2<sup>4.4</sup>-fold

downregulated. These data suggest quite strongly that there is no difference in the cytokine and chemokine mRNA profiles of cells infected with either of these viruses, and subsequently that ICP6-RIPK3 binding has no effect on cytokine regulation.

A full list of genes included in the array with their relative fold-change for both HSV-1716/uninfected and HSV-3D7/HSV-1716 can be found in appendix 8.1, Table 8.1 and Table 8.2 respectively.

## **6.2.2 Protein regulation**

To further investigate the findings from the previous chapter, it was necessary to determine levels of translated protein of chemokines that may be released into the supernatant following HSV-1716 and HSV-3D7-mediated death. As with previous experiments, the comparisons of interest in this experiment were HSV-1716 and HSV-3D7 in RIPK3-expressing cells, as well as the effect of RIPK3 itself in the HeLa-RIPK3 cell pair. Analysis of chemokines at the protein level is important when investigating necrotic death: It is possible that while overall levels of death and cytokine transcription remain the same between HSV-1716 and HSV-3D7, a shift to a more necrotic death modality could have the effect of greater cytokine release, due to the nature of death itself.

To study this, the following infection conditions were used: TOV21G cells infected with either HSV-1716 or HSV-3D7 at an MOI 2, HeLa-Lzrs infected with HSV-1716 at an MOI 2.5, and HeLa-RIPK3 cells infected with either HSV-1716 or HSV-3D7 at an MOI 2.5. In this instance, cells were incubated for 16 h in serum free medium before harvesting supernatant for the assay. MTT data was taken in parallel to determine cell viability measures (Figure 6.2).

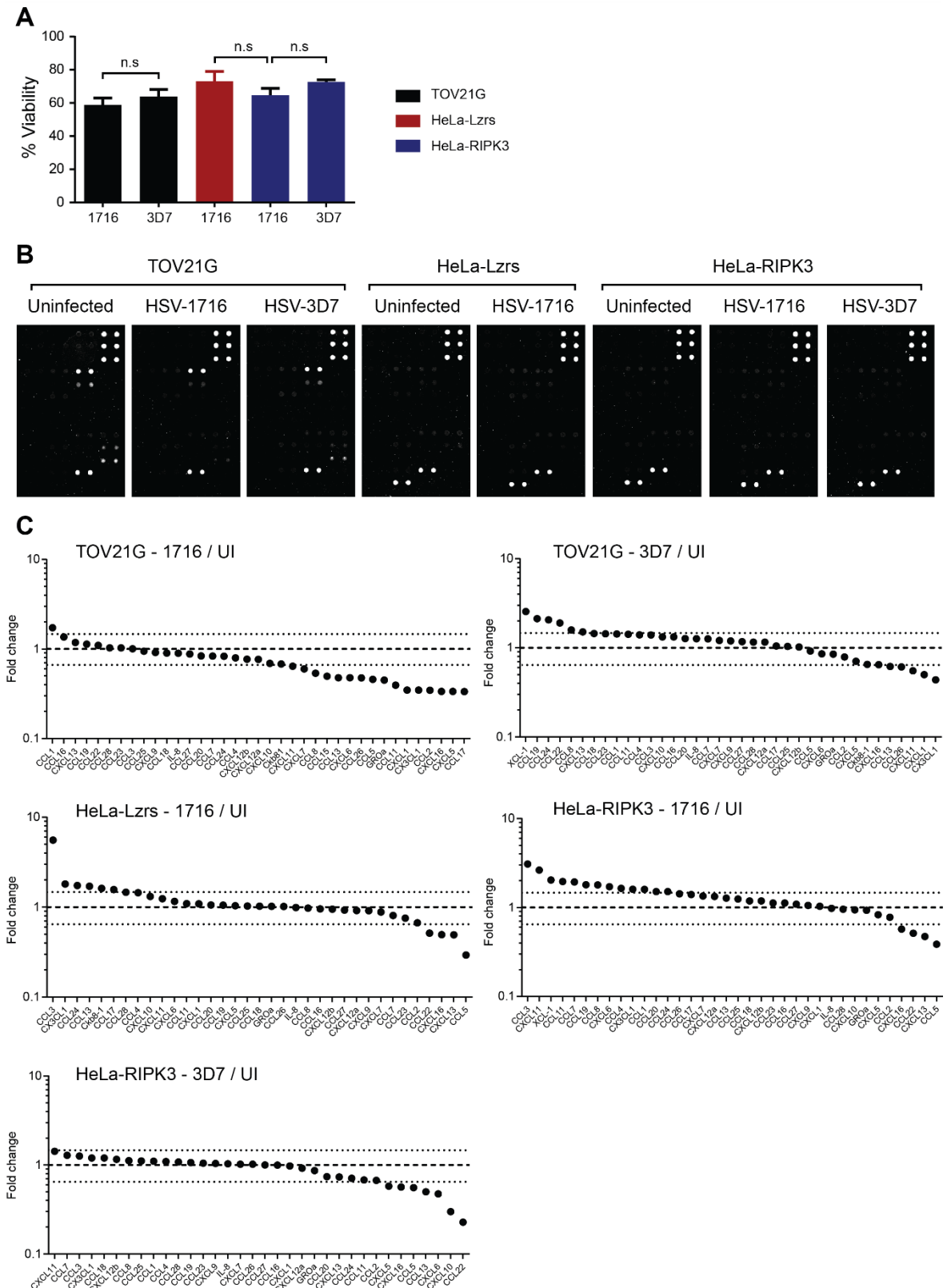


**Figure 6.2 Cytokine and Chemokine protein release following infection of cell lines with HSV-1716 or HSV-3D7.** TOV21G, HeLa-Lzrs and HeLa-RIPK3 cells were infected with either HSV-1716 or HSV-3D7 at MOI 2 (TOV21G) or 2.5 (HeLa) for 16 h in serum-free medium, before harvesting supernatants and determining viability by MTT assay. Supernatants were then analysed on a Raybiotech microchip array for cytokine and chemokine expression. 'A' shows cell viabilities plotted for each condition. Statistical significance was determined by one-way ANOVA (Tukey's multiple comparisons test). n.s, not significant. 'B' shows images obtained from chip arrays. 'C' shows waterfall graphs plotting fold-change differences compared to uninfected cells.

Conditions were chosen to induce a level of cell death approximating 50-60% viability, which was largely achieved. Comparisons done between conditions to be analysed (TOV21G, HSV-1716 vs HSV-3D7; HeLa-Lzrs vs HeLa-RIPK3, HSV-1716; HeLa-RIPK3, HSV-1716 vs HSV-3D7) showed no significant differences in cell viability, implying that any subsequent difference seen in protein levels would likely be due to protein release mechanisms (Figure 6.2a).

Supernatants were analysed using a Raybiotech chip array system, which provided a semi-quantitative means of comparing protein levels of 38 human cytokines via fluorescence signal, images of which can be seen in Figure 6.2b. Following this, waterfall graphs were produced by plotting fold-change of various conditions over uninfected cells (Figure 6.2c). A cut-off of  $\geq 1.5$ -fold increase or  $\leq 0.65$ -fold decrease was deemed to be significant and measurable as per the assay guidelines. This is illustrated in Figure 6.2c as horizontal dotted lines. In addition, data points were removed if they were not at least two standard deviations above background fluorescence, so as not to create artificially high differences in fold-change.

In TOV21G cells, HSV-1716 infection led to significant decreases in the release of 16 chemokines but increases in only two - CCL1 and CCL16. In comparison, levels of six chemokines, XCL-1, CCL19, CCL24, CCL22, CCL8 and CXCL13 were all increased when the same cells were infected with HSV-3D7, with six chemokines decreased. The largest increases in chemokine release between when comparing HSV-3D7 to HSV-1716 in TOV21G cells were - CCL11 (3.6-fold), CCL17 (3.1-fold), CCL8 (3.0-fold) and CCL24 (2.5-fold) (See appendix 8.2, Table 8.1). Overall, 31 of the 35 chemokines for which comparisons were possible were higher for HSV-3D7 than for HSV-1716.

In HeLa-Lzrs cells, six chemokines, CCL3, CX3CL1, CCL24, CCL13, Ckb8-1 and CCL17 were found to be highly increased following HSV-1716 infection (Figure 6.2c). CCL3 was the most increased with a 5.6-fold change over uninfected. Two chemokines were decreased (CXCL13 and CCL5). Comparatively, thirteen chemokines were increased in HeLa-RIPK3 cells, the highest being CCL3, CXCL11 and XCL-1. With HSV-3D7 infection of HeLa-RIPK3 cells however, no chemokines were increased, seven decreased, with relatively large decreases of the

chemokines CCL2 and CXCL10, as well as CXCL6. Twenty-two chemokines were relatively higher in HeLa-RIPK3 cells infected with HSV-1716 than in HeLa-Lzrs cells. Of these, the largest differences were in CCL7 (2.4-fold) and CXCL11 (2.1-fold) (See appendix 8.2, Table 8.4). In contrast to the TOV21G data, 28 out of the 34 chemokines for which comparisons were lower for HSV-3D7 than for HSV-1716 (See appendix 8.2, Table 8.5). The most decreased chemokines in this comparison were CXCL10 and CXCL6.

Of the 84 proteins tested in the mRNA screen, 26 of these appeared in the protein array, all of which were chemokines. To see if there was any consistency between the two arrays, a correlation and linear regression was performed between the two data sets for HSV-1716-infected over uninfected TOV21G cells (Figure 6.3). Only a moderate positive correlation was seen between the data ( $r=0.565$ ;  $p=0.0027$ ). Overall fold change was much lower for whole protein in the supernatant than for mRNA, with most protein levels decreased in comparison to uninfected cells, as mentioned previously. In contrast, transcription was upregulated for the vast majority (22/26) of the genes tested.

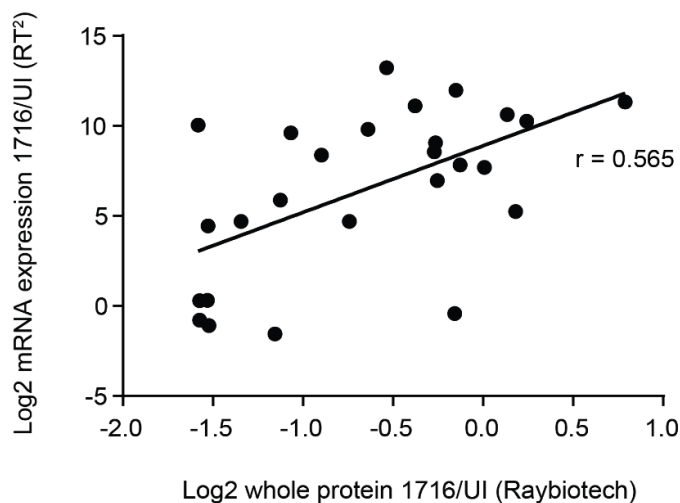


**Figure 6.3 Correlation between whole protein and mRNA expression of selected chemokines in TOV21G cells infected with HSV-1716.** Data from the RT<sup>2</sup> chemokine/cytokine profiler array and the Raybiotech chemokine array were combined and correlated. The correlation coefficient of  $r = 0.565$  is displayed.

### 6.3 NK cell killing induced by viral infection

To further touch upon the downstream immune consequences of HSV-1716-induced cell death, a co-culture assay was set up to assess whether HSV-1716 infection could promote tumour specific killing by NK-92 cells. NK-92 is an immortalised NK cell line isolated from the peripheral blood of a patient suffering from non-Hodgkin lymphoma, which has been shown to have activity against several malignant cell types in culture (Gong, Maki and Klingemann, 1994).

To get a better view of cellular killing over extended time periods, cells were analysed using an Incucyte cell imaging device. Cell death was determined by counting foci of a green, membrane impermeable, nuclear dye - Sytox. Presence of Sytox staining correlates with the number of permeabilised cells within the plate as each Sytox positive cell typically appears as a single focus. To avoid errant Sytox signalling from NK-92 cells, which are smaller than malignant cells, the processing definition was calibrated to exclude foci with a surface area below  $125 \mu\text{m}^2$ . In addition, green counts were normalised by subtracting any counts that were present in an NK-92 only well. Here, total Sytox foci counts per well are plotted (Figure 6.4).

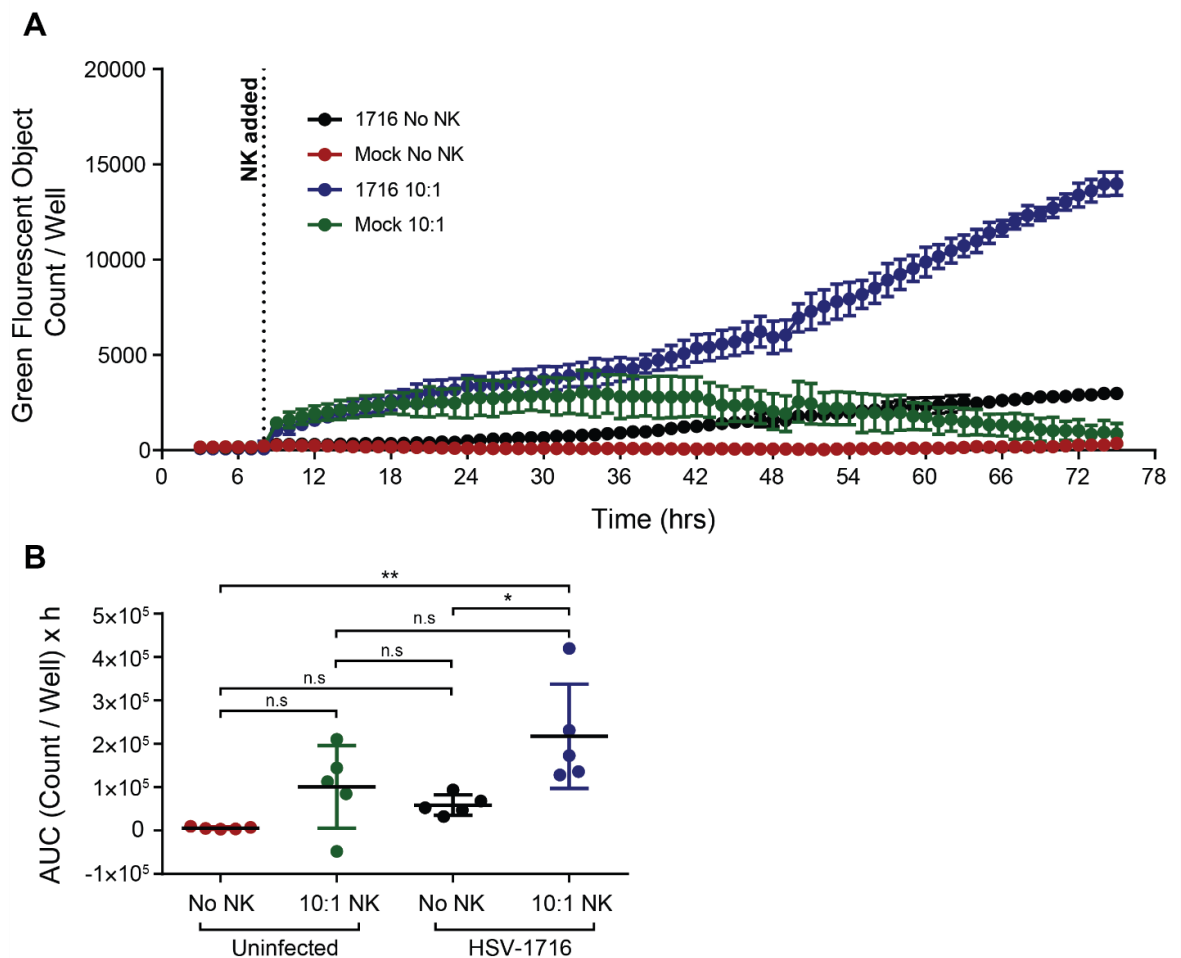


**Figure 6.4 Effect of co-treatment of TOV21G cells with NK92 cells and HSV-1716.** TOV21G cells were seeded into a 96-well plate and infected with HSV-1716 at MOI 1 for 8 h before adding NK92 cells at a 10:1 ratio, before leaving for a further 67 h and analysing uptake of the membrane-impermeable dye, Sytox. **(A)** Data points taken every hour on an Incucyte system from a single experiment are shown here. **(B)** Area under the curve analysis for five separate experiments was performed and the resulting values plotted together. Statistical significance was determined by one-way ANOVA (Tukey's multiple comparisons test). n.s., not significant; \*,  $p < 0.05$ ; \*\*,  $p < 0.01$ .

TOV21G cells were infected with HSV-1716 at MOI 1 and left for 8 h before adding in NK-92 cells at an effector: target (NK-92:TOV21G) ratio of 10:1. Cells were then placed in the cell imaging system with images and Sytox counts taken once an hour until 75 h post-infection. In Figure 6.4a, a single co-culture experiment is shown with green count per well plotted over time. Here, it can be seen that untreated cells produce essentially no green foci for the duration of the experiment, remaining in the region of several hundred counts/well. HSV-1716 infection leads to a slow increase in green fluorescent count over time, ending at ~3000 at 75 h p.i. When NK-92 cells were added to mock-infected cells at a ratio of 10:1, some TOV21G cell killing was seen, with green count rising to a maximum of ~3000/well at 33 h, before gradually declining to <1000 by 75 h.

When NK-92 cells were co-cultured with infected TOV21G cells, green counts rise in parallel with the mock-infected 10:1 cells until ~18 h, where the counts begin to diverge. From here, levels of death continue to increase in the infected co-culture cells until reaching a maximum of 14,000 counts/well at 75 h.

Similar patterns were observed across multiple experimental repeats. To determine whether changes in cell killing were of statistical significance across repeats, AUC analysis was performed on each data set, with resulting values plotted together (Figure 6.4b). For infected TOV21G cells co-cultured with NK-92 cells, average AUC was significantly higher than both untreated and infected TOV21G cells alone ( $2.1 \times 10^5$  vs  $5.8 \times 10^3$ ,  $p = 0.0027$ , and;  $2.1 \times 10^5$  vs  $5.9 \times 10^4$ ,  $p = 0.024$ ). However, there was no significant difference between infected and uninfected conditions with NK-92 cells present ( $2.1 \times 10^5$  vs  $1 \times 10^5$ ,  $p = 0.12$ ), or between any other conditions.

## 6.4 Discussion

In this chapter, I have briefly investigated some of the immunomodulatory aspects of HSV-1716 infection and touched on some of the roles that RIPK3 may play in this area. Analysing both mRNA expression and protein release of an array of cytokines and chemokines was important to get the full cell expression picture. Necrosis by definition involves permeabilization of the cell membrane and release of cellular contents. Change in mRNA expression may not therefore change the immunogenicity of cell death as significantly as protein release.

Genes that were most highly upregulated following HSV-1716 infection of TOV21G cells included interferon- $\gamma$  (*IFNG*), interferon gamma-induced protein 10 (*CXCL10*), interleukin-17F (*IL17F*), and adiponectin (*ADIPOQ*). *IFNG* is a signalling protein that has long been known for its anti-viral effects on HSV-1 (Minami *et al.*, 2002), as well as both pro and anti-tumorigenic roles in cancer (Zaidi and Merlino, 2011). *CXCL10* is a protein released by a variety of cells, typically in response to *IFNG*, and has a range of tumour promoting and inhibitory roles, as well as roles in cell death and chemotaxis (Liu, Guo and Stiles, 2011). Presence of upregulated *CXCL10* could therefore indicate an autocrine or paracrine signalling effect resulting from release of *IFNG*. *IL17F* and *ADIPOQ* are both

proinflammatory cytokines (Chang and Dong, 2009; Luo and Liu, 2016), whose roles in cancer are far less studied, with ADIPOQ being more widely known for its roles in fat metabolism. It is difficult to suggest with any certainty what the roles of these proteins might be within the context of oncolytic viral infection of a tumour, however, and much more research is needed. This suggests that during the course of infection, HSV-1716 induces a strong cellular immune response, probably as a means of combatting infection.

When comparing HSV-1716 and HSV-3D7 infected cells for their cytokine and chemokine expression directly, little change was seen between the viruses. When correlated, fold change values for each virus were shown to a coefficient of determination value of 0.943, which shows that fold-change values were extremely similar between the viruses. When comparing values by volcano plot, only 8 out of 84 genes were shown to be significantly changed. Of these, the most obvious were CCL2, CXCL2 and IL-1 $\beta$ . CCL2 is a chemokine with roles primarily in attracting immune cells such as T cells, dendritic cells and monocytes (Carr *et al.*, 1994; Qian *et al.*, 2011); CXCL3 is a cytokine which binds CXCR2 and facilitates migration and adhesion of monocytes (Smith *et al.*, 2005); IL-1 $\beta$  is a proinflammatory cytokine regulated by the NF- $\kappa$ B pathway with numerous roles in promoting proliferation as well as apoptosis. IL1 $\beta$  is associated with pyroptosis and has been shown to promote tumorigenesis in certain cases (Bergsbaken, Fink and Cookson, 2009; Lee *et al.*, 2015). When validated individually however, all of these genes were shown to be equally regulated between the viruses (Figure 6.1d).

From this it seems reasonable to confirm that there is no significant change in cytokine expression at all between HSV-1716 and HSV-3D7, of the genes tested. We can therefore conclude that the binding of RIPK3 to ICP6 does not seem to influence cytokine regulation. Links between RIPK3 function and cytokine regulation have been shown previously: RIPK3 has been shown to activate the NLRP3 inflammasome, independent of kinase activity, following LPS treatment (Lawlor *et al.*, 2015). Downstream of RIPK3, MLKL has also been shown to activate NLRP3 in conjunction with caspase-8 scaffolding activity (Kang *et al.*, 2015). One of the major effects of this pathway is an increase in IL-1 $\beta$  expression

and release, which is why it is interesting to see that this cytokine remains unchanged.

When chemokine protein release was observed, there were noticeable differences to what was seen in the RT<sup>2</sup> experiment. Firstly, relatively low numbers of chemokines were seen to increase in the supernatant following HSV-1716 infection compared to the large increase in cytokine/chemokine upregulation seen the former experiment in TOV21G cells. It is important to note that the genes studied in each experiment were not all the same; but in the subset of genes that overlapped between the data sets, there was a moderate correlation in fold change over uninfected (Figure 6.3). Overall fold changes were much higher for mRNA transcription compared to protein, which is to be expected as not all mRNA molecules will eventually become released protein. It is interesting that despite the correlation, most proteins were downregulated following infection compared to the majority of genes being upregulated. This is likely due to the fact that most of these proteins fell below the 0.65-1.5-fold cut off for significance in the protein array, and so should be interpreted as not having changed. This underscores the importance of not simply relying on mRNA regulation as a measure of the effect of a stimulus on cytokine production and the immune system.

CCL1 was the only protein that was significantly increased in the supernatant following infection in TOV21G cells and was also highly upregulated in the RT<sup>2</sup> array. CCL1 is a chemokine that has important roles in attracting monocytes, NK cells, B cells and dendritic cells by acting via the CCR8 receptor (Miller and Krangel, 1992; Roos *et al.*, 1997). This chemokine has been linked to HSV-1 infection in corneal endothelial cells, but not cancer cells (Miyazaki *et al.*, 2011).

A majority of chemokines were higher in HSV-3D7-infected cells than for HSV-1716, both overall and among those that surpassed the 1.5-fold cut off. This provides some evidence that HSV-3D7 may be inducing a more immunogenic cell death modality than HSV-1716. Despite lack of any mechanistic evidence, this matches with what has been shown in terms of greater AV/ZV staining and ATP release following HSV-3D7 infection. Taken together, these results begin to

suggest that HSV-3D7 may in fact be causing a more necrotic type of cell death alone. The fact that gene regulation of cytokine and chemokine mRNAs appear to be identical between the viruses can still fit with this theory; it may be that decreased RIPK3 inhibition by ICP6 has no effect on gene regulation, but overall change in cell death results in the release of more cellular contents.

The most pronounced differences between HSV-1716 and HSV-3D7 infected TOV21G cells in terms of chemokine release were in CCL11 (3.6-fold), CCL17 (3.1-fold) and CCL8 (3.0-fold). CCL11 is a selective chemokine which recruits eosinophils by binding to the receptor CCR3, among others (Ponath *et al.*, 1996; Forssmann *et al.*, 1997). Cell types such as neutrophils and monocytes which lack this receptor are not affected, making it quite a specific chemokine. CCL17 is a T cell chemoattractant, typically expressed in the thymus, which binds to CCR4 (Imai *et al.*, 1997). CCL8 is quite a broad spectrum chemokine, known to attract mast cells, eosinophils and basophils, as well as monocytes, T cells and NK cells by binding to a range of receptors including CCR5, CCR1 and CCR2b (Gong *et al.*, 1998; Blaszczyk *et al.*, 2000). It is hard to say with any certainty what the downstream effects of such chemokine changes could be; it is known that infiltration of CD8<sup>+</sup> T cells and NK cells are associated with positive outcomes in OC patients (Sato *et al.*, 2005; Wong *et al.*, 2013), so the effects of these chemokine changes warrant further investigation.

A similar increase in number of upregulated chemokines was seen when comparing HSV-1716-infected HeLa-Lzrs cells to HeLa-RIPK3 cells. Twenty-two out of thirty four chemokines were found at higher levels in the HeLa-RIPK3 cell condition. This can similarly be interpreted as an increase in chemokine release following overexpression of RIPK3. This fits with the theory that high levels of this protein can drive cells down a more active necroptotic pathway - as previously evidenced by higher basal HMGB1 release and MLKL phosphorylation, as well as greater cell death following HSV-1716 infection. The three most highly increased proteins in the HeLa-RIPK3 supernatant were CCL7 (2.4-fold), CXCL11 (2.1-fold), CCL8 (1.8-fold) and CCL11 (1.8-fold). CCL8 and CCL11 were both comparatively upregulated in HSV-3D7-infected TOV21G cells compared to HSV-1716, which may suggest a similar role for increased RIPK3 activation and increased release in certain chemokines. CCL7 was originally identified as a

monocyte chemoattractant, but has also been shown to have roles in attracting CD8<sup>+</sup>/CD4<sup>+</sup> T cells and NK cells (Allavena *et al.*, 1994; Loetscher *et al.*, 1994; Xu *et al.*, 1995). CXCL11 can have multiple effects, mediated by CXCR3 binding; it can attract T cells NK cells and dendritic cells, but also promote invasiveness and resistance to apoptosis in tumour cells (Burns *et al.*, 2006; Tokunaga *et al.*, 2018). CCL3 was the most increased chemokine in both HSV-1716-infected HeLa-Lzrs and HeLa-RIPK3 cells compared to uninfected cells yet was still the most decreased protein when comparing HeLa-RIPK3 to HeLa-Lzrs directly (0.55-fold). How exactly some chemokines are decreased following RIPK3 overexpression is hard to explain. There may be some transcriptional or translational regulation that is applied to certain genes, despite an overall increase in release due to necrosis.

Interestingly, there appeared to be an overall decrease in chemokine release when comparing HSV-3D7-infected HeLa-RIPK3 cells to HSV-1716. This goes against what was seen in TOV21G cells and suggests that the effect of RIPK3 activation on chemokine release may be more complicated. The most decreased proteins were CCL11 (0.35-fold), CXCL10 (0.32-fold) and CXCL6 (0.28-fold). CCL11 was one of the most upregulated chemokines in TOV21G cells for both viruses, with HSV-3D7 leading to much greater levels, so it is interesting that these cells show the complete opposite. CXCL10 was also quite highly increased following HSV-3D7 infection of TOV21G cells compared to HSV-1716.

It should be noted that while great effort was taken to ensure that cell viabilities did not differ between conditions, this was not perfect. Maintaining uniform levels of death is important when trying to compare changes that might be occurring due to the mechanism of cell death taking place. While there were no statistically significant differences in cell viability between the conditions being compared, slight differences were still noticeable and could still have a bearing on the changes in chemokine release observed. In particular, slightly reduced death in the HeLa-RIPK3/HSV-3D7 condition compared to HSV-1716 infected cells, could explain the reduction in chemokine release seen in the HSV-3D7 condition. If the differences in chemokine release were more marked than they are, then slight changes in overall death would have a smaller impact. This

needs to be taken into consideration when comparing relatively small fold-changes in chemokine release.

To more directly investigate the role of HSV-1716 on the immune system, a co-culture experiment was set up to assess the capacity of HSV-1716 to affect NK cell killing. NK-92 cells are a NK cell line that have shown a strong propensity to attack cancer cell lines *in vitro* (Gong, Maki and Klingemann, 1994). Because MTT assays cannot differentiate between the viability of two cell types in one plate, cells were treated with a green fluorescent nuclear dye to assess death via an image-based approach. This allowed for subtraction of signal from NK cells in order to focus on TOV21G cell death alone, as well as a high level of temporal information not seen with other experiments in this study.

Despite a high inter-experiment variability, a statistically significant increase in killing was seen when NK-92 cells were co-cultured with HSV-1716-infected cells compared to infected cells alone and compared to untreated cells. There was also no significant change in killing in the uninfected co-culture condition compared to untreated cells. This suggests that while NK cells are not capable of causing significant killing TOV21G cells alone, infection with HSV-1716 is sufficient to increase cell killing beyond the level of killing that the virus can induce alone. However, some level of killing is clearly visible in the NK only condition, which varied significantly between experiments - resulting in a lack of significant difference between the NK-only and the NK+HSV-1716 conditions. Overall, it seems that any benefit to co-treatment with HSV-1716 and NK-92 cells is merely additive rather than synergistic. Despite this, this is still an interesting and significant result suggesting that HSV-1716 is capable of influencing NK cell killing

This underlines the importance of CCL1 as a major upregulated and released chemokine following HSV-1716 infection. There may be an underlying mechanism between this protein and the ability of HSV-1716 to influence NK cells that would be interesting to explore.

It is of course important to point out the clear differences between the NK-92 cell line and primary NK cells. The process of transformation that has to occur

for a cell type to thrive *in vitro* could result in important functional differences that are not mirrored *in vivo*. This is, however, an interesting subject to pursue further.

## 7 Final Discussion

## 7.1 Results summary

This thesis has sought to investigate the complex roles of immunogenic cell death during the course of infection with an oncolytic agent, HSV-1716. In particular, I have tried to explore how this virus behaves in ovarian cancer cell lines while also trying to gain general mechanistic insights. I have studied a range of transformed and primary ovarian cancer lines to assess how they respond to HSV-1716 infection and to necroptosis in general. In addition, this study has led me to build upon novel gene-editing methods and apply them to HSV-1716.

Firstly, I sought to explore the suitability of HSV-1716 as an oncolytic agent for ovarian cancer. This involved showing that HSV-1716 is capable of successfully infecting, replicating within and killing a large range of ovarian cancer cell lines (Figure 3.1-Figure 3.2). This appears to be the largest panel of OC lines shown to be infected with HSV-1716. It is important to characterise potential treatments such as this in as broad a range of cell lines as possible to gain the best possible idea of how efficacious it might be. I also assessed the susceptibility of a range of OC cell lines to necroptosis induction by TSZ and analysed their expression of components of the necrosome. Crucially, I showed that despite most cell lines expressing all components of the necrosome, only one cell line, TOV21G, showed a marked sensitivity to necroptosis.

Next, I sought to create a range of genetically modified cell lines and viruses in order to fully explore the role of ICP6 in HSV-1716-induced cell death. ICP6 has been shown by others to play a key role in determining the fate of HSV-1-infected cells (Guo *et al.*, 2015; Huang, S.-Q. Wu, *et al.*, 2015), but this role has never been explored in an oncolytic herpes virus. Several OC lines expressing various modified forms of ICP6 were created, including a  $\Delta 1-243aa$  version and one containing a tetra-alanine substitution in place of the RHIM (*mutRHIM*). I also adapted my own protocol to use CRISPR/Cas9 gene editing to create a range of ICP6-null and ICP6 RHIM-modified strains of HSV-1716, HSV-3B1, -1C5 and -3D7, respectively. Importantly, I confirmed that overexpression of ICP6 has the capacity to block necroptosis in OC lines but not when the RHIM is absent. I also

showed that ICP6-null viruses replicate and kill less effectively than HSV-1716, but not when only the RHIM is modified. In addition, the RHIM-modified ICP6 of HSV-3D7 was not able to bind RIPK3, whereas HSV-1716 could.

Further exploring the cell death-inducing properties of these viruses, I showed that HSV-1716 does induce immunogenic cell death in OC cells via the release of HMGB1 and ATP, but not CAL exposure. HMGB1 and ATP release have both been associated with IA and necrosis in the past, which gives little clue as to what the underlying mechanisms of this might be. Further evidence of an explosive necrosis-like morphology was found by EM analysis of infected cells. Functionally, HSV-1716 does not respond to caspase-8 inhibition or inhibition/knockdown of RIPK1, RIPK3, or MLKL suggesting that neither pure apoptosis or necroptosis is the driving force of death. In addition, there was no increase in MLKL phosphorylation following infection, showing that necroptosis definitely is not responsible for HSV-1716-induced death in OC cells.

Crucially, none of these measures appeared to change when comparing HSV-1716 and HSV-3D7-infected cells directly. This strongly suggests that disrupting the interaction between ICP6 and RIPK3 does not lead to death proceeding in a more necrotic manner.

An interesting phenomenon was observed when assessing the HeLa-RIPK3 overexpression model. All evidence presented here seems to suggest that high levels of RIPK3 seem to drive cells down a necrotic pathway, even in the absence of other stimuli. This can be seen in both higher levels of basal HMGB1 release and MLKL phosphorylation (Figure 5.2-Figure 5.3). In addition, these cells are more sensitive to HSV-1716-induced death, although this does not seem to increase the level of necroptotic signalling. Again, no difference between any stimuli was seen in these cells when comparing HSV-1716 and HSV-3D7 infection directly. This seems to suggest that even when levels of RIPK3 are exceptionally high, HSV cannot promote any additional necroptosis beyond what is already being induced by RIPK3 alone - this is even true when no ICP6-mediated blockade of RIPK3 is present.

To test this further, HeLa-RIPK3 cells were infected with HSV-1716 or HSV-3D7 in addition to the further death stimuli, TNF- $\alpha$  and SMAC mimetic. Here it was shown that HSV-3D7-infected cells were far more sensitive to these additional stimuli than HSV-1716-infected cells. This fits with the idea that release of the ICP6-RIPK3 blockade, can open cells up to further necroptotic stimuli.

A large amount of information was gathered about the cytokine and chemokine regulation and release profiles of cell lines infected with HSV-1716 and HSV-3D7. A moderate correlation was seen between released protein and mRNA regulation, suggesting that these processes are somewhat linked. Importantly, only one chemokine was shown to be significantly raised in the supernatant, yet also highly upregulated at the transcriptional level - CCL1. No difference in cytokine regulation was seen when comparing HSV-3D7 to HSV-1716, which fits with the hypothesis that further stimulation is required to promote necroptosis. A difference was seen between the viruses in released protein, which taken together with increased ATP release and AV/ZV staining, may still suggest that some higher level of necrosis is present in HSV-3D7-infected cells, even without extra stimulus. Interestingly, NK-92 cells appeared to directly increase HSV-1716-mediated killing in TOV21G cells, providing evidence of a downstream immunostimulatory consequence of HSV-1716 killing that will need to be explored further.

## 7.2 Future directions

Having shown that TNF- $\alpha$  can increase the cell death induced by HSV-3D7 to a larger degree than HSV-1716, it would now be important to follow up this finding with further analysis of the necroptotic signalling consequences of this. It is likely that this combination will produce some necroptotic signalling - as a result it would be interesting to see to what extent this process can be blocked, and whether cell death caused by this combination is synergistic.

*In vivo* activity of these viruses is not something that has been explored in this thesis but will be important in determining the potential clinical benefit of HSV-1716 in an appropriate OC model. The most widely used transplantable model for HGSOC involves the intra-peritoneal injection of the ID8 murine cell line in

syngeneic mice (Roby *et al.*, 2000). Recently, these cells have been found to lack all of the major genetic mutations that characterise HSGOC, but new CRISPR/Cas9-generated variants of these cells have helped to correct for this (Walton *et al.*, 2016, 2017). Despite these recent advances, use of murine cell lines still poses numerous challenges for OV validation: the most obvious of these being the fact that ICP6 has been shown to have precisely opposite roles in murine and human cell types (Huang, S.-Q. Wu, *et al.*, 2015). Xenograft models based on human HGSOC cell lines have been used, including for the study of OVs (Coukos *et al.*, 1999; Fujiwara *et al.*, 2011). These models have limited applicability to the study of immune system responses, however, due to the requirement for immunocompromised mice to prevent rejection of human cells. Although, infected human cells *in vivo* can still be analysed for cytokine and chemokine regulation, which may be a potential future step for the comparison of HSV-1716 and HSV-3D7 infection.

### **7.3 Translational significance**

OVs are emerging as a potentially useful treatment option in cancer types for which clinically beneficial drugs are not available, or in cancer types that respond particularly well to immunostimulatory agents. T-VEC was the first OV approved for clinical use for unresectable recurrent metastatic melanoma by the FDA in October 2015. T-VEC was shown to improve durable response rate in patients and has been shown to effectively control local disease, although systemic effects are still arguably weak (Andtbacka *et al.*, 2015; Kaufman *et al.*, 2016). The success of T-VEC demonstrates the future utility that OVs may one day have in a range of cancer types; it also demonstrates the transformation that many current OV vectors still need to go through before they are able to interact with the body in a clinically meaningful way. Finding the right modifications to make to viral genomes and arming them with the right exogenous genes is a long and iterative process, but one that will be necessary to create a generation of OVs that can interact with cancer cells and the surrounding TME in the most optimal way.

Two elements of this project highlight ways in which this process may become more effective and streamlined in the future: firstly, I have shown that CRISPR/Cas9 gene editing can be a rapid and useful way to apply precise modifications to the genome of a large virus such as HSV-1. This process is far less time consuming and laborious than the current BAC cloning method and could become the new standard for large viral genome modification. Second, I have shown that even small modifications in the form of a single amino acid deletion can have significant impact on the way a virus responds to various stimuli. As well as highlighting the multifunctional nature of viral proteins, this could potentially open the door to an era where each region of a viral gene can be probed and modified in a way that optimises the virus for specific cancer killing and selective immune system engagement.

Demonstration that additional TNF- $\alpha$  treatment can increase cell death preferentially in HSV-3D7-infected cells compared to HSV-1716 highlights one way in which further improvement upon this virus may be possible. As the name suggests, TNF- $\alpha$  was originally identified as a serum endotoxin that could cause necrosis of tumour cells (Carswell *et al.*, 1975). While systemic toxicity of this protein has limited its use in cancer therapy, there has been interest in developing TNF- $\alpha$ -expressing OV<sub>s</sub> in order to contain expression to the desired therapeutic region (Han *et al.*, 2007; Hirvinen *et al.*, 2015). Using HSV-3D7 as a template may therefore amplify any beneficial effects that this combination might have and is one potential future avenue of interest.

## 7.4 Final remarks

The question of how OV<sub>s</sub> kill cancer cells and lead to robust anti-tumour immune responses continues to be of great importance. Here, I have shown that one such virus, HSV-1716 displays several markers of ICD, yet does not activate necroptosis. Importantly, the mechanisms that OV<sub>s</sub> employ to induce certain types of death appear to be modifiable. Much work still needs to be done to refine our definitions of cell death and identify which modes of death have the best anti-tumour immunogenic consequences. Only then can we start to build the next generation of OV<sub>s</sub> therapeutics that are able to walk the immunological

tightrope - balancing the best possible mix of immune system activation and repression to give the best possible clinical outcomes.

## 8 Appendices

## 8.1 Fold-change values for RT<sup>2</sup> chemokine/cytokine array

Table 8.1: Log<sub>2</sub> fold-change values for HSV-1716 compared to uninfected cells in TOV21G.

Gene	Log <sub>2</sub> Fold-Change	p Value	Gene	Log <sub>2</sub> Fold-Change	p Value	Gene	Log <sub>2</sub> Fold-Change	p Value
ADIPOQ	14.49	4.2	CXCL10	13.22	3.27	IL23A	5.38	2.02
BMP2	5.46	2.77	CXCL11	9.8	1.25	IL24	10.43	0.75
BMP4	-0.83	1.62	CXCL12	11.1	2.14	IL27	3.02	0.65
BMP6	8.68	1.12	CXCL13	10.25	1.76	IL3	12.91	0.72
BMP7	6.72	0.67	CXCL16	0.29	0.43	IL4	5.76	0.47
C5	-1.65	0.19	CXCL2	-1.56	0.79	IL5	9.37	1.5
CCL1	11.32	2.43	CXCL5	-0.79	0.53	IL6	-0.74	0.84
CCL11	4.7	0.97	CXCL9	7.83	1.33	IL7	5.55	0.8
CCL13	9.6	0.41	FASLG	14.4	0.36	CXCL8	-0.42	0.34
CCL17	10.04	0.74	GPI	1.85	4.34	IL9	8.47	0.51
CCL18	11.97	2.44	IFNA2	13.25	0.51	LIF	-3.29	0.52
CCL19	5.24	0.9	IFNG	12.89	2.04	LTA	7.97	1.48
CCL2	0.31	0.09	IL10	11.66	1.31	LTB	2.19	0.93
CCL20	6.96	2.85	IL11	4.55	2.03	MIF	-1.64	1.48
CCL21	4.32	0.42	IL12A	-0.31	0.22	MSTN	8.72	2.69
CCL22	10.63	1.13	IL12B	10.79	0.94	NODAL	3.46	0.94
CCL24	8.56	0.48	IL13	7.68	2.18	OSM	3.41	0.68
CCL3	7.69	0.46	IL15	-1.38	0.86	PPBP	4.69	1.39
CCL5	5.88	0.75	IL16	5.31	0.67	SPP1	-1.99	3.13
CCL7	9.06	0.9	IL17A	8.62	0.46	TGFB2	4.48	1.72
CCL8	8.38	2.91	IL17F	14.2	2.3	THPO	5.19	2.51
CD40LG	8.48	2.75	IL18	-1.54	3.04	TNF	2.11	2.79
CNTF	0.13	0.06	IL1A	-0.44	1	TNFRSF11B	-4.19	2.79
CSF1	2.89	0.47	IL1B	4.69	1.2	TNFSF10	8.18	1.1
CSF2	8.37	1.05	IL1RN	8.78	0.79	TNFSF11	8.38	2.1
CSF3	9.47	1.94	IL2	8.56	0.52	TNFSF13B	1.21	0.7
CX3CL1	4.44	4.37	IL21	7.04	2.81	VEGFA	2.94	3.91
CXCL1	-1.09	0.88	IL22	8.27	1.89	XCL1	10.28	0.67

Table 8.2: Log2 fold-change values for HSV-1716 infection compared to HSV-3D7 in TOV21G cells.

Gene	Log2 Fold-Change	Log2 p Value	Gene	Log2 Fold-Change	Log2 p Value	Gene	Log2 Fold-Change	p Value
ADIPOQ	1.21	2.35	CXCL10	0.71	2.15	IL23A	-0.36	0.22
BMP2	0.2	0.37	CXCL11	-2.03	0.26	IL24	-2.83	0.7
BMP4	1.21	1.47	CXCL12	0.97	1.13	IL27	-3.46	0.77
BMP6	0.07	0.05	CXCL13	0.79	0.96	IL3	-3.13	0.7
BMP7	-5.12	0.82	CXCL16	-1	0.19	IL4	1.43	0.62
C5	1.1	0.18	CXCL2	1.36	3.27	IL5	-2.17	0.17
CCL1	-2.25	1.14	CXCL5	0.2	0.24	IL6	0.54	1.14
CCL11	0.56	0.5	CXCL9	-1.06	0.04	IL7	-0.9	0.33
CCL13	-4.37	0.52	FASLG	-5.77	0.45	CXCL8	0.14	0.04
CCL17	-2.02	0.05	GPI	0.15	1.01	IL9	-1.85	0.49
CCL18	-0.87	0.3	IFNA2	-2.64	0.3	LIF	0.76	0.23
CCL19	-2.92	0.89	IFNG	1.12	1.55	LTA	1.19	0.97
CCL2	-1.62	2.43	IL10	-1.27	0.78	LTB	-0.12	0.53
CCL20	1.25	2.03	IL11	-0.68	0.34	MIF	0.57	4.08
CCL21	-0.56	0.13	IL12A	-0.29	0.17	MSTN	0.1	0.08
CCL22	0.14	0.22	IL12B	-4.45	1.22	NODAL	-1.7	0.11
CCL24	-1.94	0.48	IL13	-1.22	0.63	OSM	-3.49	0.5
CCL3	-1.37	0.42	IL15	1.16	0.63	PPBP	0.11	0.15
CCL5	0.09	0.3	IL16	-1.61	0.04	SPP1	0.81	2.8
CCL7	-2.37	0.74	IL17A	-0.29	0.19	TGFB2	1.01	0.94
CCL8	-1.06	0.27	IL17F	-0.04	0.04	THPO	-1.43	0.19
CD40LG	-0.7	0.19	IL18	1.11	3.84	TNF	0.89	2.17
CNTF	1.9	1.29	IL1A	2.32	1	TNFRSF11B	2.73	0.9
CSF1	-1.1	0.01	IL1B	-4.41	1.45	TNFSF10	-3.27	0.83
CSF2	-1.67	0.62	IL1RN	-1.1	0.14	TNFSF11	-0.73	0.24
CSF3	1.07	1.52	IL2	-0.31	0.14	TNFSF13B	1.03	0.13
CX3CL1	0.43	0.81	IL21	0.71	0.43	VEGFA	0.69	2.68
CXCL1	0.12	0.4	IL22	0.82	0.77	XCL1	-2.23	0.38

## 8.2 Fold change values for Raybiotech chemokine array

**Table 8.3: Relative fold changes in chemokine expression for TOV21G cells infected with HSV-1716 or HSV-3D7.**

Chemokine	TOV21G		
	HSV-1716*	HSV-3D7*	HSV-3D7/HSV-1716
CCL11	0.394	1.421	3.61
CCL17	0.334	1.048	3.14
CCL8	0.537	1.587	2.96
CCL24	0.829	2.063	2.49
CCL2	0.346	0.791	2.29
CXCL5	0.336	0.706	2.10
CXCL7	0.598	1.208	2.02
CCL5	0.458	0.921	2.01
CXCL10	0.69	1.328	1.92
CXCL16	0.336	0.646	1.92
GROa	0.449	0.848	1.89
CCL19	1.134	2.125	1.87
CXCL6	0.477	0.856	1.79
CCL4	0.797	1.397	1.75
CCL22	1.098	1.902	1.73
CCL18	0.901	1.449	1.61
CCL20	0.838	1.27	1.52
CCL7	0.833	1.26	1.51
CXCL12a	0.765	1.157	1.51
CXCL1	0.348	0.5	1.44
CCL23	1.03	1.437	1.40
CCL3	1.005	1.396	1.39
CCL27	0.881	1.171	1.33
CXCL12b	0.77	1.02	1.32
CXCL9	0.915	1.194	1.30
CCL13	0.477	0.618	1.30
CCL26	0.475	0.61	1.28
CXCL13	1.183	1.513	1.28
CX3CL1	0.347	0.437	1.26
CCL28	1.03	1.161	1.13
CCL25	0.947	1.037	1.10
CCL16	1.36	1.324	0.97
Ckb81	0.68	0.651	0.96
CXCL11	0.642	0.553	0.86
CCL1	1.729	1.43	0.83
IL-8	0.897	1.264	1.41
XCL-1	nil†	2.555	N/A
CCL15	0.496	nil†	N/A

\* Fold change values compared to uninfected cells

† Fluorescence values < 2 SD above background

**Table 8.4: Relative fold changes in chemokine expression for HeLa cells infected with HSV-1716.**

Chemokine	HeLa - HSV-1716		
	HeLa-Lzrs*	HeLa-RIPK3*	HSV-3D7/HSV-1716
CCL7	0.809	1.942	2.40
CXCL11	1.244	2.64	2.12
CCL8	0.977	1.797	1.84
CCL11	1.093	1.962	1.80
CCL19	1.052	1.802	1.71
CXCL7	0.882	1.347	1.53
CCL23	0.753	1.124	1.49
CXCL6	1.16	1.717	1.48
CXCL12a	0.916	1.333	1.46
CCL20	1.056	1.51	1.43
CCL26	1.017	1.428	1.40
CCL5	0.293	0.387	1.32
CXCL12b	0.948	1.186	1.25
CCL25	1.03	1.245	1.21
CCL27	0.927	1.092	1.18
CCL16	0.957	1.124	1.17
CXCL16	0.494	0.573	1.16
CCL2	0.67	0.777	1.16
CCL18	1.026	1.186	1.16
CXCL9	0.915	1.057	1.16
CCL4	1.447	1.643	1.14
CCL22	0.514	0.513	1.00
IL-8	0.99	0.979	0.99
CXCL13	0.492	0.472	0.96
CXCL1	1.09	1.034	0.95
GROa	1.022	0.933	0.91
CCL17	1.571	1.398	0.89
CX3CL1	1.809	1.607	0.89
CCL24	1.739	1.51	0.87
CXCL5	1.037	0.831	0.80
CCL13	1.708	1.274	0.75
CXCL10	1.316	0.943	0.72
CCL28	1.467	0.955	0.65
CCL3	5.576	3.082	0.55
Ckb8-1	1.619	nil†	N/A
XCL-1	nil†	2.035	N/A
CCL1	nil†	1.598	N/A
CCL15	nil†	nil†	N/A

\* Fold change values compared to uninfected cells

† Fluorescence values < 2 SD above background

**Table 8.5: Relative fold changes in chemokine expression for HeLa-RIPK3 cells infected with HSV-1716 or HSV-3D7.**

Chemokine	HeLa RIPK3		
	HSV-1716*	HSV-3D7*	HSV-3D7/HSV-1716
CXCL13	0.472	0.735	1.56
CCL5	0.387	0.556	1.44
CCL28	0.955	1.08	1.13
IL-8	0.979	1.033	1.06
CCL18	1.186	1.2	1.01
CXCL16	0.573	0.565	0.99
CXCL9	1.057	1.041	0.98
CXCL12b	1.186	1.159	0.98
CXCL1	1.034	0.977	0.94
CCL23	1.124	1.049	0.93
GROa	0.933	0.866	0.93
CCL27	1.092	1	0.92
CCL25	1.245	1.111	0.89
CCL16	1.124	0.997	0.89
CCL2	0.777	0.671	0.86
CXCL7	1.347	1.023	0.76
CX3CL1	1.607	1.201	0.75
CCL26	1.428	1.02	0.71
CXCL5	0.831	0.578	0.70
CXCL12a	1.333	0.92	0.69
CCL1	1.598	1.101	0.69
CCL4	1.643	1.096	0.67
CCL7	1.942	1.288	0.66
CCL8	1.797	1.122	0.62
CCL19	1.802	1.067	0.59
CXCL11	2.64	1.424	0.54
CCL20	1.51	0.741	0.49
CCL24	1.51	0.709	0.47
CCL22	0.513	0.228	0.44
CCL3	3.082	1.261	0.41
CCL13	1.274	0.501	0.39
CCL11	1.962	0.681	0.35
CXCL10	0.943	0.299	0.32
CXCL6	1.717	0.474	0.28
CCL17	1.398	nil†	N/A
XCL-1	2.035	nil†	N/A
CCL15	nil†	nil†	N/A
Ckb8-1	nil†	nil†	N/A

\* Fold change values compared to uninfected cells

† Fluorescence values < 2 SD above background

## 9 List of References

- Abal, M., Andreu, J. M. and Barasoain, I. (2003) 'Taxanes: microtubule and centrosome targets, and cell cycle dependent mechanisms of action.', *Current cancer drug targets*, 3(3), pp. 193-203. Available at: <http://www.ncbi.nlm.nih.gov/pubmed/12769688> (Accessed: 15 December 2017).
- Abdoli, S. *et al.* (2017) 'Construction of Various  $\gamma$ 34.5 Deleted Fluorescent-Expressing Oncolytic herpes Simplex type 1 (oHSV) for Generation and Isolation of HSV-Based Vectors', *Iranian biomedical journal*. Pasteur Institute of Iran, 21(4), pp. 206-217. doi: 10.18869/ACADPUB.IBJ.21.4.206.
- Aghajanian, C. *et al.* (2012) 'OCEANS: A Randomized, Double-Blind, Placebo-Controlled Phase III Trial of Chemotherapy With or Without Bevacizumab in Patients With Platinum-Sensitive Recurrent Epithelial Ovarian, Primary Peritoneal, or Fallopian Tube Cancer', *Journal of Clinical Oncology*, 30(17), pp. 2039-2045. doi: 10.1200/JCO.2012.42.0505.
- Ahmed, A. A. *et al.* (2010) 'Driver mutations in TP53 are ubiquitous in high grade serous carcinoma of the ovary', (February), pp. 49-56.
- Aletti, G. D. *et al.* (2006) 'Ovarian cancer surgical resectability: Relative impact of disease, patient status, and surgeon', *Gynecologic Oncology*, 100(1), pp. 33-37. doi: 10.1016/j.ygyno.2005.07.123.
- Alipour, S. *et al.* (2016) 'Specific immunotherapy in ovarian cancer: a systematic review', *Immunotherapy*, 8(10), pp. 1193-1204. doi: 10.2217/imt-2016-0034.
- Allavena, P. *et al.* (1994) 'Induction of natural killer cell migration by monocyte chemotactic protein-1, -2 and -3', *European Journal of Immunology*, 24(12), pp. 3233-3236. doi: 10.1002/eji.1830241249.
- Allavena, P. *et al.* (2010) 'Engagement of the Mannose Receptor by Tumoral Mucins Activates an Immune Suppressive Phenotype in Human Tumor-Associated Macrophages', *Clinical and Developmental Immunology*, 2010, pp. 1-10. doi: 10.1155/2010/547179.
- Andersson, U. and Tracey, K. J. (2011) 'HMGB1 Is a Therapeutic Target for Sterile Inflammation and Infection', *Annual Review of Immunology*, 29(1), pp. 139-162. doi: 10.1146/annurev-immunol-030409-101323.
- Andrabi, S. A. *et al.* (2014) 'Poly(ADP-ribose) polymerase-dependent energy depletion occurs through inhibition of glycolysis', *Proceedings of the National Academy of Sciences*, 111(28), pp. 10209-10214. doi: 10.1073/pnas.1405158111.
- Andtbacka, R. H. I. *et al.* (2015) 'Talimogene laherparepvec improves durable response rate in patients with advanced melanoma', *Journal of Clinical Oncology*, 33(25), pp. 2780-2788. doi: 10.1200/JCO.2014.58.3377.
- Angelova, A. L. *et al.* (2014) 'Complementary induction of immunogenic cell death by oncolytic parvovirus H-1PV and gemcitabine in pancreatic cancer.', *Journal of virology*, 88(10), pp. 5263-76. doi: 10.1128/JVI.03688-13.
- Anglesio, M. S. *et al.* (2015) 'Synchronous Endometrial and Ovarian Carcinomas: Evidence of Clonality', *Journal of the National Cancer Institute*. Oxford University Press, 108(6), p. djv428. doi: 10.1093/jnci/djv428.

- Antoniou, A. *et al.* (2003) 'Average Risks of Breast and Ovarian Cancer Associated with BRCA1 or BRCA2 Mutations Detected in Case Series Unselected for Family History: A Combined Analysis of 22 Studies', *The American Journal of Human Genetics*, 72(5), pp. 1117-1130. doi: 10.1086/375033.
- Ardighieri, L. *et al.* (2014) 'Mutational analysis of BRAF and KRAS in ovarian serous borderline (atypical proliferative) tumours and associated peritoneal implants.', *The Journal of pathology*, 232(1), pp. 16-22. doi: 10.1002/path.4293.
- Asea, A. *et al.* (2002) 'Novel signal transduction pathway utilized by extracellular HSP70: role of toll-like receptor (TLR) 2 and TLR4.', *The Journal of biological chemistry*, 277(17), pp. 15028-34. doi: 10.1074/jbc.M200497200.
- Ashkenazi, A. and Dixit, V. M. (1998) 'Death receptors: signaling and modulation.', *Science (New York, N.Y.)*, 281(5381), pp. 1305-8. Available at: <http://www.ncbi.nlm.nih.gov/pubmed/9721089> (Accessed: 9 January 2018).
- Atanasiu, D. *et al.* (2007) 'Bimolecular complementation reveals that glycoproteins gB and gH/gL of herpes simplex virus interact with each other during cell fusion', *Proceedings of the National Academy of Sciences*, 104(47), pp. 18718-18723. doi: 10.1073/pnas.0707452104.
- Ataseven, B. *et al.* (2016) 'FIGO stage IV epithelial ovarian, fallopian tube and peritoneal cancer revisited', *Gynecologic Oncology*, 142(3), pp. 597-607. doi: 10.1016/j.ygyno.2016.06.013.
- Baek, S.-J. *et al.* (2008) 'Stage IIIc epithelial ovarian cancer classified solely by lymph node metastasis has a more favorable prognosis than other types of stage IIIc epithelial ovarian cancer.', *Journal of gynecologic oncology*. Korean Society of Gynecologic Oncology and Colposcopy, 19(4), pp. 223-8. doi: 10.3802/jgo.2008.19.4.223.
- Bailer, S. M. *et al.* (2017) 'Herpesviral vectors and their application in oncolytic therapy, vaccination, and gene transfer', *Virus Genes*. Springer US, 53(5), pp. 741-748. doi: 10.1007/s11262-017-1482-7.
- Bast, R. C. *et al.* (1981) 'Reactivity of a monoclonal antibody with human ovarian carcinoma.', *The Journal of clinical investigation*, 68(5), pp. 1331-7. Available at: <http://www.ncbi.nlm.nih.gov/pubmed/7028788> (Accessed: 5 February 2018).
- Basu, S. *et al.* (2001) 'CD91 is a common receptor for heat shock proteins gp96, hsp90, hsp70, and calreticulin.', *Immunity*, 14(3), pp. 303-13. Available at: <http://www.ncbi.nlm.nih.gov/pubmed/11290339> (Accessed: 19 December 2017).
- Bauerschmitz, G. J. *et al.* (2002) 'Treatment of ovarian cancer with a tropism modified oncolytic adenovirus.', *Cancer research*, 62(5), pp. 1266-70. Available at: <http://www.ncbi.nlm.nih.gov/pubmed/11888888> (Accessed: 16 February 2018).
- Bell, D., Berchuck, A. and Birrer, M. (2011) 'Integrated genomic analyses of ovarian carcinoma.', *Nature*, 474(7353), pp. 609-15. doi: 10.1038/nature10166.
- Bello-Morales, R. *et al.* (2005) 'High susceptibility of a human oligodendroglial cell line to herpes simplex type 1 infection', *Journal of Neurovirology*, 11(2), pp. 190-198. doi: 10.1080/13550280590924179.

- Benencia, F., Courrèges, M. C., Conejo-García, J. R., Mohamed-Hadley, A., *et al.* (2005) 'HSV oncolytic therapy upregulates interferon-inducible chemokines and recruits immune effector cells in ovarian cancer', *Molecular Therapy*, 12(5), pp. 789-802. doi: 10.1016/j.ymthe.2005.03.026.
- Benencia, F., Courrèges, M. C., Conejo-García, J. R., Buckanovich, R. J., *et al.* (2005) 'Oncolytic HSV exerts direct antiangiogenic activity in ovarian carcinoma.', *Human gene therapy*, 16(6), pp. 765-78. doi: 10.1089/hum.2005.16.765.
- Benencia, F. *et al.* (2008) 'Herpes virus oncolytic therapy reverses tumor immune dysfunction and facilitates tumor antigen presentation.', *Cancer biology & therapy*, 7(8), pp. 1194-205. Available at: <http://www.ncbi.nlm.nih.gov/pubmed/18458533> (Accessed: 3 January 2015).
- Berghe, T. Vanden *et al.* (2014) 'Regulated necrosis: the expanding network of non-apoptotic cell death pathways', *Nature Reviews Molecular Cell Biology*. Nature Publishing Group, 15(2), pp. 135-147. doi: 10.1038/nrm3737.
- Bergsbaken, T., Fink, S. L. and Cookson, B. T. (2009) 'Pyroptosis: host cell death and inflammation.', *Nature reviews. Microbiology*. NIH Public Access, 7(2), pp. 99-109. doi: 10.1038/nrmicro2070.
- Bi, Y. *et al.* (2014) 'High-Efficiency Targeted Editing of Large Viral Genomes by RNA-Guided Nucleases', *PLoS Pathog*, 10(5), p. e1004090. doi: 10.1371/journal.ppat.1004090.
- Bilsland, A. E., Spiliopoulou, P. and Evans, T. R. J. (2016) 'Virotherapy: cancer gene therapy at last?', *F1000Research*, 5(0), p. 2105. doi: 10.12688/f1000research.8211.1.
- Blaszczyk, J. *et al.* (2000) 'Complete crystal structure of monocyte chemotactic protein-2, a CC chemokine that interacts with multiple receptors.', *Biochemistry*, 39(46), pp. 14075-81. Available at: <http://www.ncbi.nlm.nih.gov/pubmed/11087354> (Accessed: 30 April 2018).
- Bolovan, C. A., Sawtell, N. M. and Thompson, R. L. (1994) 'ICP34.5 mutants of herpes simplex virus type 1 strain 17syn+ are attenuated for neurovirulence in mice and for replication in confluent primary mouse embryo cell cultures.', *Journal of virology*, 68(1), pp. 48-55. Available at: <http://www.pubmedcentral.nih.gov/articlerender.fcgi?artid=236262&tool=pmcentrez&rendertype=abstract> (Accessed: 2 January 2015).
- Bouzari, Z. *et al.* (2011) 'Risk of malignancy index as an evaluation of preoperative pelvic mass.', *Caspian journal of internal medicine*. Babol University of Medical Sciences, 2(4), pp. 331-5. Available at: <http://www.ncbi.nlm.nih.gov/pubmed/24551441> (Accessed: 5 February 2018).
- Bowtell, D. D. L. (2010) 'The genesis and evolution of high-grade serous ovarian cancer.', *Nature reviews. Cancer*, 10(11), pp. 803-8. doi: 10.1038/nrc2946.
- Brennan, M. A. and Cookson, B. T. (2000) 'Salmonella induces macrophage death by caspase-1-dependent necrosis.', *Molecular microbiology*, 38(1), pp. 31-40. Available at: <http://www.ncbi.nlm.nih.gov/pubmed/11029688> (Accessed: 11 January 2018).
- Brinkmann, V. *et al.* (2004) 'Neutrophil Extracellular Traps Kill Bacteria', *Science*, 303(5663), pp. 1532-1535. doi: 10.1126/science.1092385.

- Burattini, S. and Falcieri, E. (2013) 'Analysis of Cell Death by Electron Microscopy', in. Humana Press, Totowa, NJ, pp. 77-89. doi: 10.1007/978-1-62703-383-1\_7.
- Burger, R. A. *et al.* (2011) 'Incorporation of Bevacizumab in the Primary Treatment of Ovarian Cancer', *New England Journal of Medicine*, 365(26), pp. 2473-2483. doi: 10.1056/NEJMoa1104390.
- Burns, J. M. *et al.* (2006) 'A novel chemokine receptor for SDF-1 and I-TAC involved in cell survival, cell adhesion, and tumor development.', *The Journal of experimental medicine*. Rockefeller University Press, 203(9), pp. 2201-13. doi: 10.1084/jem.20052144.
- Cabon, L. *et al.* (2012) 'BID regulates AIF-mediated caspase-independent necroptosis by promoting BAX activation.', *Cell death and differentiation*. Nature Publishing Group, 19(2), pp. 245-56. doi: 10.1038/cdd.2011.91.
- Cai, D. L. and Jin, L.-P. (2017) 'Immune Cell Population in Ovarian Tumor Microenvironment.', *Journal of Cancer*. Ivyspring International Publisher, 8(15), pp. 2915-2923. doi: 10.7150/jca.20314.
- Cai, Z. *et al.* (2014) 'Plasma membrane translocation of trimerized MLKL protein is required for TNF-induced necroptosis.', *Nature cell biology*. Nature Publishing Group, a division of Macmillan Publishers Limited. All Rights Reserved., 16(1), pp. 55-65. doi: 10.1038/ncb2883.
- Campbell, I. G. *et al.* (2004) 'Mutation of the *PIK3CA* Gene in Ovarian and Breast Cancer', *Cancer Research*, 64(21), pp. 7678-7681. doi: 10.1158/0008-5472.CAN-04-2933.
- Cantrell, L. A. *et al.* (2010) 'Metformin is a potent inhibitor of endometrial cancer cell proliferation--implications for a novel treatment strategy.', *Gynecologic oncology*, 116(1), pp. 92-8. doi: 10.1016/j.ygyno.2009.09.024.
- Cardone, M. H. *et al.* (1998) 'Regulation of cell death protease caspase-9 by phosphorylation.', *Science (New York, N.Y.)*, 282(5392), pp. 1318-21. Available at: <http://www.ncbi.nlm.nih.gov/pubmed/9812896> (Accessed: 12 January 2018).
- Carew, J. F. *et al.* (2001) 'A novel approach to cancer therapy using an oncolytic herpes virus to package amplicons containing cytokine genes.', *Molecular therapy: the journal of the American Society of Gene Therapy*, 4(3), pp. 250-6. doi: 10.1006/mthe.2001.0448.
- Carr, M. W. *et al.* (1994) 'Monocyte chemoattractant protein 1 acts as a T-lymphocyte chemoattractant.', *Proceedings of the National Academy of Sciences of the United States of America*. National Academy of Sciences, 91(9), pp. 3652-6. Available at: <http://www.ncbi.nlm.nih.gov/pubmed/8170963> (Accessed: 26 April 2018).
- Carswell, E. A. *et al.* (1975) 'An endotoxin-induced serum factor that causes necrosis of tumors.', *Proceedings of the National Academy of Sciences of the United States of America*, 72(9), pp. 3666-70. Available at: <http://www.ncbi.nlm.nih.gov/pubmed/1103152> (Accessed: 2 May 2018).
- Casares, N. *et al.* (2005) 'Caspase-dependent immunogenicity of doxorubicin-induced tumor cell death.', *The Journal of experimental medicine*. The Rockefeller University Press, 202(12), pp. 1691-701. doi: 10.1084/jem.20050915.

- Catasús, L. *et al.* (2004) 'Molecular genetic alterations in endometrioid carcinomas of the ovary: Similar frequency of beta-catenin abnormalities but lower rate of microsatellite instability and PTEN alterations than in uterine endometrioid carcinomas', *Human Pathology*, 35(11), pp. 1360-1368. doi: 10.1016/j.humpath.2004.07.019.
- Chambers, S. K. *et al.* (1997) 'Overexpression of epithelial macrophage colony-stimulating factor (CSF-1) and CSF-1 receptor: a poor prognostic factor in epithelial ovarian cancer, contrasted with a protective effect of stromal CSF-1.', *Clinical cancer research : an official journal of the American Association for Cancer Research*, 3(6), pp. 999-1007. Available at: <http://www.ncbi.nlm.nih.gov/pubmed/9815777> (Accessed: 3 January 2018).
- Chan, F. K.-M., Luz, N. F. and Moriwaki, K. (2015) *Programmed Necrosis in the Cross Talk of Cell Death and Inflammation*, *Annual Review of Immunology*. doi: 10.1146/annurev-immunol-032414-112248.
- Chang, S. H. and Dong, C. (2009) 'IL-17F: regulation, signaling and function in inflammation.', *Cytokine*. NIH Public Access, 46(1), pp. 7-11. doi: 10.1016/j.cyto.2008.12.024.
- Chao, M. P. *et al.* (2010) 'Calreticulin is the dominant pro-phagocytic signal on multiple human cancers and is counterbalanced by CD47.', *Science translational medicine*, 2(63), p. 63ra94. doi: 10.1126/scitranslmed.3001375.
- Chen, D., Yu, J. and Zhang, L. (2016) 'Necroptosis: An alternative cell death program defending against cancer', *Biochimica et Biophysica Acta (BBA) - Reviews on Cancer*. Elsevier B.V. doi: 10.1016/j.bbcan.2016.03.003.
- Chen, G.-X. *et al.* (2014) 'Clinical utility of recombinant adenoviral human p53 gene therapy: current perspectives', *OncoTargets and Therapy*, 7, p. 1901. doi: 10.2147/OTT.S50483.
- Chen, W. *et al.* (2013) 'Diverse Sequence Determinants Control Human and Mouse Receptor Interacting Protein 3 (RIP3) and Mixed Lineage Kinase domain-Like (MLKL) Interaction in Necroptotic Signaling', *Journal of Biological Chemistry*, 288(23), pp. 16247-16261. doi: 10.1074/jbc.M112.435545.
- Chen, X. *et al.* (2014) 'Translocation of mixed lineage kinase domain-like protein to plasma membrane leads to necrotic cell death', *Cell Research*. Nature Publishing Group, 24(1), pp. 105-121. doi: 10.1038/cr.2013.171.
- Chen, X. *et al.* (2016) 'Pyroptosis is driven by non-selective gasdermin-D pore and its morphology is different from MLKL channel-mediated necroptosis.', *Cell research*. Nature Publishing Group, 26(9), pp. 1007-20. doi: 10.1038/cr.2016.100.
- Cho, Y. S. *et al.* (2009) 'Phosphorylation-driven assembly of the RIP1-RIP3 complex regulates programmed necrosis and virus-induced inflammation.', *Cell*, 137(6), pp. 1112-23. doi: 10.1016/j.cell.2009.05.037.
- Choudhary, S. *et al.* (2011) 'Herpes Simplex Virus Type-1 (HSV-1) Entry into Human Mesenchymal Stem Cells Is Heavily Dependent on Heparan Sulfate', *Journal of Biomedicine and Biotechnology*, 2011, pp. 1-11. doi: 10.1155/2011/264350.
- Chumakov, P. M. *et al.* (2012) '[Oncolytic enteroviruses]', *Mol Biol (Mosk)*, 46(5), pp. 712-725. doi: 10.1134/S0026893312050032.

Clarke, P. G. (1990) 'Developmental cell death: morphological diversity and multiple mechanisms.', *Anatomy and embryology*, 181(3), pp. 195-213. Available at: <http://www.ncbi.nlm.nih.gov/pubmed/2186664> (Accessed: 8 January 2018).

Clarke, R. W. (2015) 'Forces and Structures of the Herpes Simplex Virus (HSV) Entry Mechanism', *ACS Infectious Diseases*. American Chemical Society, 1(9), pp. 403-415. doi: 10.1021/acsinfecdis.5b00059.

Clement, C. *et al.* (2006) 'A novel role for phagocytosis-like uptake in herpes simplex virus entry.', *The Journal of cell biology*. The Rockefeller University Press, 174(7), pp. 1009-21. doi: 10.1083/jcb.200509155.

De Clercq, E. (2004) 'Antiviral drugs in current clinical use.', *Journal of clinical virology: the official publication of the Pan American Society for Clinical Virology*, 30(2), pp. 115-33. doi: 10.1016/j.jcv.2004.02.009.

Coleman, R. L. *et al.* (2015) 'A phase III randomized controlled clinical trial of carboplatin and paclitaxel alone or in combination with bevacizumab followed by bevacizumab and secondary cytoreductive surgery in platinum-sensitive, recurrent ovarian, peritoneal primary and fallopian tube cancer (Gynecologic Oncology Group 0213)', *Gynecologic Oncology*. Elsevier, 137, pp. 3-4. doi: 10.1016/j.ygyno.2015.01.005.

Coleman, R. L. *et al.* (2017) 'Rucaparib maintenance treatment for recurrent ovarian carcinoma after response to platinum therapy (ARIEL3): a randomised, double-blind, placebo-controlled, phase 3 trial.', *Lancet (London, England)*, 390(10106), pp. 1949-1961. doi: 10.1016/S0140-6736(17)32440-6.

Colunga, A. G., Laing, J. M. and Aurelian, L. (2010) 'The HSV-2 mutant DeltaPK induces melanoma oncolysis through nonredundant death programs and associated with autophagy and pyroptosis proteins.', *Gene therapy*. NIH Public Access, 17(3), pp. 315-27. doi: 10.1038/gt.2009.126.

Conner, J. *et al.* (1993) 'Herpes simplex virus type 1 ribonucleotide reductase large subunit: regions of the protein essential for subunit interaction and dimerization.', *Biochemistry*, 32(49), pp. 13673-80. Available at: <http://www.ncbi.nlm.nih.gov/pubmed/8257701> (Accessed: 7 February 2018).

Contreras, R. G. *et al.* (1999) 'Relationship between Na(+),K(+)-ATPase and cell attachment.', *Journal of cell science*, 112 ( Pt 23), pp. 4223-32. Available at: <http://www.ncbi.nlm.nih.gov/pubmed/10564641> (Accessed: 25 January 2018).

Copeland, A. M., Newcomb, W. W. and Brown, J. C. (2009) 'Herpes Simplex Virus Replication: Roles of Viral Proteins and Nucleoporins in Capsid-Nucleus Attachment', *Journal of Virology*, 83(4), pp. 1660-1668. doi: 10.1128/JVI.01139-08.

Coukos, G. *et al.* (1999) 'Use of carrier cells to deliver a replication-selective herpes simplex virus-1 mutant for the intraperitoneal therapy of epithelial ovarian cancer.', *Clinical cancer research: an official journal of the American Association for Cancer Research*, 5(6), pp. 1523-37. Available at: <http://www.ncbi.nlm.nih.gov/pubmed/10389942> (Accessed: 3 January 2015).

Coukos, G. *et al.* (2000) 'Oncolytic Herpes Simplex Virus-1 Lacking ICP34 . 5 Induces p53-independent Death and Is Efficacious against Chemotherapy-resistant Ovarian Cancer Oncolytic Herpes Simplex Virus-1 Lacking ICP34 . 5 Induces p53- independent Death and Is Efficacious against ', pp. 3342-3353.

- Cuatrecasas, M. *et al.* (1997) 'K-ras mutations in mucinous ovarian tumors: a clinicopathologic and molecular study of 95 cases.', *Cancer*, 79(8), pp. 1581-6. Available at: <http://www.ncbi.nlm.nih.gov/pubmed/9118042> (Accessed: 12 December 2017).
- Curiel, T. J. *et al.* (2004) 'Specific recruitment of regulatory T cells in ovarian carcinoma fosters immune privilege and predicts reduced survival', *Nature Medicine*, 10(9), pp. 942-949. doi: 10.1038/nm1093.
- Davison, A. J. *et al.* (2009) 'The order Herpesvirales.', *Archives of virology*. NIH Public Access, 154(1), pp. 171-7. doi: 10.1007/s00705-008-0278-4.
- Debbas, M. and White, E. (1993) 'Wild-type p53 mediates apoptosis by E1A, which is inhibited by E1B', *Genes & Development*, 7, pp. 546-554.
- Degterev, A. *et al.* (2005) 'Chemical inhibitor of nonapoptotic cell death with therapeutic potential for ischemic brain injury', *Nature Chemical Biology*, 1(2), pp. 112-119. doi: 10.1038/nchembio711.
- Degterev, A. *et al.* (2014) *Assays for necroptosis and activity of RIP kinases*. 1st edn, *Methods in enzymology*. 1st edn. Elsevier Inc. doi: 10.1016/B978-0-12-801430-1.00001-9.
- Delaleu, N. and Bickel, M. (2004) 'Interleukin-1beta and interleukin-18: regulation and activity in local inflammation', *Periodontology 2000*, 35(1), pp. 42-52. doi: 10.1111/j.0906-6713.2004.003569.x.
- Delwar, Z. M. *et al.* (2016) 'Tumour-specific triple-regulated oncolytic herpes virus to target glioma', 7(19).
- Derubertis, B. G. *et al.* (2007) 'Cytokine-secreting herpes viral mutants effectively treat tumor in a murine metastatic colorectal liver model by oncolytic and T-cell-dependent mechanisms.', *Cancer gene therapy*, 14(6), pp. 590-7. doi: 10.1038/sj.cgt.7701053.
- Deshmane, S. L. and Fraser, N. W. (1989) 'During latency, herpes simplex virus type 1 DNA is associated with nucleosomes in a chromatin structure.', *Journal of virology*, 63(2), pp. 943-7. Available at: <http://www.ncbi.nlm.nih.gov/pubmed/2536115> (Accessed: 5 December 2017).
- Deveraux, Q. L. *et al.* (1998) 'IAPs block apoptotic events induced by caspase-8 and cytochrome c by direct inhibition of distinct caspases', *The EMBO Journal*, 17(8), pp. 2215-2223. doi: 10.1093/emboj/17.8.2215.
- Diaconu, I. *et al.* (2012) 'Immune response is an important aspect of the antitumor effect produced by a CD40L-encoding oncolytic adenovirus', *Cancer Research*, 72(9), pp. 2327-2338. doi: 10.1158/0008-5472.CAN-11-2975.
- Dilokthornsakul, P. *et al.* (2013) 'The Effects of Metformin on Ovarian Cancer', *International Journal of Gynecological Cancer*, 23(9), pp. 1544-1551. doi: 10.1097/IGC.0b013e3182a80a21.
- Dinkic, C. *et al.* (2017) 'Pazopanib (GW786034) and cyclophosphamide in patients with platinum-resistant, recurrent, pre-treated ovarian cancer - Results of the PACOVAR-trial.', *Gynecologic oncology*. Elsevier, 146(2), pp. 279-284. doi: 10.1016/j.ygyno.2017.05.013.
- Dinulescu, D. M. *et al.* (2005) 'Role of K-ras and Pten in the development of mouse models of endometriosis and endometrioid ovarian cancer', *Nature*

*Medicine*, 11(1), pp. 63-70. doi: 10.1038/nm1173.

Dixon, S. J. *et al.* (2012) 'Ferroptosis: an iron-dependent form of nonapoptotic cell death.', *Cell*. NIH Public Access, 149(5), pp. 1060-72. doi: 10.1016/j.cell.2012.03.042.

Domcke, S. *et al.* (2013) 'Evaluating cell lines as tumour models by comparison of genomic profiles.', *Nature communications*. Nature Publishing Group, 4, p. 2126. doi: 10.1038/ncomms3126.

Dosch, M. *et al.* (2018) 'Mechanisms of ATP Release by Inflammatory Cells', *International Journal of Molecular Sciences*, 19(4), p. 1222. doi: 10.3390/ijms19041222.

Dufour, F. *et al.* (2011) 'The ribonucleotide reductase R1 subunits of herpes simplex virus types 1 and 2 protect cells against TNF $\alpha$ - and FasL-induced apoptosis by interacting with caspase-8', *Apoptosis*, 16(3), pp. 256-271. doi: 10.1007/s10495-010-0560-2.

Duluc, D. *et al.* (2007) 'Tumor-associated leukemia inhibitory factor and IL-6 skew monocyte differentiation into tumor-associated macrophage-like cells', *Blood*, 110(13), pp. 4319-4330. doi: 10.1182/blood-2007-02-072587.

Duncan, M. R., Stanish, S. M. and Cox, D. C. (1978) 'Differential sensitivity of normal and transformed human cells to reovirus infection.', *Journal of virology*, 28(2), pp. 444-9. Available at: <http://www.pubmedcentral.nih.gov/articlerender.fcgi?artid=354293&tool=pmcentrez&rendertype=abstract>.

Dutch, R. E., Bianchi, V. and Lehman, I. R. (1995) 'Herpes simplex virus type 1 DNA replication is specifically required for high-frequency homologous recombination between repeated sequences.', *Journal of virology*. American Society for Microbiology, 69(5), pp. 3084-9. Available at: <http://www.ncbi.nlm.nih.gov/pubmed/7707536> (Accessed: 4 December 2017).

Elgendy, M. *et al.* (2011) 'Oncogenic Ras-Induced Expression of Noxa and Beclin-1 Promotes Autophagic Cell Death and Limits Clonogenic Survival', *Molecular Cell*, 42(1), pp. 23-35. doi: 10.1016/j.molcel.2011.02.009.

Elion, G. *et al.* (1977) 'Selectivity of action of an antiherpetic agent, 9-(2-hydroxyethoxymethyl) guanine', *National Acad Sciences*, 74(12), pp. 5716-5720. Available at: <http://www.pnas.org/content/74/12/5716.short> (Accessed: 18 December 2017).

Elliott, M. R. *et al.* (2009) 'Nucleotides released by apoptotic cells act as a find-me signal to promote phagocytic clearance.', *Nature*, 461(7261), pp. 282-6. doi: 10.1038/nature08296.

Elmore, S. (2007) 'Apoptosis: A Review of Programmed Cell Death', *Toxicologic Pathology*, 35(4), pp. 495-516. doi: 10.1080/01926230701320337.

Fadok, V. A. *et al.* (1992) 'Exposure of phosphatidylserine on the surface of apoptotic lymphocytes triggers specific recognition and removal by macrophages.', *Journal of immunology (Baltimore, Md. : 1950)*, 148(7), pp. 2207-16. Available at: <http://www.ncbi.nlm.nih.gov/pubmed/1545126> (Accessed: 10 January 2018).

Fadok, V. A. *et al.* (2001) 'Loss of phospholipid asymmetry and surface exposure of phosphatidylserine is required for phagocytosis of apoptotic cells by

- macrophages and fibroblasts.’, *The Journal of biological chemistry*. American Society for Biochemistry and Molecular Biology, 276(2), pp. 1071-7. doi: 10.1074/jbc.M003649200.
- Fajardo, C. A. *et al.* (2017) ‘Oncolytic Adenoviral Delivery of an EGFR-Targeting T-cell Engager Improves Antitumor Efficacy’, *Cancer Research*, 77(8), pp. 2052-2063. doi: 10.1158/0008-5472.CAN-16-1708.
- Fatokun, A. A., Dawson, V. L. and Dawson, T. M. (2014) ‘Parthanatos: mitochondrial-linked mechanisms and therapeutic opportunities’, *British Journal of Pharmacology*, 171(8), pp. 2000-2016. doi: 10.1111/bph.12416.
- Feldmeyer, L. *et al.* (2007) ‘The Inflammasome Mediates UVB-Induced Activation and Secretion of Interleukin-1 $\beta$  by Keratinocytes’, *Current Biology*, 17(13), pp. 1140-1145. doi: 10.1016/j.cub.2007.05.074.
- Fink, S. L. and Cookson, B. T. (2006) ‘Caspase-1-dependent pore formation during pyroptosis leads to osmotic lysis of infected host macrophages’, *Cellular Microbiology*, 8(11), pp. 1812-1825. doi: 10.1111/j.1462-5822.2006.00751.x.
- Florey, O. *et al.* (2011) ‘Autophagy machinery mediates macroendocytic processing and entotic cell death by targeting single membranes’, *Nature Cell Biology*, 13(11), pp. 1335-1343. doi: 10.1038/ncb2363.
- Florey, O., Kim, S. E. and Overholtzer, M. (2015) ‘Entosis: Cell-in-Cell Formation that Kills Through Entotic Cell Death.’, *Current molecular medicine*, 15(9), pp. 861-6. Available at: <http://www.ncbi.nlm.nih.gov/pubmed/26511711> (Accessed: 26 January 2018).
- Folkins, A. K. *et al.* (2008) ‘A candidate precursor to pelvic serous cancer (p53 signature) and its prevalence in ovaries and fallopian tubes from women with BRCA mutations’, *Gynecologic Oncology*, 109(2), pp. 168-173. doi: 10.1016/j.ygyno.2008.01.012.
- Forssmann, U. *et al.* (1997) ‘Eotaxin-2, a novel CC chemokine that is selective for the chemokine receptor CCR3, and acts like eotaxin on human eosinophil and basophil leukocytes.’, *The Journal of experimental medicine*. Rockefeller University Press, 185(12), pp. 2171-6. doi: 10.1084/JEM.185.12.2171.
- Frantz, S. *et al.* (2003) ‘Targeted deletion of caspase-1 reduces early mortality and left ventricular dilatation following myocardial infarction.’, *Journal of molecular and cellular cardiology*, 35(6), pp. 685-94. Available at: <http://www.ncbi.nlm.nih.gov/pubmed/12788386> (Accessed: 11 January 2018).
- Fu, X., Wang, H. and Zhang, X. (2002) ‘High-frequency intermolecular homologous recombination during herpes simplex virus-mediated plasmid DNA replication.’, *Journal of virology*. American Society for Microbiology, 76(12), pp. 5866-74. doi: 10.1128/JVI.76.12.5866-5874.2002.
- Fujiwara, S. *et al.* (2011) ‘Carrier cell-based delivery of replication-competent HSV-1 mutants enhances antitumor effect for ovarian cancer’, *Cancer Gene Therapy*, 18(2), pp. 77-86. doi: 10.1038/cgt.2010.53.
- Fukuhara, H. *et al.* (2005) ‘Triple gene-deleted oncolytic herpes simplex virus vector double-armed with interleukin 18 and soluble B7-1 constructed by bacterial artificial chromosome-mediated system.’, *Cancer research*, 65(23), pp. 10663-8. doi: 10.1158/0008-5472.CAN-05-2534.
- Fuster, M. M. and Esko, J. D. (2005) ‘The sweet and sour of cancer: glycans as

novel therapeutic targets', *Nature Reviews Cancer*, 5(7), pp. 526-542. doi: 10.1038/nrc1649.

Gaillard, S. L., Secord, A. A. and Monk, B. (2016) 'The role of immune checkpoint inhibition in the treatment of ovarian cancer', *Gynecologic Oncology Research and Practice*. BioMed Central, 3(1), p. 11. doi: 10.1186/s40661-016-0033-6.

Galluzzi, L. *et al.* (2012) 'Molecular definitions of cell death subroutines: recommendations of the Nomenclature Committee on Cell Death 2012', *Cell Death and Differentiation*, 19(1), pp. 107-120. doi: 10.1038/cdd.2011.96.

Galluzzi, L. *et al.* (2014) 'Molecular mechanisms of regulated necrosis.', *Seminars in cell & developmental biology*. Elsevier Ltd, pp. 1-9. doi: 10.1016/j.semcd.2014.02.006.

Galluzzi, L. *et al.* (2015) 'Essential versus accessory aspects of cell death: recommendations of the NCCD 2015', *Cell Death & Differentiation*, 22(1), pp. 58-73. doi: 10.1038/cdd.2014.137.

Galva, C., Artigas, P. and Gatto, C. (2012) 'Nuclear Na<sup>+</sup>/K<sup>+</sup>-ATPase plays an active role in nucleoplasmic Ca<sup>2+</sup> homeostasis', *Journal of Cell Science*, 125(24), pp. 6137-6147. doi: 10.1242/jcs.114959.

Gamallo, C. *et al.* (1999) 'beta-catenin expression pattern in stage I and II ovarian carcinomas : relationship with beta-catenin gene mutations, clinicopathological features, and clinical outcome.', *The American journal of pathology*, 155(2), pp. 527-36. Available at: <http://www.ncbi.nlm.nih.gov/pubmed/10433945> (Accessed: 13 December 2017).

Garber, K. (2006) 'China Approves World 's First Oncolytic Virus Therapy for Cancer Treatment', *J Natl Cancer Inst*, 98(5), pp. 298-300. doi: 98/5/298 [pii]10.1093/jnci/djj111 [doi].

Gardella, S. *et al.* (2002) 'The nuclear protein HMGB1 is secreted by monocytes via a non-classical, vesicle-mediated secretory pathway', *EMBO reports*, 3(10), pp. 995-1001. doi: 10.1093/embo-reports/kvf198.

Geevarghese, S. K. *et al.* (2010) 'Phase I/II study of oncolytic herpes simplex virus NV1020 in patients with extensively pretreated refractory colorectal cancer metastatic to the liver.', *Human gene therapy*, 21(9), pp. 1119-28. doi: 10.1089/hum.2010.020.

Gentle, I. E. *et al.* (2011) 'In TNF-stimulated Cells, RIPK1 Promotes Cell Survival by Stabilizing TRAF2 and cIAP1, which Limits Induction of Non-canonical NF- $\kappa$ B and Activation of Caspase-8', *Journal of Biological Chemistry*, 286(15), pp. 13282-13291. doi: 10.1074/jbc.M110.216226.

Gershenson, D. M. *et al.* (2006) 'Clinical Behavior of Stage II-IV Low-Grade Serous Carcinoma of the Ovary', *Obstetrics & Gynecology*, 108(2), pp. 361-368. doi: 10.1097/01.AOG.0000227787.24587.d1.

Gey, G. O., Coffman, W. D. and Kubicek, M. T. (1952) 'Tissue culture studies of the proliferative capacity of cervical carcinoma and normal epithelium', *Cancer Res.*, 12, pp. 264-265. Available at: <https://ci.nii.ac.jp/naid/10006432514/> (Accessed: 30 March 2018).

Gobeil, P. A. M. and Leib, D. A. (2012) 'Herpes simplex virus  $\gamma$ 34.5 interferes

- with autophagosome maturation and antigen presentation in dendritic cells.’, *mBio*, 3(5), pp. e00267-12. doi: 10.1128/mBio.00267-12.
- Gong, J. *et al.* (2016) ‘Clinical development of reovirus for cancer therapy: An oncolytic virus with immune-mediated antitumor activity.’, *World journal of methodology*, 6(1), pp. 25-42. doi: 10.5662/wjm.v6.i1.25.
- Gong, J. H., Maki, G. and Klingemann, H. G. (1994) ‘Characterization of a human cell line (NK-92) with phenotypical and functional characteristics of activated natural killer cells.’, *Leukemia*, 8(4), pp. 652-8. Available at: <http://www.ncbi.nlm.nih.gov/pubmed/8152260> (Accessed: 25 April 2018).
- Gong, W. *et al.* (1998) ‘Monocyte chemotactic protein-2 activates CCR5 and blocks CD4/CCR5-mediated HIV-1 entry/replication.’, *The Journal of biological chemistry*, 273(8), pp. 4289-92. Available at: <http://www.ncbi.nlm.nih.gov/pubmed/9468473> (Accessed: 30 April 2018).
- Goodell, V. *et al.* (2006) ‘Antibody Immunity to the p53 Oncogenic Protein Is a Prognostic Indicator in Ovarian Cancer’, *Journal of Clinical Oncology*, 24(5), pp. 762-768. doi: 10.1200/JCO.2005.03.2813.
- Granstein, R. D. *et al.* (2005) ‘Augmentation of cutaneous immune responses by ATP gamma S: purinergic agonists define a novel class of immunologic adjuvants.’, *Journal of immunology (Baltimore, Md. : 1950)*, 174(12), pp. 7725-31. Available at: <http://www.ncbi.nlm.nih.gov/pubmed/15944274> (Accessed: 18 January 2018).
- Green, D. and Ferguson, T. (2009) ‘Immunogenic and tolerogenic cell death’, *Nature Reviews ...*, 9(5), pp. 1-25. doi: 10.1038/nri2545.IMMUNOGENIC.
- Greiner, S. *et al.* (2006) ‘The highly attenuated vaccinia virus strain modified virus Ankara induces apoptosis in melanoma cells and allows bystander dendritic cells to generate a potent anti-tumoral immunity’, *Clinical and Experimental Immunology*, 146(2), pp. 344-353. doi: 10.1111/j.1365-2249.2006.03177.x.
- Grote, D., Cattaneo, R. and Fielding, A. K. (2003) ‘Neutrophils contribute to the measles virus-induced antitumor effect: enhancement by granulocyte macrophage colony-stimulating factor expression.’, *Cancer research*, 63(19), pp. 6463-8. Available at: <http://www.ncbi.nlm.nih.gov/pubmed/14559838> (Accessed: 14 February 2018).
- de Gruijl, T. D., Janssen, A. B. and van Beusechem, V. W. (2015) ‘Arming oncolytic viruses to leverage antitumor immunity’, *Expert Opinion on Biological Therapy*, pp. 1-13. doi: 10.1517/14712598.2015.1044433.
- Guillerme, J.-B. *et al.* (2013) ‘Measles Virus Vaccine-Infected Tumor Cells Induce Tumor Antigen Cross-Presentation by Human Plasmacytoid Dendritic Cells’, *Clinical Cancer Research*, 19(5), pp. 1147-1158. doi: 10.1158/1078-0432.CCR-12-2733.
- Gujar, S. A. *et al.* (2010) ‘Reovirus Virotherapy Overrides Tumor Antigen Presentation Evasion and Promotes Protective Antitumor Immunity’, *Molecular Cancer Therapeutics*, 9(11), pp. 2924-2933. doi: 10.1158/1535-7163.MCT-10-0590.
- Guo, F. *et al.* (2005) ‘Mechanistic role of heat shock protein 70 in Bcr-Abl-mediated resistance to apoptosis in human acute leukemia cells.’, *Blood*, 105(3), pp. 1246-55. doi: 10.1182/blood-2004-05-2041.

- Guo, H. *et al.* (2015) 'Herpes simplex virus suppresses necroptosis in human cells', *Cell Host and Microbe*. Elsevier Inc., 17(2), pp. 243-251. doi: 10.1016/j.chom.2015.01.003.
- Guo, Z. S. *et al.* (2005) 'The enhanced tumor selectivity of an oncolytic vaccinia lacking the host range and antiapoptosis genes SPI-1 and SPI-2', *Cancer Research*, 65(21), pp. 9991-9998. doi: 10.1158/0008-5472.CAN-05-1630.
- Hackenbrock, C. R. (1966) 'Ultrastructural bases for metabolically linked mechanical activity in mitochondria. I. Reversible ultrastructural changes with change in metabolic steady state in isolated liver mitochondria.', *The Journal of cell biology*, 30(2), pp. 269-97. Available at: <http://www.ncbi.nlm.nih.gov/pubmed/5968972> (Accessed: 7 March 2018).
- Hackenbrock, C. R. (1968) 'Ultrastructural bases for metabolically linked mechanical activity in mitochondria. II. Electron transport-linked ultrastructural transformations in mitochondria.', *The Journal of cell biology*, 37(2), pp. 345-69. Available at: <http://www.ncbi.nlm.nih.gov/pubmed/5656397> (Accessed: 7 March 2018).
- Hafezi, W. *et al.* (2012) 'Entry of Herpes Simplex Virus Type 1 (HSV-1) into the Distal Axons of Trigeminal Neurons Favors the Onset of Nonproductive, Silent Infection', *PLoS Pathogens*. Edited by K. L. Mossman, 8(5), p. e1002679. doi: 10.1371/journal.ppat.1002679.
- Hamanishi, J. *et al.* (2007) 'Programmed cell death 1 ligand 1 and tumor-infiltrating CD8+ T lymphocytes are prognostic factors of human ovarian cancer', *Proceedings of the National Academy of Sciences*, 104(9), pp. 3360-3365. doi: 10.1073/pnas.0611533104.
- Hamanishi, J. *et al.* (2015) 'Safety and Antitumor Activity of Anti-PD-1 Antibody, Nivolumab, in Patients With Platinum-Resistant Ovarian Cancer', *Journal of Clinical Oncology*, 33(34), pp. 4015-4022. doi: 10.1200/JCO.2015.62.3397.
- Han, Z. Q. *et al.* (2007) 'Development of a second-generation oncolytic Herpes simplex virus expressing TNF $\alpha$  for cancer therapy', *The Journal of Gene Medicine*, 9(2), pp. 99-106. doi: 10.1002/jgm.999.
- Hanahan, D. and Weinberg, R. A. (2000) 'The hallmarks of cancer.', *Cell*, 100(1), pp. 57-70. Available at: <http://www.ncbi.nlm.nih.gov/pubmed/10647931> (Accessed: 2 February 2018).
- Hanahan, D. and Weinberg, R. A. (2011) 'Hallmarks of Cancer: The Next Generation', *Cell*, 144(5), pp. 646-674. doi: 10.1016/j.cell.2011.02.013.
- Harada, J. N. and Berk, A. J. (1999) 'p53-Independent and -dependent requirements for E1B-55K in adenovirus type 5 replication', *J Virol*, 73(7), pp. 5333-5344. Available at: <http://www.ncbi.nlm.nih.gov/pubmed/10364280> <http://jvi.asm.org/content/73/7/5333.full.pdf>.
- Hardy, W. R. and Sandri-Goldin, R. M. (1994) 'Herpes simplex virus inhibits host cell splicing, and regulatory protein ICP27 is required for this effect.', *Journal of virology*, 68(12), pp. 7790-9. Available at: <http://www.ncbi.nlm.nih.gov/pubmed/7966568> (Accessed: 1 December 2017).
- Harrap, K. R. (1985) 'Preclinical studies identifying carboplatin as a viable cisplatin alternative.', *Cancer treatment reviews*, 12 Suppl A, pp. 21-33.

Available at: <http://www.ncbi.nlm.nih.gov/pubmed/3910219> (Accessed: 15 December 2017).

Harrow, S. *et al.* (2004) 'HSV1716 injection into the brain adjacent to tumour following surgical resection of high-grade glioma: safety data and long-term survival', *Gene Therapy*, 11(22), pp. 1648-1658. doi: 10.1038/sj.gt.3302289.

Hart, K. M. *et al.* (2011) 'IL-10 Immunomodulation of Myeloid Cells Regulates a Murine Model of Ovarian Cancer', *Frontiers in Immunology*, 2, p. 29. doi: 10.3389/fimmu.2011.00029.

Hartkopf, A. D. *et al.* (2011) 'Oncolytic virotherapy of gynecologic malignancies', *Gynecologic Oncology*, 120(2), pp. 302-310. doi: 10.1016/j.ygyno.2010.10.031.

Hashiro, G., Loh, P. C. and Yau, J. T. (1977) 'The preferential cytotoxicity of reovirus for certain transformed cell lines.', *Archives of virology*, 54(4), pp. 307-15. Available at: <http://www.ncbi.nlm.nih.gov/pubmed/562142> (Accessed: 21 September 2016).

Hayward, G. S. *et al.* (1975) 'Anatomy of herpes simplex virus DNA: evidence for four populations of molecules that differ in the relative orientations of their long and short components.', *Proceedings of the National Academy of Sciences of the United States of America*, 72(11), pp. 4243-7. Available at: <http://www.ncbi.nlm.nih.gov/pubmed/172900> (Accessed: 30 November 2017).

He, B., Gross, M. and Roizman, B. (1997) 'The gamma(1)34.5 protein of herpes simplex virus 1 complexes with protein phosphatase 1alpha to dephosphorylate the alpha subunit of the eukaryotic translation initiation factor 2 and preclude the shutoff of protein synthesis by double-stranded RNA-activated protein kinase.', *Proceedings of the National Academy of Sciences of the United States of America*, 94(3), pp. 843-8. Available at: <http://www.ncbi.nlm.nih.gov/pubmed/9023344> (Accessed: 3 January 2018).

Heath, W. R. and Carbone, F. R. (2001) 'Cross-presentation, dendritic cells, tolerance and immunity.', *Annual Review of Immunology*, 19(1), pp. 47-64. doi: 10.1146/annurev.immunol.19.1.47.

Heinrich, B. *et al.* (2017) 'Immunogenicity of oncolytic vaccinia viruses JX-GFP and TG6002 in a human melanoma in vitro model: studying immunogenic cell death, dendritic cell maturation and interaction with cytotoxic T lymphocytes.', *OncoTargets and therapy*. Dove Press, 10, pp. 2389-2401. doi: 10.2147/OTT.S126320.

Hildebrand, J. M. *et al.* (2014) 'Activation of the pseudokinase MLKL unleashes the four-helix bundle domain to induce membrane localization and necroptotic cell death', 111(42). doi: 10.1073/pnas.1408987111.

Hill, M. M. *et al.* (2004) 'Analysis of the composition, assembly kinetics and activity of native Apaf-1 apoptosomes', *The EMBO Journal*, 23(10), pp. 2134-2145. doi: 10.1038/sj.emboj.7600210.

Hirvonen, M. *et al.* (2015) 'Immunological Effects of a Tumor Necrosis Factor Alpha-Armed Oncolytic Adenovirus', *Human Gene Therapy*, 26(3), pp. 134-144. doi: 10.1089/hum.2014.069.

Honess, R. W. and Roizman, B. (1975) 'Regulation of herpesvirus macromolecular synthesis: sequential transition of polypeptide synthesis requires functional viral

- polypeptides.’, *Proceedings of the National Academy of Sciences of the United States of America*, 72(4), pp. 1276-80. Available at: <http://www.ncbi.nlm.nih.gov/pubmed/165503> (Accessed: 30 November 2017).
- Hu, J. C. C. *et al.* (2006) ‘A phase I study of OncoVEXGM-CSF, a second-generation oncolytic herpes simplex virus expressing granulocyte macrophage colony-stimulating factor’, *Clinical Cancer Research*, 12(22), pp. 6737-6747. doi: 10.1158/1078-0432.CCR-06-0759.
- Huang, Z., Wu, S., *et al.* (2015) ‘Necroptosis to Restrict Virus Propagation in Mice Article Initiates Necroptosis to Restrict Virus Propagation in Mice’, *Cell Host and Microbe*. Elsevier Inc., 17(2), pp. 229-242. doi: 10.1016/j.chom.2015.01.002.
- Huang, Z., Wu, S.-Q., *et al.* (2015) ‘RIP1/RIP3 Binding to HSV-1 ICP6 Initiates Necroptosis to Restrict Virus Propagation in Mice.’, *Cell host & microbe*. Elsevier Inc., 17(2), pp. 229-42. doi: 10.1016/j.chom.2015.01.002.
- Ichim, G. and Tait, S. W. (2015) ‘Necroptosis: Fifty shades of RIPKs.’, *Molecular & cellular oncology*. Taylor & Francis, 2(2), p. e965638. doi: 10.4161/23723548.2014.965638.
- Idzko, M. *et al.* (2007) ‘Extracellular ATP triggers and maintains asthmatic airway inflammation by activating dendritic cells.’, *Nature medicine*, 13(8), pp. 913-9. doi: 10.1038/nm1617.
- Imai, T. *et al.* (1997) ‘The T cell-directed CC chemokine TARC is a highly specific biological ligand for CC chemokine receptor 4.’, *The Journal of biological chemistry*, 272(23), pp. 15036-42. Available at: <http://www.ncbi.nlm.nih.gov/pubmed/9169480> (Accessed: 30 April 2018).
- Irving, J. A. *et al.* (2005) ‘Synchronous endometrioid carcinomas of the uterine corpus and ovary: alterations in the  $\beta$ -catenin (CTNNB1) pathway are associated with independent primary tumors and favorable prognosis’, *Human Pathology*, 36(6), pp. 605-619. doi: 10.1016/j.humpath.2005.03.005.
- Itamochi, H. *et al.* (2002) ‘Low proliferation activity may be associated with chemoresistance in clear cell carcinoma of the ovary.’, *Obstetrics and gynecology*, 100(2), pp. 281-7. Available at: <http://www.ncbi.nlm.nih.gov/pubmed/12151151> (Accessed: 13 December 2017).
- Iwahori, K. *et al.* (2015) ‘Engager T Cells: A New Class of Antigen-specific T Cells That Redirect Bystander T Cells’, *Molecular Therapy*, 23(1), pp. 171-178. doi: 10.1038/mt.2014.156.
- Jacobs, I. *et al.* (1990) ‘A risk of malignancy index incorporating CA 125, ultrasound and menopausal status for the accurate preoperative diagnosis of ovarian cancer.’, *British journal of obstetrics and gynaecology*, 97(10), pp. 922-9. Available at: <http://www.ncbi.nlm.nih.gov/pubmed/2223684> (Accessed: 5 February 2018).
- Jayson, G. C. *et al.* (2014) ‘Ovarian cancer.’, *Lancet*. Elsevier Ltd, 384(9951), pp. 1376-1388. doi: 10.1016/S0140-6736(13)62146-7.
- Jeeninga, R. E. *et al.* (2005) ‘Construction of a minimal HIV-1 variant that selectively replicates in leukemic derived T-cell lines: Towards a new virotherapy approach’, *Cancer Research*, 65(8), pp. 3347-3355. doi:

10.1158/0008-5472.CAN-04-4280.

Jeeninga, R. E. *et al.* (2006) 'Construction of doxycycline-dependent mini-HIV-1 variants for the development of a virotherapy against leukemias.', *Retrovirology*, 3, p. 64. doi: 10.1186/1742-4690-3-64.

Jenkins, H. L. and Spencer, C. A. (2001) 'RNA polymerase II holoenzyme modifications accompany transcription reprogramming in herpes simplex virus type 1-infected cells.', *Journal of virology*, 75(20), pp. 9872-84. doi: 10.1128/JVI.75.20.9872-9884.2001.

Jensen, E. C. (2012) 'Use of Fluorescent Probes: Their Effect on Cell Biology and Limitations', *The Anatomical Record: Advances in Integrative Anatomy and Evolutionary Biology*. Wiley Subscription Services, Inc., A Wiley Company, 295(12), pp. 2031-2036. doi: 10.1002/ar.22602.

Jin, L. *et al.* (2016) 'The double life of RIPK1', *Molecular & Cellular Oncology*, 3(1), p. e1035690. doi: 10.1080/23723556.2015.1035690.

Jones, S. *et al.* (2012) 'Low-grade serous carcinomas of the ovary contain very few point mutations', *The Journal of Pathology*, 226(3), pp. 413-420. doi: 10.1002/path.3967.

Jurak, I. *et al.* (2010) 'Numerous Conserved and Divergent MicroRNAs Expressed by Herpes Simplex Viruses 1 and 2', *Journal of Virology*, 84(9), pp. 4659-4672. doi: 10.1128/JVI.02725-09.

Kaiser, W. J., Upton, J. W. and Mocarski, E. S. (2013) 'Viral modulation of programmed necrosis', *Current Opinion in Virology*, 3(3), pp. 296-306. doi: 10.1016/j.coviro.2013.05.019.

Kang, S. *et al.* (2015) 'Caspase-8 scaffolding function and MLKL regulate NLRP3 inflammasome activation downstream of TLR3', *Nature Communications*, 6(1), p. 7515. doi: 10.1038/ncomms8515.

Karasneh, G. A. and Shukla, D. (2011) 'Herpes simplex virus infects most cell types in vitro: clues to its success', *Virology Journal*. BioMed Central, 8(1), p. 481. doi: 10.1186/1743-422X-8-481.

Kato, N., Sasou, S. and Motoyama, T. (2006) 'Expression of hepatocyte nuclear factor-1beta (HNF-1beta) in clear cell tumors and endometriosis of the ovary', *Modern Pathology*, 19(1), pp. 83-89. doi: 10.1038/modpathol.3800492.

Kaufman, H. L. *et al.* (2016) 'Systemic versus local responses in melanoma patients treated with talimogene laherparepvec from a multi-institutional phase II study', *Journal for ImmunoTherapy of Cancer*, 4(1), p. 12. doi: 10.1186/s40425-016-0116-2.

Kehoe, S. *et al.* (2015) 'Primary chemotherapy versus primary surgery for newly diagnosed advanced ovarian cancer (CHORUS): an open-label, randomised, controlled, non-inferiority trial.', *Lancet (London, England)*. Elsevier, 386(9990), pp. 249-57. doi: 10.1016/S0140-6736(14)62223-6.

Kelland, L. (2007) 'The resurgence of platinum-based cancer chemotherapy', *Nature Reviews Cancer*. Nature Publishing Group, 7(8), pp. 573-584. doi: 10.1038/nrc2167.

Kelly, K. J., Wong, J. and Fong, Y. (2008) 'Herpes simplex virus NV1020 as a novel and promising therapy for hepatic malignancy', *Expert Opinion on*

- Investigational Drugs*, 17(7), pp. 1105-1113. doi: 10.1517/13543784.17.7.1105.
- Kemeny, N. *et al.* (2006) 'Phase I, Open-Label, Dose-Escalating Study of a Genetically Engineered Herpes Simplex Virus, NV1020, in Subjects with Metastatic Colorectal Carcinoma to the Liver', *Human Gene Therapy*, 17(12), pp. 1214-1224. doi: 10.1089/hum.2006.17.1214.
- Kerr, J. F., Wyllie, A. H. and Currie, A. R. (1972) 'Apoptosis: a basic biological phenomenon with wide-ranging implications in tissue kinetics.', *British journal of cancer*, 26(4), pp. 239-57. Available at: <http://www.ncbi.nlm.nih.gov/pubmed/4561027> (Accessed: 12 January 2018).
- Kesari, S. *et al.* (1995) 'Therapy of experimental human brain tumors using a neuroattenuated herpes simplex virus mutant.', *Laboratory investigation; a journal of technical methods and pathology*, 73(5), pp. 636-48. Available at: <http://www.ncbi.nlm.nih.gov/pubmed/7474937> (Accessed: 4 January 2018).
- Kettle, S. *et al.* (1997) 'Vaccinia virus serpin B13R (SPI-2) inhibits interleukin-1beta-converting enzyme and protects virus-infected cells from TNF- and Fas-mediated apoptosis, but does not prevent IL-1beta-induced fever.', *The Journal of general virology*, 78 ( Pt 3), pp. 677-85. doi: 10.1099/0022-1317-78-3-677.
- Kim, K. H. *et al.* (2012) 'A phase I clinical trial of Ad5.SSTR/TK.RGD, a novel infectivity-enhanced bicistronic adenovirus, in patients with recurrent gynecologic cancer.', *Clinical cancer research : an official journal of the American Association for Cancer Research*. NIH Public Access, 18(12), pp. 3440-51. doi: 10.1158/1078-0432.CCR-11-2852.
- Kim, S. E. *et al.* (2016) 'Ultrasml nanoparticles induce ferroptosis in nutrient-deprived cancer cells and suppress tumour growth', *Nature Nanotechnology*, 11(11), pp. 977-985. doi: 10.1038/nnano.2016.164.
- Kischkel, F. C. *et al.* (1995) 'Cytotoxicity-dependent APO-1 (Fas/CD95)-associated proteins form a death-inducing signaling complex (DISC) with the receptor.', *The EMBO journal*, 14(22), pp. 5579-88. Available at: <http://www.ncbi.nlm.nih.gov/pubmed/8521815> (Accessed: 9 January 2018).
- Kit, S. (1985) 'Thymidine kinase.', *Microbiological sciences*, 2(12), pp. 369-75. Available at: <http://www.ncbi.nlm.nih.gov/pubmed/3939993> (Accessed: 4 January 2018).
- Knipe, E. *et al.* (2014) 'Chapter 60 Herpes Simplex Viruses', in *Fields Virology*, pp. 1-140.
- Knox, R. J. *et al.* (1986) 'Mechanism of cytotoxicity of anticancer platinum drugs: evidence that cis-diamminedichloroplatinum(II) and cis-diammine-(1,1-cyclobutanedicarboxylato)platinum(II) differ only in the kinetics of their interaction with DNA.', *Cancer research*, 46(4 Pt 2), pp. 1972-9. Available at: <http://www.ncbi.nlm.nih.gov/pubmed/3512077> (Accessed: 15 December 2017).
- Köbel, M. *et al.* (2008) 'Ovarian carcinoma subtypes are different diseases: implications for biomarker studies.', *PLoS medicine*, 5(12), p. e232. doi: 10.1371/journal.pmed.0050232.
- Köbel, M. *et al.* (2009) 'A Limited Panel of Immunomarkers Can Reliably Distinguish Between Clear Cell and High-grade Serous Carcinoma of the Ovary', *The American Journal of Surgical Pathology*, 33(1), pp. 14-21. doi: 10.1097/PAS.0b013e3181788546.

- Koks, C. A. *et al.* (2015) 'Newcastle disease virotherapy induces long-term survival and tumor-specific immune memory in orthotopic glioma through the induction of immunogenic cell death.', *International journal of cancer*, 136(5), pp. E313-25. doi: 10.1002/ijc.29202.
- Komdeur, F. L. *et al.* (2016) 'CD103+ intraepithelial T cells in high-grade serous ovarian cancer are phenotypically diverse TCR $\alpha$ ; $\beta$ ;+ CD8 $\alpha$ ; $\beta$ ;+ T cells that can be targeted for cancer immunotherapy', *Oncotarget*, 7(46), pp. 75130-75144. doi: 10.18632/oncotarget.12077.
- Komiyama, S. *et al.* (1999) 'Prognosis of Japanese patients with ovarian clear cell carcinoma associated with pelvic endometriosis: clinicopathologic evaluation.', *Gynecologic oncology*, 72(3), pp. 342-6. Available at: <http://www.ncbi.nlm.nih.gov/pubmed/10053105> (Accessed: 13 December 2017).
- Koo, G.-B. *et al.* (2015) 'Methylation-dependent loss of RIP3 expression in cancer represses programmed necrosis in response to chemotherapeutics', *Cell Research*. Nature Publishing Group, 25(6), pp. 707-725. doi: 10.1038/cr.2015.56.
- Kothakota, S. *et al.* (1997) 'Caspase-3-generated fragment of gelsolin: effector of morphological change in apoptosis.', *Science (New York, N.Y.)*, 278(5336), pp. 294-8. Available at: <http://www.ncbi.nlm.nih.gov/pubmed/9323209> (Accessed: 10 January 2018).
- Kramer, M. F. *et al.* (2011) 'Herpes simplex virus 1 microRNAs expressed abundantly during latent infection are not essential for latency in mouse trigeminal ganglia', *Virology*, 417(2), pp. 239-247. doi: 10.1016/j.virol.2011.06.027.
- Krishna, S. and Overholtzer, M. (2016) 'Mechanisms and consequences of entosis', *Cellular and Molecular Life Sciences*, 73(11-12), pp. 2379-2386. doi: 10.1007/s00018-016-2207-0.
- Krockenberger, M. *et al.* (2008) 'Macrophage migration inhibitory factor contributes to the immune escape of ovarian cancer by down-regulating NKG2D.', *Journal of immunology (Baltimore, Md. : 1950)*, 180(11), pp. 7338-48. Available at: <http://www.ncbi.nlm.nih.gov/pubmed/18490733> (Accessed: 13 February 2018).
- Kroemer, G. *et al.* (2009) 'Classification of cell death: recommendations of the Nomenclature Committee on Cell Death 2009.', *Cell death and differentiation*, 16(1), pp. 3-11. doi: 10.1038/cdd.2008.150.
- Kroemer, G. *et al.* (2013) 'Immunogenic cell death in cancer therapy.', *Annual review of immunology*, 31, pp. 51-72. doi: 10.1146/annurev-immunol-032712-100008.
- Kroemer, G. and Levine, B. (2008) 'Autophagic cell death: the story of a misnomer', *Nature Reviews Molecular Cell Biology*, 9(12), pp. 1004-1010. doi: 10.1038/nrm2529.
- Kroemer, G., Mariño, G. and Levine, B. (2010) 'Autophagy and the Integrated Stress Response', *Molecular Cell*, 40(2), pp. 280-293. doi: 10.1016/j.molcel.2010.09.023.
- Kronlage, M. *et al.* (2010) 'Autocrine purinergic receptor signaling is essential for

- macrophage chemotaxis.’, *Science signaling*, 3(132), p. ra55. doi: 10.1126/scisignal.2000588.
- Krysko, D. V. *et al.* (2008) ‘Apoptosis and necrosis: Detection, discrimination and phagocytosis’, *Methods*. Academic Press, 44(3), pp. 205-221. doi: 10.1016/J.YMETH.2007.12.001.
- Kuo, K.-T. *et al.* (2009) ‘Analysis of DNA copy number alterations in ovarian serous tumors identifies new molecular genetic changes in low-grade and high-grade carcinomas.’, *Cancer research*, 69(9), pp. 4036-42. doi: 10.1158/0008-5472.CAN-08-3913.
- Landskron, J. *et al.* (2015) ‘Activated regulatory and memory T-cells accumulate in malignant ascites from ovarian carcinoma patients’, *Cancer Immunology, Immunotherapy*, 64(3), pp. 337-347. doi: 10.1007/s00262-014-1636-6.
- LaRocca, C. J. *et al.* (2015) ‘Oncolytic adenovirus expressing interferon alpha in a syngeneic Syrian hamster model for the treatment of pancreatic cancer.’, *Surgery*, 157(5), pp. 888-98. doi: 10.1016/j.surg.2015.01.006.
- Lasner, T. M. *et al.* (1996) ‘Therapy of a murine model of pediatric brain tumors using a herpes simplex virus type-1 ICP34.5 mutant and demonstration of viral replication within the CNS.’, *Journal of neuropathology and experimental neurology*, 55(12), pp. 1259-69. Available at: <http://www.ncbi.nlm.nih.gov/pubmed/8957450> (Accessed: 4 January 2018).
- Lawlor, K. E. *et al.* (2015) ‘RIPK3 promotes cell death and NLRP3 inflammasome activation in the absence of MLKL’, *Nature Communications*, 6(1), p. 6282. doi: 10.1038/ncomms7282.
- Ledermann, J. *et al.* (2012) ‘Olaparib Maintenance Therapy in Platinum-Sensitive Relapsed Ovarian Cancer’, *New England Journal of Medicine*, 366(15), pp. 1382-1392. doi: 10.1056/NEJMoa1105535.
- Ledermann, J. *et al.* (2014) ‘Olaparib maintenance therapy in patients with platinum-sensitive relapsed serous ovarian cancer: a preplanned retrospective analysis of outcomes by BRCA status in a randomised phase 2 trial’, *The Lancet Oncology*, 15(8), pp. 852-861. doi: 10.1016/S1470-2045(14)70228-1.
- Ledermann, J. A. *et al.* (2013) ‘Newly diagnosed and relapsed epithelial ovarian carcinoma: ESMO Clinical Practice Guidelines for diagnosis, treatment and follow-up’, *Annals of Oncology*, 24(suppl 6), p. vi24-vi32. doi: 10.1093/annonc/mdt333.
- Ledermann, J. A. *et al.* (2016) ‘Cediranib in patients with relapsed platinum-sensitive ovarian cancer (ICON6): a randomised, double-blind, placebo-controlled phase 3 trial’, *The Lancet*, 387(10023), pp. 1066-1074. doi: 10.1016/S0140-6736(15)01167-8.
- Lee, C.-H. *et al.* (2015) ‘IL-1 $\beta$  Promotes Malignant Transformation and Tumor Aggressiveness in Oral Cancer’, *Journal of Cellular Physiology*. Wiley-Blackwell, 230(4), pp. 875-884. doi: 10.1002/jcp.24816.
- Lee, J. S., Raja, P. and Knipe, D. M. (2016) ‘Herpesviral ICP0 Protein Promotes Two Waves of Heterochromatin Removal on an Early Viral Promoter during Lytic Infection’, *mBio*, 7(1), pp. e02007-15. doi: 10.1128/mBio.02007-15.
- Leib, D. A. *et al.* (2009) ‘Interaction of ICP34.5 with Beclin 1 modulates herpes simplex virus type 1 pathogenesis through control of CD4 $^{+}$  T-cell responses.’,

*Journal of virology*, 83(23), pp. 12164-71. doi: 10.1128/JVI.01676-09.

Leopardi, R., Van Sant, C. and Roizman, B. (1997) 'The herpes simplex virus 1 protein kinase US3 is required for protection from apoptosis induced by the virus.', *Proceedings of the National Academy of Sciences of the United States of America*, 94(15), pp. 7891-6. Available at: <http://www.ncbi.nlm.nih.gov/pubmed/9223283> (Accessed: 4 December 2017).

Li, J. *et al.* (2012) 'The RIP1/RIP3 necrosome forms a functional amyloid signaling complex required for programmed necrosis.', *Cell*, 150(2), pp. 339-50. doi: 10.1016/j.cell.2012.06.019.

Li, S. *et al.* (2012) 'Oncolytic virotherapy for ovarian cancer', *Oncolytic Virotherapy*, 1, pp. 1-21. doi: 10.2147/OV.S31626.

Li, Y. *et al.* (2011) 'ICP34.5 protein of herpes simplex virus facilitates the initiation of protein translation by bridging eukaryotic initiation factor 2alpha (eIF2alpha) and protein phosphatase 1.', *The Journal of biological chemistry*. American Society for Biochemistry and Molecular Biology, 286(28), pp. 24785-92. doi: 10.1074/jbc.M111.232439.

Liashkovich, I. *et al.* (2011) 'Nuclear delivery mechanism of herpes simplex virus type 1 genome', *Journal of Molecular Recognition*, 24(3), pp. 414-421. doi: 10.1002/jmr.1120.

Lin, C. *et al.* (2016) 'Increasing the Efficiency of CRISPR/Cas9-mediated Precise Genome Editing of HSV-1 Virus in Human Cells.', *Scientific reports*. Nature Publishing Group, 6, p. 34531. doi: 10.1038/srep34531.

Lin, C. and Zhang, J. (2017) 'Inflammasomes in Inflammation-Induced Cancer.', *Frontiers in immunology*. Frontiers Media SA, 8, p. 271. doi: 10.3389/fimmu.2017.00271.

Linkermann, A. *et al.* (2014) 'Synchronized renal tubular cell death involves ferroptosis', *Proceedings of the National Academy of Sciences*, 111(47), pp. 16836-16841. doi: 10.1073/pnas.1415518111.

Linkermann, A., Kunzendorf, U. and Krautwald, S. (2014) 'Phosphorylated MLKL causes plasma membrane rupture', *Molecular & Cellular Oncology*, 1(1), p. e29915. doi: 10.4161/mco.29915.

Liu, B. L. *et al.* (2003) 'ICP34.5 deleted herpes simplex virus with enhanced oncolytic, immune stimulating, and anti-tumour properties.', *Gene therapy*, 10(4), pp. 292-303. doi: 10.1038/sj.gt.3301885.

Liu, M., Guo, S. and Stiles, J. K. (2011) 'The emerging role of CXCL10 in cancer (Review).', *Oncology letters*. Spandidos Publications, 2(4), pp. 583-589. doi: 10.3892/ol.2011.300.

Liu, X. *et al.* (2016) 'Key roles of necroptotic factors in promoting tumor growth'.

Liu, Y. *et al.* (2013) 'Autosis is a Na<sup>+</sup>,K<sup>+</sup>-ATPase-regulated form of cell death triggered by autophagy-inducing peptides, starvation, and hypoxia-ischemia', *Proceedings of the National Academy of Sciences*, 110(51), pp. 20364-20371. doi: 10.1073/pnas.1319661110.

Liu, Y. and Levine, B. (2015) 'Autosis and autophagic cell death: the dark side of autophagy.', *Cell death and differentiation*. Nature Publishing Group, 22(3), pp.

367-76. doi: 10.1038/cdd.2014.143.

Locksley, R. M., Killeen, N. and Lenardo, M. J. (2001) 'The TNF and TNF receptor superfamilies: integrating mammalian biology.', *Cell*, 104(4), pp. 487-501. Available at: <http://www.ncbi.nlm.nih.gov/pubmed/11239407> (Accessed: 9 January 2018).

Loetscher, P. *et al.* (1994) 'Monocyte chemotactic proteins MCP-1, MCP-2, and MCP-3 are major attractants for human CD4+ and CD8+ T lymphocytes.', *FASEB journal : official publication of the Federation of American Societies for Experimental Biology*, 8(13), pp. 1055-60. Available at: <http://www.ncbi.nlm.nih.gov/pubmed/7926371> (Accessed: 1 May 2018).

Lu, B. *et al.* (2012) 'Novel role of PKR in inflammasome activation and HMGB1 release', *Nature*, 488(7413), pp. 670-674. doi: 10.1038/nature11290.

Lu, B. *et al.* (2014) 'JAK/STAT1 signaling promotes HMGB1 hyperacetylation and nuclear translocation', *Proceedings of the National Academy of Sciences*, 111(8), pp. 3068-3073. doi: 10.1073/pnas.1316925111.

Luo, Y. and Liu, M. (2016) 'Adiponectin: a versatile player of innate immunity', *Journal of Molecular Cell Biology*, 8(2), pp. 120-128. doi: 10.1093/jmcb/mjw012.

Luxton, G. W. G. *et al.* (2005) 'Targeting of herpesvirus capsid transport in axons is coupled to association with specific sets of tegument proteins', *Proceedings of the National Academy of Sciences*, 102(16), pp. 5832-5837. doi: 10.1073/pnas.0500803102.

Mace, A. T. M. *et al.* (2008) 'Potential for efficacy of the oncolytic Herpes simplex virus 1716 in patients with oral squamous cell carcinoma.', *Head & neck*, 30(8), pp. 1045-51. doi: 10.1002/hed.20840.

MacKie, R. M., Stewart, B. and Brown, S. M. (2001) 'Intralesional injection of herpes simplex virus 1716 in metastatic melanoma.', *Lancet*, 357(9255), pp. 525-6. doi: 10.1016/S0140-6736(00)04048-4.

MacLean, a R. *et al.* (1991) 'Herpes simplex virus type 1 deletion variants 1714 and 1716 pinpoint neurovirulence-related sequences in Glasgow strain 17+ between immediate early gene 1 and the "a" sequence.', *The Journal of general virology*, 72 ( Pt 3), pp. 631-9. Available at: <http://www.ncbi.nlm.nih.gov/pubmed/1848598>.

Mariathasan, S. *et al.* (2006) 'Cryopyrin activates the inflammasome in response to toxins and ATP', *Nature*, 440(7081), pp. 228-232. doi: 10.1038/nature04515.

Markert, J. *et al.* (2015) 'Extended disease-free interval of 6 years in a recurrent glioblastoma multiforme patient treated with G207 oncolytic viral therapy', *Oncolytic Virotherapy*, 4, p. 33. doi: 10.2147/OV.S62461.

Markert, J. M. *et al.* (1992) 'Expanded spectrum of viral therapy in the treatment of nervous system tumors', *Journal of Neurosurgery*, 77(4), pp. 590-594. doi: 10.3171/jns.1992.77.4.0590.

Markert, J. M. *et al.* (1993) 'Reduction and elimination of encephalitis in an experimental glioma therapy model with attenuated herpes simplex mutants that retain susceptibility to acyclovir.', *Neurosurgery*, 32(4), pp. 597-603. Available at: <http://www.ncbi.nlm.nih.gov/pubmed/8386343> (Accessed: 4 January 2018).

- Markert, J. M. *et al.* (2009) 'Phase Ib Trial of Mutant Herpes Simplex Virus G207 Inoculated Pre- and Post-tumor Resection for Recurrent GBM', *17(1)*, pp. 199-207. doi: 10.1038/mt.2008.228.
- Markert, J. M. *et al.* (2014) 'A phase 1 trial of oncolytic HSV-1, G207, given in combination with radiation for recurrent GBM demonstrates safety and radiographic responses.', *Molecular therapy: the journal of the American Society of Gene Therapy*, *22(5)*, pp. 1048-55. doi: 10.1038/mt.2014.22.
- Markowska, A. *et al.* (2017) 'Angiogenesis and cancer stem cells: New perspectives on therapy of ovarian cancer.', *European journal of medicinal chemistry*, *142*, pp. 87-94. doi: 10.1016/j.ejmech.2017.06.030.
- Martuza, R. L. *et al.* (1991) 'Experimental therapy of human glioma by means of a genetically engineered virus mutant.', *Science (New York, N.Y.)*, *252(5007)*, pp. 854-6. Available at: <http://www.ncbi.nlm.nih.gov/pubmed/1851332>.
- Matis, J. and Kúdelová, M. (2001) 'Early shutoff of host protein synthesis in cells infected with herpes simplex viruses.', *Acta virologica*, *45(5-6)*, pp. 269-77. Available at: <http://www.ncbi.nlm.nih.gov/pubmed/12083325> (Accessed: 1 December 2017).
- McCabe, K. E. *et al.* (2014) 'Triggering necroptosis in cisplatin and IAP antagonist-resistant ovarian carcinoma.', *Cell death & disease*. Nature Publishing Group, *5(10)*, p. e1496. doi: 10.1038/cddis.2014.448.
- McGeoch, D. J. *et al.* (1988) 'The Complete DNA Sequence of the Long Unique Region in the Genome of Herpes Simplex Virus Type 1', *Journal of General Virology*, *69(7)*, pp. 1531-1574. doi: 10.1099/0022-1317-69-7-1531.
- McGeoch, D. J., Rixon, F. J. and Davison, A. J. (2006) 'Topics in herpesvirus genomics and evolution', *Virus Research*, *117(1)*, pp. 90-104. doi: 10.1016/j.virusres.2006.01.002.
- McKie, E. A. *et al.* (1996) 'Selective in vitro replication of herpes simplex virus type 1 (HSV-1) ICP34.5 null mutants in primary human CNS tumours--evaluation of a potentially effective clinical therapy.', *British journal of cancer*, *74(5)*, pp. 745-52. Available at: <http://www.ncbi.nlm.nih.gov/pubmed/8795577> (Accessed: 4 January 2018).
- McKie, E. A. *et al.* (1998) 'Histopathological responses in the CNS following inoculation with a non-neurovirulent mutant (1716) of herpes simplex virus type 1 (HSV 1): relevance for gene and cancer therapy.', *Neuropathology and applied neurobiology*, *24(5)*, pp. 367-72. Available at: <http://www.ncbi.nlm.nih.gov/pubmed/9821167> (Accessed: 2 January 2015).
- McQuade, T., Cho, Y. and Chan, F. K.-M. (2013) 'Positive and negative phosphorylation regulates RIP1- and RIP3-induced programmed necrosis', *Biochemical Journal*, *456(3)*, pp. 409-415. doi: 10.1042/BJ20130860.
- Medeiros, F. *et al.* (2006) 'The tubal fimbria is a preferred site for early adenocarcinoma in women with familial ovarian cancer syndrome.', *The American journal of surgical pathology*, *30(2)*, pp. 230-6. Available at: <http://www.ncbi.nlm.nih.gov/pubmed/16434898> (Accessed: 11 December 2017).
- Meignier, B. and Roizman, B. (1985) 'Herpes simplex virus vaccines.', *Antiviral research*, Suppl 1, pp. 259-65. Available at:

- <http://www.ncbi.nlm.nih.gov/pubmed/3002260> (Accessed: 5 January 2018).
- Meshij, N. *et al.* (2013) 'Enhancement of systemic tumor immunity for squamous cell carcinoma cells by an oncolytic herpes simplex virus', *Cancer Gene Therapy*, 20(9), pp. 493-498. doi: 10.1038/cgt.2013.45.
- Michaud, M. *et al.* (2011) 'Autophagy-dependent anticancer immune responses induced by chemotherapeutic agents in mice.', *Science (New York, N.Y.)*, 334(6062), pp. 1573-7. doi: 10.1126/science.1208347.
- Miller, M. D. and Krangel, M. S. (1992) 'The human cytokine I-309 is a monocyte chemoattractant.', *Proceedings of the National Academy of Sciences of the United States of America*, 89(7), pp. 2950-4. Available at: <http://www.ncbi.nlm.nih.gov/pubmed/1557400> (Accessed: 30 April 2018).
- Minami, M. *et al.* (2002) 'Role of IFN-  $\gamma$  and Tumor Necrosis Factor-  $\alpha$  in Herpes Simplex Virus Type 1 Infection', *Journal of Interferon & Cytokine Research*, 22(6), pp. 671-676. doi: 10.1089/10799900260100150.
- Mineta, T. *et al.* (1995) 'Attenuated multi-mutated herpes virus-1 for the treatment of malignant gliomas', *Nature*, 1, pp. 938-943. doi: 10.1038/nm0995-938.
- Mirza, M. R. *et al.* (2016) 'Niraparib Maintenance Therapy in Platinum-Sensitive, Recurrent Ovarian Cancer', *New England Journal of Medicine*, 375(22), pp. 2154-2164. doi: 10.1056/NEJMoa1611310.
- Mitamura, T. *et al.* (2017) 'Induction of anti-VEGF therapy resistance by upregulated expression of microseminoprotein (MSMP)', *Oncogene*. doi: 10.1038/onc.2017.348.
- Miyamoto, S. *et al.* (2012) 'Coxsackievirus B3 is an oncolytic virus with immunostimulatory properties that is active against lung adenocarcinoma.', *Cancer research*, 72(10), pp. 2609-21. doi: 10.1158/0008-5472.CAN-11-3185.
- Miyazaki, D. *et al.* (2011) 'Herpes Simplex Virus Type 1-Induced Transcriptional Networks of Corneal Endothelial Cells Indicate Antigen Presentation Function', *Investigative Ophthalmology & Visual Science*, 52(7), p. 4282. doi: 10.1167/iovs.10-6911.
- Mohr, I. and Gluzman, Y. (1996) 'A herpesvirus genetic element which affects translation in the absence of the viral GADD34 function.', *The EMBO journal*, 15(17), pp. 4759-66. Available at: <http://www.pubmedcentral.nih.gov/articlerender.fcgi?artid=452208&tool=pmcentrez&rendertype=abstract>.
- Monk, B. J. *et al.* (2014) 'Anti-angiopoietin therapy with trebananib for recurrent ovarian cancer (TRINOVA-1): a randomised, multicentre, double-blind, placebo-controlled phase 3 trial.', *The Lancet. Oncology*, 15(8), pp. 799-808. doi: 10.1016/S1470-2045(14)70244-X.
- Moon, K. B., Turner, P. C. and Moyer, R. W. (1999) 'SPI-1-dependent host range of rabbitpox virus and complex formation with cathepsin G is associated with serpin motifs.', *Journal of virology*, 73(11), pp. 8999-9010. Available at: <http://www.ncbi.nlm.nih.gov/pubmed/10516006> (Accessed: 4 October 2016).
- Moquin, D. M., McQuade, T. and Chan, F. K.-M. (2013) 'CYLD Deubiquitinates RIP1 in the TNF $\alpha$ -Induced Necrosome to Facilitate Kinase Activation and Programmed Necrosis', *PLoS ONE*. Edited by E. W. Harhaj, 8(10), p. e76841. doi:

10.1371/journal.pone.0076841.

Morgan, J. (2007) 'Vero Cells in Vaccine Production', *BioProcessing Journal*, 6(3), pp. 12-17. doi: 10.12665/J63.Morgan.

Mou, F., Wills, E. and Baines, J. D. (2009) 'Phosphorylation of the UL31 Protein of Herpes Simplex Virus 1 by the US3-Encoded Kinase Regulates Localization of the Nuclear Envelopment Complex and Egress of Nucleocapsids', *Journal of Virology*, 83(10), pp. 5181-5191. doi: 10.1128/JVI.00090-09.

Mundschau, L. J. and Faller, D. V (1994) 'Endogenous inhibitors of the dsRNA-dependent eIF-2 alpha protein kinase PKR in normal and ras-transformed cells.', *Biochimie*, 76(8), pp. 792-800. Available at: <http://www.ncbi.nlm.nih.gov/pubmed/7893828> (Accessed: 5 February 2018).

Muruve, D. A. *et al.* (2008) 'The inflammasome recognizes cytosolic microbial and host DNA and triggers an innate immune response', *Nature*, 452(7183), pp. 103-107. doi: 10.1038/nature06664.

Negus, R. P. *et al.* (1995) 'The detection and localization of monocyte chemoattractant protein-1 (MCP-1) in human ovarian cancer.', *Journal of Clinical Investigation*, 95(5), pp. 2391-2396. doi: 10.1172/JCI117933.

Nemunaitis, J. *et al.* (2000) 'Selective replication and oncolysis in p53 mutant tumors with ONYX-015, an E1B-55kD gene-deleted adenovirus, in patients with advanced head and neck cancer: A phase II trial', *Cancer Research*, 60(22), pp. 6359-6366. doi: 10.1126/science.1905840.

Neumann, L. *et al.* (1997) 'The active domain of the herpes simplex virus protein ICP47: a potent inhibitor of the transporter associated with antigen processing.', *Journal of molecular biology*, 272(4), pp. 484-92. Available at: <http://www.ncbi.nlm.nih.gov/pubmed/9325106> (Accessed: 1 December 2017).

Newcomb, W. W. *et al.* (2001) 'The UL6 Gene Product Forms the Portal for Entry of DNA into the Herpes Simplex Virus Capsid', *Journal of Virology*, 75(22), pp. 10923-10932. doi: 10.1128/JVI.75.22.10923-10932.2001.

Newton, K. and Manning, G. (2016) 'Necroptosis and Inflammation', *Annual Review of Biochemistry*, 85(1), p. annurev-biochem-060815-014830. doi: 10.1146/annurev-biochem-060815-014830.

NHS (2017) *National Cancer Drugs Fund List Drug Indication*. Available at: <https://www.england.nhs.uk/wp-content/uploads/2013/03/ncdf-list.pdf> (Accessed: 19 December 2017).

O'Shea, C. C. *et al.* (2004) 'Late viral RNA export, rather than p53 inactivation, determines ONYX-015 tumor selectivity.', *Cancer cell*, 6(6), pp. 611-23. doi: 10.1016/j.ccr.2004.11.012.

Obeid, M. *et al.* (2007) 'Calreticulin exposure dictates the immunogenicity of cancer cell death.', *Nature medicine*, 13(January), pp. 54-61. doi: 10.1038/nm1523.

Obermajer, N. *et al.* (2011) 'PGE2-Induced CXCL12 Production and CXCR4 Expression Controls the Accumulation of Human MDSCs in Ovarian Cancer Environment', *Cancer Research*, 71(24), pp. 7463-7470. doi: 10.1158/0008-5472.CAN-11-2449.

Ojala, P. M. *et al.* (2000) 'Herpes simplex virus type 1 entry into host cells:

- reconstitution of capsid binding and uncoating at the nuclear pore complex in vitro.', *Molecular and cellular biology*, 20(13), pp. 4922-31. Available at: <http://www.ncbi.nlm.nih.gov/pubmed/10848617> (Accessed: 1 December 2017).
- Omoto, S. *et al.* (2015) 'Suppression of RIP3-dependent Necroptosis by Human Cytomegalovirus', *Journal of Biological Chemistry*, (404), p. jbc.M115.646042. doi: 10.1074/jbc.M115.646042.
- Orzalli, M. H., DeLuca, N. A. and Knipe, D. M. (2012) 'Nuclear IFI16 induction of IRF-3 signaling during herpesviral infection and degradation of IFI16 by the viral ICP0 protein.', *Proceedings of the National Academy of Sciences of the United States of America*, 109(44), pp. E3008-17. doi: 10.1073/pnas.1211302109.
- Owen, D., Crump, C. and Graham, S. (2015) 'Tegument Assembly and Secondary Envelopment of Alpha herpesviruses', *Viruses*, 7(12), pp. 5084-5114. doi: 10.3390/v7092861.
- Oza, A. M., Cibula, D., *et al.* (2015) 'Olaparib combined with chemotherapy for recurrent platinum-sensitive ovarian cancer: a randomised phase 2 trial', *The Lancet Oncology*, 16(1), pp. 87-97. doi: 10.1016/S1470-2045(14)71135-0.
- Oza, A. M., Cook, A. D., *et al.* (2015) 'Standard chemotherapy with or without bevacizumab for women with newly diagnosed ovarian cancer (ICON7): overall survival results of a phase 3 randomised trial', *The Lancet Oncology*, 16(8), pp. 928-936. doi: 10.1016/S1470-2045(15)00086-8.
- Ozols, R. F. *et al.* (2003) 'Phase III trial of carboplatin and paclitaxel compared with cisplatin and paclitaxel in patients with optimally resected stage III ovarian cancer: a Gynecologic Oncology Group study.', *Journal of clinical oncology: official journal of the American Society of Clinical Oncology*, 21(17), pp. 3194-200. doi: 10.1200/JCO.2003.02.153.
- Panaretakis, T. *et al.* (2009) 'Mechanisms of pre-apoptotic calreticulin exposure in immunogenic cell death', *The EMBO Journal*, 28(5), pp. 578-590. doi: 10.1038/emboj.2009.1.
- Papanastassiou, V. *et al.* (2002) 'The potential for efficacy of the modified (ICP 34.5-) herpes simplex virus HSV1716 following intratumoural injection into human malignant glioma: a proof of principle study', *Gene Therapy*, 9(6), pp. 398-406. doi: 10.1038/sj.gt.3301664.
- Park, S. Y. *et al.* (2002) 'Expression of cytokeratins 7 and 20 in primary carcinomas of the stomach and colorectum and their value in the differential diagnosis of metastatic carcinomas to the ovary', *Human Pathology*, 33(11), pp. 1078-1085. doi: 10.1053/hupa.2002.129422.
- Parviainen, S. *et al.* (2015) 'GMCSF-armed vaccinia virus induces an antitumor immune response.', *International journal of cancer*, 136(5), pp. 1065-72. doi: 10.1002/ijc.29068.
- Pasparakis, M. and Vandenabeele, P. (2015) 'Necroptosis and its role in inflammation', 5. doi: 10.1038/nature14191.
- Patch, A.-M. *et al.* (2015) 'Whole-genome characterization of chemoresistant ovarian cancer', *Nature*, 521(7553), pp. 489-494. doi: 10.1038/nature14410.
- Patrone, M. *et al.* (2003) 'The human cytomegalovirus UL45 gene product is a late, virion-associated protein and influences virus growth at low multiplicities of infection', *Journal of General Virology*, 84(12), pp. 3359-3370. doi:

10.1099/vir.0.19452-0.

Pattingre, S. *et al.* (2005) 'Bcl-2 Antiapoptotic Proteins Inhibit Beclin 1-Dependent Autophagy', *Cell*, 122(6), pp. 927-939. doi: 10.1016/j.cell.2005.07.002.

Pawaria, S. and Binder, R. J. (2011) 'CD91-dependent programming of T-helper cell responses following heat shock protein immunization.', *Nature communications*, 2, p. 521. doi: 10.1038/ncomms1524.

Perkins, D., Pereira, E. F. R. and Aurelian, L. (2003) 'The herpes simplex virus type 2 R1 protein kinase (ICP10 PK) functions as a dominant regulator of apoptosis in hippocampal neurons involving activation of the ERK survival pathway and upregulation of the antiapoptotic protein Bag-1.', *Journal of virology*, 77(2), pp. 1292-305. Available at: <http://www.ncbi.nlm.nih.gov/pubmed/12502846> (Accessed: 28 September 2016).

Pesce, S. *et al.* (2015) 'B7-H6-mediated downregulation of NKp30 in NK cells contributes to ovarian carcinoma immune escape', *Oncolmmunology*, 4(4), p. e1001224. doi: 10.1080/2162402X.2014.1001224.

Phelan, D., Barrozo, E. R. and Bloom, D. C. (2017) 'HSV1 latent transcription and non-coding RNA: A critical retrospective', *Journal of Neuroimmunology*, 308, pp. 65-101. doi: 10.1016/j.jneuroim.2017.03.002.

Piek, J. M. *et al.* (2001) 'Tubal ligation and risk of ovarian cancer', *The Lancet*, 358(9284), p. 844. doi: 10.1016/S0140-6736(01)05992-X.

Pignata, S. *et al.* (2015) 'Pazopanib plus weekly paclitaxel versus weekly paclitaxel alone for platinum-resistant or platinum-refractory advanced ovarian cancer (MITO 11): a randomised, open-label, phase 2 trial', *The Lancet Oncology*. Elsevier Ltd, 16(5), pp. 561-568. doi: 10.1016/S1470-2045(15)70115-4.

Ponath, P. D. *et al.* (1996) 'Molecular cloning and characterization of a human eotaxin receptor expressed selectively on eosinophils.', *The Journal of experimental medicine*. Rockefeller University Press, 183(6), pp. 2437-48. doi: 10.1084/JEM.183.6.2437.

Post, L. E. and Roizman, B. (1981) 'A generalized technique for deletion of specific genes in large genomes: alpha gene 22 of herpes simplex virus 1 is not essential for growth.', *Cell*. Elsevier, 25(1), pp. 227-32. doi: 10.1016/0092-8674(81)90247-6.

Prat, J. (2012) 'Ovarian carcinomas: five distinct diseases with different origins, genetic alterations, and clinicopathological features', *Virchows Archiv*, 460(3), pp. 237-249. doi: 10.1007/s00428-012-1203-5.

Prat, J. and FIGO Committee on Gynecologic Oncology (2014) 'Staging classification for cancer of the ovary, fallopian tube, and peritoneum', *International Journal of Gynecology & Obstetrics*, 124(1), pp. 1-5. doi: 10.1016/j.ijgo.2013.10.001.

Pujade-Lauraine, E. *et al.* (2012) 'AURELIA: A randomized phase III trial evaluating bevacizumab (BEV) plus chemotherapy (CT) for platinum (PT)-resistant recurrent ovarian cancer (OC).', *Journal of Clinical Oncology*. American Society of Clinical Oncology, 30(18\_suppl), p. LBA5002-LBA5002. doi: 10.1200/jco.2012.30.18\_suppl.lba5002.

- Purvanov, V. *et al.* (2014) 'G-protein-coupled receptor signaling and polarized actin dynamics drive cell-in-cell invasion.', *eLife*. eLife Sciences Publications, Ltd, 3. doi: 10.7554/eLife.02786.
- Qian, B.-Z. *et al.* (2011) 'CCL2 recruits inflammatory monocytes to facilitate breast-tumour metastasis', *Nature*, 475(7355), pp. 222-225. doi: 10.1038/nature10138.
- Radtke, K. *et al.* (2010) 'Plus- and minus-end directed microtubule motors bind simultaneously to herpes simplex virus capsids using different inner tegument structures.', *PLoS pathogens*. Edited by B. Damania, 6(7), p. e1000991. doi: 10.1371/journal.ppat.1000991.
- Rampling, R. *et al.* (2000) 'Toxicity evaluation of replication-competent herpes simplex virus (ICP 34.5 null mutant 1716) in patients with recurrent malignant glioma.', *Gene therapy*, 7(10), pp. 859-66. Available at: <http://www.ncbi.nlm.nih.gov/pubmed/10845724> (Accessed: 7 December 2016).
- Randazzo, B. P. *et al.* (1996) 'Herpes Simplex 1716—an ICP 34.5 Mutant—Is Severely Replication Restricted in Human Skin Xenografts in Vivo', *Virology*, 223(2), pp. 392-395. doi: 10.1006/viro.1996.0493.
- Rattan, R. *et al.* (2011) 'Metformin suppresses ovarian cancer growth and metastasis with enhancement of cisplatin cytotoxicity in vivo.', *Neoplasia (New York, N.Y.)*, 13(5), pp. 483-91. Available at: <http://www.ncbi.nlm.nih.gov/pubmed/21532889> (Accessed: 19 December 2017).
- Reef, S. *et al.* (2006) 'A Short Mitochondrial Form of p19ARF Induces Autophagy and Caspase-Independent Cell Death', *Molecular Cell*, 22(4), pp. 463-475. doi: 10.1016/j.molcel.2006.04.014.
- Reinartz, S. *et al.* (2014) 'Mixed-polarization phenotype of ascites-associated macrophages in human ovarian carcinoma: Correlation of CD163 expression, cytokine levels and early relapse', *International Journal of Cancer*, 134(1), pp. 32-42. doi: 10.1002/ijc.28335.
- Reinthaller, A. (2016) 'Antiangiogenic therapies in ovarian cancer.', *Memo. Springer*, 9(3), pp. 139-143. doi: 10.1007/s12254-016-0282-4.
- Remijnsen, Q. *et al.* (2011) 'Dying for a cause: NETosis, mechanisms behind an antimicrobial cell death modality.', *Cell death and differentiation*. Nature Publishing Group, 18(4), pp. 581-8. doi: 10.1038/cdd.2011.1.
- Remijnsen, Q. *et al.* (2011) 'Neutrophil extracellular trap cell death requires both autophagy and superoxide generation', *Cell Research*, 21(2), pp. 290-304. doi: 10.1038/cr.2010.150.
- Rieger, A. M. *et al.* (2011) 'Modified annexin V/propidium iodide apoptosis assay for accurate assessment of cell death.', *Journal of visualized experiments : JoVE*, (50), pp. 37-40. doi: 10.3791/2597.
- Rimon, G. *et al.* (1997) 'Increased surface phosphatidylserine is an early marker of neuronal apoptosis.', *Journal of neuroscience research*, 48(6), pp. 563-70. Available at: <http://www.ncbi.nlm.nih.gov/pubmed/9210526> (Accessed: 3 April 2018).
- Roby, K. F. *et al.* (2000) 'Development of a syngeneic mouse model for events related to ovarian cancer.', *Carcinogenesis*, 21(4), pp. 585-91. Available at:

<http://www.ncbi.nlm.nih.gov/pubmed/10753190> (Accessed: 2 May 2018).

Rode, K. *et al.* (2011) 'Uncoupling uncoating of herpes simplex virus genomes from their nuclear import and gene expression.', *Journal of virology*. American Society for Microbiology (ASM), 85(9), pp. 4271-83. doi: 10.1128/JVI.02067-10.

Rodriguez, D. A. *et al.* (2016) 'Characterization of RIPK3-mediated phosphorylation of the activation loop of MLKL during necroptosis', *Cell Death & Differentiation*. Nature Publishing Group, 23(1), pp. 76-88. doi: 10.1038/cdd.2015.70.

Rodríguez, I. M. and Prat, J. (2002) 'Mucinous tumors of the ovary: a clinicopathologic analysis of 75 borderline tumors (of intestinal type) and carcinomas.', *The American journal of surgical pathology*, 26(2), pp. 139-52. Available at: <http://www.ncbi.nlm.nih.gov/pubmed/11812936> (Accessed: 12 December 2017).

Roehm, P. C. *et al.* (2016) 'Inhibition of HSV-1 Replication by Gene Editing Strategy.', *Scientific reports*. Nature Publishing Group, 6, p. 23146. doi: 10.1038/srep23146.

Roizman, B., Zhou, G. and Du, T. (2011) 'Checkpoints in productive and latent infections with herpes simplex virus 1: conceptualization of the issues', *Journal of NeuroVirology*, 17(6), pp. 512-517. doi: 10.1007/s13365-011-0058-x.

Roos, R. S. *et al.* (1997) 'Identification of CCR8, the receptor for the human CC chemokine I-309.', *The Journal of biological chemistry*, 272(28), pp. 17251-4. Available at: <http://www.ncbi.nlm.nih.gov/pubmed/9211859> (Accessed: 30 April 2018).

Russell, S. J., Peng, K.-W. and Bell, J. C. (2012) 'Oncolytic virotherapy.', *Nature biotechnology*. Nature Publishing Group, 30(7), pp. 658-70. doi: 10.1038/nbt.2287.

Le Sage, V. and Banfield, B. W. (2012) 'Dysregulation of autophagy in murine fibroblasts resistant to HSV-1 infection.', *PloS one*. Edited by D. A. Leib, 7(8), p. e42636. doi: 10.1371/journal.pone.0042636.

Sakahira, H., Enari, M. and Nagata, S. (1998) 'Cleavage of CAD inhibitor in CAD activation and DNA degradation during apoptosis', *Nature*, 391(6662), pp. 96-99. doi: 10.1038/34214.

Sakahira, H. and Nagata, S. (2002) 'Co-translational folding of caspase-activated DNase with Hsp70, Hsp40, and inhibitor of caspase-activated DNase.', *The Journal of biological chemistry*, 277(5), pp. 3364-70. doi: 10.1074/jbc.M110071200.

Sandbaumhüter, M. *et al.* (2013) 'Cytosolic herpes simplex virus capsids not only require binding inner tegument protein pUL36 but also pUL37 for active transport prior to secondary envelopment', *Cellular Microbiology*, 15(2), pp. 248-269. doi: 10.1111/cmi.12075.

Sander, J. D. and Joung, J. K. (2014) 'CRISPR-Cas systems for editing, regulating and targeting genomes.', *Nature biotechnology*. Nature Publishing Group, 32(4), pp. 347-55. doi: 10.1038/nbt.2842.

Santin, A. D. *et al.* (2001) 'Phenotypic and functional analysis of tumor-infiltrating lymphocytes compared with tumor-associated lymphocytes from ascitic fluid and peripheral blood lymphocytes in patients with advanced ovarian

- cancer.’, *Gynecologic and obstetric investigation*. Karger Publishers, 51(4), pp. 254-61. doi: 10.1159/000058060.
- Sarinella, F. *et al.* (2006) ‘Oncolysis of pancreatic tumour cells by a  $\gamma$ 34.5-deleted HSV-1 does not rely upon Ras-activation, but on the PI 3-kinase pathway’, *Gene Therapy*, 13(14), pp. 1080-1087. doi: 10.1038/sj.gt.3302770.
- Sato, E. *et al.* (2005) ‘Intraepithelial CD8+ tumor-infiltrating lymphocytes and a high CD8+/regulatory T cell ratio are associated with favorable prognosis in ovarian cancer’, *Proceedings of the National Academy of Sciences*, 102(51), pp. 18538-18543. doi: 10.1073/pnas.0509182102.
- Sato, N. *et al.* (2000) ‘Loss of heterozygosity on 10q23.3 and mutation of the tumor suppressor gene PTEN in benign endometrial cyst of the ovary: possible sequence progression from benign endometrial cyst to endometrioid carcinoma and clear cell carcinoma of the ovary.’, *Cancer research*, 60(24), pp. 7052-6. Available at: <http://www.ncbi.nlm.nih.gov/pubmed/11156411> (Accessed: 13 December 2017).
- Scaffidi, C. *et al.* (1999) ‘The role of c-FLIP in modulation of CD95-induced apoptosis.’, *The Journal of biological chemistry*, 274(3), pp. 1541-8. Available at: <http://www.ncbi.nlm.nih.gov/pubmed/9880531> (Accessed: 9 January 2018).
- Scaffidi, P., Misteli, T. and Bianchi, M. E. (2002) ‘Release of chromatin protein HMGB1 by necrotic cells triggers inflammation’, *Nature*, 418(6894), pp. 191-195. doi: 10.1038/nature00858.
- Schiraldi, M. *et al.* (2012) ‘HMGB1 promotes recruitment of inflammatory cells to damaged tissues by forming a complex with CXCL12 and signaling via CXCR4.’, *The Journal of experimental medicine*, 209(3), pp. 551-63. doi: 10.1084/jem.20111739.
- Schmidt, S. V *et al.* (2015) ‘RIPK3 expression in cervical cancer cells is required for PolyIC-induced necroptosis, IL-1 $\alpha$  release, and efficient paracrine dendritic cell activation.’, *Oncotarget*. Impact Journals, LLC, 6(11), pp. 8635-47. doi: 10.18632/oncotarget.3249.
- Schneider, U. *et al.* (2000) ‘Recombinant Measles Viruses Efficiently Entering Cells through Targeted Receptors’, *Journal of Virology*, 74(21), pp. 9928-9936. doi: 10.1128/JVI.74.21.9928-9936.2000.
- Schweichel, J.-U. and Merker, H.-J. (1973) ‘The morphology of various types of cell death in prenatal tissues’, *Teratology*, 7(3), pp. 253-266. doi: 10.1002/tera.1420070306.
- Scott, E. M. *et al.* (2018) ‘Solid Tumor Immunotherapy with T Cell Engager-Armed Oncolytic Viruses’, *Macromolecular Bioscience*, 18(1), p. 1700187. doi: 10.1002/mabi.201700187.
- Senzer, N. N. *et al.* (2009) ‘Phase II Clinical Trial of a Granulocyte-Macrophage Colony-Stimulating Factor-Encoding, Second-Generation Oncolytic Herpesvirus in Patients With Unresectable Metastatic Melanoma’, *Journal of Clinical Oncology*, 27(34), pp. 5763-5771. doi: 10.1200/JCO.2009.24.3675.
- Sharma, K. *et al.* (2014) ‘Cytotoxic Autophagy in Cancer Therapy’, *International Journal of Molecular Sciences*, 15(6), pp. 10034-10051. doi: 10.3390/ijms150610034.
- Sheldrick, P. and Berthelot, N. (1975) ‘Inverted repetitions in the chromosome

of herpes simplex virus.’, *Cold Spring Harbor symposia on quantitative biology*, 39 Pt 2, pp. 667-78. Available at: <http://www.ncbi.nlm.nih.gov/pubmed/169022> (Accessed: 30 November 2017).

Shi, J. *et al.* (2015) ‘Cleavage of GSDMD by inflammatory caspases determines pyroptotic cell death’, *Nature*, 526(7575), pp. 660-665. doi: 10.1038/nature15514.

Shimizu, S. *et al.* (2004) ‘Role of Bcl-2 family proteins in a non-apoptotic programmed cell death dependent on autophagy genes’, *Nature Cell Biology*, 6(12), pp. 1221-1228. doi: 10.1038/ncb1192.

Shimizu, S. *et al.* (2010) ‘Involvement of JNK in the regulation of autophagic cell death’, *Oncogene*, 29(14), pp. 2070-2082. doi: 10.1038/onc.2009.487.

Shimizu, S. *et al.* (2014) ‘Autophagic Cell Death and Cancer’, *International Journal of Molecular Sciences*, 15(2), pp. 3145-3153. doi: 10.3390/ijms15023145.

Shoji-Kawata, S. *et al.* (2013) ‘Identification of a candidate therapeutic autophagy-inducing peptide’, *Nature*, 494(7436), pp. 201-206. doi: 10.1038/nature11866.

Sica, A. *et al.* (2000) ‘Defective expression of the monocyte chemotactic protein-1 receptor CCR2 in macrophages associated with human ovarian carcinoma.’, *Journal of immunology (Baltimore, Md. : 1950)*, 164(2), pp. 733-8. Available at: <http://www.ncbi.nlm.nih.gov/pubmed/10623817> (Accessed: 3 January 2018).

da Silva, R. *et al.* (2017) ‘Natural Killer Cells Response to IL-2 Stimulation Is Distinct between Ascites with the Presence or Absence of Malignant Cells in Ovarian Cancer Patients’, *International Journal of Molecular Sciences*, 18(12), p. 856. doi: 10.3390/ijms18050856.

Simchoni, S. *et al.* (2006) ‘Familial clustering of site-specific cancer risks associated with BRCA1 and BRCA2 mutations in the Ashkenazi Jewish population.’, *Proceedings of the National Academy of Sciences of the United States of America*, 103(10), pp. 3770-4. doi: 10.1073/pnas.0511301103.

Simpson-Holley, M. *et al.* (2005) ‘Identification and functional evaluation of cellular and viral factors involved in the alteration of nuclear architecture during herpes simplex virus 1 infection.’, *Journal of virology*, 79(20), pp. 12840-51. doi: 10.1128/JVI.79.20.12840-12851.2005.

Smith, D. F. *et al.* (2005) ‘GRO family chemokines are specialized for monocyte arrest from flow’, *American Journal of Physiology-Heart and Circulatory Physiology*. American Physiological Society, 289(5), pp. H1976-H1984. doi: 10.1152/ajpheart.00153.2005.

Sodeik, B., Ebersold, M. W. and Helenius, A. (1997) ‘Microtubule-mediated transport of incoming herpes simplex virus 1 capsids to the nucleus.’, *The Journal of cell biology*, 136(5), pp. 1007-21. Available at: <http://www.ncbi.nlm.nih.gov/pubmed/9060466> (Accessed: 1 December 2017).

Song, G.-Y. *et al.* (2007) ‘An MVA vaccine overcomes tolerance to human p53 in mice and humans’, *Cancer Immunology, Immunotherapy*, 56(8), pp. 1193-1205. doi: 10.1007/s00262-006-0270-3.

Song, G.-Y. *et al.* (2011) ‘Recombinant Modified Vaccinia Virus Ankara (MVA) Expressing Wild-Type Human p53 Induces Specific Antitumor CTL Expansion’,

- Cancer Investigation*, 29(8), pp. 501-510. doi: 10.3109/07357907.2011.606248.
- Speck, T. *et al.* (2018) 'Targeted BiTE expression by an oncolytic vector augments therapeutic efficacy against solid tumors', *Clinical Cancer Research*, p. clincanres.2651.2017. doi: 10.1158/1078-0432.CCR-17-2651.
- Stockwell, B. R. *et al.* (2017) 'Ferroptosis: A Regulated Cell Death Nexus Linking Metabolism, Redox Biology, and Disease', *Cell*, 171(2), pp. 273-285. doi: 10.1016/j.cell.2017.09.021.
- Streby, K. A. *et al.* (2017) 'Intratumoral Injection of HSV1716, an Oncolytic Herpes Virus, Is Safe and Shows Evidence of Immune Response and Viral Replication in Young Cancer Patients', *Clinical Cancer Research*, 23(14), pp. 3566-3574. doi: 10.1158/1078-0432.CCR-16-2900.
- Street, C. (2016) 'Identification of a Herpes Simplex Virus Type 1 Polypeptide Which Is a Component of the Virus-induced Ribonucleotide Reductase B E R N A D E T T E M . D U T I A', (1984), pp. 1457-1466.
- Su, L. *et al.* (2014) 'A plug release mechanism for membrane permeation by MLKL.', *Structure (London, England : 1993)*, 22(10), pp. 1489-500. doi: 10.1016/j.str.2014.07.014.
- Su, Z. *et al.* (2016) 'Cancer therapy in the necroptosis era', pp. 1-9. doi: 10.1038/cdd.2016.8.
- Suenaga, T. *et al.* (2014) 'Engineering large viral DNA genomes using the CRISPR-Cas9 system', (May), pp. 513-522. doi: 10.1111/1348-0421.12180.
- Sun, L. *et al.* (2012) 'Mixed lineage kinase domain-like protein mediates necrosis signaling downstream of RIP3 kinase.', *Cell*. Elsevier Inc., 148(1-2), pp. 213-27. doi: 10.1016/j.cell.2011.11.031.
- Swisher, E. M. *et al.* (2017) 'Rucaparib in relapsed, platinum-sensitive high-grade ovarian carcinoma (ARIEL2 Part 1): an international, multicentre, open-label, phase 2 trial', *The Lancet Oncology*, 18(1), pp. 75-87. doi: 10.1016/S1470-2045(16)30559-9.
- Tada, S., Hamada, M. and Yura, Y. (2018) 'Proteomic Analysis of Secretomes of Oncolytic Herpes Simplex Virus-Infected Squamous Cell Carcinoma Cells', *Cancers*. Multidisciplinary Digital Publishing Institute, 10(2), p. 28. doi: 10.3390/cancers10020028.
- Takaoka, A. *et al.* (2007) 'DAI (DLM-1/ZBP1) is a cytosolic DNA sensor and an activator of innate immune response.', *Nature*, 448(7152), pp. 501-5. doi: 10.1038/nature06013.
- Takaoka, H. *et al.* (2011) 'A novel fusogenic herpes simplex virus for oncolytic virotherapy of squamous cell carcinoma.', *Virology journal*, 8, p. 294. doi: 10.1186/1743-422X-8-294.
- Takasu, A. *et al.* (2016) 'Immunogenic cell death by oncolytic herpes simplex virus type 1 in squamous cell carcinoma cells.', *Cancer gene therapy*, 23(4), pp. 107-13. doi: 10.1038/cgt.2016.8.
- Tanida, I., Ueno, T. and Kominami, E. (2008) 'LC3 and Autophagy', in *Methods in molecular biology (Clifton, N.J.)*, pp. 77-88. doi: 10.1007/978-1-59745-157-4\_4.
- Tanida, S. *et al.* (2012) 'Mechanisms of Cisplatin-Induced Apoptosis and of Cisplatin Sensitivity: Potential of BIN1 to Act as a Potent Predictor of Cisplatin

Sensitivity in Gastric Cancer Treatment', *International Journal of Surgical Oncology*. Hindawi, 2012, pp. 1-8. doi: 10.1155/2012/862879.

Thornberry, N. A. and Lazebnik, Y. (1998) 'Caspases: enemies within.', *Science (New York, N.Y.)*, 281(5381), pp. 1312-6. Available at: <http://www.ncbi.nlm.nih.gov/pubmed/9721091> (Accessed: 9 January 2018).

Tiwari, V. *et al.* (2005) 'A Role for Herpesvirus Entry Mediator as the Receptor for Herpes Simplex Virus 1 Entry into Primary Human Trabecular Meshwork Cells', *Journal of Virology*, 79(20), pp. 13173-13179. doi: 10.1128/JVI.79.20.13173-13179.2005.

Tiwari, V. *et al.* (2006) 'Role for 3-O-Sulfated Heparan Sulfate as the Receptor for Herpes Simplex Virus Type 1 Entry into Primary Human Corneal Fibroblasts', *Journal of Virology*, 80(18), pp. 8970-8980. doi: 10.1128/JVI.00296-06.

Toda, M. (2000) 'Tumor Growth Inhibition by Intratumoral Inoculation of Defective Herpes Simplex Virus Vectors Expressing Granulocyte-Macrophage Colony-Stimulating Factor', *Molecular Therapy*, 2(4), pp. 324-329. doi: 10.1006/mthe.2000.0130.

Tokunaga, R. *et al.* (2018) 'CXCL9, CXCL10, CXCL11/CXCR3 axis for immune activation - A target for novel cancer therapy.', *Cancer treatment reviews*, 63, pp. 40-47. doi: 10.1016/j.ctrv.2017.11.007.

Tothill, R. W. *et al.* (2008) 'Novel Molecular Subtypes of Serous and Endometrioid Ovarian Cancer Linked to Clinical Outcome', *Clinical Cancer Research*, 14(16), pp. 5198-5208. doi: 10.1158/1078-0432.CCR-08-0196.

Turner, A. *et al.* (1998) 'Glycoproteins gB, gD, and gHgL of herpes simplex virus type 1 are necessary and sufficient to mediate membrane fusion in a Cos cell transfection system.', *Journal of virology*. American Society for Microbiology, 72(1), pp. 873-5. Available at: <http://www.ncbi.nlm.nih.gov/pubmed/9420303> (Accessed: 30 November 2017).

Umbach, J. L. *et al.* (2008) 'MicroRNAs expressed by herpes simplex virus 1 during latent infection regulate viral mRNAs', *Nature*, 454(7205), pp. 780-3. doi: 10.1038/nature07103.

Upton, J. W., Kaiser, W. J. and Mocarski, E. S. (2008) 'Cytomegalovirus M45 Cell Death Suppression Requires Receptor-interacting Protein (RIP) Homotypic Interaction Motif (RHIM)-dependent Interaction with RIP1', *Journal of Biological Chemistry*, 283(25), pp. 16966-16970. doi: 10.1074/jbc.C800051200.

Upton, J. W., Kaiser, W. J. and Mocarski, E. S. (2012) 'DAI/ZBP1/DLM-1 complexes with RIP3 to mediate virus-induced programmed necrosis that is targeted by murine cytomegalovirus vIRA', *Cell Host and Microbe*. Elsevier Inc., 11(3), pp. 290-297. doi: 10.1016/j.chom.2012.01.016.

Urbanaviciute, V. *et al.* (2008) 'Induction of inflammatory and immune responses by HMGB1-nucleosome complexes: implications for the pathogenesis of SLE.', *The Journal of experimental medicine*, 205(13), pp. 3007-18. doi: 10.1084/jem.20081165.

Vanags, D. M. *et al.* (1996) 'Protease involvement in fodrin cleavage and phosphatidylserine exposure in apoptosis.', *The Journal of biological chemistry*, 271(49), pp. 31075-85. Available at: <http://www.ncbi.nlm.nih.gov/pubmed/8940103> (Accessed: 3 April 2018).

- Vandenabeele, P. *et al.* (2010) 'Molecular mechanisms of necroptosis: an ordered cellular explosion', *Nature Reviews Molecular Cell Biology*, 11(10), pp. 700-714. doi: 10.1038/nrm2970.
- Vandenabeele, P. *et al.* (2016) 'Immunogenic Apoptotic Cell Death and Anticancer Immunity', in *Advances in experimental medicine and biology*, pp. 133-149. doi: 10.1007/978-3-319-39406-0\_6.
- Vandenabeele, P., Vanden Berghe, T. and Festjens, N. (2006) 'Caspase inhibitors promote alternative cell death pathways.', *Science's STKE: signal transduction knowledge environment*. American Association for the Advancement of Science, 2006(358), p. pe44. doi: 10.1126/stke.3582006pe44.
- Vang, R. *et al.* (2006) 'Immunohistochemical expression of CDX2 in primary ovarian mucinous tumors and metastatic mucinous carcinomas involving the ovary: comparison with CK20 and correlation with coordinate expression of CK7', *Modern Pathology*, 19(11), pp. 1421-1428. doi: 10.1038/modpathol.3800698.
- Vanlangenakker, N., Vanden Berghe, T. and Vandenabeele, P. (2012) 'Many stimuli pull the necrotic trigger, an overview.', *Cell death and differentiation*. Nature Publishing Group, 19(1), pp. 75-86. doi: 10.1038/cdd.2011.164.
- Varga, A. *et al.* (2015) 'Antitumor activity and safety of pembrolizumab in patients (pts) with PD-L1 positive advanced ovarian cancer: Interim results from a phase Ib study.', *Journal of Clinical Oncology*, 33(15), pp. 5510-5510. Available at: [http://ascopubs.org/doi/abs/10.1200/jco.2015.33.15\\_suppl.5510](http://ascopubs.org/doi/abs/10.1200/jco.2015.33.15_suppl.5510) (Accessed: 2 January 2018).
- Vasey, P. A. *et al.* (2004) 'Phase III randomized trial of docetaxel-carboplatin versus paclitaxel-carboplatin as first-line chemotherapy for ovarian carcinoma.', *Journal of the National Cancer Institute*, 96(22), pp. 1682-91. doi: 10.1093/jnci/djh323.
- Vega, V. L. *et al.* (2008) 'Hsp70 translocates into the plasma membrane after stress and is released into the extracellular environment in a membrane-associated form that activates macrophages.', *Journal of immunology (Baltimore, Md. : 1950)*, 180(6), pp. 4299-307. Available at: <http://www.ncbi.nlm.nih.gov/pubmed/18322243> (Accessed: 12 January 2018).
- Vergote, I. *et al.* (2010) 'Neoadjuvant Chemotherapy or Primary Surgery in Stage IIIC or IV Ovarian Cancer', *New England Journal of Medicine*, 363(10), pp. 943-953. doi: 10.1056/NEJMoa0908806.
- Verpooten, D. *et al.* (2009) 'Control of TANK-binding Kinase 1-mediated Signaling by the  $\gamma_1$  34.5 Protein of Herpes Simplex Virus 1', *Journal of Biological Chemistry*, 284(2), pp. 1097-1105. doi: 10.1074/jbc.M805905200.
- Vittone, V. *et al.* (2005) 'Determination of interactions between tegument proteins of herpes simplex virus type 1.', *Journal of virology*, 79(15), pp. 9566-71. doi: 10.1128/JVI.79.15.9566-9571.2005.
- Wadsworth, S., Jacob, R. J. and Roizman, B. (1975) 'Anatomy of herpes simplex virus DNA. II. Size, composition, and arrangement of inverted terminal repetitions.', *Journal of virology*, 15(6), pp. 1487-97. Available at: <http://www.ncbi.nlm.nih.gov/pubmed/167196> (Accessed: 30 November 2017).
- Wajant, H. (2002) 'The Fas signaling pathway: more than a paradigm.', *Science (New York, N.Y.)*, 296(5573), pp. 1635-6. doi: 10.1126/science.1071553.

- Wales, S. Q. *et al.* (2008) 'ICP10PK inhibits calpain-dependent release of apoptosis-inducing factor and programmed cell death in response to the toxin MPP+'.', *Gene therapy*, 15(20), pp. 1397-409. doi: 10.1038/gt.2008.88.
- Walton, J. *et al.* (2016) 'CRISPR/Cas9-Mediated Trp53 and Brca2 Knockout to Generate Improved Murine Models of Ovarian High-Grade Serous Carcinoma', *Cancer Research*, 76(20), pp. 6118-6129. doi: 10.1158/0008-5472.CAN-16-1272.
- Walton, J. B. *et al.* (2017) 'CRISPR/Cas9-derived models of ovarian high grade serous carcinoma targeting Brca1, Pten and Nf1, and correlation with platinum sensitivity', *Scientific Reports*, 7(1), p. 16827. doi: 10.1038/s41598-017-17119-1.
- Wang, H. *et al.* (2014) 'Mixed Lineage Kinase Domain-like Protein MLKL Causes Necrotic Membrane Disruption upon Phosphorylation by RIP3', *Molecular Cell*, 54(1), pp. 133-146. doi: 10.1016/j.molcel.2014.03.003.
- Wang, M. *et al.* (2015) 'Impaired formation of homotypic cell-in-cell structures in human tumor cells lacking alpha-catenin expression', *Scientific Reports*, 5(1), p. 12223. doi: 10.1038/srep12223.
- Wang, X. *et al.* (2014) 'Direct activation of RIP3/MLKL-dependent necrosis by herpes simplex virus 1 (HSV-1) protein ICP6 triggers host antiviral defense.', *Proceedings of the National Academy of Sciences of the United States of America*, 111(43), pp. 15438-43. doi: 10.1073/pnas.1412767111.
- Wang, Y. *et al.* (2016) 'A nuclease that mediates cell death induced by DNA damage and poly(ADP-ribose) polymerase-1', *Science*, 354(6308), p. aad6872-aad6872. doi: 10.1126/science.aad6872.
- Waters, A. M. *et al.* (2017) 'Rationale and Design of a Phase 1 Clinical Trial to Evaluate HSV G207 Alone or with a Single Radiation Dose in Children with Progressive or Recurrent Malignant Supratentorial Brain Tumors', *Human Gene Therapy Clinical Development*, 28(1), pp. 7-16. doi: 10.1089/humc.2017.002.
- Webb, J. R. *et al.* (2014) 'Tumor-Infiltrating Lymphocytes Expressing the Tissue Resident Memory Marker CD103 Are Associated with Increased Survival in High-Grade Serous Ovarian Cancer', *Clinical Cancer Research*, 20(2), pp. 434-444. doi: 10.1158/1078-0432.CCR-13-1877.
- Weigert, M. *et al.* (2017) 'RIPK3 promotes adenovirus type 5 activity', *Cell Death & Disease*. Nature Publishing Group, 8(12), p. 3206. doi: 10.1038/s41419-017-0110-8.
- Weller, S. K. and Coen, D. M. (2012) 'Herpes simplex viruses: mechanisms of DNA replication.', *Cold Spring Harbor perspectives in biology*. Cold Spring Harbor Laboratory Press, 4(9), p. a013011. doi: 10.1101/cshperspect.a013011.
- Whilding, L. M. *et al.* (2013) 'Vaccinia virus induces programmed necrosis in ovarian cancer cells.', *Molecular therapy: the journal of the American Society of Gene Therapy*, 21(11), pp. 2074-86. doi: 10.1038/mt.2013.195.
- Whitley, R. J. *et al.* (1993) 'Replication, establishment of latency, and induced reactivation of herpes simplex virus gamma 1 34.5 deletion mutants in rodent models.', *The Journal of clinical investigation*. American Society for Clinical Investigation, 91(6), pp. 2837-43. doi: 10.1172/JCI116527.
- Wiegand, K. C. *et al.* (2010) 'ARID1A Mutations in Endometriosis-Associated Ovarian Carcinomas', *New England Journal of Medicine*, 363(16), pp. 1532-1543. doi: 10.1056/NEJMoa1008433.

- Wild, P. *et al.* (2015) 'Herpes Simplex Virus 1 Us3 Deletion Mutant is Infective Despite Impaired Capsid Translocation to the Cytoplasm', *Viruses*, 7(12), pp. 52-71. doi: 10.3390/v7010052.
- Wong, J. L. *et al.* (2013) 'IL-18-Primed Helper NK Cells Collaborate with Dendritic Cells to Promote Recruitment of Effector CD8+ T Cells to the Tumor Microenvironment', *Cancer Research*, 73(15), pp. 4653-4662. doi: 10.1158/0008-5472.CAN-12-4366.
- Workenhe, S. T. *et al.* (2014) 'Immunogenic HSV-mediated oncolysis shapes the antitumor immune response and contributes to therapeutic efficacy.', *Molecular therapy: the journal of the American Society of Gene Therapy*. Nature Publishing Group, 22(1), pp. 123-31. doi: 10.1038/mt.2013.238.
- Xia, B. *et al.* (2016) 'MLKL forms cation channels.', *Cell research*. Nature Publishing Group, 26(5), pp. 517-528. doi: 10.1038/cr.2016.26.
- Xia, Z.-J. *et al.* (2004) '[Phase III randomized clinical trial of intratumoral injection of E1B gene-deleted adenovirus (H101) combined with cisplatin-based chemotherapy in treating squamous cell cancer of head and neck or esophagus].', *Ai zheng = Aizheng = Chinese journal of cancer*, 23(12), pp. 1666-70. Available at: <http://www.ncbi.nlm.nih.gov/pubmed/15601557> (Accessed: 15 September 2016).
- Xing, D. *et al.* (2017) 'Mutation of NRAS is a rare genetic event in ovarian low-grade serous carcinoma.', *Human pathology*. Elsevier, 68, pp. 87-91. doi: 10.1016/j.humpath.2017.08.021.
- Xu, J. *et al.* (2014) 'Macrophage endocytosis of high-mobility group box 1 triggers pyroptosis', *Cell Death & Differentiation*, 21(8), pp. 1229-1239. doi: 10.1038/cdd.2014.40.
- Xu, L. L. *et al.* (1995) 'Monocyte chemotactic protein-3 (MCP3) interacts with multiple leukocyte receptors: binding and signaling of MCP3 through shared as well as unique receptors on monocytes and neutrophils.', *European journal of immunology*, 25(9), pp. 2612-7. doi: 10.1002/eji.1830250931.
- Yamano, T. *et al.* (2016) 'Whole cell vaccination using immunogenic cell death by an oncolytic adenovirus is effective against a colorectal cancer model', *Molecular Therapy - Oncolytics*, 3, p. 16031. doi: 10.1038/mto.2016.31.
- Yang, B. *et al.* (2004) 'Inhibitors Directed towards Caspase-1 and -3 Are Less Effective than Pan Caspase Inhibition in Preventing Renal Proximal Tubular Cell Apoptosis', *Nephron Experimental Nephrology*, 96(2), pp. e39-e51. doi: 10.1159/000076403.
- Yang, H. *et al.* (2010) 'A critical cysteine is required for HMGB1 binding to Toll-like receptor 4 and activation of macrophage cytokine release', *Proceedings of the National Academy of Sciences*, 107(26), pp. 11942-11947. doi: 10.1073/pnas.1003893107.
- Yang, H. *et al.* (2015) 'High Mobility Group Box Protein 1 (HMGB1): The Prototypical Endogenous Danger Molecule.', *Molecular medicine (Cambridge, Mass.)*. The Feinstein Institute for Medical Research, 21 Suppl 1(Suppl 1), pp. S6-S12. doi: 10.2119/molmed.2015.00087.
- Yang, W. S. *et al.* (2014) 'Regulation of Ferroptotic Cancer Cell Death by GPX4', *Cell*, 156(1-2), pp. 317-331. doi: 10.1016/j.cell.2013.12.010.

- Yang, Y. *et al.* (2014) 'Antitumor effects of oncolytic adenovirus armed with PSA-IZ-CD40L fusion gene against prostate cancer', *Gene Therapy*, 21(8), pp. 723-731. doi: 10.1038/gt.2014.46.
- Yap, T. A. *et al.* (2011) 'Poly(ADP-Ribose) polymerase (PARP) inhibitors: Exploiting a synthetic lethal strategy in the clinic', *CA: A Cancer Journal for Clinicians*, 61(1), pp. 31-49. doi: 10.3322/caac.20095.
- Yee, S.-B. *et al.* (2006) 'zVAD-fmk, unlike BocD-fmk, does not inhibit caspase-6 acting on 14-3-3/Bad pathway in apoptosis of p815 mastocytoma cells', *Experimental & Molecular Medicine*, 38(6), pp. 634-642. doi: 10.1038/emm.2006.75.
- Yi, S. *et al.* (2017) 'Antiangiogenic drugs used with chemotherapy for patients with recurrent ovarian cancer: a meta-analysis', *OncoTargets and Therapy*, Volume 10, pp. 973-984. doi: 10.2147/OTT.S119879.
- Yin, Z., Pascual, C. and Klionsky, D. (2016) 'Autophagy: machinery and regulation', *Microbial Cell*, 3(12), pp. 588-596. doi: 10.15698/mic2016.12.546.
- Yoon, M. and Spear, P. G. (2002) 'Disruption of adherens junctions liberates nectin-1 to serve as receptor for herpes simplex virus and pseudorabies virus entry.', *Journal of virology*, 76(14), pp. 7203-8. Available at: <http://www.ncbi.nlm.nih.gov/pubmed/12072519> (Accessed: 5 January 2018).
- Young, R. C. *et al.* (1979) 'cis-Dichlorodiammineplatinum(II) for the treatment of advanced ovarian cancer.', *Cancer treatment reports*, 63(9-10), pp. 1539-44. Available at: <http://www.ncbi.nlm.nih.gov/pubmed/387224> (Accessed: 13 December 2017).
- Yu, F. *et al.* (2014) 'T-cell engager-armed oncolytic vaccinia virus significantly enhances antitumor therapy.', *Molecular therapy: the journal of the American Society of Gene Therapy*, 22(1), pp. 102-11. doi: 10.1038/mt.2013.240.
- Yu, Z. *et al.* (2007) 'Nectin-1 Expression by Squamous Cell Carcinoma is a Predictor of Herpes Oncolytic Sensitivity', *Molecular Therapy*, 15(1), pp. 103-113. doi: 10.1038/sj.mt.6300009.
- Zaidi, M. R. and Merlino, G. (2011) 'The two faces of interferon- $\gamma$  in cancer.', *Clinical cancer research: an official journal of the American Association for Cancer Research*. NIH Public Access, 17(19), pp. 6118-24. doi: 10.1158/1078-0432.CCR-11-0482.
- Zamarin, D. *et al.* (2014) 'Localized Oncolytic Virotherapy Overcomes Systemic Tumor Resistance to Immune Checkpoint Blockade Immunotherapy', *Science Translational Medicine*, 6(226), p. 226ra32-226ra32. doi: 10.1126/scitranslmed.3008095.
- Zamzami, N. *et al.* (1998) 'Subcellular and submitochondrial mode of action of Bcl-2-like oncoproteins', *Oncogene*, 16(17), pp. 2265-2282. doi: 10.1038/sj.onc.1201989.
- Zhang, B. *et al.* (2017) 'Revisiting ovarian cancer microenvironment: a friend or a foe?', *Protein & Cell*. Higher Education Press, pp. 1-19. doi: 10.1007/s13238-017-0466-7.
- Zhang, F. (2015) 'CRISPR/Cas9: Prospects and Challenges', *Human Gene Therapy*, 26(7), pp. 409-410. doi: 10.1089/hum.2015.29002.fzh.

- Zhang, L. *et al.* (2003) 'Intratumoral T Cells, Recurrence, and Survival in Epithelial Ovarian Cancer', *New England Journal of Medicine*, 348(3), pp. 203-213. doi: 10.1056/NEJMoa020177.
- Zhang, Q. *et al.* (2012) 'Prognostic Significance of Tumor-Associated Macrophages in Solid Tumor: A Meta-Analysis of the Literature', *PLoS ONE*. Edited by M. O. Hoque. Public Library of Science, 7(12), p. e50946. doi: 10.1371/journal.pone.0050946.
- Zhang, T. *et al.* (2016) 'Knockdown of HVEM, a Lymphocyte Regulator Gene, in Ovarian Cancer Cells Increases Sensitivity to Activated T Cells', *Oncology Research Featuring Preclinical and Clinical Cancer Therapeutics*, 24(3), pp. 189-196. doi: 10.3727/096504016X14641336229602.
- Zhou, Y. *et al.* (2015) 'B7-H6 expression correlates with cancer progression and patient's survival in human ovarian cancer.', *International journal of clinical and experimental pathology*, 8(8), pp. 9428-33. Available at: <http://www.ncbi.nlm.nih.gov/pubmed/26464699> (Accessed: 13 February 2018).
- Zhou, Z. H. *et al.* (2000) 'Seeing the herpesvirus capsid at 8.5 Å.', *Science (New York, N.Y.)*, 288(5467), pp. 877-80. Available at: <http://www.ncbi.nlm.nih.gov/pubmed/10797014> (Accessed: 27 November 2017).
- Zhu, H. *et al.* (2016) 'Membrane-bound heat shock proteins facilitate the uptake of dying cells and cross-presentation of cellular antigen', *Apoptosis*, 21(1), pp. 96-109. doi: 10.1007/s10495-015-1187-0.
- Zilka, O. *et al.* (2017) 'On the Mechanism of Cytoprotection by Ferrostatin-1 and Liproxstatin-1 and the Role of Lipid Peroxidation in Ferroptotic Cell Death', *ACS Central Science*, 3(3), pp. 232-243. doi: 10.1021/acscentsci.7b00028.